INFORMATION TO USERS

This manuscript has been reproduced from the microfilm master. UMI films the text directly from the original or copy submitted. Thus, some thesis and dissertation copies are in typewriter face, while others may be from any type of computer printer.

The quality of this reproduction is dependent upon the quality of the copy submitted. Broken or indistinct print, colored or poor quality illustrations and photographs, print bleedthrough, substandard margins, and improper alignment can adversely affect reproduction.

In the unlikely event that the author did not send UMI a complete manuscript and there are missing pages, these will be noted. Also, if unauthorized copyright material had to be removed, a note will indicate the deletion.

Oversize materials (e.g., maps, drawings, charts) are reproduced by sectioning the original, beginning at the upper left-hand corner and continuing from left to right in equal sections with small overlaps.

Photographs included in the original manuscript have been reproduced xerographically in this copy. Higher quality 6" x 9" black and white photographic prints are available for any photographs or illustrations appearing in this copy for an additional charge. Contact UMI directly to order.

Bell & Howell Information and Learning
300 North Zeeb Road, Ann Arbor, MI 48106-1346 USA
800-521-0600

Studies of the Response to Polycyclic Aromatic Compounds of Liquid Introduction - Atmospheric Pressure Ionisation Mass Spectrometry

By

Beata M. Kolakowski

Submitted in Partial Fulfillment of the
Requirements for the Degree of
Doctor of Philosophy

at

Dalhousie University
Halifax, Nova Scotia
August 1999

DALHOUSIE UNIVERSITY

FACULTY OF GRADUATE STUDIES

The undersigned hereby certify that they have read and recommend to the Faculty of Graduate Studies for acceptance a thesis entitled "Studies of the Response to Polycyclic Aromatic Compounds of Liquid Introduction - Atmospheric Pressure Ionisation Mass Spectrometry"

by Beata Kolakowski

in partial fulfillment of the requirements for the degree of Doctor of Philosophy.

Dated: August 31, 1999

External Examiner

Research Supervisor

Examining Committee

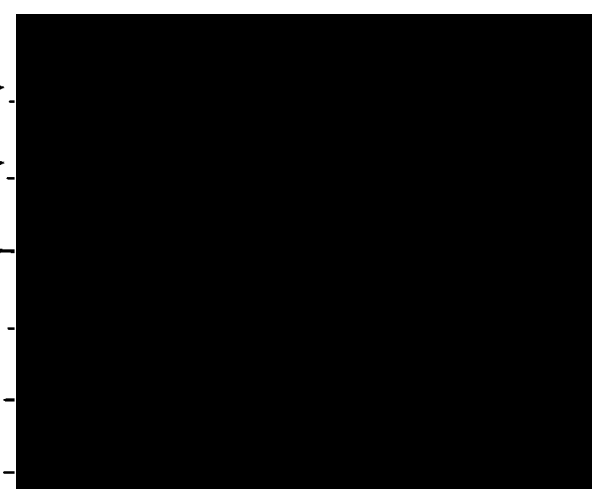

DALHOUSIE UNIVERSITY

DATE: August 31, 1999.

AUTHOR: Beata Maria Kolakowski

TITLE: Studies of the Response to Polycyclic Aromatic Compounds of Liquid Introduction – Atmospheric Pressure Chemical Ionisation Mass Spectrometry

DEPARTMENT OR SCHOOL: Chemistry

DEGREE: Ph.D. **CONVOCATION:** October **YEAR:** 1999

Permission is hereby granted to Dalhousie University to circulate and to have copied for non-commercial purposes, at its discretion, the above title upon the request of individuals or institutions.

Signature of Author

W świetej pamieńczy
Ciocią moją,
Halina Kołakowska Anglart

Table of Contents

List of Figures

List of Tables

Abstract

Polycyclic aromatic compounds are ubiquitous environmental contaminants which are difficult to analyse for in real matrices and havestructure-specfic carcinogenic and mutagenic properties. Atmospheric pressure ionisation mass spectrometric methods provide a means of characterising PACs but poor sensitivity led to detailed studies of the methods, aimed at understanding the chemistry inside the source. Response, in this study, refers both to signal intensity and to predominant ionisation mechanism, represented as the ratio of protonated molecule to molecular ion ($[M+H]^+/M^{+\bullet}$).

The instrumental parameters studied in APCI could be divided into two groups - Group 1 was associated with changes in signal but not $[M+H]^+/M^{+\bullet}$ and Group 2 with changes in both. Bath gas flow rate, nebuliser flow rate, probe position, data acquisition routine, source temperature, and probe temperature were all group 1 parameters. Skimmer cone orifice size, sheath gas flow rate, corona voltage, cone voltage, injection solvent, and source gas belonged to group 2. When optimising PAC detection in a new solvent, gas flow rates, source and probe temperatures, and cone and corona voltages were studied.

Of the solvents tested, organic solvents showed better results than aqueous solvents, likely the result of better nebulisation. Dichloromethane gave the highest signal, probably due to offering the best nebulisation and highest PAC solubility. The best protonation was observed in 50:50 (v/v) acetonitrile-water and hexanes. With the C_5 to C_9 alkanes, *m/z* 59 was correlated with high signal but *m/z* 43 with the highest protonation (consistent with it being the better gas phase acid of the two). These results revealed no correlation between sensitivity and ionisation mechanism. However, protonation and sensitivity were closely related to analyte structure. Ketones and carbazoles were most readily protonated and detected while partially reduced carbazoles were most poorly detected and protonated. The other PACs were of intermediate reactivity.

ESI of PACs was successful with acetic acid addition to acetonitrile (in fact, provided an order of magnitude better detection than APCI for biphenylene) and with the following chemical electron transfer reagents (CETRs): 2,3-dichloro-5,6-dicyano-1,4-benzoquinone, chloranil and 6,7-dichloro-1,4-dihydroxyanthraquinone. The largest increase in signal intensity was for perylene with choranil. Naphthalene and pyrene derivatives differed in their reactivity to CETRs, providing a potential means of isomer discrimination.

Preliminary experiments with one, two and three gas systems indicated that Extradry™ air as bath gas and carbon dioxide as sheath and nebuliser gas was optimal for PAC detection in aqueous and neat acetonitrile, and dichloromethane, and nitrogen as bath gas and carbon dioxide as sheath and nebuliser gas was optimal with hexanes. Later experiments showed that an all CO_2 system was best for hexanes while all Extradry™ air or nitrogen (bath and sheath)- carbon dioxide (nebuliser) was best for aqueous and neat acetonitrile, and dichloromethane. When applied to real world analysis of PACs in a light gas oil, the latter gas system with acetonitrile resulted in a fourfold increase in signal intensity.

List of Abbreviations and Acronyms

API	atmospheric pressure ionisation
APCI	atmospheric pressure chemical ionisation
B	bath
BaP	benzo[*a*]pyrene
CE	capillary electrophoresis
CETR	chemical electron transfer reagent
CI	chemical ionisation
CID	collision-induced dissociation
dc	direct current
DCM	dichloromethane
DDAQ	6,7-dichloro-1,4-dihydroxyanthraquinone
DDQ	2,3-dichloro-5,6-dicyano-1,4-benzoquinone
DNA	deoxyribonucleic acid
EI	electron ionisation
EPA	U.S. Environmental Protection Agency
ESI	electrospray ionisation
eV	electron volts
FID	flame ionisation detector
FPD	flame photometric detection
GB	gas phase basicity $-\Delta G^\circ$ for the reaction: $B + H^+ \rightarrow BH^+$
GC	gas chromatography
GC/CI-MS	gas chromatography/chemical ionisation mass spectrometry
GC/EI-MS	gas chromatography/electron ionisation mass spectrometry
GC/NICI-MS	gas chromatography negative ion chemical ionisation mass spectrometry
GC/MS	gas chromatography/mass spectrometry
HP	Hewlett-Packard
HFC	hydrofluorocarbon

HFE	hydrofluorocarbon ether
HPLC	high performance liquid chromatography
HPLC/MS	high performance liquid chromatography/mass spectrometry
kV	kilovolt
L/B	length-to-breadth ratio
LC	liquid chromatography
LC/APCI-MS	liquid chromatography/atmospheric pressure chemical ionisation mass spectrometry
LC/CI-MS	liquid chromatography/chemical ionisation mass spectrometry
LC/MS	liquid chromatography/mass spectrometry
MeCN	acetonitrile
MeOH	methanol
MS/MS	tandem mass spectrometry
MTC	6-methyl-1,2,3,4-tetrahydrocarbazole
MW	molecular weight
m/z	mass to charge ratio
N	nebuliser
PAC	polycyclic aromatic compound
PAH	polycyclic aromatic hydrocarbon
PANH	polycyclic aromatic nitrogen hydrocarbons
PASH	polycyclic aromatic sulfur hydrocarbon
PEEK	polyetheretherketone
PSC	phenyl-stabilised cation
PFC	perfluoroalkene
rf	radiofrequency
RP-HPLC	reversed phase - high performance liquid chromatography
S	sheath
SIR	signal ion recording
SFC	supercritical fluid chromatography

SFC-MS	supercritical fluid chromatography - mass spectrometry
sLph	standard litres per hour
S/N	signal-to-noise ratio
TBN	1,2:3,4:5,6:7,8-tetrabenzonaphthalene
TCP	tetrachlorophthalamidopropyl column
TCQ	7,7,8,8-tetracyanoquinodimethane
tetralin	1,2,3,4-tetrahydronaphthalene
TFA	trifluoroacetic acid
TIC	total ion count
TNF	2,4,7-trinitro-9-fluorenone
TNFM	(2,4,7-trinitro-9-fluoenylidene)malonitrile
TPC	triphenylcarbenium tetrafluoroborate
TPP	triphenylpyrylium tetrafluoroborate
TTZ	2,3,5-triphenyl-*2H*-tetrazolium chloride
UV	ultraviolet

Acknowledgments

I would like to thank Dr. L. Ramaley for providing me with this opportunity to broaden my research skills, and for his encouragement, assistance and guidance in carrying out this research and in the preparation of this thesis.

Many thanks to Drs. R.D. Guy and J.S. Grossert for providing training, advice and technical assistance to carry out this project. Also, thanks to Michael Potvin and Panos Hatsis for doing the initial studies with the cutting of the distillation fractions and light gas oils, and to Alex Tan for synthesising PAC standards. Thanks to the Dalhousie Chemistry Machine Shop for always having a supply of liquid nitrogen, an endless supply of regulators and their tireless assistance.

I wish to acknowledge Dr. Jean Cooley and the R & D staff at Syncrude for graciously providing suggestions and interesting samples. I would also like to thank Dr. S. Roussis at Imperial Oil for useful discussions.

I wish to thank NSERC, Imperial Oil, the Dalhousie Graduate Student Travel Fund, and the Walter C. Sumner Fellowship Foundation for their financial support of this project and my graduate studies.

A special thank you to Javier Giorgi and my parents for their support and encouragement.

Chapter 1

Introduction

Interest in polycyclic aromatic compounds (PACs) dates back to 1775 when Dr. Percival Pott, a British physician, recognised soot and coal tar as the cause of the abnormally high incidence of scrotal cancer in chimney sweeps [1]. It was not until the 1930s that a potent chemical carcinogen in coal tar was isolated by Kennaway and Cook [2,3]. The molecule, benzo[*a*]pyrene consists of five fused aromatic rings. This discovery sparked interest in understanding the mechanisms of PAC formation, and metabolic transformation into ultimate carcinogens, in assessing their potential carcinogenic and mutagenic properties, in determining their fate in the environment and in developing methods to measure their presence in environmental and industrial samples. Their impact on engine performance and their deleterious effects on 1) petroleum product quality and shelf life and 2) on refinery equipment spurred further interest in their study. Their identification as a class of carcinogens and mutagens whose properties are highly structure-dependent led to legislation regarding emission standards and gave further impetus to the development of trace analytical techniques capable of isomer discrimination in a variety of complex matrices.

1.1 What are polycyclic aromatic compounds (PACs)?

Polycyclic aromatic compounds form a broad class of compounds consisting of polycyclic aromatic hydrocarbons (PAHs), their derivatives and their heteroatomic analogues. PAHs, as their name suggests, are aromatic compounds consisting purely of carbon and hydrogen compounds arranged into fused, 5- and 6-membered rings. The hydrogens on the rings can be replaced by alkyl, amino, halo, hydroxy or nitro groups to

yield PAH derivatives. The carbons in the rings can be replaced in one or more positions by oxygen, nitrogen or sulfur atoms or some combination of these. These compounds constitute the heterocyclic analogues [4]. Examples of these compounds are presented in Figure 1.1.

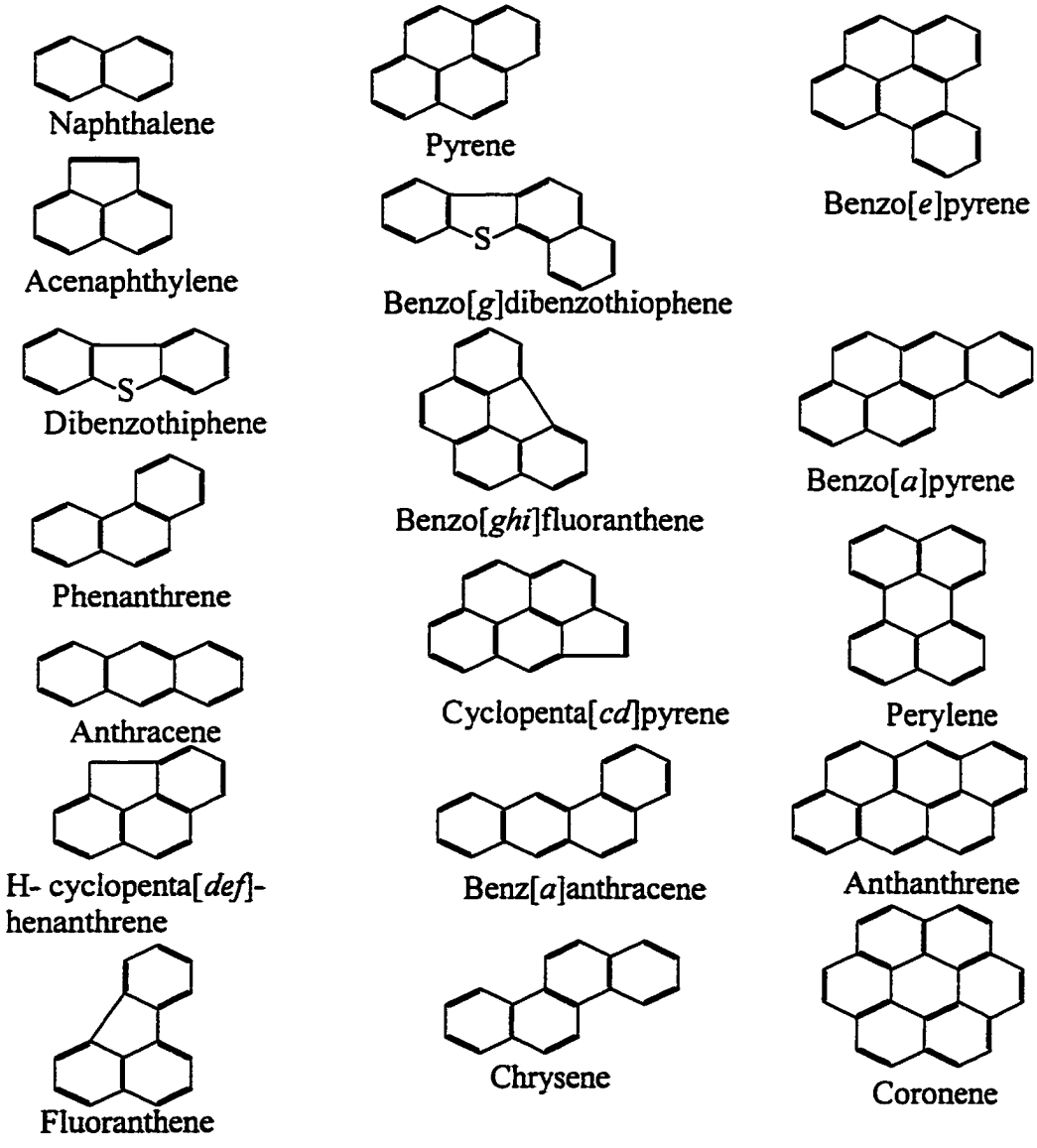

Figure 1.1. Examples of polycyclic aromatic compounds

1.2 Why the interest in PACs?

Researchers, regulatory bodies such as the U.S. Environmental Protection Agency (EPA) and Health Canada, and petroleum companies such as Syncrude Canada (which converts Athabasca tar sands into synthetic crude oils) and Imperial Oil, among others, are interested in the identification of PACs because of their impact on the environment, on human health, on the refining process and on the quality of fuel products.

PACs have been described as ubiquitous environmental contaminants, having been detected in the atmosphere, soot [5], soil, agricultural crops, marine environments, plankton, seaweeds and filter feeding organisms [6]. Soil and marine contamination is derived mainly from petroleum spills, runoff from roads, sewage, effluents from industrial processes and fall out from the atmosphere while urban contamination comes mainly from internal combustion engine exhaust. Although PACs are formed by natural processes, most PAC release to the environment occurs during combustion, coal coking or petroleum catalytic cracking, coal and shale conversion, transportation and use of synthetic fuels and petroleum products. Formation is optimal under pyrolytic conditions at 650-900°C, with alkylated PACs being formed at the lower end of this temperature range. During pyrolysis, gas phase ethylenic radicals are formed and condense to form larger polycyclic compounds.[7-13]

Upon being released into the environment, some PACs can be activated or transformed to more harmful products by chemical reactions with oxidants or sunlight. For example, some PAHs can react with singlet oxygen[14-16], ozone [17-24], hydroxyl radicals [25-26], N_2O_5 [27], SO_2, SO_3 and H_2SO_4 [28]. Atmospheric temperature, the physical properties of the various PACs and the nature of the substrates upon which the PACs are

adsorbed are all implicated in the extent of chemical conversion of PACs [4]. For example, in gas stacks, cooling allows gaseous PACs to condense into microparticles which can subsequently agglomerate into larger particles although the extent to which a particular PAC molecule will exist in the gas phase or the particle phase is determined by both the vapour pressure of the compound and ambient temperature [29]. At 25°C in an urban aerosol, 3-ring PACs are in the vapour phase, 4- and 5-ring PACs exist both in the particle and in the vapour phases while 6-ring (and larger) compounds exist only in the particle phase [30,31].

Because of the widespread nature of the environmental contamination, PACs are inhaled, ingested and absorbed through the skin. They are adsorbed to phospholipids and distributed to various organs in the body. The health concerns of PACs are related to the identification of many of these compounds as potent carcinogens and/or mutagens. The carcinogenic activity varies widely with the shape, size and electronic state of the particular compound [32]. For example, benzo[*a*]pyrene is strongly carcinogenic while the benzo[*e*]pyrene isomer is relatively innocuous.

The electrophilic properties of PAC metabolites allow them to react with the nucleophilic centres in proteins and nucleic acids to form covalent adducts [33-36]. The fate of the adducts is related to their stability. Less stable adducts will be spontaneously removed via a chemical depurination mechanism. More stable adducts will be enzymatically excised during cellular repairs but the most stable adducts will remain in the deoxyribonucleic acid (DNA) and accumulate with repeated exposure [37]. Most of the past emphasis was on smaller PAHs because they were easier to isolate and detect but it has been observed that as the number of rings increases so does the mutagenic and carcinogenic activity [38].

The third reason for the interest in PACs is their effect on industrial processes and equipment. Syncrude isolates bitumen from the Athabasca tar sands. This bitumen contains 22-25% saturates, 10.3-10.8% monoaromatics, 4.6-5.3% diaromatics, 28.6% polyaromatics and polar compounds, 16.5% acids, 7.8% bases and 1.6% neutral nitrogenous compounds. The monoaromatic fraction is composed of alkylbenzenes, naphthenebenzenes, and dinaphthenebenzenes while the diaromatic fraction contains naphthalenes, acenaphthenes, dibenzofurans and fluorenes. The other fractions were not characterized due to problems with handling high-mass compounds [39]. Bitumen is transformed through upgrading to produce a residue-free, low-sulfur, low-nitrogen synthetic crude [40-44]. It is preferable to remove PACs because they poison catalysts, corrode refinery equipment, and alter odour and shelf lifetime of the final products [4,45]. PAC coating in gas stacks necessitates cleaning which can cause shutdown of equipment. All of this increases the cost of generating the final product and impacts on the economic health of the company.

The final factor in the interest in PACs is in their effect on fuel performance. PACs in gasoline are beneficial, in that their presence leads to cleaner burning and better fuel performance. In diesel fuel, PACs are undesirable as they reduce fuel performance. In producing a good diesel fuel, it is thus necessary to minimize PACs to improve engine performance and to reduce toxic emissions to meet (or surpass) federal emission limits.

Emission limits are related to the identification by the U.S. Environmental Protection Agency (EPA) of priority pollutant PACs in a number of matrices, such as drinking water, soil and automobile emissions. The EPA has certified reference materials to facilitate identification and quantification of PACs in each of these matrices. To be certified, results

of 3 or more independent analytical techniques must be in agreement. The EPA-recommended methods of analysis are reversed phase liquid chromatography (LC) with fluorescence detection, multidimensional liquid chromatography, and gas chromatography with electron ionisation mass spectrometry (GC/EI-MS) or chemical ionisation mass spectrometry (GC/CI-MS) with methane or isobutane on two GC stationary phases with different selectivities for PAC separation. Multidimensional LC refers to using one column, for example a normal phase column, to separate PACs according to the ring number, and then using one or more other columns to separate and quantify the isomers of each ring number by reversed phase high performance liquid chromatography (HPLC) with fluorescence detection [46].

These methods are excellent for the identification and quantification of parent PAHs and basic, acidic and neutral nitrogen-containing PACs at trace levels. They do not readily permit the detection of heterocyclic PACs which frequently co-elute with their hydrocarbon analogues but whose biological and/or industrial implications may be quite dissimilar. Nor do they permit the detailed analysis of complex mixtures encompassing many different ring sizes and degree/type of substitution [4]. In particular, high-mass compounds are too involatile to be identified by GC/MS, and alkylated substituents may be degraded in the GC injector or in the EI or CI source. These classes of compounds (high mass, heterocyclic and alkylated PACs) are particularly prevalent in synthetic fuels [4].

For the reasons that PACs are harmful to human health, the environment, and refinery equipment and the difficulty in analysing the afore-mentioned classes of PACs, Syncrude and Imperial Oil are very interested in the analysis of their products through the different

stages of the refining process in an effort to determine how and where PACs are formed and which compounds are being formed. Once identified, method development can begin to find ways to eliminate the formation of these compounds which should increase the performance of the products, reduce maintenance costs and decrease the deleterious occupational health effects. This project is intended to assist Syncrude in the identification of compounds formed and in tracking the progress made in improving their product.

Due to the difficulties in analysing high mass PAC components, which include the lack of standards, the trace amounts of these compounds, the complexity of the matrix and the rapid proliferation of isomers as the mass increases, prior liquid chromatographic separation in one or more dimensions with appropriate detection is required. Mass spectrometry, in particular, using the atmospheric pressure chemical ionisation technique, offers the advantage of being able to accept the entire flow from an HPLC column and it can yield molecular weight and structural information that can assist in compound identification. It is both a sensitive and a selective detection technique.

It has been experimentally observed in this laboratory and elsewhere [92] that the sensitivity of the API techniques (atmospheric pressure chemical ionisation (APCI) and electrospray (ESI)) was lower than desired. This spurred interest in another project undertaken with the collaboration of Dr. S. Roussis at Imperial Oil to understand the nature of the APCI plasma and its effects on the ability to identify and quantify PACs in petroleum matrices. This plasma is initiated by application of a high voltage to the tip of the corona discharge needle. The ensuing corona discharge will ionise gas, solvent and analyte molecules in its vicinity. How changing the nature of the gas and/or solvent alters the plasma

chemistry and how these changes are correlated with sensitivity to the analytes of interest were examined.

1.3 Research Objectives

The research objectives of this project were two-fold. The first was to study the response of liquid introduction – atmospheric pressure ionisation mass spectrometry to polycyclic aromatic compounds. The response to PACs was studied as a function of: a) instrumental parameters, b) solvent identity, c) source gas, solvent and analyte identity and d) API technique (atmospheric pressure chemical ionisation vs. electrospray ionisation). The second objective was to apply the knowledge gained from these studies to the analysis of standards and real-world samples. The main applications were in the characterisation of the PAC content of distillation fractions of synthetic fuels by normal phase chromatography coupled to atmospheric pressure chemical ionisation mass spectrometry (APCI-MS), the characterisation of the PAC content of a synthetic fuel by cold column liquid chromatography–APCI-MS, and the differentiation amongst naphthalene and pyrene derivatives by electrospray ionisation.

Chapter 2

Liquid Introduction and Mass Spectral Analysis for PAC Detection

The focus of this thesis is to study the response of liquid sample introduction – API mass spectrometric methods to polycyclic aromatic compounds as a function of API technique, instrumental parameters, solvents and gases used. This chapter will focus primarily on mass spectral techniques for PAC identification with some description of relevant sample introduction methods (flow injection analysis and chromatography).

2.1. Mass Spectrometry

2.1.1. Instrumentation and Ionisation Mechanisms

A basic mass spectrometer consists of an ion source where species are ionised, a mass analyser where ions are separated, a detector where ions are counted, a recording system where the mass spectrum is displayed and a vacuum system. With the exception of the recording system which is usually a computer outfitted with the proper software, all of these will be discussed, beginning with the mass analysers of which there are four major types: 1) time-of-flight, 2) ion traps, 3) magnetic sector and 4) quadrupole instruments.

2.1.1.1. Mass Analysers

The quadrupole design was used for these studies so it will be described in detail. A brief description of the advantages and disadvantages of the other mass analysers is provided but more detailed descriptions are available in the cited references.

The advantages of time-of-flight analysers include simplicity, speed, good dynamic range, high sensitivity due to the absence of slits and the very high *m/z* range. Disadvantages include the requirements for pulse formation of ions and high acceleration [47-49].

Radiofrequency ion traps (also called quadrupole ion stores, electrostatic ion traps and qaudrupole ion traps) are distinct from other mass spectrometers in that the ion source and analyser are the same. The advantages of this instrument include its high sensitivity (a limit of detection similar to a flame ionisation detector), its unit mass resolution for high mass ions, its compactness, simplicity, inexpensiveness, its ease of interface with chromatographic equipment and the accessibility to chemical ionisation libraries for compound identification. Its disadvantages include a limited dynamic range and a small mass range [47 - 50].

Magnetic ion traps include the omegatron and the Fourier Transform Ion Cyclotron Resonance instruments. The omegatron is simple, very sensitive, and its resolution is proportional to B^2 which is a limitation. The Fourier Transform Ion Cyclotron Resonance instrument has the advantages of non-destructive ion analysis, a linear mass scale, a constant precision over the entire mass range, high accuracy, ion generation and analysis occur in the same region thereby reducing ion loss in transit, all ions can be detected simultaneously, the instrument can be rapidly switched between positive and negative ionisation modes, there is no requirement for complex optics or high voltages and the resolution is greater than 10^6. It can be interfaced with difficulty to GC and the sensitivity increases with increasing mass resolution. Its drawbacks include high cost, large size, complicated operation, long scan times to maintain high accuracy and resolution, the requirement for vacuum of 10^{-9} Torr, its limitation to low sample gas pressures, relatively low dynamic range, and problematic interface to LC systems [47-49].

The magnetic sector instrument is the classical mass analyser. Both single and double focussing designs are available and offer the advantages of high resolution, the ability to perform high mass determination, and the ability to observe metastable ions. Its principal drawbacks include a modest mass range, difficulty in coupling to GC and the inability to couple to LC [47-52].

Quadrupole instruments are the most commonly used mass spectrometers. Both electric and magnetic quadrupoles have been developed but only the former are used as they are easier to operate and control. In these instruments, ions are generated in the source, accelerated into the analyser and separated by an electrostatic and radiofrequency field created by four parallel rods [49, 50]. This instrumental design consists of four electrodes (commonly called rods) arranged in a diamond. These rods may be hyperbolic or cylindrical, the latter being easier to machine. A typical quadrupole design in presented in Figure 2.1. It consists of two pairs of parallel rods, rods 1 and 3 forming one pair and rods 2 and 4 forming the second pair. Voltages equal in magnitude but opposite in sign are applied to each pair of rods, generating an electric field that directs ion motion in the XY plane. If dc voltages without a radiofrequency (rf) component are applied to the rods, the sample cations will be attracted to one pair and repelled by the others but will follow an erratic path through the analyser and the ions will not reach the detector in any predictable fashion, if at all. If only an rf potential is applied, all ions are guided through the rods and will reach the detector. Finally, if both a dc potential and an rf component are applied to both sets of rods with the proper amplitude ratio to generate opposing fields, only the ion of a particular *m/z* range will be able to pass through the rods and reach the detector.

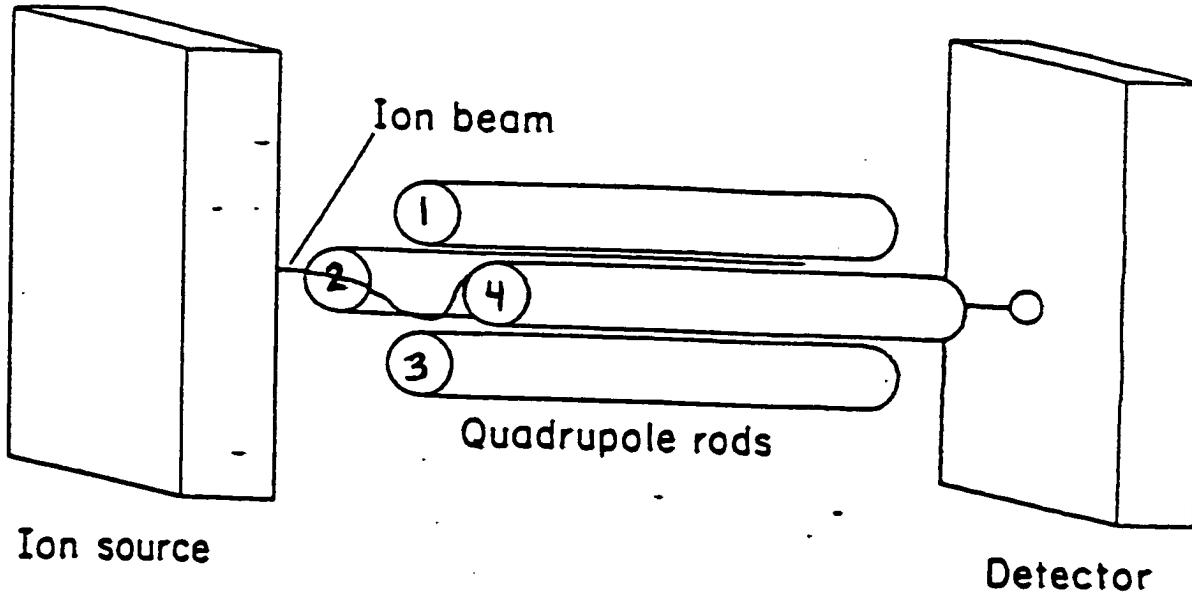

Figure 2.1 A typical quadrupole design [51]

Thus, the field generated by rods 1 and 3 will correspond to:

$$U + V_p \cos\omega t \qquad \text{(eq.2.1)}$$

and the field at rods 2 and 4 will be:

$$-U - V_p \cos\omega t \qquad \text{(eq.2.2)}$$

where U is the dc voltage, V_p is the peak applied rf potential, ω is the angular frequency of the rf field and t is the time. In other words, by properly selecting the potential and frequency, some masses will pass through undeflected and others will be collected by one of the electrodes. Thus, the ion of interest will proceed to the detector while heavier ions will hit the negative poles and lighter ions will hit the positive poles. By varying the dc and rf

voltages whilst maintaining a constant ratio between them so that controlled ion paths are possible, the ions of different *m/z* will able to pass through to the detector. This is called mass scanning. With a computer-controlled quadrupole, the fields can be rapidly altered so that successive *m/z* ions can be detected. The mass resolution of this design increases with increasing rod length. The advantages include fast scanning, linear mass scale, programmability, compactness, ease of operation, low cost, simple calibration, no requirement for high accelerating voltages, and ready interfacing with gas and liquid chromatographs. Its principal disadvantages are that its resolution and mass range are poorer than a sector instrument [47-53].

The design of the VG-Fisons-Micromass™ instrument used in this thesis is presented in Figure 2.2. It consists of three sets of "quadrupoles". The first and third operate like the single quadrupoles described above and are identified as MS1 and MS2, respectively. The

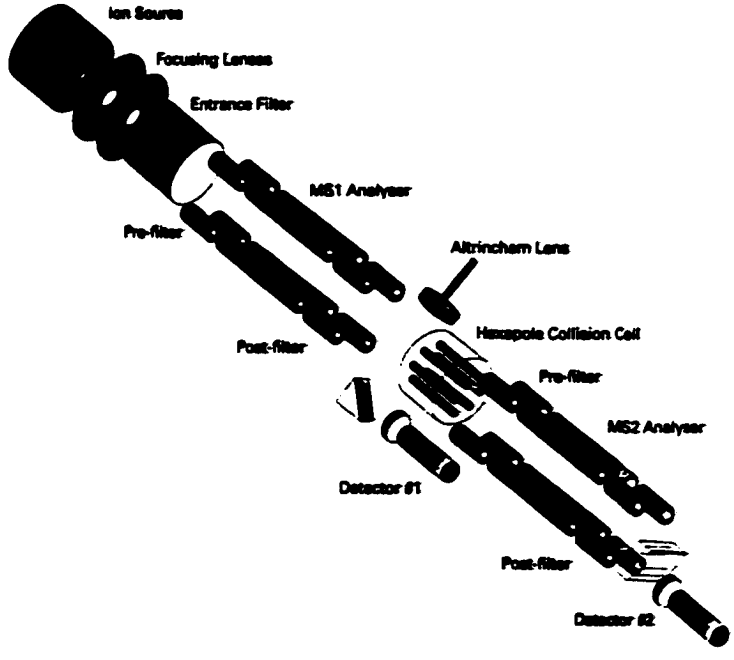

Figure 2.2 VG-Fisons-Micromass Triple Quadrupole design [54]

second quadrupole is actually a hexapole and forms a collision cell where ions are made to fragment further through ion-molecule reactions with a collision gas, usually argon. It operates as an ion guide in rf mode only. Scanning mass spectrometry can be performed in either or in both MS1 and MS2 [54].

2.1.1.2 Ion Sources

2.1.1.2.1 *Electron Ionisation*

Although not the oldest form of ionisation in mass spectrometry, electron ionisation (also called electron impact) is the classical means of generating ions in a mass spectrometer. When used in sector instruments, it offers the benefits of high mass resolution, well-characterised fragmentation pathways, and large spectral libraries for compound identification. In this method, a filament is electrically heated until electron ejection occurs. These electrons are guided into an ion chamber and accelerated to an anode on the opposite side of the chamber, at an energy of 70 electron volts (eV) under normal conditions. A stream of gaseous sample molecules is introduced into the chamber which may collide with these high energy electrons. These collisions may result in the ionisation of the molecule and the deposition of the excess kinetic energy of the electrons as internal energy of the ionic species. Depending on the amount of energy transferred and the lability of bonds in the molecule, this may induce fragmentation, yielding a series of characteristic ions for a given compound class (e.g. alcohols frequently show a loss of 18 mass units due to dehydration). The ions formed, whether molecular ions or fragment ions, will be pushed out of the source by small voltages on the repeller plates and are accelerated into a mass analysing device. Ionisation efficiency is quite low and unreacted species are removed by continuous pumping.

Electron ionisation spectra of unsubstituted PACs are usually simple with abundant molecular ions and little fragmentation, making it impossible to distinguish isomers. The spectral simplicity is related to the ability of the aromatic ring system to distribute any charges and extra stabilisation energy. In general, the molecular ion is the most abundant peak, the loss of 2 hydrogens to give $[M-2]^{+\cdot}$ is the second most abundant and doubly charged ions are of medium intensity. These latter peaks' abundance will increase with the number of aromatic rings available to disperse the charge.

For alkylated PACs, the highly energetic beam of electrons tends to break off some or even all alkyl substituents, making it difficult to distinguish amongst non-isobaric alkyl derivatives and the parent compound unless the energy of the ionising electrons is reduced in such a way that fragmentation is reduced. Small alkylated PAC spectra are dominated by the molecular ion and fused ring tropylium ions, but the differences amongst isomers are too small to allow positional assignment. With larger alkyl substituents, similar behaviour is observed as the instrumental response is insensitive to the site or nature of the alkyl substitution and only the number of unsaturated carbons can be determined.

Examination of non-alkylated PACs indicates predominance of a molecular ion and a characteristic loss. Hydroxy PACs lose COH; aldehyde substituted PACs lose hydrogen, and carbon monoxide; carboxylic functionalities lose hydroxy and carboxy groups; amides lose NH_2 and halogenated PACs lose HX. Heteroatomic and heterocyclic analogues will give spectra equivalent to the parent hydrocarbons while thiophenic sulfur generates strong $[M-1]^+$ ions. With electron ionisation, the exact mass of an ion can be determined but this does not assist in isomass-isomer discrimination.

Gas chromatography/mass spectrometry (GC/MS) employs electron ionisation for sample ionisation. This is the most widely used method for PAC analysis in environmental samples [4, 53, 54].

2.1.1.2.2 *Chemical Ionisation (CI)*

Positive Ion CI:

Overloading of an EI source has long been known to be associated with an increase in the $[M+H]^+$ ion due to bimolecular collisions in the ion source leading to proton transfer. Munson in 1967 was the first to envisage these reactions as acid/base gas phase reactions that could be harnessed for selective ionisation of analytes. To accomplish this, a reagent gas is introduced at a pressure of ~1 Torr, thus at a much higher pressure than the sample. Using electron ionisation, this sample gas will be ionised, generating reagent ions that will ionise the sample. The sensitivity of the CI-MS system is fundamentally determined by the equilibrium between ion formation and ion loss by ion-electron, ion-ion, and ion-molecule reactions, collisions with source walls and detachment of electrons from negative ions [55].

Typical CI reagents in order of decreasing acidity are shown in Table 2.1. All of these reagent ions, despite their high acidity provide much softer ionisation, more molecular weight information and less fragmentation than EI. However, they are associated with high backgrounds, distinct fragmentation patterns (different from EI), and no spectral library searching capability. CI sources require more maintenance due to the need for frequent source cleaning [4, 49, 52].

Table 2.1. Typical CI Reagent Gases [49]

Reagent Gas	Reagent ion	Proton Affinity (kJ/mol)	Ionisation Ability
Hydrogen	H_3^+	421.3	All Organics
Nitrogen/Hydrogen	N_2H^+	491.2	All Organics
Carbon dioxide/Hydrogen	CO_2H^+	538.1	All Organics
Methane	CH_5^+, $C_2H_5^+$	546.0, 684.1	All Organics
Water	$(H_2O)_NH^+$	723.8	All Organics
Propane	$C_3H_7^+$	773.6	Selective
Isobutane	$C_4H_9^+$	823.8	Selective
Ammonia	$(NH_3)H^+$	857.7	Selective

Among these species, methane is the most widely used and best characterised reagent gas. Inelastic collisions of energetic electrons with methane will result in the production of positive ions (H^+, $H_2^{+\bullet}$, $C^{+\bullet}$, CH^+, $CH_2^{+\bullet}$, CH_3^+, $CH_4^{+\bullet}$), neutral particles ($H^\bullet$, H_2, C, $CH^\bullet$, $:CH_2$, $CH_3^\bullet$) and negative particles (H^-, $C^{-\bullet}$, CH^-, $CH_2^{-\bullet}$, CH_3^-). These species may undergo ion-molecule reactions, leading to secondary and tertiary ions though only the reactions with rates of about 10^{-9} mol/s will be observed. These reactions will yield $CH_4^{+\bullet}$, $H^\bullet$, CH_3^+, H_2, CH_5^+, $C_2H_2^{+\bullet}$, $C_2H_3^+$, $C_2H_4^{+\bullet}$, $C_2H_5^+$, $CH_3^\bullet$, $C_3H_4^{+\bullet}$, $C_3H_5^+$, $C_3H_7^+$, $O_2^{-\bullet}$, CH_4, H_3O^+, C_2H_4, HCO^+, HCO_2^+, and CO_2. CH_5^+ and $C_2H_5^+$ are the principal reagent ions involved in proton transfer to the sample molecules to yield protonated molecules and can be useful for distinguishing isomers [56].

Some reagents have been specifically investigated for reaction with particular compound classes. Dimethyl ether forms fragment ion-molecule adducts with substituted aromatics, amino alcohols, lactams, lactones, polyethylene glycols, benzodiazepines,

azepines, trichothecenes, certain alkaloids, nucleoside antibiotics and PACs which can be used for substrate characterisation and isomer discrimination [57]. Acetone chemical ionisation was observed to result in acetylated products of benzonitrile, phenol, anisole and aniline [58] and was used to distinguish alkenes from cycloalkanes, the former forming $[m+43]^+$ species with acetone [59]. Acetonitrile was successfully applied to the analysis of long chain hydrocarbons which formed $[M + CH_2CN^+]$ species [60]. Tetramethylsilane chemical ionisation resulted in the gas phase trimethylsilyation of monosubstituted aromatics, yielding both molecular ion and $[M+ (CH_3)_3Si]^+$ adduct ions, the molecular ion being particularly abundant in compounds with electron-donating groups [61]. Mixtures of predominantly methane and tetramethylsilane, with a smaller amount of a Lewis base (B) such as water, acetone or dimethyl ether will form $(CH_3)_3Si\text{-}B^+$ as the principal chemical ionisation reagent ion. If the sample has a higher affinity for the reagent ion than the Lewis base, the adduct and sample will react by a displacement mechanism, to regenerate the base and form the trimethylsilyl adduct of the sample [62]. Methyl iodide [63] reacted with ketones and alcohols to yield molecular ions, protonated molecules and methylated sample molecules. In addition, alcohols formed $[M - OH + CH_3I]^+$ and $[M - H_2O + I]^+$ ions. Nitrous oxide was used for the determination of sites of unsaturation in deep sea shark glycerol ether lipids through the production of characteristic R_1CO^+ and/or R_2CO^+ [64] and was effective as a means of characterising the alkanes, alkenes and arenes of automotive exhausts [65].

As described above, CI generally results in the formation of protonated molecules. However, a fair amount of molecular ion is also formed and Hazell et al. in 1988 [66] studied the origin of this ion. This ion could result from dissociation of the $[M+H]^+$ ion, charge

exchange ionisation of the sample or residual electron ionisation. The first is a violation of the even-electron rule. This rule does not hold in very high-energy environments but the average CI source is not such an environment. Charge exchange with accompanying dissociation of CH_5^+ is also energetically unfavourable, indicating residual electron ionisation as the principal route to molecular ion formation, confirmed by the methyl radical loss from the molecular ion which is typical of EI conditions.

Charge Exchange CI:

In this case, a non-acidic reagent gas, such as argon, is used. The argon is pumped into the source and is then ionised and reacts with a molecule, M, by the following reactions:

$$Ar + e^- \rightarrow Ar^{+\bullet} + 2e^-$$

$$Ar^{+\bullet} + M \rightarrow M^{+\bullet} + Ar$$

This type of ionisation yields EI-like spectra though this is a softer ionisation technique so less fragmentation is observed. However, it is less sensitive than EI [49].

Metastable Ion Bombardment CI:

This technique involves the formation of energetic atoms although metastable excited state helium atoms are preferred. These metastable ions are used to bombard sample molecules, resulting in the formation of a radical cation of the sample, the release of an electron and the regeneration of ground state helium. This technique exhibits a low background, a relatively high sensitivity and the softness of the ionisation technique is controllable by careful selection of the bombarding metastable, the ionisation technique getting softer as one descends the noble gas row of the periodic table [49].

Negative Ion CI (NICI):

The most common mechanism is by electron capture which yields $M^{-\bullet}$ which typically loses $H^{\bullet}$ to form $[M-H]^-$ as the most intense peak. A compound's reactivity is determined by its electron affinity which is related to the energy of the lowest unoccupied molecular orbital (LUMO). For PACs, if the electron affinity is greater than 0.5 eV, $[M-H]^-$ is formed with little molecular ion while if less than 0.5 eV, the opposite is true. This method is particularly useful for PACs substituted with electronegative substituents [4, 52].

Another mechanism in negative ion mode is to react the PACs with oxygen to yield $[M+15]^-$ which corresponds to $[M+O_2-OH]^-$. The actual reaction between PACs and $O_2^{-\bullet}$ is by charge transfer. With hydroxyl ions, they can undergo charge transfer to yield a molecular anion, abstract a proton to yield $[M-H]^-$ ions or add an analyte to yield $[M+OH]^-$ ions [3, 49].

A third mechanism involves the use of CO_2 plasma to react with PACs to generate M+n[O]-m[H] where the number of oxygen atoms added and the relative intensities of the fragment ions are compound-specific enough for characterisation. For example, pyrene and fluoranthene have very different behaviours. Fluoranthene yields only an intense molecular anion cluster around *m/z* 202, regardless of the source temperature or reagent gas pressure while pyrene exhibits rich ion chemistry with formation of anion clusters around *m/z* 200, 218 and 234. *M/z* 200 and 234 clusters are more intense than the molecular anion and the intensity ratios of *m/z* 217/218 and of *m/z* 234/232 will increase with increasing reagent pressure [67, 68].

A fourth mechanism in NICI is proton extraction. This requires a strong base, such as NH_2^-, that is capable of extracting a proton from a sample molecule [49]. This mechanism is typically one thousand times less efficient than electron capture [55].

NICI mass spectra tend to be significantly richer and distinct from positive ion spectra but there is much instrument-to-instrument variation which among other factors is related to the cleanliness of the source. The method is a sensitive, selective, quantitative and qualitative technique for the detection of PAHs and their alkylated analogues [69, 70]. Methylbenzo[e]pyrenes and/or methylperylenes could be identified only with the selectivity of NICI. It was also possible to distinguish benzo[*a*]pyrene and benzo[*e*]pyrene as the former was extremely sensitive to NICI while the latter was completely insensitive [69].

Comparison Amongst CI Techniques and Between EI and CI Techniques:

A comparison of positive and negative ion chemical ionisation was performed for hydrofluorocarbons (HFCs), hydrofluorocarbon ethers (HFEs) and perfluororalkenes (PFCs) with methane, isobutane, ammonia, nitric oxide, and chloroform CI and EI. CI was observed to be far more useful for GC/MS characterisation of these compounds than EI. In positive ion mode, CI reagent gases, such as methane, isobutane and ammonia, engage in acid/base reactions with the compounds of interest, resulting in the formation of protonated molecules, though $[M\text{-}F]^+$ is predominant with methane and PFCs/HFCs. Nitrous oxide, tetrafluoromethane, 1,1,1,2-tetrafluoroethane and hexafluorosulfide are non acid/base reagent gases used for positive ion CI. Tetrafluoromethane, 1,1,1,2-tetrafluoroethane and hexafluorosulfide give methane CI-like spectra with a little more fragmentation in the case of the first two and extensive fragmentation for the third. NO yields an EI-like spectra with

a strong $[M+NO]^-$ peak with several HFCs and HFEs . In negative ion mode, HFEs exhibit an ether bond cleavage to form $[M-O]^-$ with methane and isobutane while chloroform results in the formation of strong $[M+Cl]^-$ ions with HFCs and HFEs having a -CHF- linkage [71]. A comparison of plasma desorption (PD), electron ionisation, and methane and ammonia positive chemical ionisation of aromatic pesticides demonstrated that plasma desorption spectra gave more information than EI or methane CI with PD yielding a more abundant molecular ion than EI and the same relative abundance of fragment ions. Although the level of molecular ion is higher in the methane CI spectra, the greater fragmentation in the PD spectra allows better structural determination. The ammonia spectra were of little analytical value [72].

2.1.1.2.3 *Half-Mass Detection*

With both positive ion CI and EI, selective detection of PAHs using half-masses has been attempted. The specificity of detection increases with the abundance of M^{+2} formed by electron ionisation, which in turn is related to the molecular structure. The more rings available, the more likely it is to form. Once formed, doubly charged ions can be reacted with a variety of collision gases thus forming a series of doubly charged ions by successive losses of acetylene for confirmatory purposes in conjunction with the first ^{13}C isotope peaks of M^{+2}. These ions have half-integral values of *m/z* and are readily distinguished from singly charged interferences [73, 74]. Biphenyl, diphenylacetylene and phenanthrene under energetic EI conditions will form doubly and several triply charged ions as well as ions from the loss of H, H_2, C_2H_2, C_3H_3, and $2C_2H_2$. The results indicate that all fragmentation reactions with an energy above the ionisation energy of the compound will occur by ring opening [75].

2.1.1.2.4 Atmospheric Pressure Chemical Ionisation (APCI)

Atmospheric pressure chemical ionisation is a soft ionization technique ideal for LC and CE interfacing because it can tolerate flow rates up to 2 mL/min, can tolerate any aqueous or organic mobile phases, can ionise a broad range of compounds and can be directly coupled to LC without a split. APCI gives less structural information than CI but is recommended for studies of ionisation reaction sequences under equilibrium control and for quantitative and qualitative analyses.

This technique involves the introduction of sample chromatographically, by flow injection, by direct injection of a sample in solution or by direct sample insertion into an ion source held at atmospheric pressure. The samples and solvents introduced must be vapourised by heating as all reactions observed in an APCI source are gas phase reactions. A ^{63}Ni foil or a corona discharge needle held at high voltage (the corona discharge needle is more efficient and reproducible) supply an electron flow that ionises the carrier gas molecules, initiating a series of reactions, culminating in the ionisation of the sample. The vacuum system and the ion lenses are critical in maintaining ion transmission from the source to the analyser region. The distance between the corona discharge needle and the skimmer cone is an important variable in the ion residence time and hence, the nature of the ions observed. At a distance of 0.5 mm, ion residence time is very small and the spectra are dominated by carrier gas ions formed by relatively high energy processes with high internal energy under nonequilibrium conditions. At a distance of 4 mm, only long-lived ions at thermal and chemical equilibrium are observed [76-79].

APCI⁻:

The carrier gas being the predominant species in the ion source, even with HPLC introduction of solvent and sample, is the first to be ionised. Nitrogen is the most common carrier gas used and is ionised by the following series of reactions:

$$N_2 + e^- \rightarrow N_2^{-\bullet} + 2e^-$$

$$N_2^{-\bullet} + 2N_2 \rightarrow N_4^{-\bullet} + N_2$$

$$N_4^{-\bullet} + H_2O \rightarrow H_2O^{-\bullet} + 2N_2$$

$$H_2O^{-\bullet} + H_2O \rightarrow H_3O^- + HO^\bullet$$

$$H_3O^- + H_2O + N_2 \rightarrow H^-(H_2O)_2 + N_2$$

$$H^-(H_2O)_{n-1} + H_2O + N_2 \rightarrow H^-(H_2O)_n + N_2$$

with the formation of N^-, N_3^-, $O_2^{-\bullet}$, NO^-, $NO^-(H_2O)_n$ and NO_2^- [76-79].

These primary reagent ions will act to ionise other species introduced into the source. Hence, charge exchange will occur to species with an ionisation potential lower than that of the carrier gas or its impurities and proton transfer will occur to compounds with a higher proton affinity (or gas phase basicity) than the protonated water clusters, thus generating solvent-derived reagent ions. Benzene will be ionised to its molecular ion and engage in charge exchange with sample molecules. Chloroform with its high ionisation energy forms ions that rapidly react with solvent impurities so only impurity-derived ions appear [80, 81].

There are a number of mechanisms by which species are ionised in APCI. These include proton transfer, charge exchange, hydride abstraction, addition , cluster formation and ipso-substitution..

Proton transfer can be depicted as:

$$A + BH^+ \rightarrow AH^+ + B$$

and will occur if A is a better gas phase base than B. The ease of this reaction can be predicted by molecular orbital calculations of gas phase basicities or based on compilations of experimentally determined values. These tables predict that both methane and isobutane are fairly weak gas phase bases and will transfer a proton to other species. Ammonia, water and alcohols are weak gas phase bases capable of proton transfer to other species but are not recommended as they result in a high degree of clustering and thus, potential interferences. Chloroform with its ethanol additive provides both a reagent ion for proton transfer (derived from the ethanol), a low background and unreactivity to other species.

Charge exchange can be depicted as:

$$A + B^{+\bullet} \rightarrow A^{+\bullet} + B$$

and will occur if the ionisation energy of A is below that of B, making it energetically favourable. Benzene and NO^+ with their higher ionisation energies readily ionise PACs by charge exchange.

Hydride abstraction is less readily observed. NO^+ will abstract a tertiary hydrogen from a hydrocarbon or a secondary hydrogen from a secondary alcohol to form the deprotonated molecule [76].

Covalently bound adducts of ammonium, pyridinium and nitrous oxide ions with various types of compounds have been observed. This is the ionisation by addition mechanism [82, 83].

Cluster formation by hydrogen bonding and sharing of protons occurs readily in an APCI source, with the extent of cluster formation being dependent on source temperature, gas flow rates, cone voltage and reagent concentration. In general, cluster formation is not desirable as it spreads out a sample over a number of different ions, increases background and is a potential source of mass interference [84].

Ipso-substitution occurs as an intermediate step in the radical-mediated aromatic substitutions. This intermediate may dissociate either by rearrangement to an ortho or para intermediate or without rearrangement. the final step in the reaction results in a charged species and a radical. For example, chlorobenzene in reaction with ammonia will generate protonated aniline and the chlorine radical [85].

APCI⁻:

In APCI⁻ mode, ions are generated by ion/molecule reactions or by thermalised electron/molecule reactions which yield even-electron negative ions, neutral radicals and negative radical ions. A number of mechanisms exist for generating negative ions.

The first mechanism is electron attachment to form molecular radical anions. Quinones and α-ketones have relatively high electron affinities, producing radical anions of high stability. In this reaction, the attachment of a thermal electron is exothermic. For PACs with their lower electron affinities, the reaction is not as energetically favourable, thus requiring electrons to have an initial energy greater than thermal energy and yielding more unstable radical anions. These thermalised electrons can be generated with the usual carrier gases, a low concentration of methane in argon or 0.1% isobutane in nitrogen [86].

Electron attachment may also proceed by dissociative means. In this case, the radical anion is formed as an intermediate, quickly followed by the elimination of a stable negative ion. This is particularly common for halogenated compounds, though the energetics of the reaction depend on the strength of the carbon-halogen bond [87-88].

Proton transfer is another mechanism which can be operative. The chloride ion in the presence of a stronger acid will form hydrogen chloride and yield the molecular anion of the sample, with the solvent serving as the chlorine source. Alternatives to the chloride ion include the superoxide, hydroxide and fluoride ions [89-90].

Comparing APCI with EI and CI shows that there is a fundamental difference in product distribution with EI and CI reflecting relative rates of reactions whereas APCI product ion distribution reflects chemical and thermal equilibrium. However, CI and APCI are similar in their design requirements, reagents and ionisation processes. With CI, the reagent gas is present in large excess relative to the sample, making it difficult to exhaust the supply of reagent ions. In APCI, the level and type of reagent ions available is highly dependent on the sample introduction method and competition may occur between several reagent ions. For example, proton attachment from protonated water clusters will compete with ammonium ion attachment where both are present [91]. With chromatographic sample introduction, reagent ions are present at all times, continually ionising sample molecules which will produce mass chromatograms reflective of the chromatographic separation in a manner similar to UV, refractive index or fluorescence detection. Comparing APCI and CI spectra in positive and negative ion mode for single compounds and a single reagent gas, are quite similar and the differences are explicable based on physical properties of the analytes

and different ion residence times. However, when mixtures are analysed , the spectra can be quite distinct. Ionisation of the carrier gas and the generation of reagent gas species are believed to be quite similar for APCI and CI but the final product distribution can be quite different [76].

Later work indicated that the APCI product distribution was not completely thermodynamically controlled. In fact, whether the reactions in an APCI plasma consisting only of carrier gas and analyte were kinetically controlled or thermodynamically controlled was dependent on the analyte's gas phase basicity. If this basicity was greater than 200 kcal/mol (836.8 kJ/mol), the reaction was kinetically controlled whereas if less than 200 kcal/mol (836.8 kJ/mol), the reaction was thermodynamically controlled. A larger gas phase basicity difference is necessary to compensate for the energetically unfavourable dissociation of the stable water clusters to form analyte clusters or protonated molecule. Sensitivity tended to increase with the degree of kinetic control of the reaction until the supply of reagent ions was exhausted which could be as little as 0.1 ppm for highly reactive pyridine. PACs were particularly unreactive and were less sensitive than what would be predicted based on their gas phase basicity [92]. This lower sensitivity can be partially overcome by increasing the temperature of the source with the optimum temperature being determined by the analyte(s) involved [93].

Optimising source temperature or any other variable can be difficult when analysing a mixture of components with their own optima. Kektar mathematically demonstrated that the API response of a two-component mixture is dependent on their relative concentrations and their proton affinities, and can be predicted from their relative rates of ionisation [94].

If reagent gases are mixed, protons are transferred such that the weakest possible reagent ion is formed, causing the plasma chemistry and the corresponding product ion spectra to change dramatically [95].

APCI-MS has found wide application. It has been used extensively for the monitoring of microimpurites in air [96-98], for studying negative ions [99], for detecting nicotine [100], for analysing alkanes, alkenes and cycloalkanes [101] and for analysing dimethylenedihydrothiophene in methylene chloride [102] to name a few applications. In all cases, charge transfer reactions tend to predominate when the water concentration in the solvent is reduced and when energetics are not favourable to proton transfer. However, reducing the water content reduces the degree of solvation, making for more exposed protons and better proton transfer.

2.1.1.2.5 *Electrospray Ionisation (ESI)*

The electrospray interface is presented in Figure 2.3A. It is similar to the APCI interface (Figure 2.3B) except that the corona discharge needle is exchanged for a high voltage on the capillary through which the liquid flow exits into the source. Compared to APCI, it works best with much lower flow rates (1-40 μL/min), is much more rigorous with solvent demands (solvents must be filtered and degassed and 50:50 (v/v) acetonitrile (MeCN) or methanol (MeOH)/H_2O with 1% acetic or formic acid are preferred), works well for previously ionized samples and a split must be used to reduce HPLC flow rates. It does, however, permit the determination of very high mass compounds not amenable to detection by other mass spectrometric techniques by multiple charging.

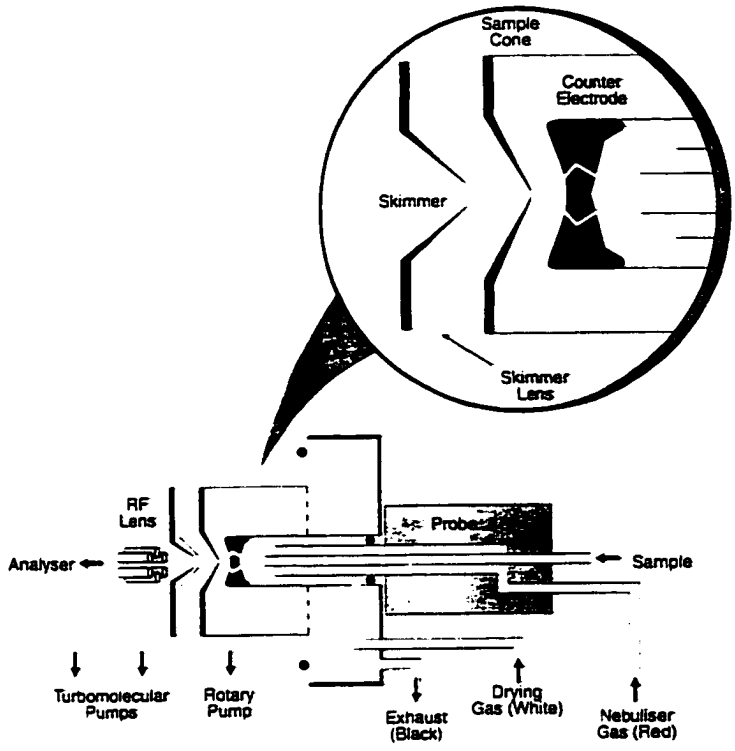

Figure 2.3A. Diagram of the ESI Interface [35]

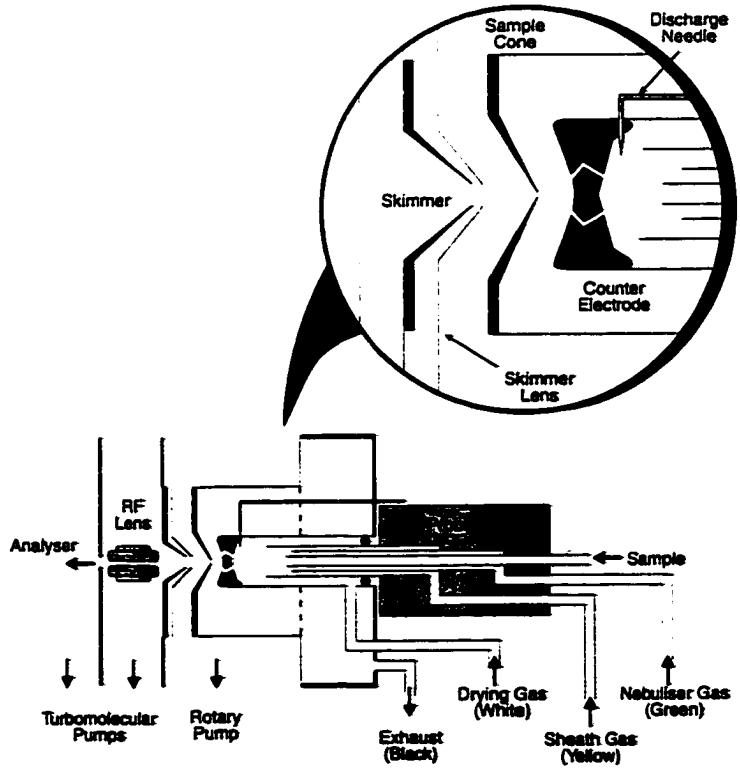

Figure 2.3B Diagram of the APCI Interface [35]

As mentioned, electrospray is most efficient if a compound will ionize by acid/base chemistry or if non-ionic compounds can associate with small ions. The sample will enter he heated probe in a mobile phase, and then encounter the high voltage capillary which aids in expelling the ions from the solvent, and these ions are passed through lenses into the mass spectrometer and detected [54]. A refinement is to add a nebulising gas which will produce a fine mist of electrically charged droplets. The solvent will first evaporate, causing the droplet size to decrease and the charge density on the droplet to increase.

Low molecular weight compounds tend to form protonated species in positive ion mode electrospray (ESI^+) and deprotonated species in negative ion mode (ESI^-). This proton abstraction/proton loss behaviour is probably due to a similar acid/base mechanism as was described for APCI [103]. The type of ion observed can be tailored by use of the appropriate solvent and reagents.

2.1.1.3 Ion Detectors

Having generated the ions and separated them by mass, detection of the ions is required. A number of detectors are available including single and multiple Faraday collectors, ion sensitive emulsions, electron multipliers, and scintillation/photomultiplier detectors. Only the scintillation/photomultiplier detector, the detector used in the experiments described in this thesis, will be described.

In this detector (see Figure 2.4.), the ions are accelerated towards a negatively charged electrode to generate secondary electrons. These secondary electrons are accelerated by the same electrostatic field, and impinge on a phosphor which is coupled to a photomultiplier. The sensitive dynodes of the photomultiplier are sealed from the vacuum

system. The advantages include prolonged phosphor lifetime because these secondary electrons are much less damaging than a beam of primary ions, better sensitivity because light generated by electron impact is much stronger than by ion impact, and many more electrons are generated by impact of accelerated ions. The activated surfaces of the photomultiplier are never exposed to the environment with the ensuing loss of gain [47].

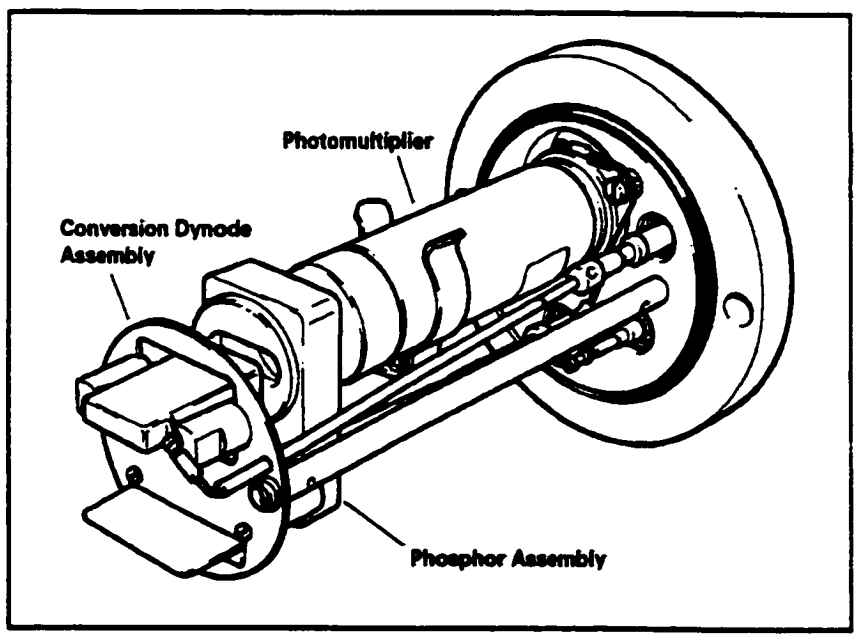

Figure 2.4 The phosphor detection system in the Fisons Triple Quadrupole instrument [54]

2.1.1.4. Vacuum System

The vacuum system is critical in pumping out the source region, thus preventing memory effects and assisting in the transmission of ions into the mass spectrometer. The pressure in the source will also determine the number of ion/molecule reactions occurring, the ion residence time and the final distribution of ion products. The vacuum system consists of a number of vacuum pumps and gauges for measuring the vacuum. In order to get a high

vacuum, at least two pumps - a fore pump and a high vacuum pump - are required. The standard fore pump is a rotary vane pump, usually consisting of two stages and containing an inert, low vapour pressure oil. This pump is capable of maintaining a vacuum of 10^{-2} to 10^{-3} Torr. The turbomolecular pump functions like a prop jet engine in reverse, requires no oil so there is no oil background in the spectra, is not damaged if vented, requires yearly lubrication of its high-speed bearings, pumps down rapidly and provides a better vacuum than the normal diffusion pump. It can provide vacua in the range of 10^{-9} to 10^{-10} Torr.

The pressure is measured by a system of gauges. In this instrument, both low and high vacuum gauges are found, the former indicating whether the roughing pumps are functioning and the high vacuum gauges indicating the goodness of the high vacuum. A Pirani gauge is a thermal conductivity-based low vacuum gauge which consists of two filaments joined in a bridge circuit. It provides a non-linear response, can read pressures from 10 to 10^{-4} Torr, is reasonably rugged but can get contaminated with species from roughing pumps. The high vacuum gauge used is the Penning gauge which is a cold cathode gauge that uses a very high voltage to create high energy electrons, using a magnetic field to constrain their movement , collides them with gas molecules, generating gas ions which are collected by the central electrode. It must be periodically cleaned [49].

2.1.2 Tandem Mass Spectrometry (MS/MS)

This is a powerful method for mixture analysis and structural determination. It can be considered to be two separations of ionised sample components. In the first step, ions are formed, usually from mixture components, and separated by mass analysis. Selected ions are then subjected to further fragmentation by collision induced dissociation (CID). In the next

step, ions are again separated by mass analysis to yield a secondary mass spectrum used to identify individual components.

This can be done with coupling of almost any two mass analysers or in single units for trap instruments, but only MS/MS in a triple quadrupole instrument will be described. The first step occurs in the MS1 region (Figure 2.2). Ions are generated in the source and separated by mass analysis in the 1st quadrupole. They are then introduced into the collision cell (quadrupole #2) and subjected to collisional dissociations with a reagent gas. The fragments generated from these ion-molecule reactions will then be separated in MS2 [23]. If two ions are present with different structures, their decomposition patterns will be distinct and will thus permit identification.

The advantages of this arrangement over others include: 1) fast analysis, 2) increased separability, 3) easy interfacing to a computer for instrument control, calibration and data acquisition, 4) compactness, 5) the capability of analysing for specific component in a mixture, 6) virtually simultaneous separations relative to chromatographic methods, 7) excellence as a structural analysis technique and 8) the ability to use a number of scan modes. The scan modes include product ion scans, precursor ion scans and neutral loss scans.

In daughter or product ion scans, MS1 will select an ion or ions of a particular *m/z* or a series of *m/z* will undergo CID in the collision cell. The resulting ions, called daughter or product ions, are analysed by either full scan or single ion monitoring in MS2. These types of scans yield all the product ions generated from a particular precursor, yielding a mass spectrum of the selected ion(s). These scans are used mainly for identifying individual components in mixtures or for studying fragmentation to obtain structural information.

In parent or precursor ion scans, all masses of interest are scanned in MS1 and are passed into the collision cell to undergo ion-molecule reactions. MS2 is operated in single ion monitoring mode so that only the precursor ions which yield product ions of particular *m/z* ratios will be detected. These scans are useful for compound class identification.

The neutral loss scans involve setting both MS1 and MS2 to perform a scanning analysis with a constant mass difference. An ion will only appear in MS2 when it has undergone the proper neutral loss. The mass of the neutral species lost in the collision cell is characteristic of a particular class of compounds or a specific functional group. This allows fast identification of a series of related compounds. For example, chlorinated species are readily identified by the loss of 35 mass units which corresponds to loss of the chlorine.

The main disadvantage of MS/MS is the difficulty in finding ionisation conditions that will permit efficient detection of all mixture components [47, 51, 52].

MS/MS is mostly easily performed in quadrupole or ion trap instruments but it can be performed with magnetic sector instruments. Linked B/E scans can be used for isomeric discrimination of PACs and for examining the fragmentation behaviour of PAH metastable ions [104-105]. The metastable ions of four isomers of $C_{18}H_{12}$ were examined by this method. The results indicated strong $M^{+\bullet}$, $[M\text{-}H]^{+}$ and $[M\text{-}2H]^{+\bullet}$ whose abundance was characteristic of the particular isomer. The use of a collision gas was not observed to result in better structural information or fragmentation. No simple correlation of ionisation energies, average internal energy or appearance energy with the abundance of a given molecular or fragment ion could be made.

2.2 Sample Introduction Techniques

These techniques fall into one of two categories: flow injection and chromatography. The former is used to introduce a fixed quantity of material with one or more components of interest. It is employed to illustrate the sample complexity and to identify the major components of the mixture. It is also well-suited to optimisation studies, calibration and tuning, as the solvent composition is easily changed and manipulation of sample loop size can result in pseudo-infusion conditions of a calibrant or test solution. Chromatography: 1) separates the components of a mixture, thereby reducing the complexity of the mixture, 2) may assist in isomer discrimination, 3) offers the potential for improving sensitivity by monitoring a select mass rather than scanning a broad range, 4) provides retention time data which can assist in component identification and 5) can be sued with complimentary detectors, i.e. fluorescence and diode array UV .

2.2.1 Flow Injection Analysis (FIA)

This sample introduction technique consists of a pump which delivers a continuous stream of mobile phase and reagent solution, an injection device for sample introduction into the mobile phase stream as a plug of material, a reaction coil where the sample is mixed with reagent solution, a length of tubing which connects the reaction coil with the flow cell, a flow cell where the products of the chemical reaction are delivered and a detector whose response is dependent on the nature and amount of the product in the flow cell at any given time. In the case of an API mass spectrometric detector, an HPLC or syringe pump is used for generating the constant stream of solvent, an injection valve is used for sample introduction, analytes are ionised in solution or in the gas phase via mechanisms that are specific to given

mass spectral techniques, and are then detected by ion detectors. Like the conventional FIA output, the mass spectral output is a peak, the height of which is related to the detectability of the analyte [106].

2.2.2 Chromatographic Sample Introduction

Due to the complexity of the matrices in which PACs are found, their trace level concentrations in these matrices, the wide variation in physical properties and states of PACs, and the rapid proliferation of isomers as the carbon number increases, a number of chromatographic methods have been investigated for their efficient separation and characterisation by retention time indices.

Gas chromatography with its extremely efficient separations, the availability of a wide range of detectors and its excellent quantitative and qualitative capabilities makes this a first choice for sample analysis. It was applied to the analysis of volatile PACs via flame ionisation [107-109], flame photometric [110-111], thermionic [110-111], chemiluminescent [112], plasma emission [113-115] and EI [4], CI [4] or tandem mass spectrometric [4] detection for the analysis of PACs whose retention time was dependent on structure, size and shape. Hence, an increase in the number of carbons, a more condensed structure and greater degree of planarity were associated with lower volatility and hence, longer retention times. This technique is unsurpassed for the analysis of the smaller, more volatile PACs that have been identified as carcinogens and for which standards are available, permitting determination by comparison of retention indices. Its principal limitations include the requirement for volatile, thermally stable compounds and the inability to differentiate isomeric PACs either by reference to their physical properties or their fragmentation patterns

[4]. To address these limitations, research is underway into the development of PAH-specific stationary phases [116, 117], more heat-stable GC columns and stationary phases[118, 119] and other methods of chromatographic separation.

Liquid chromatography lacks the requirements for sample volatility and thermal stability required in GC analysis and offers a cornucopia of stationary phases, mobile phase formulations, separation mechanisms, pressures [120], flow rates, and temperatures [121] to customise separations. Optimisation of these separation parameters can be performed manually or via computer software systems [8, 10]. LC chromatography with long chromatographic columns is employed for fractionation of fossil fuels into saturates, aromatics, N and S-containing compounds (acids, bases and neutrals) and polar compounds. These smaller fractions are easier to analyse because the mixtures are less complex, homocyclic and heterocyclic compounds have been separated, separation conditions can be tailor made to each group of compounds and more selective detection schemes can be employed [123]. For example, thiophenic compounds (PASHs) frequently coelute and have similar masses to their PAH analogues whilst having a greater number of possible isomers due to sulfur substitution in non-equivalent positions in the rings. Their efficient characterisation necessitates isolating the sulfur-containing fraction by alumina or silica chromatography, then separating the components by ligand exchange chromatography with palladium chloride-doped silica. The palladium catalyses desulfurisation of the PASH upon complex formation if the sulfur is accessible and Pd-PASH complexes are eluted [124].

Separation according to ring number or compound class is usually performed using normal phase conditions in which underivatised silica separates compounds based on

hydrogen-bonding and acid/base interactions (type I) [4, 125] or based on polarisability and induction effects (type II). The separation is not purely dependent on the number of aromatic rings or of π electrons [126-129] but rather is mediated by molecular shape, planarity and substitution pattern. Planar molecules are better able to penetrate into the stationary phase, have a larger surface area for interaction and are retained longer. With alkyl substitution, the number and position of the substituents, their chain length and whether or not saturated rings are present must be considered [4]. Monoalkylation of a polar compound will most strongly impact on elution if the substituent is in a sterically hindered position relative to the polar substituent, causing strong alkyl-polar interactions, most notably the ortho position in benzene [129]. In general, alkylation decreases retention time due to shielding of the aromatic ring from the stationary phase, whilst saturated rings increase retention time by increasing available surface area [4]. All of these factors were considered when compound class separation of bitumens was tested on three different media (attapulgus clay, silica and alumina). Although the elution order of fractions varied between the media, attapulgite separations were highly irreproducible due to wide structural variations of the clay from lot to lot, alumina was poorly adapted to fractionation of polar compounds and was not rugged enough while chromatographic grade silica offered the most reproducible compound-class fractionation [130].

HPLC offers shorter analysis time, better separation efficiency, better detector response and less solvent consumption than conventional low pressure LC, mainly due to smaller stationary phase particle sizes, small diameter columns and low void volumes [131]. The major effect is related to particle size as the surface area for interaction increases with

decreasing particle size. However, more C_{18} groups can be bonded to the silica surface of high pore diameter species than to smaller ones. Thus, the size of the pores and particles needs to be balanced between good carbon loading and speed of analysis [132].

Reversed phase chromatography can also be used to fractionate compound mixtures but is more commonly used for fractional analysis of compound classes. Early research demonstrated that PACs could be separated on C_{18} columns with water-acetonitrile gradients but there were great differences in separation capabilities of columns. This was traced to the monomeric or polymeric nature of the stationary phase, with polymeric phases being very orderly, structured phases held in a rigid three-dimensional configuration, ideal for the separation of PACs [4, 133, 134].

The mechanism of retention is also different between the two column types. Adsorption usually involves van der Waals forces, ion exchange, electrostatic interactions and hydrogen bonding [136]. With monomeric phases, the analytes are separated by the number of carbon atoms in the molecule while the polymeric phase will separate PACs by their shape, size, planarity, dispersive effects, permeation effects and quadrupolar interactions [137]. The slotted structure of the polymeric C_{18} column allows PACs to stack into the gaps between the hydrocarbon sheet, causing them to interact more strongly with the bonded phase and be more retained. Less planar molecules do not permeate as well and so elute earlier [127]. One way of describing the size and shape of a molecule is to generate two perpendicular axes through the molecule of maximum length, giving the length-to-breadth (L/B) ratio, retention increasing with increasing L/B ratio. Methylation can significantly alter the L/B ratio and if the effect is large enough, can provide a means of isomer

discrimination. In particular, 1-methylbenzo[*a*]phenanthrene eluted anomalously because of its non-planarity due to steric crowding of the methyl group [138]. More recent work has demonstrated that oligomeric, non-endcapped C_{18} columns are the best for separating PACs as they offer better surface coverage and smaller pore sizes [139].

With a given column type, the type of modifier in the mobile phase affects elution order by altering the selectivity and efficiency of the column. Alcohols, other organics or surfactants can be used as modifiers. The addition of alcohols generally improves the separation and reduces analysis time [140]. An alternative is the incorporation of β-cyclodextrin or its derivatives on the stationary or into the mobile phases. β-cyclodextrin-poly(allyl)amine has been successfully used to separate substituted phenols through the formation of inclusion complexes with the interaction proceeding in the order: para> meta > ortho. These complexes are stabilised by increasing the methanol content of the mobile phase, reducing the elution time without changing elution order [141].

The temperature at which a column is run is also important. In general, increasing the temperature will reduce the analysis time at the cost of poorer resolution in reversed phase mode. The effect on elution order will depend on the size and shape of the analytes, with increasing structural compactness being associated with sharper decreases in retention time, causing a reversal in elution order with increasing temperature. The explanation for this phenomenon may reside with the changes in the separabilities with temperature [142, 143].

Synchronous gradients of mobile phase flow rate and column temperature halved the analysis time while preserving the separation efficiency. However, these gradients must be simultaneous to realise these benefits for the separation of PACs [121].

Having separated the compounds by either normal or reversed phase chromatography, the sample composition can then be determined by an appropriate detection method. With HPLC, the most commonly used detection schemes involve ultraviolet/visible spectrophotometry, fluorescence or atmospheric pressure ionisation mass spectrometry.

Supercritical fluid chromatography (SFC) is of interest in filling the gap between GC and LC by maintaining or extending the range of compounds tolerated in HPLC while gaining some of the efficiency of GC [4]. In fact, this technique permits faster, less solvent-consuming separation than HPLC [144]. Supercritical fluids are gases maintained at a temperature just above their critical temperature and compressed to a pressure where "liquid-like" interactions become important. This causes the physical properties to be intermediate between those of a gas and of a liquid. By altering the temperature and the pressure and thus the density, different solvent characteristics are exhibited [145 - 146].

Capillary electrophoresis is a relatively new separation method. In capillary zone electrophoresis, a sample is hydrodynamically or electrokinetically injected into a capillary, a high electrical field is applied and the compounds elute according to mass and charge. Neutral molecules, like PACs, usually elute quite slowly. However, when incorporated into inclusion complexes, their mobility can be quite good. Differing sizes and shapes of the PACs will influence their ability to form a good inclusion complex, thus determining their elution profile. A mixture of negatively charged sulfoether-β-cyclodextrin and neutral methyl-β-cyclodextrin was used to separate PAH components based on their relative abilities to form inclusion complexes. All 16 priority PAHs isolated from contaminated soils could be determined in under 20 minutes with efficiencies up to 100 000 theoretical plates [151].

A similar separation with prior solid phase microextraction was instituted for PAC analysis. Using a mixture of sulfobutyloxy-β-cyclodextrin, methyl-β-cyclodextrin and α-cyclodextrin, 16 PAHS were separated and detected by absorbance measurements at 254 nm with limits of detection ranging from 8 to 75 ppb [152].

2.3 Chromatography with Mass Spectrometric Detection

The popularity of chromatography with mass spectrometric detection is rooted in the ability of a chromatographic procedure to separate out the components of a complex mixture and assist in isomer discrimination and the flexibility, high sensitivity and selectivity and high amount of information (mass, structural) provided by the mass spectrometer [153]. This section will illustrate how mass spectral techniques have been coupled to GC, LC and SFC for the analysis of PACs.

2.3.1. Gas Chromatography/Mass Spectrometry (GC/MS)

This technique has been applied to the analysis of nitrogen-containing PACs (PNAHs), sulfur-containing PACs (PSAHs), PAHs, a variety of PACs and polyaromatic ketones. The following table provides a summary of the literature applications of GC/MS to the characterisation of PACs in petroleum samples. Dzidic *et al.* [155] used a 30 m DB-5 fused-silica column to separate PNAHs and PSAHs. Low *et al.* [156] used a BP-1 vitreous silica column, Bayona *et al.* [157] used a methylpolysiloxane-coated silica column and Canton *et al.* [158] used a SPB-5-coated silica column to separate PAHs. Brotherton *et al.* [159] used a 25 m SE-54-coated silica column to separate isomeric PAHs. Pyle *et al.* [160] used a 30-m , 5% phenyl-95% dimethyl polysiloxane was used for PAC separation. Mosi *et al.* [161] 30 m db5 capillary column to separate polyaromatic ketones.

Table 2.2. GC/MS Analyses of PACs

Mode	Compounds	Conclusions	Ref.
EI	PNAHs	- separation by ring number only - excellent reproducibility, sensitivity, resolution - unable to identify isomers	155
CI	PNAHs PSAHs	- with ammonia, unable to protonate S compounds - with isobutane, able to determine parent ion of all N, S and hydrocarbon-containing PACs	155
NICI	PAHs	- selectivity and sensitivity were ion source pressure- and temperature-dependent - larger PACs form $[M+H]^-$ - $[M-H]^-$ formed by nucleophilic deprotonation	156 - 158
CI	isomeric PAHs	- H_2 gave best isomer discrimination, highest reproducibility, highest sensitivity - ion form of PAH was reagent gas-dependent	159
MS/MS	PACs	- differentiation of m/z 252 isomers - fragmentation dependent on number of ortho proton interactions	160
MS/MS	polyaromatic quinones	- $[M-CO]^+$ for unsubstituted compounds - $[M-CO-CH_3]^+$ for substituted compounds	161

2.3.2 Liquid Chromatography/Mass Spectrometry (LC/MS)

The principal justification for liquid chromatography/mass spectrometry (LC/MS) techniques is that as the PACs get larger, it becomes more and more difficult to elute them with GC methods [4], and the number of possible isomers increases as the mass of the PAC increases. With the number of alkyl-substituted PACs in petroleum-based samples, the use of multidimensional LC techniques for sample separation and fractionation is necessary.

However, LC on its own yields little information about the chemical identity of the separated substances but when combined with mass spectrometry, information about MW, structure and elution order can be gained [162]. For example, high performance liquid chromatography/mass spectrometry (HPLC/MS) can be used to completely characterise a fully hydrogenated coal liquefaction sample. The saturated hydrocarbons elute first, the aromatics will be separated by the number of aromatic rings and then back flush techniques will yield the polar compounds [163].

The main difficulty encountered in coupling LC with MS detection is to design the interface to remove much of the solvent without the loss of trace analytes. The ideal LC/MS interface does not restrict LC or MS operating conditions, does not degrade LC resolution, has a detection limit below one nanogram and a dynamic range of at least four orders of magnitude, must not chemically modify the sample and permits at least 30% passage of sample and solvent [164]. These characteristics and the high flow rates typically used in HPLC make the method most amenable to APCI-MS analysis which can tolerate flow rates of up to 2 mL/min. However, HPLC column effluents have been analysed by EI, CI, ESI and MS/MS. HPLC was also interfaced to a tandem mass spectrometer. However, the best choice of LC/MS system will depend on the samples to be analysed, the mass spectrometer available, the types of chromatographic equipment necessary, the available infrastructure, cost considerations, maintenance issues and the experience of the operators [165]. To counter some of the problems encountered in these detectors, micro column (capillary column) technology has also been employed.

When capillary-column HPLC was interfaced to a mass-flow selective detector, the low flow rate meant that all of the HPLC effluent could be introduced directly into the mass spectrometer, rather than having to vent a large portion of the solvent and thus causing some sample loss. This improved the sensitivity relative to conventional LC/MS and provided a better detection limit. The column effluent was subjected to CI analysis after desolvation of the micro droplets through a combination of a heated ion source and a high vacuum. The major drawback was that in gradient modes, the need for very low flow rates makes it difficult to get stable flows, though work in this area is continuing. In fact when micro column HPLC was applied to the analysis of 5-to-9 ring parent and alkylated PACs, the resolution of components was dramatically improved on these extremely efficient columns but isomers could not be distinguished using either the columns or the mass spectrometer [166]. This inability to chromatographically resolve isomers is not limited to micro column technology. Conventional columns also have difficulty in separating isomers although they are more successful with cata-condensed (linearly fused benzene rings, such as in anthracene) than peri-condensed (nonlinearly fused systems such as in perylene), which is likely due to a molecular shape effect. Microcolumn LC was also successfully coupled to a particle beam mass spectrometer for the analyis of PAC metabolites in water, resulting in the identification of six main metabolites [167].

LC/CI-MS also was applied to the analysis of mono- and diaromatic fractions. These fractions were originally isolated by normal-phase chromatography with hexane as the mobile phase, then separated and detected by a direct interface of the reversed phase high-performance liquid chromatography (RP-HPLC) μBondapak C18 column with the mass

spectrometer. The mass number, retention time and simultaneous UV detection at 254 and 313 nm allowed benzenes, alkylbenzenes, para bonded benzene compounds and compounds with a naphthalene-like structure to be identified and quantified [168].

An EI-like mechanism was applied to the analysis of high-mass PAHs. As the ability to form doubly charged molecular ions increases with molecular weight due to a decrease in the second ionisation potential, when these high-mass PAHs were subjected to 70 eV electrons they readily formed M^{+2} ions. As mentioned earlier, these half-masses are much more unique and provide a more selective means of quantification [169].

ESI is a wonderful method for the analysis of proteins, peptides and oligonucleotides as it can generate many charges, thereby reducing the *m/z* ratio to a level where most instruments can reliably detect the species. It has been applied to the analysis of hydroxylated PACs and compared to APCI detection of these compounds. A detection limit of 1.5 to 35 µg/mL for ESI and 0.3-50 µg/mL for APCI was observed. These are quite similar despite the fact that the flow rate tolerances and ionisation methods are very different. Because of the low flow rates required in ESI, a split is necessary to reduce the total amount of material reaching the source [51, 54]. In another application, a simple packed capillary column capable of gradient separations was combined with electrospray mass spectrometry for trace analysis of urinary metabolites, protein mapping and pharmaceutical impurity analysis in the pg range [170].

LC/APCI-MS has been widely used for basic and applied research, method development and routine analysis. Operating in simple scanning mode, it can be used for sample identification with structural confirmation by tandem mass spectrometry [171]. By

using a semi-microcolumn, the sensitivity of the mass spectrometer could be improved by more than an order of magnitude [172]. In fact, when comparing a dual electrospray/APCI interface at low flow rates (~50 μL/min) for flow injection analysis, demonstrated that these techniques could be complementary, extending the range of detectable compounds and providing easier characterisation of complex mixtures [173]. The greatest drawback to the use of APCI is the high background noise due to clusters which often require starting scanning from *m/z* 100-200, depending on the species present. These cluster ions make it difficult to observe low mass analytes [174]. One way to solve this is to use background subtraction, which is usually ineffective. Another is to use a computer program to select mass chromatograms with low noise and background and combine these spectra to give a reduced total ion chromatogram. This offers a considerable improvement in the TIC appearance and in analysis time [175]. These difficulties as well as problematic isomer discrimination can be addressed by tandem mass spectrometry.

MS/MS techniques may be more selective for identification of analytes in complex matrices as they monitor both the precursor ion and the subsequent fragmentation of this ion which may reveal structural differences that will facilitate identification. Another peak in the original spectrum may be used if it were more informative. The technique was found to be much more sensitive when the molecular ion was subjected to further degradation than when the protonated molecule was used. A single fragmentation reaction (examine each precursor ion as it degrades to a characteristic fragment ion) or multiple fragmentation reactions (examine each precursor ion's degradation to two or more fragment ions) can be monitored. The latter was able to distinguish thiophenic compounds in a mixture [176]. Liquid

chromatography in conjunction with APCI tandem mass spectrometry was used to analyse sulfadiazine residues in Coho salmon [177], a 5α-reductase inhibitor [178], Tenidap and its stable isotope analog [179], and stanozolol and its metabolites [180]. Isotope dilution LC/ APCI tandem mass spectrometry was used to identify and quantify levels of heterocyclic amine carcinogens in grilled meat. Using isotopically labelled internal standards for isotope dilution improved the reproducibility of the results. With MS/MS capability, the structures could be confirmed and quantification down to 0.1 ppb was possible [181]. APCI-MS/MS in conjunction with LC separation was used to identify and quantify isomers of PAHs in environmental samples. This study indicated that the predominant ionisation method (proton transfer or charge exchange) could not be correlated by reference to ionisation energies or proton affinities. However, there was a general trend toward improved protonation with increasing size of the PACs. The collision gas pressure and the collision energy was an important factor in the degree of fragmentation exhibited, with fragmentation and mass spectral resolution increasing with increasing collision gas thickness and the optimal collision energy increasing with increasing mass of the PACs. With this method, sixteen PACs were identified and twelve were quantified [182]. LC/electrospray tandem mass spectrometry has been successfully applied to the analysis of preionised acids, salts, amino acids, peptides, nucleosides and nucleotides [183].

2.3.3 Supercritical Fluid Chromatography/Mass Spectrometry (SFC/MS)

SFC has been coupled to both CI and APCI sources for the analysis of PACs. The typical carrier gas for SFC, carbon dioxide, is capable of acting as a primary reagent gas [184]. With CI detection, a thermospray ion source and probe were used to handle the

effluent from a packed column. A discharge electrode was used to improve the ionisation efficiency and methane gas was added to maintain the source pressure so that ion-molecule reactions were observed. Although the CO_2 gas produced little in the way of background, the methanol used as a modifier generated substantial background, thereby reducing the sensitivity for the ions of interest and increasing the detection limit [185].

With APCI detection, a short interface is required to rapidly reduce the pressure of the SFC mobile phase to ambient pressure. With a proper interface and the lack of background from carbon dioxide, the method is capable of detecting low picogram levels of material although the sensitivities of individual PACs will depend on their ionisation energies and proton affinities. These properties will also affect the ionisation mechanism. Low mass compounds will be the most sensitive under charge transfer conditions, especially with benzene available while with high-mass compounds, proton transfer conditions are preferred. These preferences are unaffected by alkylation [186].

Chapter 3

Experimental Methods and Materials

3.1 Introduction

The APCI plasma is generated by the interplay between the mobile phase components and the analytes in the liquid introduction step, the gases introduced into the source as nebuliser, sheath and bath gases and the corona discharge generated by the corona discharge needle. Hence, changing the analyte, mobile phase, source gases or discharge voltage should directly impact the nature of the ionised species present in the plasma and the consequent ion-molecule reactions that occur in the source to generate ions of the analyte of interest. To probe the plasma chemistry, standards of PACs were prepared in typical solvents used for the separation of PACs, such as 50:50 acetonitrile/water, acetonitrile, hexanes and dichloromethane. The effect of these solvents was then assessed in one, two and three gas systems. The gases introduced into the gas streams included Dewar nitrogen, Prepurified™ nitrogen, building air, Extradry™ air, Extradry™ oxygen, Bonedry™ carbon dioxide, Bonedry™ carbon monoxide, methane and hydrogen. An in-house built gas box with attached valves was used to introduce gases separately into the nebuliser, sheath and bath gas streams and to control their flow rates. The ultimate purpose of this study is to improve detection limits of different classes of PACs, as illustrated by those selected as probes of the plasma chemistry in Figure 3.1.

3.2 Materials

Benzene, naphthalene, ethylene glycol monoethyl ether, ethylene glycol monomethyl ether, and cyclohexane were purchased from Fisher. Chloroform, pentane, and acetonitrile

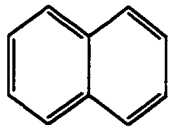

Naphthalene

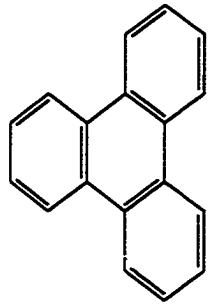

Triphenylene

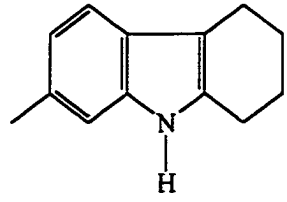

6-methyl-1,2,3,4-tetrahydro carbazole

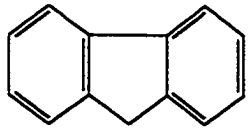

Fluorene

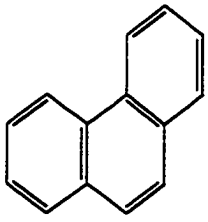

Phenanthrene

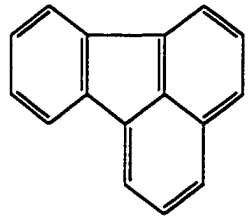

Fluoranthene

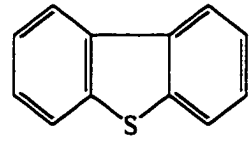

Dibenzothiophene

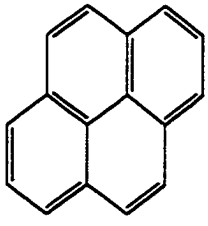

Pyrene

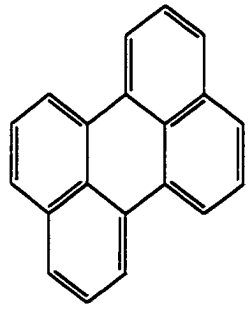

Perylene

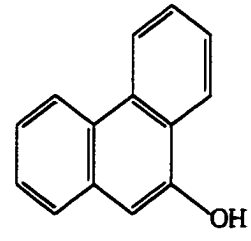

9-Phenanthrol

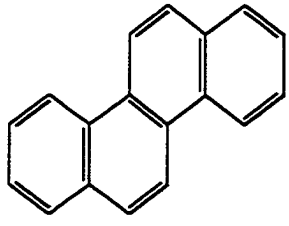

Chrysene

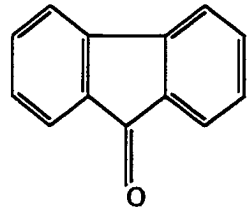

Fluorenone

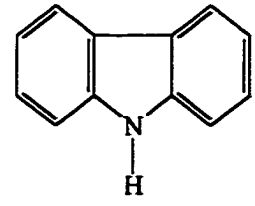

Carbazole

Figure 3.1. PACs used as probes of APCI plasma

(ACS reagent and HPLC grades) were obtained from Caledon. Biphenyl, ethylamine, tetracyanoethylene, isooctane and chloranil were obtained from Eastman. Anachemia supplied tetralin (1,2,3,4-tetrahydronaphthalene), phenanthrene and toluene. 1-methylnaphthalene, 2-methylnaphthalene, 2,3-dimethylnaphthalene, 2,6-dimethylnaphthalene, 2,7-dimethylnaphthalene and 9,10-dihydroanthracene were obtained from Chem Service. Xylenes were purchased from Analar, hexanes and methanol from Van Waters & Rogers, isopropanol and dichloromethane from ACP Chemicals and *n*-octane from Phillips. BDH supplied acetic acid, trifluoroacetic acid, formic acid and *n*-hexane. Active aluminum oxide, activity I, used in column chromatography was obtained from Brinkman. Aldrich supplied heptane, α,α,α-trifluorinated toluene, nonane, sodium iodide, ammonium acetate, benzo[*a*]pyrene, biphenylene, chrysene, pyrene, fluorenone, 6-methyl-1,2,3,4-tetrahydrocarbazole (MTC), anthracene, perylene, 9,10-dihydrophenanthrene, 2,3-benzanthracene, 2,3-dichloro-5,6-dicyano-1,4-benzoquinone (DDQ), 6,7-dichloro-1,4-dihydroxyanthraquinone (DDAQ), 2,3,5-triphenyl-*2H*-tetrazolium chloride (TTZ), triphenylcarbenium tetrafluoroborate (TPC), (2,4,7-trinitro-9-fluorenylidene)malonitrile (TNFM), 7,7,8,8,-tetracyanoquinodimethane (TCQ), and 2,4,7-trinitro-9-fluorenone (TNF), all other dimethylnaphthalenes (1,2-, 1,3-, 1,4-, 1,5-, 1,6-, 1,7-), 2,3,5-trimethylnaphthalene, 1,2,4,5-tetramethylbenzene, pentamethylbenzene, hexamethylbenzene, mesitylene, 4-ethyltoluene, 2-methylphenanthrene, 9-ethylfluorene, 1,2,6,7-tetrahydropyrene, 1,2,3,6,7,8-hexahydropyrene, and naphtho[2,3-*a*]pyrene. 1-Ethylnaphthalene, 2-ethylnaphthalene, 3-ethylphenanthrene, 2-ethylphenanthrene, 1-ethylpyrene, 1-methylpyrene, 5,7-dimethyltetralin, 2-methyltetralin, 4-methyltetralin, 1-propylnaphthalene, 1-butylnaphthalene, 9-methylphenanthrene, 3,6-

dimethylphenanthrene, 2-ethylfluorene, ethylmethylpyrenes, 1,8-diethylpyrene, 1,3-diethylpyrene, 1,6-diethylpyrene and 9,10-dihydrobenzo[a]prene were prepared in-house by Alex Tan. These were prepared by Friedel Crafts acylations, followed by Wolff-Kishner reductions. In all cases, chemicals were used without further purification with the exception of the alkane and dichloromethane solvents which were distilled before use. Distilled water was obtained in-house while Milli-Q water was obtained from a Barnstead NANOpure™ purification system.

Extradry™ air (less than 10 ppm water), industrial grade compressed air (97% purity), Extradry™ oxygen, Prepurified™ tank nitrogen, (99.998% pure) Bone-dry ™ carbon dioxide (99.8% purity), Bone-dry ™ carbon monoxide (99 - 99.5% purity), hydrogen (97% pure), and CP grade methane (99% purity) were obtained from Praxair. Compressed helium and argon were purchased from Liquid Carbonic. Building air was furnished by the Dalhousie University Dentistry Department. Liquid nitrogen (prepared by liquefaction of air) was supplied by the Dalhousie University Chemistry or Physics Departments, stored in a 100L stainless, pressurised steel Dewar (referred to as Dewar nitrogen in the thesis).

3.3 Equipment

All mass spectral studies were conducted with a VG-Fisons-Micromass Quattro triple quadrupole mass spectrometer controlled by a 133 MHz K-PC Pentium S (IBM-compatible computer clone) using Masslynx 2.1 software. Three skimmer cones were used in this study - skimmer cone A was delivered with the instrument when purchased. Skimmer cone A was dropped, the orifice collapsed and an attempt to drill out a new orifice was made. A misalignment of the drill and the cone and a larger than desired drill bit yielded a larger

orifice, approximately 20° off-normal. This is referred to as skimmer cone B. Skimmer cone C was purchased new in November 1998.

The mass spectrometer was usually interfaced to a liquid delivery system consisting of an HPLC pump or a syringe pump, a Rheodyne model 4593 injector and where applicable, HPLC column(s). For flow injection analysis or isocratic chromatography, one of the Micromeritics 750, the Shimadzu LC-6A, the Shimadzu LC-10AT or the LC-10AT*VP* HPLC pumps was used. The latter three were the most commonly used. The LC-6A model was used for optimising instrumental parameters (see Chapter 4), the LC-10AT for the effects of solvent characteristics and flow rate (see Chapter 5), and the LC-10AT*VP* for the plasma characterisation studies (see Chapter 6). Analyses requiring gradient elution were performed with a Hewlett Packard series 1100 or a Waters 600 Controller quaternary HPLC pump. The two syringe pumps used were the Sage model 341A or the Cole Palmer model 74900. The HPLC columns used included a Vydac™ polymeric C_{18} column, a Chromatographic Specialties silica column, Supelco monomeric C_{18} columns, and a tetrachlorophthalamidopropyl (TCP) column prepared in-house. A Hamilton model 705 50 µL HPLC syringe or a Hamilton model 1001 one mL gas tight syringe were used for sample injection. A Hamilton model #1725 250 µL gas tight syringe or a Popper & Sons two mL syringe was used to rinse the injection valve. Hamilton model 1010 ten mL gas tight syringes were used with the syringe pumps. All injections were made with appropriately sized stainless steel loops. Tubing connections from the pump to the injector were made with 1/16" o.d., 0.25 or 0.50 mm i.d. polyetheretherketone (PEEK) tubing, all other connections were made with 1/16" o.d., 0.13 or 0.17 mm i.d. PEEK tubing, all supplied by Chromatographic

Specialties. In the plasma characterisation studies, PEEK and teflon tubing (for connecting solvent bottles to pump, pump to injection valve, injection valve outlet to probe) and glass bottles were dedicated to one of four solvents (50:50 (v/v) acetonitrile-water, acetonitrile, dichloromethane and hexanes). The tubing and bottles were purchased from Chromatographic Specialties. Diagrams of gas boxes 1 (the original gas box) and 2 (the modified gas box) are presented in Figures 3.2 and 3.3.

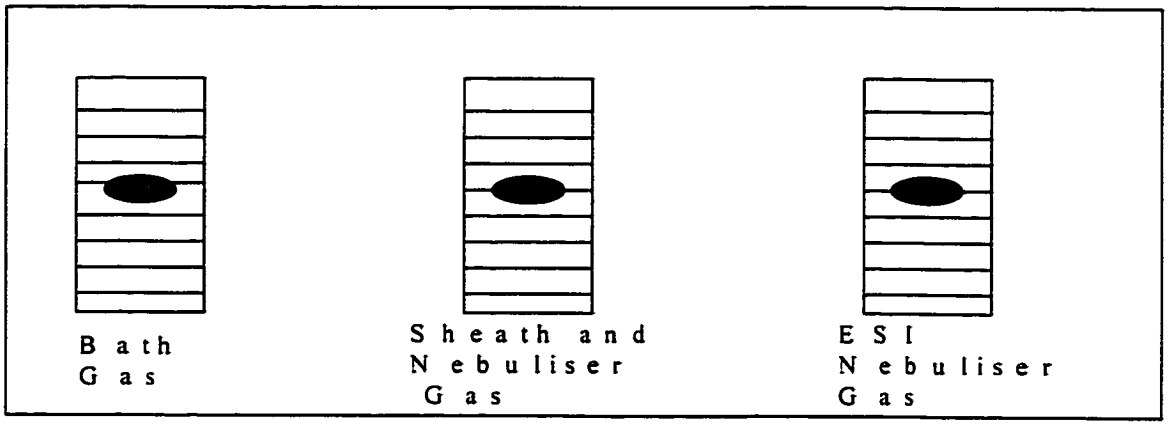

Figure 3.2. Original gas box

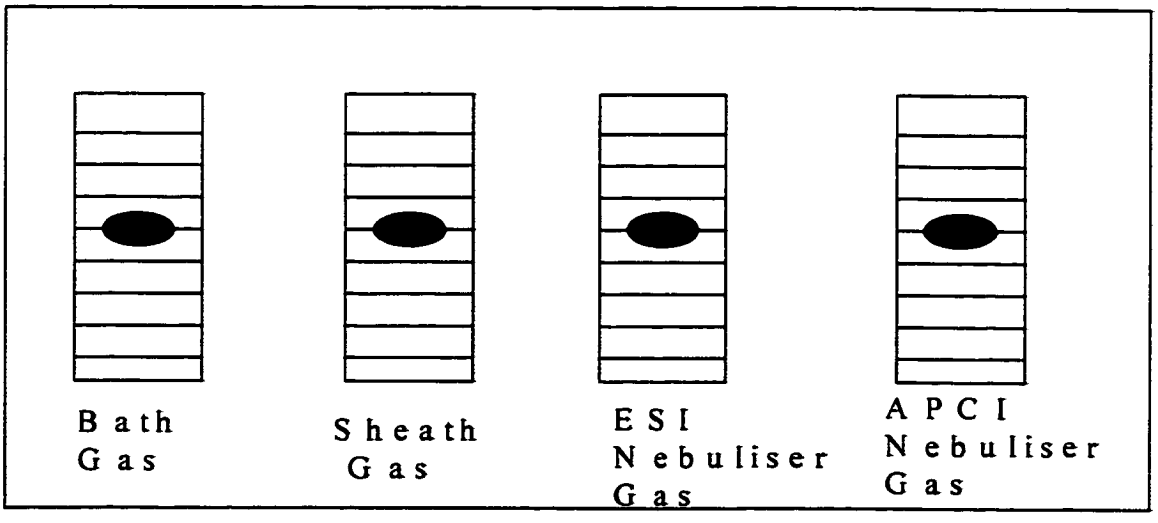

Figure 3.3. Modified Gas Box

3.4 Methods

3.4.1 Calibration of the Mass Spectrometer

The original calibrations were performed with polyethylene glycol-200 to -1000 (PEG) standards in electron ionisation mode, as described in Brent Jewett's thesis [187]. This calibration covered the range from *m/z* 20 to 2000 and was checked periodically by the analysis of a PEG standard in electrospray mode with reference to the manufacturer's instructions.

Plasma characterisation studies required calibration from *m/z* 5 to 500. To perform this calibration, a 3 mg/mL solution in both sodium iodide and ammonium acetate was prepared in degassed 50:50 (v/v) isopropanol/water. This solution was loaded into a 10 mL syringe, placed in a syringe pump and the flow set to 1.8 mL/h. Using either gas box design, the bath gas flow rate of 300 standard litres per hour (sLph) and the nebuliser flow rate of 20 sLph were set with either Dewar nitrogen or air as the source gas. The system was allowed to stabilise for 15 minutes. The ESI^+ run conditions were set as follows: 3.5 kV capillary voltage, 50 V skimmer cone voltage, and 105°C source temperature. The calibration should be performed with reference to the sodium iodide and ammonium acetate clusters, as detailed in the Table 3.1, with 0.25 u as the acceptable mass error.

To check calibration in the *m/z* 5-20 range, inject 3 mg/mL of lithium iodide with 50:50 (v/v) isopropanol/water flowing. Characteristic isotope peaks of Li at *m/z* 6 (7.5%) and 7 (92.5%) should be observed.

Table 3.1 Calibration file for *m/z* 5-500

m/z	Ion
18.0344	NH_4^+
22.9898	Na^+
78.0919	$(NH_4^+)(CH_3COOH)$
83.0473	$(Na^+)(CH_3COOH)$
104.7	$(Na^+)_2(CH_3COO^-)$
138.1494	$(NH_4^+)(CH_3COOH)_2$
143.1048	$(Na^+)(CH_3COOH)_2$
172.8840	$[(Na^+)NaI]$
322.7782	$[(Na^+)(NaI)_2]$
472.6725	$[(Na^+)(NaI)_3]$
622.5667	$[(Na^+)(NaI)_4]$
772.4610	$(Na)_6(I)_5^+$
922.3552	$(Na)_7(I)_6^+$
1072.2494	$(Na)_8(I)_7^+$

3.4.2 Standard Preparation

A number of stock solutions were used in the course of these studies. These are described in detail in Table 3.2. In all cases, the appropriate amount of standard was weighed, dissolved in the appropriate solvent in a volumetric flask with sonication, and then diluted to the mark once the flask had been cooled to room temperature. Serial dilutions were performed with volumetric pipettes and flasks.

Table 3.2 Description of Stock Solutions Used

Stock Solution	Solvent	Components	Concentration (M)
PAH mix 1	Acetonitrile	benzene naphthalene tetralin biphenyl fluorene anthracene pyrene chrysene perylene	1.24e-3 1.04e-3 1.20e-3 1.05e-3 1.00e-3 9.90e-4 1.08e-3 1.75e-4 1.20e-4
LC mix 1	Acetonitrile	benzene naphthalene fluorene phenanthrene anthracene pyrene 3-ethylphenanthrene 2-ethylphenanthrene 1-ethylpyrene 2-methylpyrene	1.24e-3 1.04e-3 1.00e-3 1.06e-3 9.90e-4 1.08e-3 1.48e-3 1.46e-4 1.35e-4 9.30e-4
LC mix 2	Acetonitrile	benzene toluene naphthalene 4-ethyltoluene fluorene phenanthrene anthracene pyrene 3-ethylphenanthrene 2-ethylphenanthrene 1-ethylpyrene 2-methylpyrene 1,2,3,4-tetrahydro-benzo(a)pyrene	*not determined, see end of table

LC mix 3	Hexanes	benzene toluene naphthalene 4-ethyltoluene fluorene phenanthrene anthracene pyrene 3-ethylphenanthrene 2-ethylphenanthrene 1-ethylpyrene 2-methylpyrene 1,2,3,4-tetrahydro- benzo(a)pyrene	*not determined, see end of table
GLC -1	Acetonitrile	benzene toluene xylene tetralin mesitylene pentamethylbenzene 2-methylnaphthalene 9-methylanthracene 2-ethylphenanthrene 3,6-dimethylphenanthrene	7.4e-3 5.3e-3 6.3e-3 1.0e-2 5.9e-3 6.1e-3 1.14e-2 5.2e-3 1.7e-3 5.7e-3
AB-1	Acetonitrile	benzene toluene xylene mesitylene 4-ethyltoluene 1,2,3,5-tetramethylbenzene pentamethylbenzene hexamethylbenzene 5,7-dimethyltetralin 4-methyltetralin	0.0124 0.0119 0.0116 0.0106 0.0098 0.0028 0.0022 0.0023 0.0027 0.0040

N-1	Acetonitrile	naphthalene 2-methylnaphthalene 1-Ethylnaphthalene 2-Ethylnaphthalene 2,3-dimethylnaphthalene 2,6-dimethylnaphthalene 1-propylnaphthalene 1-butylnaphthalene tetralin	2.7e-3 3.4e-3 2.6e-3 2.4e-3 2.5e-3 1.2e-3 2.1e-3 2.2e-3 3.3e-3
P-1	Acetonitrile	phenanthrene 2-methylphenanthrene 9-methylphenanthrene 3,6-dimethylphenanthrene 3-ethylphenanthrene 2-ethylphenanthrene	3.0e-3 2.7e-3 2.2e-3 3.1e-3 3.4e-3 4.8e-3
PF-1	Acetonitrile	pyrene fluorene 2-ethylfluorene 9-ethylfluorene 1-ethylpyrene 9,10- dihydrobenzo(a)pyrene	3.4e-3 3.4e-3 3.0e-3 3.9e-3 1.1e-3 4.0e-4
Benz -1	Acetonitrile	benzene toluene xylene mesitylene tetramethylbenzene pentamethylbenzene hexamethylbenzene	2.89e-2 2.61e-2 1.91e-2 2.16e-2 2.59e-2 2.22e-2 2.11e-2
Alkanes 1	pentane	Naphthalene Phenanthrene Pyrene Fluorene	1.81e-2 1.17e-2 7.46e-3 1.24e-3
Alkanes 2	*n*-hexane	Naphthalene Phenanthrene Pyrene Fluorene	1.18e-2 1.08e-2 1.39e-2 1.30e-2

Alkanes 3	hexanes	Naphthalene Phenanthrene Pyrene Fluorene	1.50e-2 1.69e-2 1.15e-2 1.89e-2
Alkanes 4	heptane	Naphthalene Phenanthrene Pyrene Fluorene	1.35e-2 1.33e-2 8.50e-3 1.29e-2
Alkanes 5	octane	Naphthalene Phenanthrene Pyrene Fluorene	1.96e-2 1.28e-2 9.74e-3 1.12e-2
Alkanes 6	isooctane	Naphthalene Phenanthrene Pyrene Fluorene	2.02e-2 2.17e-2 1.30e-2 1.05e-2
Alkanes 7	nonane	Naphthalene Phenanthrene Pyrene Fluorene	2.40e-2 2.55e-2 1.08e-2 1.09e-2
Alkanes 8	cyclohexane	Naphthalene Phenanthrene Pyrene Fluorene	2.04e-2 1.69e-2 1.04e-2 1.06e-2
ES-1	Acetonitrile - 1% acetic acid	benzene naphthalene fluorene phenanthrene anthracene 3-ethylphenanthrene 1-methylpyrene 1-ethylpyrene pyrene chrysene	2.07e-3 1.73e-3 1.67e-3 1.76e-3 1.65e-3 2.47e-3 1.55e-4 2.25e-4 1.80e-3 2.92e-4

ES-2	dichloromethane/ 0.1% trifluoroacetic acid	naphthalene phenanthrene pyrene perylene 2,3-benzanthracene	4.525e-4 4.623e-4 4.529e-4 4.581e-4 4.713e-4
Imperial -1	Acetonitrile	naphthalene phenanthrene pyrene fluorene chrysene fluorenone MTC**	2.12e-3 2.56e-3 2.39e-3 2.05e-3 2.16e-3 2.65e-3 2.23e-3
Imperial-2	Hexanes	naphthalene phenanthrene pyrene fluorene fluorenone	9.30e-4 8.38e-4 7.94e-4 9.42e-4 8.76e-4
Imperial -3	Dichloromethane	naphthalene phenanthrene pyrene fluorene chrysene fluorenone MTC**	3.713e-3 3.928e-3 4.845e-3 4.163e-3 4.170e-3 6.437e-3 4.771e-3
IO-1	Acetonitrile	naphthalene fluorene phenanthrene chrysene dibenzothiophene pyrene 9-phenanthrol	2.08e-3 1.64e-3 1.08e-3 1.18e-3 9.82e-4 7.86e-4 1.06e-3
IO-2	Acetonitrile	naphthalene carbazole triphenylene phenanthrene fluoranthene perylene	2.66e-3 1.11e-3 5.12e-4 8.36e-4 1.15e-3 1.08e-3

IO-3	Dichloromethane	naphthalene fluorene phenanthrene chrysene dibenzothiophene pyrene 9-phenanthrol	1.94e-3 1.43e-3 1.21e-3 8.19e-4 1.35e-3 1.32e-3 1.25e-3
IO-4	Dichloromethane	naphthalene carbazole triphenylene phenanthrene fluoranthene perylene	2.38e-3 1.45e-3 2.28e-4 1.05e-3 1.13e-3 6.62e-4
IO-5	Hexanes	naphthalene fluorene phenanthrene chrysene dibenzothiophene pyrene 9-phenanthrol	1.83e-3 1.37e-3 1.21e-3 9.20e-4 1.06e-3 1.30e-3 1.26e-3
IO-6	Hexanes	naphthalene carbazole triphenylene phenanthrene fluoranthene	1.81e-3 1.42e-3 4.25e-4 1.15e-3 9.69e-4

* standards prepared non-analytically by Dr. R.D. Guy for chromatographic optimisation, concentrations are unknown
** abbreviation for 6-methyl-1,2,3,4-tetrahydrocarbazole

3.4.3 Liquid Introduction Techniques

3.4.3.1. Flow Injection Analysis

This technique was used mainly for two purposes: one was for optimisation of instrumental parameters to optimise PAC detection in a particular solvent and the second was for studies of PAC response as a function of solvent and gas.

General Procedure:

The general procedure for mass spectrometric analysis with flow injection analysis is as follows: Unless otherwise stated, the mobile phase flow rate is 0.200 mL/min. After initiating the flow and turning on the bath and sheath gases (each set at 250 sLph), the probe was inserted in the mass spectrometer. The probe and the source temperatures were set to 200°C and 120°C, respectively, and the cone voltage was set to 30 V. These parameter settings are those recommended by the manufacturer. The mass spectrometer was then tuned using the solvent ions. Tuning implied adjusting the corona voltage, ion energy and the voltages on the lenses to give maximum response and a symmetrical peak shape. Having completed the tuning, sample analysis could begin. To this end, a 100 μL sample loop was then filled with the analyte via a appropriately sized syringe. The mass spectrometer was set to scan from *m/z* 70 to *m/z* 350 at a rate of 3 sec/scan to get a total ion current. After acquiring thirty spectra of background, the sample was injected into the stream of mobile phase and scanned for 50 scans. The spectrum would indicate a distinct peak where the sample was detected. The data were then processed by MassLynx™ software which combined the "sample scans" and the "background scans" and subtracted the backgound from the sample scans.

Standard APCI Conditions:

The following are the experimentally determined standard $APCI^+$ instrumental settings: 1) source T = 120°C (optimum is solvent-dependent), 2) probe T = 350-400°C, 3) Dewar nitrogen regulator at 100 psi, 4) bath gas flow = 300 sLph, 5) sheath gas flow = 375 sLph (if using original gas box) and 300 sLph (if using modified gas box), 6) nebuliser flow

= 30 sLph, 7) corona voltage of ~ 4.00 kV (optimum is solvent-dependent), 8) probe position adjustor 1 turn down from maximum upward position, and 9) cone voltage = 30V (optimum is solvent-dependent).

3.4.3.2 Isocratic Reversed Phase HPLC

LC mix 1 was used for all isocratic LC-MS analyses and optimisation. In all cases, the mobile phase was 70:30 (v/v) MeCN/H_2O and was run at 1.00 mL/min. The mobile phase was run into an injector valve, through the Vydac™ column, then through an absorbance detector set at 250 nm and then into the mass spectrometer.

Under these conditions, the components elute in the order of benzene, naphthalene, fluorene, phenanthrene, anthracene, pyrene coeluting with 3-ethylphenanthrene, 2-ethylphenanthrene, 1-methylpyrene and 2-ethylpyrene. The total run time was 30 minutes under these solvent conditions. The absorbance detector monitored the elution order. The effluent from the absorbance detector was introduced into the mass spectrometer probe through a small internal diameter PEEK tube (o.d. = 1/16", i.d. = 0.13 mm) to minimize peak broadening.

As in flow injection analysis, the response to PACs was optimised by examining the effect of probe temperature, gas flow rates, scan rate, cone voltage and number of synchronous functions being controlled by the data system on the signal-to-noise ratio and the peak appearance. Most parameters were identical to the standard $APCI^+$ conditions described above except that the signal-to-noise ratio was better at a probe T= 400°C than at 200°C.

3.4.3.3 Gradient Elution Reversed Phase Liquid Chromatography

LC mixes 2 and 3 and GLC-1 standards were used for these studies.

Three different gradients were explored. All consisted of an initial isocratic portion of 50:50 (v/v) acetonitrile/water and a later rise to 100% acetonitrile. The 503010030 gradient maintained the isocratic portion for thirty minutes, then linearly increased to 100% acetonitrile over 30 minutes. The 50310060 gradient maintained the isocratic portion for three minutes followed by a linear increase to 100% acetonitrile over the next 60 minutes. The 50310010 featured a three minute isocratic portion, followed by a linear increase to 100% acetonitrile over the next ten minutes. All gradients were run at 1.00 mL/min and the Vydac™ column was used for all separations. The gradient affected compound retention time but not compound elution order. The elution order was as described in the previous section except 1,2,3,4-tetrahydrobenzo[*a*]pyrene emerged last.

In addition to the three gradients tested, the response of PACs as a function of the probe temperature, source temperature, cone voltage, carrier gas, sample solvent and single ion monitoring vs. scanning was examined. The results were the same as those observed for the isocratic reversed phase chromatographic sample introduction.

LC mixes 2 and 3, and Fraction #9 (a naphthalene-rich fraction of a Syncrude crude oil sample #2HPP 105) were analysed by gradient reversed phase liquid chromatography-mass spectrometry. All samples were injected neat.

3.4.3.4 Normal Phase High Performance Liquid Chromatography

3.4.3.4.1. Sample Preparation

The distillation was performed at Syncrude on 200 mL of crude oil Lot # 2HPP 1106. The 0-10% fraction was collected at a distillation pressure of 712 mm Hg (atmospheric pressure that day) over a temperature range of 62.4 to 166.3°C. The 10-20% fraction was collected at a distillation pressure of 712 mm Hg over a temperature range of 155.6 to 207.4°C, and all subsequent fractions were collected at a distillation pressure of 5 mm Hg. The 20-30% fraction was collected from 191.6 to 231.1°C, the 30-40% cut from 212.4 to 246.8°C, 40-50% fraction from 233.2 to 262.4°C, the 50-60% fraction from 250.4 to 275.9°C, the 60-70% fraction from 265.8 to 290.5°C, the 70-80% fraction from 284.0 to 307.9°C, the 80-90% fraction from 297.4 to 329.7°C and the 90-100% fraction is all that is left over. As some of the distillation fractions were collected at atmospheric temperature and others were collected at reduced pressure, all the measured temperatures were scaled to what they would have been if the distillation had been performed at the atmospheric pressure. This is called the atmospheric equivalent temperature.

3.4.3.4.2. Procedures

3.4.3.4.2.1 Isocratic elution

Hexane was pumped by a Shimadzu isocratic pump through the silica column at a flow rate of 1 mL/min. Sample was injected by full-loop injection (5 or 20 μL) with a Rheodyne injection valve. The column eluent was monitored at 336 nm by the Shimadzu computer-interfaced single-wavelength detector. The eluent was then passed into a Rheodyne cutting valve fitted with a 100, 200 or 500 μL loop. The loop of this valve was continuously

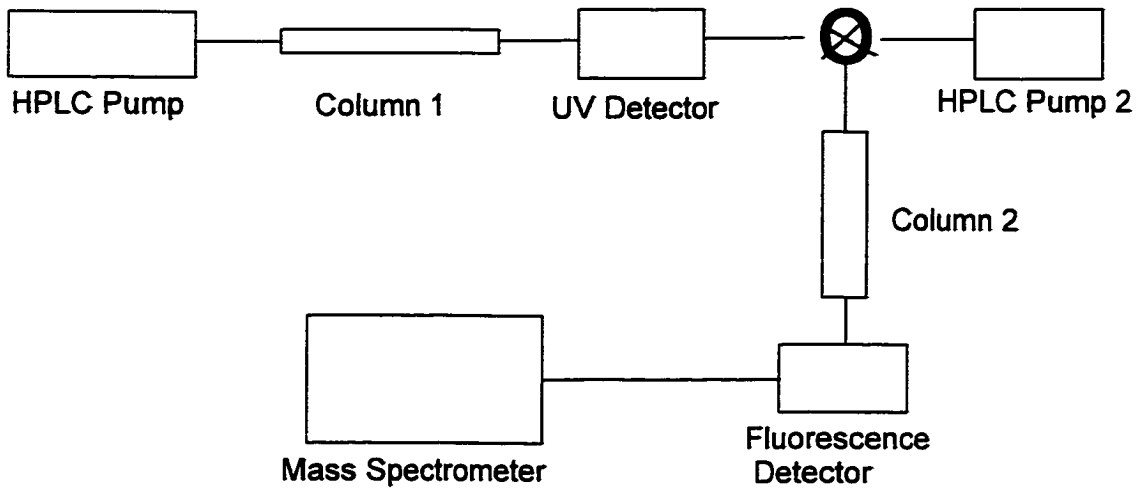

Figure 3.4. Instrumental set-up for cutting experiments.

being filled with column effluent and was connected to a second Shimadzu isocratic pump which provided a continuous flow of 30% dichloromethane/70% hexane at a rate of 0.4 mL/min. When a peak of interest was trapped in the loop, it was injected and the mobile phase carried it directly into the mass spectrometer for detection.

An alternative was to inject the sample trapped in the loop onto the tetrachlorophthalamidopropyl (TCP) column for further separation (Figure 3.4). The effluent from the TCP column was monitored by a fluorometer programmed with an excitation wavelength of 230 nm and an emission wavelength of 380 nm and then detected by APCI-MS in tandem.

In either case, the mass spectrometer was allowed to perform a number of background scans before sample introduction.

All distillation fractions were injected directly into the mass spectrometer to characterise the composition of each distillation fraction. When separated on a silica column,

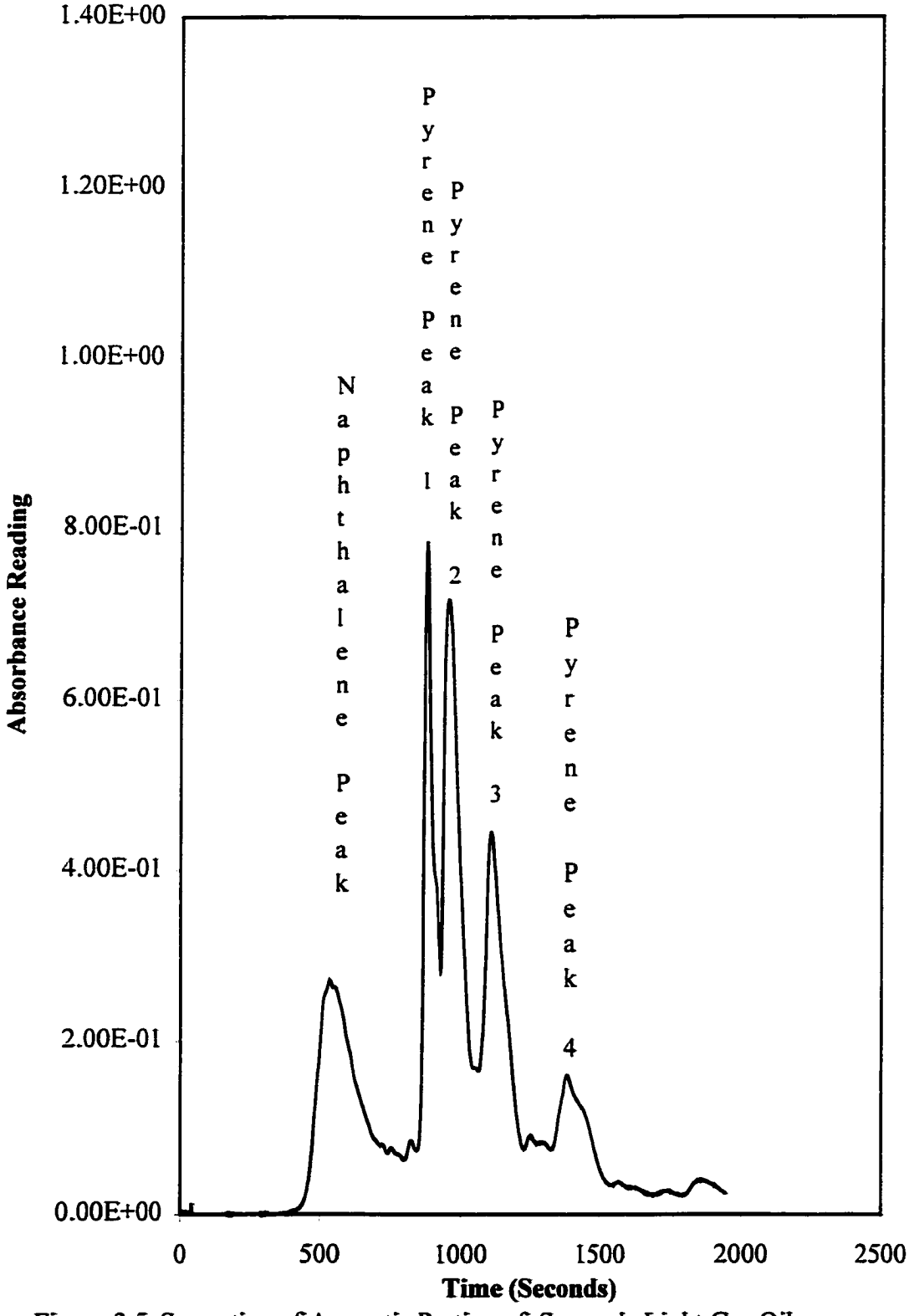

Figure 3.5. Separation of Aromatic Portion of Syncrude Light Gas Oils on a 4.6 x 25 cm silica column, hexane as eluent, UV detection at 336 nm.

the 80-90% and 90-100% distillation cuts (see Figure 3.5) gave a broad peak due to diaromatics (identified as the naphthalene peak), and three to four peaks with a pyrene backbone (defined as pyrene peaks 1 through 4). The three-ring systems would elute between the naphthalene peak and pyrene peak 1 but were present at too low a concentration to be clearly visible using 336 nm detection. The naphthalene peak of the 80-90% fraction was selected and a cut of this fraction was sent to the mass spectrometer for analysis. Similarly, the pyrene peaks of the 80-90% and 90-100% cuts were selected on the silica column and were analysed after separation on the TCP column both for compound identification purposes and to determine the effect of cutting position on the observed response.

3.4.3.4.2.2 *Gradient Elution*

The set-up of the experiment is similar with the following exceptions. The Hewlett-Packard pump was used to introduce 0.4 mL/min of 30% dichloromethane/70% hexane to the TCP column for 30 minutes before increasing the DCM content to 100% over 30 minutes. An excitation wavelength of 325 nm and an emission wavelength of 380nm were used for analysing pyrene peaks. A new corona needle was used in the analysis of the 90-100% distillation cut.

3.4.3.5 Cold Column Chromatography

These separations were performed on two linked C_{18} columns with acetonitrile as the mobile phase. Connections were made with PEEK tubing from the injector to the column 1, from the exit of column 2 to the UV detector and from the UV detector to the APCI probe. The HPLC pump was primed and then the line meant to connect the pump to the injector was flushed thoroughly with acetonitrile. The pump was then connected to the injector and a flow

of mobile phase was started into the columns which had been submerged in an ice bath. The low temperature permitted 100% organic elution rather than 50% organic, thus improving mass spectrometric detection. The UV detector was set at 336 nm for analysis of the valley between pyrene peaks 2 and 3 and to permit the detection of pyrene and its derivatives. Temperature equilibration of the column, warming up of the UV lamp, and stabilisation of the mass spectrometer required fifteen minutes.

Once the system was fully equilibrated, the UV detector was zeroed and the mass spectrometer was tuned. A corona voltage of 4 kV, cone voltages of 15, 30 or 50 volts, a source temperature of 120°C, a probe temperature of 350°C, bath and sheath gas flow rates of 300 sLph each and a nebuliser gas flow rate of 30 sLph were found to be optimal for analysing analytes eluting from the column with a mobile phase (100% MeCN) flow rate of 1 mL/min. A single-ion recording (SIR) function of all suspected molecular and quasi-molecular ion masses (determined previously from fluorescence spectra) was set up with a 0.2 sec dwell time at each mass at each cone voltage. The sample was injected and data acquisition by the UV detector and mass spectrometer initiated. Acquisition continued until all peaks had eluted.

3.5 Experiments

3.5.1 Optimisation of Instrumental Parameters

Optimisable parameters in APCI and electrospray ionisation (ESI) include the corona voltage (APCI) or capillary voltage (ESI), cone voltage, probe temperature, source temperature, mass spectral scan range, scanning vs. single ion monitoring, bath gas flow rate, sheath gas flow rate, nebuliser gas flow rate (in the modified gas box), and solvent flow rate.

To test the effect of these parameters on signal intensity, an appropriate dilution of standard was made. Standard $APCI^+$ conditions were used as listed in Section 3.4.3.1. Each parameter was optimised individually by varying it between the minium and maximum permitted values and monitoring the ion abundance response of standard compounds. Having determined the optimum value, this value was used for subsequent optimisation experiments. Some or all of these parameters had to be evaluated when changing solvents for flow injection analysis, when switching between isocratic reversed and normal phase separations, and when switching to gradient techniques in an effort to obtain optimal signal-to-noise ratios.

In addition to examining the instrumental parameters for optimisation of signal intensity, the comparability of detectors and pumps were compared. For comparing isocratic pumps, the Shimadzu, HP and Micromeritics HPLC pumps and the Sage syringe pump were used to provide a flow rate of 200 μL/min of 50:50 acetonitrile/water. Both the background spectra and the response to a 500 μL injection of a hundredfold dilution of Imperial -1 standard with mobile phase were examined, specifically looking at noisiness in TICs and in mass spectral response to the components of the standard mixture.

For the case of comparing gradient pumps, the gradient separation of LC mix 1 was performed with the Waters and HP systems. 100 μL of this mixture was injected onto a Vydac™ column and separated with a gradient starting at 50:50 acetonitrile/water at 1 mL/min. These conditions were maintained for 30 minutes and then the %acetonitrile was increased linearly to 100% over the next thirty minutes. This was maintained for 5 minutes and then returned to initial conditions over 2 minutes, followed by a 10 minute equilibration

time before the next injection. In a similar manner, the Waters and Shimadzu absorbance detectors were compared. The same standard was separated on the column and gradient separation was performed with the HP system with detection at 250 nm. The absorbance spectra were compared for number and intensity of peaks.

3.5.2 Solvent Effects

The nature of the solvent affects both the observed signal strength and the ionisation mechanisms of analytes as it may be the source of collision-induced charge exchange or proton transfer to the analyte molecules. In addition to affecting the signal, the nature of the solvent will determine the identity and intensity of background ions.

3.5.2.1 Solvent Purity

3.5.2.1.A Distilled vs. Milli-Q water

Trace impurities in solvents can induce great changes in the background and sample ions observed. To test the effect of water quality, isocratic LC/MS conditions with 70:30 (v/v) acetonitrile/water were set up with Milli-Q and building distilled water. Using standard $APCI^+$ conditions (except for a probe T = 400°C), the background and the response to LC mix 1 was monitored by UV at 250 nm in tandem with mass spectrometric detection.

3.5.2.1.B Alumina column purification of hexanes and dichloromethane

An analysis of the background ions of hexanes and dichloromethane solvents seemed to indicate the presence of oxygen-containing species, derived either from the solvent or the gas streams.

To test this hypothesis, two separate experiments were performed. In experiment 1, the background of hexanes (200 µL/min solvent flow, 300 sLph bath and sheath gas flow,

30 sLph nebuliser flow, 4.00 kV corona voltage, 15, 30 and 50 V cone, source T = 120°C, probe T = 350°C) was determining by scanning *m/z* 5-300 in 1 second scans in triplicate with Dewar nitrogen as the only gas in the system. The solvent flow was turned off, tank nitrogen was introduced into all streams and the solvent flow re-started. After a stabilisation period, the background spectra were re-obtained. Tank nitrogen was selected as it should be drier and contain less oxygen that Dewar nitrogen.

In experiment 2, a 75 cm high, 3 cm wide column was filled to 50 cm height with activity I, dry alumina. 100 mL of hexanes or dichloromethane was then passed through the column, 25 mL being used to wet the column, 75 mL being collected. Precautions were taken to keep air and light (in the case of DCM) out of the solvent. This purification should remove all polar impurities, especially oxygen-containing species. In the meantime, thousandfold dilutions of Imperial-2 and Imperial-3 standards were performed with purified and unpurified solvent. Dedicated tubing and glassware was used for all analyses. The HPLC pump was primed with unpurified solvent, the tubing flushed and the flow to the probe initiated. With Dewar nitrogen as the source gas, the system was allowed to equilibrate for 20 minutes after which time the instrument was tuned. A data acquisition file was set up to scan the background (*m/z* 5 to 300) in one second scans and to analyse for sample peaks (0.2 s/mass at 15, 30 and 50 V cone) of the standard mixture components. Ten scans of background were obtained, the sample was injected and the acquisition continued until the TIC returned to baseline. The background signal was subtracted from the analyte signal to give the corrected analytical signal. Once the solvent had been filtered, it was then immediately analysed in the same fashion as the analytical standard in unfiltered solvent. The filtered and unfiltered

solvent spectra were compared on the basis of the *m/z* and intensity of the background peaks and on the signal intensity and predominant ionisation mechanism of the PAC standards.

3.5.2.2 Protonation and Signal Intensity in aqueous CH_3CN and aqueous CH_3OH

Solutions of naphthalene (60 mg added to 5 mL of solvent) were prepared in solutions varying from 100% aqueous to 100% organic. The solvent used was also used as the mobile phase for the flow injection analysis. Standard $APCI^+$ conditions were used for the analysis. 100 µL was injected and the response was monitored at *m/z* 128 (molecular ion) and *m/z* 129 (protonated molecule). The $[M+H]^+/M^{+\bullet}$ vs. % organic was plotted.

3.5.2.3 Injection Solvent vs. Mobile Phase

A 1 mM solution of fluorene was prepared in 100% acetonitrile, 90% (v/v) acetonitrile/water, 70% (v/v) acetonitrile/water and 50% (v/v) acetonitrile/water. Standard $APCI^+$ conditions were used. Initial experiments were conducted with 100% acetonitrile as the mobile phase with 100 µL injections of fluorene in each of the injection solvents. The responses at *m/z* 166 and 167 were extracted from the scanned data (*m/z* 70-250). This was repeated with each of the remaining three combinations of acetonitrile with water and the response recorded. Both the total signal intensity and the $[M+H]^+/M^{+\bullet}$ ratio were plotted as a function of mobile phase composition to determine whether the mobile phase or the injection solvent were more critical to the behaviour of analyte molecules.

3.5.2.4 Effect of Solvent Additives

PAH mix 1 was used to evaluate the ability of ethylene glycol monoethyl ether and ethylene glycol monomethyl ether to break up water and acetonitrile clusters and thus reduce the background in an APCI system. To 50:50 acetonitrile/water (plagued with a high level

of background noise) was added 0, 1, 2, 3, 4, 5, 6, 7, 8, 9, 10, 20 and 50 % by volume of these additives. These mobile phases were used both to dilute the stock solution fivefold and for the flow injection analysis. Standard APCI$^+$ conditions were used, except that the sheath gas flow rate was 300 sLph. 100 µL injections were made. Scanned spectra (*m/z* 20 -250) were taken to assess the effects on both the noise and signal simultaneously.

PAH mix 1 was used as a probe to determine whether the addition of acetic acid, trifluoroacetic acid, formic acid, and chloroform would affect the ionisation mechanism or signal intensity. The additive was added to 50:50 acetonitrile/water to a final concentration of 0, 0.1, 0.2, 0.5, 1.0 and 2.0% additive. These solvents were then used to dilute the stock solution one thousandfold. Using the same mass spectral conditions as above, the analytical standards were analysed in triplicate. The total signal intensity and ratio of protonated molecule to molecular ion were plotted as a function of % additive. This study was repeated with a stock solution not containing benzene, tetralin or biphenyl to assess the effect of benzene-like species on the ionisation mechanism.

3.5.2.5. Alkane Solvents

Alkane solvents such as pentane, n-hexane, hexanes, heptane, octane, isooctane, nonane and cyclohexane will differ in their fragmentation behaviour. Whether this will affect ionisation mechanism, detection limit and sensitivity for PACs was tested using serial dilutions of Alkanes-1 through 8 standards. A 0.200 mL/min flow rate of solvent which matched the injection solvent and standard APCI$^+$ conditions were used except the probe temperature was set at 350 °C. A scan range from *m/z* 5-300 for background and SIR function with 0.25s dwell time/mass were set up. The samples were analysed in triplicate from lowest

to highest concentration. The injector was rinsed with 0.750 mL of solvent between standards. When changing solvents, the pump was primed, the system flushed for 10 minutes at 1 mL/min to remove all traces of the previous solvent or sample. The concentration - normalised total signal intensities were plotted as a function of solvent as were the $[M+H]^+/M^{+\bullet}$ ratios.

3.5.2.6 % Acetic Acid for Electrospray

0.5 mL of ~0.01 M benzene, naphthalene, fluorene, phenanthrene, anthracene, 3-ethylphenanthrene, 1-methylpyrene, 1-ethylpyrene, pyrene and ~ 0.001 M chrysene stock solutions in MeCN were diluted with 3 mL of MeCN and acetic acid concentrations ranging from 0 to 10%. Using the Cole-Palmer syringe pump to deliver a constant flow of 600 μL/h (10 μL/min), 10 μL of each solution was injected into the mobile phase stream, and carried into the mass spectrometer for analysis.

The following ESI-MS conditions were used: capillary voltage = 3.5 kV, cone voltage = 30V, and source T = 80°C.

3.5.3 Electrospray of PACs

Standard ESI^+/ESI^- conditions: capillary voltage = 3.5 kV, cone voltage = 30V, source T = 120°C, bath gas flow = 300 sLph, ESI nebuliser gas flow = 17 sLph, minimum distance between ESI capillary and skimmer cone, and probe position adjustment one turn below full upward position.

3.5.3.1 ESI^+/ESI^- of PAHs in MeCN/1% Acetic Acid

0.5 mL each of ~0.01 M benzene, naphthalene, fluorene, phenanthrene, anthracene, 3-ethylphenanthrene, 1-methylpyrene, 1-ethylpyrene, pyrene and ~ 0.001 M chrysene stock

solutions in MeCN were diluted with 3 mL of MeCN/1% acetic acid to produce discrete solutions. Using the Cole-Palmer syringe pump to deliver a constant flow of 600 μL/h (10 μL/min), 10 μL of each solution was injected into the acetonitrile-acetic acid mobile phase stream, and carried into the mass spectrometer for analysis under standard ESI^+ conditions.

3.5.3.2 ESI^+/ESI^- of PAHs in dichloromethane/hexanes (1:4)

Using the stock solutions of benzene, naphthalene, tetralin, biphenyl, fluorene, phenanthrene, 3-ethylphenanthrene, pyrene and 1-methylpyrene, ESI^+/ESI^- analyses of these PACs were attempted. A Cole-Palmer syringe pump delivered the dichloromethane-hexanes (1:4) mobile phase at a flow rate of 1.8 mL/hr and 100 μL of solution were injected through a Rheodyne valve into the flowing stream. Standard ESI^+/ESI^- conditions were used, except cone voltage = 22V.

3.5.3.3 ESI^+/ESI^- of Standard ES-1

ES-1 stock solution was diluted 1:1 with MeCN+ 2% ethylamine or with MeCN + 2% acetic acid and the solvent used as the mobile phase. In each case, the Waters HPLC pump was set to deliver 0.030 mL/min. Standard ESI^+/ESI^- conditions were used.

3.5.3.4 $APCI^+$ vs ESI^+

A 0.0105 M solution of biphenylene in acetonitrile and acetonitrile+1% acetic acid were prepared. Standard ESI^+ and standard $APCI^+$ conditions were used for analysis with 10 μL sample injection.

3.5.3.5 ESI^+ with Chemical Electron Transfer Reagents (CETRs) and Phenyl-stabilised Cations (PSCs)

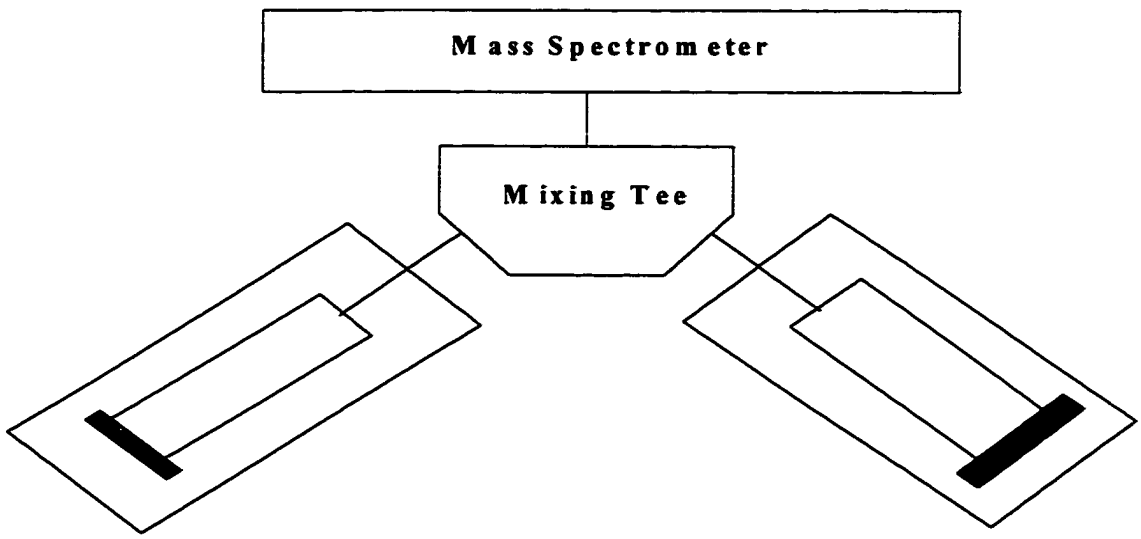

Figure 3.6. Setup for PAC analysis with CETRs and PSCs

3.5.3.5.1 Original Evaluations

2,3-dichloro-5,6-dicyano-1,4-benzoquinone (DDQ) was prepared in CH_2Cl_2/0.1% trifluoroacetic acid (TFA) and diluted to a final concentration of 0.280 mM with the same solvent. ES-2 stock or a 2.5 mM solution of 2,3-benzanthracene was prepared in dichloromethane and diluted 1/50 with 50%methanol-50% dichloromethane, 70%hexane/30% DCM, DCM , DCM/0.1% TFA. The diluted PAH solution was placed in a 10 mL syringe, fitted into the Cole-Palmer syringe pump (see Figure 3.6) and joined to the left hand side of the mixing tee. The DDQ solution was placed in another 10 mL syringe, fitted into the Sage pump and connected to the right hand side of the mixing tee. Both syringe pumps were raised so that the tee junction could be attached directly to the ESI

probe. A continuous stream of PAH standard (0.3 or 1.8 mL/h) was maintained into the spectrometer. 30 scans were obtained, then the DDQ pump was turned on at a flow of 0.35 mL/h for 90 seconds, then turned off and the mass spectrometric response was recorded before and after initiating the flow of DDQ. Standard ESI^+/ESI^- conditions were used but the capillary voltage was increased to 4.00 kV.

This was repeated with similar concentrations of chloranil, (2,4,7-trinitro-9-fluorenylidene)malonitrile, tetracyanoethylene, 7,7,8,8,-tetracyanoquinodimethane, 2,4,7,-trinitro-9-fluorenone and 6,7-dicholoro-1,4-dihydroxyanthraquinone.

3.5.3.5.2 Later Evaluations

Later evaluations used individual PACs from the ES-2 standard to test chemical electron transfer reagents (CETRs) or phenyl-stabilised cations (PSCs). The same MS conditions and experimental setup were used as with complete ES-2 standard with dichloromethane + 0.1% trifluoroacetic acid used throughout. In the first step, solvent was placed in syringe 1 and a constant stream at 1.8 mL/h was introduced into a mixing tee and then into the mass spectrometer source. Air was used as the source gas. After acquiring 30 background spectra, the flow of the CETR/PSC reagent was turned on at 1.5, 3.9 or 21 mL/h from syringe pump 2 into the mixing tee for 30 more scans. Triplicate analyses were performed at each flow rate. The difference in the signal intensity of the solvent alone and the solvent + CETR/PSC was determined. This was the "background" due to the electron transfer reagent.

The syringe containing the solvent was emptied and filled with the appropriate PAC solution. A constant stream of 1.8 mL/h was introduced. After acquiring 30 background

spectra, the flow of the CETR/PSC reagent was turned on at 1.5, 3.9 or 21 mL/h from syringe pump 2 into the mixing tee for 30 more scans. Triplicate analyses were performed at each flow rate. The difference in the signal intensity of the PAC alone and the PAC + CETR/PSC was determined. This was the"analytical signal". The "background signal" was subtracted from the "analytical" signal to give the "corrected" signal.

This sequence was repeated with naphthalene, phenanthrene, pyrene, 2,3-benzanthracene and perylene with each of the chemical electron transfer reagents (DDQ, Chloranil, 6,7-dichloro-1,4-dihydroxyanthraquinone (DDAQ)) and phenyl-stabilised cations (2,3,5-triphenyl–2*H*-tetrazolium chloride (TTZ), triphenylcarbenium tetrafluoroborate (TPSC) and 2,4,6-triphenylpyrylium tetrafluoroborate (TPP)).

3.5.3.5.3 Discrimination of Alkylated Aromatics

Discrimination of Alkylated Naphthalenes by APCI

Solutions of naphthalene (1 mM) and its methyl, ethyl, dimethyl, propyl and1-butyl derivatives were prepared in acetonitrile. These were analysed by flow injection with a flow of 0.200 mL/min flow of 90:10 (v/v) acetonitrile/water, 100 µL injection under standard $APCI^+$ conditions except the cone voltage was varied from 10 to 60 volts. This was to indicate whether these isomers could be distinguished amongst each other at typical APCI conditions.

Discrimination of Alkylated PACs by APCI

Solutions (20 mM) of benzene and some of its mono-, di-,tri-, tetra-, penta- and hexa-methyl derivatives were prepared in acetonitrile. With conditions similar to those used for naphthalene derivatives with the exception of using a cone voltage of 30 volts, the

samples were analysed in scanning (*m/z* 70-170 in 2.90 seconds) and in SIR (0.21 seconds per mass) to determine the extent of derivative discrimination and the effect of substitution on APCI response.

The ability of LC/APCI-MS to distinguish alkylated PACs of a given ring size was tested with standards AB-1 N-1, P-1, PF-1 by the 50301030 gradient with standard $APCI^+$ conditions and a probe temperature of 400°C.

ESI Discrimination of Alkylated Naphthalenes and Pyrenes

Solutions (20 μM) of naphthalene, its mono and dimethyl derivatives, and 2,3,5-trimethylnaphthalene were tested with DDQ and chloranil to determine whether the number and location of alkyl substituents affects the ability of an electron transfer reagent to oxidise PACs and if so, whether differences in reactivity of CETRs can be exploited for derivative discrimination. Standard ESI^+/ESI^- conditions were used, except capillary voltage = 4.00 kV.

Similar experiments were performed with pyrene, 1-methylpyrene, 4-methylpyrene, a mixture of methylethylpyrenes, 1-ethylpyrene, 1,8-diethylpyrene, 1,3-diethylpyrene and 1,6-diethyl-pyrene to determine the effect of number and position of substituents on the ability of PACs to be oxidised by DDQ, chloranil or DDAQ. In addition, 1,2,6,7-tetrahydropyrene, 1,2,3,6,7,8-hexahydropyrene and naphtho[2,3-*a*]pyrene where aromatic rings are reduced or added were tested to determine their effect on electron transfer.

In addition to the evaluation of CETRs and PSCs, and examining the effects of substitution/ring reduction, adduct formation between PAC and CETRS/PSCs was assessed. This was done by maintaining a low cone voltage (15V cone) and broadening the mass spectral range to *m/z* 1000. The most likely complexes to form are 1:1, charged complexes.

3.5.4 Imperial Oil Project

3.5.4.1 Analysis of Imperial Standards 1 through 3 with Skimmer Cone A

The purpose of these studies was to attempt to characterise the nature of the APCI plasma formed by the interplay of analyte molecules, solvent molecules, gas molecules and a corona discharge. This discharge initiates ionisation of species which through ion-molecule reactions ionise the analytes via proton transfer or charge transfer mechanisms. The PAC standards were used to probe the plasma in an effort to better understand the plasma chemistry and its impact on the signal intensity and ionisation mechanism of PACs, with the ultimate goal of optimising the response to these analytes.

Naphthalene, fluorene, phenanthrene, pyrene and chrysene were selected as representatives of the low to mid-mass range of PACs while fluorenone and 6-methyl-1,2,3,4-tetrahydrocarbazole (MTC) were chosen as representatives of the heterocyclic, partially ring reduced and alkylated compounds which may be present in petroleum samples. These standards were prepared in typical HPLC solvents (50:50 (v/v) acetonitrile/water, acetonitrile, hexanes, dichloromethane). Chrysene and MTC were insoluble in hexanes so were left out of the hexanes test mixture. Analytical standards were prepared by a hundredfold dilution of Imperial standards 1 to 3 of the appropriate solvent.

In all cases, the HPLC pump was primed with the selected solvent, all tubing lines were flushed thoroughly and the flow rate of 200 μL/min initiated to the probe. Dewar nitrogen was introduced into all streams (300 sLph for bath and sheath gas, 30 sLph for nebuliser flow) and the mass spectrometer stabilised for 20 minutes. The instrument was then tuned to the optimum running parameters for a given solvent as detailed in Table 3.3.

Table 3.3. Optimum Mass Spectral Parameters for Given Solvents

Solvent	Cone V	Corona V	Source T	Probe T
MeCN/H_2O	30 V	4.00 kV	120°C	350°C
MeCN	30	4.00	120	350
DCM	22	4.50	120	350
Hexanes	22	4.00	100	350

The one mL stainless steel sampling loop was filled with the appropriate analytical standard via a 10 mL syringe loop. This gave about 5 minutes of run time. As this was a pseudo-infusion experiment, background spectra were not acquired. Both scan and SIR functions were used in a data acquisition. The scan function scanned the range from *m/z* 120 to 250 every 2.90 seconds. The SIR function was set up at the appropriate cone voltage with a dwell time of 0.20 seconds at *m/z* 128, 129, 166, 167, 178, 179, 180, 181, 202, 203, 228 and 229 corresponding to the molecular ion and protonated molecule of each component.

Gas Studies

Using one solvent at a time to maximise efficiency, the following experiments were performed using the modified gas box to manipulate gas flows. Gases studied included Dewar N_2, tank N_2, Extradry™ air, building air, O_2, CO_2, CO, CH_4 and H_2.

Table 3.4. Gas Study Experiments Performed

Experiment Type	Description
One gas	one gas in bath (B), sheath (S) and nebuliser (N) streams
Two Gas, Type I	Gas 1 (B+S) - Gas 2 (N)
Two Gas, Type II	Gas 1 (B) - Gas 2 (S+N)
Three Gas	Gas 1 (B) - Gas 2 (S) - Gas 3 (N)

NB: Air and oxygen were not used with hexanes as the mobile phase. A gas or gas combination would be selected and then nebuliser or bath-sheath gas studies undertaken as listed in Table 3.4. Whenever a new gas combination was undertaken, the machine was taken out of operate mode, the solvent flow was stopped, and the appropriate gas valve(s) emptied. The desired gas was introduced, the flow rate adjusted, the solvent flow resumed, and the system allowed to stabilise for five minutes. Nebuliser and bath-sheath gas flow rate studies were then initiated.

As an example, one would begin with Dewar nitrogen, then introduce carbon dioxide in the nebuliser stream, then have nitrogen as bath gas and carbon dioxide as sheath and nebuliser gas, then have an all carbon dioxide system, then introduce tank nitrogen in the bath gas with carbon dioxide in the other two streams and so on. This was repeated as necessary to allow all desired combinations of gases to be studied.

Concerns

In the course of this work, a number of concerns were raised. These included memory effects, cross-contamination, interaction among sample components, effect of orifice size, incorrect calibration, reproducibility of results and applicability of results to real-world analysis of refined petroleum products. These concerns were addressed in a variety of ways. 1) To reduce memory effects and cross contamination, tubing and glassware was labelled "general use" and "solvent-dedicated". When switching solvents, general use materials were used to prime the pump and all lines were flushed for five minutes at 2 mL/min. The lines to and from the pump and probe were removed, dedicated glassware and tubing installed, the

pump primed and the lines flushed for five minutes at 2 mL/min. The flow was reduced to 0.200 mL/min and a stabilisation time of 5 - 20 minutes instituted. Whenever the solvent needed to be changed, general use materials would be installed and the system cleaned to ensure no carryover from the previous solvent. 2) To assess the effect of orifice size and sample interaction, eight solutions were prepared as in Table 3.5 in hexanes.

Table 3.5 Solutions used for Testing Orifice Size and Sample Interaction

Solution #	Components
1	pyrene
2	pyrene + naphthalene
3	pyrene + phenanthrene
4	pyrene + chrysene
5	pyrene + naphthalene + MTC
6	pyrene + naphthalene + phenanthrene + chrysene + MTC
7	pyrene + fluorene + phenanthrene + chrysene + MTC
8	pyrene + MTC

These were analysed with dedicated glassware and tubing with skimmer cones B and C. In addition, the analytical standards derived from Imperial Oil standards were re-analysed with cone C and the results from cones A and C compared, except that only SIR data was used and selected gases or gas combinations were studied. 3) To select the proper calibration range, the instrument was re-calibrated from *m/z* 5-500, rather than *m/z* 20-2000. 4) To address reproducibility issues, all subsequent analyses were done at least with triplicate injections and the appropriate statistics (mean, standard deviation, % relative standard

deviation) calculated. 5) IO standards 1 through 6 were prepared with compounds previously identified in sample fuels and analysed as described below.

3.5.4.2 Analysis of IO Standards 1 through 6 with Skimmer Cone C

In all cases before a study was initiated, the skimmer cone and pepper pot of the APCI source were checked for cleanliness and if required, sonicated in concentrated formic acid for twenty minutes. After sonication, they were rinsed thoroughly with water, rinsed with isopropanol, blotted dry with a Kimwipe, allowed to air dry for thirty minutes and then reinstalled in the source, taking every precaution to ensure no fingerprints were left on the source.

Gas Studies

One solvent at a time was used to ensure efficiency. Each was tested with Dewar nitrogen (all), tank nitrogen (all), building air (all), Extradry™ air (all), carbon dioxide (all), nitrogen or air (bath and sheath gas) - carbon dioxide (nebuliser gas) and nitrogen or air (bath gas) - carbon dioxide (sheath and nebuliser gas). Using dedicated glassware and tubing, a 200 μL/min flow was initiated, the gases were turned on (300 sLph for bath and sheath gas, 30 sLph for nebuliser gas) and the system allowed to stabilise for five to twenty minutes.

IO standards 1 and 2 were diluted one hundredfold with either 50:50 (v/v) acetonitrile/water or acetonitrile while the others were diluted one part in a hundred with the appropriate solvent. Hexanes and dichloromethane were freshly distilled and used within the day to ensure lack of degradation.

A 250 μL stainless steel loop was used for all sample injections. Between standards, the 1mL sample syringe was rinsed with 3 portions of 300 μL and the sample loop rinsed

with three portions of 250 μL via a 250 μL syringe. In all cases, 200 μL of each standard was loaded into the loop and replicate injections made.

Four data acquisition functions were set up. Analyses of the standard and background were performed by single ion recording with a 0.2 sec dwell time at each mass of *m/z* 128, 129, 166, 167, 168, 178, 179, 184, 185, 194, 195, 202, 203, 228, 229, 252 and 253 at 15, 30 and 50 volts cone. The solvent background was obtained by scanning the *m/z* range from 5 to 300 every second.

Ten scans of background were acquired, the analyte injected, the TICs monitored and the acquisition continued for 5 - 10 scans after returning to baseline. In each of the SIR runs of standard, the background at that cone voltage for that function was subtracted for the analytical signal at these conditions to give the corrected signal at each *m/z*. The mass lists were obtained and plots of total intensity or $[M+H]^+/M^{+\bullet}$ for a given ion as a function of gas combination were prepared. For the background spectra, the first ten scans were averaged and the intensity of the background ions as a function of gas combination statistically analysed.

Background Studies

To prevent memory effects from previous analyses, the solvent lines were disconnected, the probe plugged up, and the probe and source were heated to their maximum temperatures, 500°C and 190°C, respectively, with a constant stream of nitrogen. This was maintained for twenty to thirty minutes to allow vapourisation of all samples or solvents remaining in the probe or adsorbing to source walls. The source and probe were cooled down to 120°C and 350°C, respectively. The gas background spectra were acquired at 4.25 kV

corona, gas flows of 300 sLph for bath and sheath gases and 30 sLph for nebuliser gas and 15, 30 and 50 volts cone with Dewar nitrogen, tank nitrogen, building air and Extradry™ air with scan functions of *m/z* 5 - 300 with one second scans. Whenever a gas was changed, ten to fifteen minute equilibrations were instituted.

All solvent background studies were performed with dedicated glassware. A flow rate of 0.200 mL/min was used for all runs and analysed by the same procedure as the gases.

Ion Confirmation

The structural formulae of gas and solvent background ions were confirmed where possible by MS/MS or by cone voltage studies. Ions were selected and enough collision gas introduced to reduce their intensities 50 -75%. Cone voltages of 15V were used throughout the MS/MS experiments. For precursor ion studies, collision energies were set to 30 or 50 eV while for product ion studies, 20, 40 and 60 eV collision energies were used. For precursor ion studies, the mass range studied would cover $M^{+\bullet}$ mass up to *m/z* 250 while for product ions, the range from *m/z* 5 to $[M + 5]^{+\bullet}$.

Contrasting the spectra of ions at cone voltages of 15, 30 and 50 V also served to give indications of the source and fate of ions. These reinforced the data from the MS/MS experiments.

Chapter 4

Optimisation of Instrumental Parameters for the Analysis of PACs

4.1 Optimisation of APCI-MS

There are a number of instrumental parameters which can have an impact on the performance of the mass spectrometer and thus, the analysis of polycyclic aromatic compounds. These include the reliability of the liquid delivery system, the solvent flow rate, the source gas flow rates (bath, sheath and nebuliser), the vertical position of the APCI probe relative to the skimmer cone, scanning vs. single ion recording, the scan range, the corona voltage, the cone voltage, the source temperature and the probe temperature. Other factors which can also have an impact include the injection solvent, the concentration of the species, the source gas used and the mobile phase composition. All of these factors, with the exception of the mobile phase composition which is dealt with in Chapter 5, will be addressed.

NB: The terms response, signal, signal intensity and signal strength are used throughout the thesis. Unless otherwise stated, these terms refer to the sum of the background-corrected peak height for the molecular ion and for the protonated molecule of the species of interest. Also, most optimisation experiments were carried out with single injections under a given set of conditions. Thus, it is not possible to statistically evaluate the results and the graphs lack error bars.

4.1.1 Effect of the Liquid Delivery System

The liquid delivery system must deliver a constant stream of solvent and where applicable, analyte, to the mass spectrometer. Pulses in the rate of delivery will cause

variations in ion yields which can lead to errors in averaging and subtraction routines. Comparability of LC pumps is also an issue where a dedicated LC pump is not available. These issues were addressed by comparing the Shimadzu LC-10AT pump, the Sage syringe pump, the Micromeritics pump and the Hewlett-Packard (HP) pump for their ability to deliver 0.3 mL/min of 50:50 (v/v) acetonitrile/water. The results indicate that: 1) the APCI probe provided a high back pressure which interfered with the proper functioning of the syringe pump, 2) the Micromeritics pump, not commonly used, proved difficult to purge and to control the flow rate and 3) the Shimadzu and HP pumps were comparable. This indicates that some pumps can be used interchangeably but caution should be exercised. Another issue is the comparability of two pumps to deliver a gradient. The HP and Waters pumps were compared for their ability to separate the components of LC mix-1 by the 503010030 gradient (50:50 (v/v) acetonitrile/water for the first thirty minutes, then a linear increase to100% acetonitrile over the next thirty minutes) on a Vydac™ column. The results, presented in Table 4.1, show that the order of elution and the but the intensity of the ions with the Waters system are somewhat higher. The latter may be due to injection irreproducibility but the other observations are consistent with the two pumps delivering similar flows and combinations of solvents at a given time. The peaks tend to emerge later in the Waters system which may be the result of different dead volumes and/or the intolerance of the Waters pump for 100% water, which necessitated premixing of the 50:50 (v/v) acetonitrile/water and the slight adjustment of the gradient to ensure that at a given point in the gradient, the composition of the Waters and HP mobile phases was identical.

Table 4.1. Signal Intensity and Retention Time of LC mix-1 Components by Gradient Separation

Compound	Signal with HP System	Signal with Waters System	Retention Time with HP System (sec)	Retention Time with Waters System (sec)
Benzene				
Naphthalene	1.26e4	1.71e4	630	765
Fluorene	1.50e4	2.44e4	960	1260
Anthracene	4.36e4	4.19e4	1170	1560
Phenanthrene	1.04e5	6.11e4	1410	1980
Pyrene	4.54e4	1.14e5	2160	2790
3-ethylphenanthrene	5.73e3	1.82e4	2160	2790
2-ethylphenanthrene	5.60e2	8.50e3	2490	3030
1-methylpyrene	2.15e4	1.67e5	2730	3240
1-ethylpyrene	1.00e4	1.55e4	2940	3420

4.1.2 Effect of the Solvent Flow Rate

The effect of pump pulsations is likely to be more apparent at low flow rates than at high ones but solvent flow rate can also have an impact on the yield of reagent ions, the nebulisation and desolvation efficiency, and the number of collisions an ion will undergo in the mass spectrometer source. To test the effect of this parameter, a 50:50 (v/v) acetonitrile/water mobile phase was prepared. The Shimadzu LC-10AT pump was used to deliver flow rates from 0.020 to 1.800 mL/min of solvent. Figure 4.1 shows the TIC (*m/z* 100 to 400) as a function of solvent flow rate. The ion yields seem to rise linearly up to between

0.3 and 0.4 mL/min, then appear to saturate at higher flows, seeming to indicate that an upper limit for ion production exists. These results indicate that the flow rate does have an impact on ion yields for solvent backgrounds. The standard deviation for the case of 1.8 mL/min is particularly bad though no explanation can be offered for this behaviour. There is no advantage, in terms of solvent ionisation, to using flows above 0.500 mL/min and the system is useable down to 0.020 mL/min, which indicates that both flow injection analysis (typically 200 μL/min) and column chromatography (typically 1 mL/min) can be successfully coupled to APCI-MS.

4.1.3 Effect of the Bath and Sheath Gas Flow (Original Gas Box)

With the original gas box, only two streams were available - the bath gas and sheath gas streams. A portion of the gas flow from the sheath gas stream was used for nebulisation. The bath gas is responsible for preventing collisions of ions with the walls of the mass spectrometer source, the sheath gas guides the ions into the skimmer cone orifice and the nebuliser gas assists in converting the liquid introduced into a fine mist of small droplets. Dewar nitrogen in all gas streams, an acetonitrile mobile phase and 100 μL injections of 0.5 mM fluorene were used to probe the effect of the bath gas and sheath gas flow on signal intensity and ionisation mechanism, plotted in Figures 4.2 and 4.3, respectively. The results indicate that the bath gas flow rate, except for the anomalous result at 100 sLph, has little effect either on the total signal or on the $[M+H]^+/M^{+\bullet}$ ratio. This suggests that the bath gas flow rate is not a major contributor to controlling ion residence time nor does the bath gas appear to participate in ion-molecule reactions with the solvent or analyte. The sheath and nebuliser gas flow rates do have an impact both on the signal intensity.

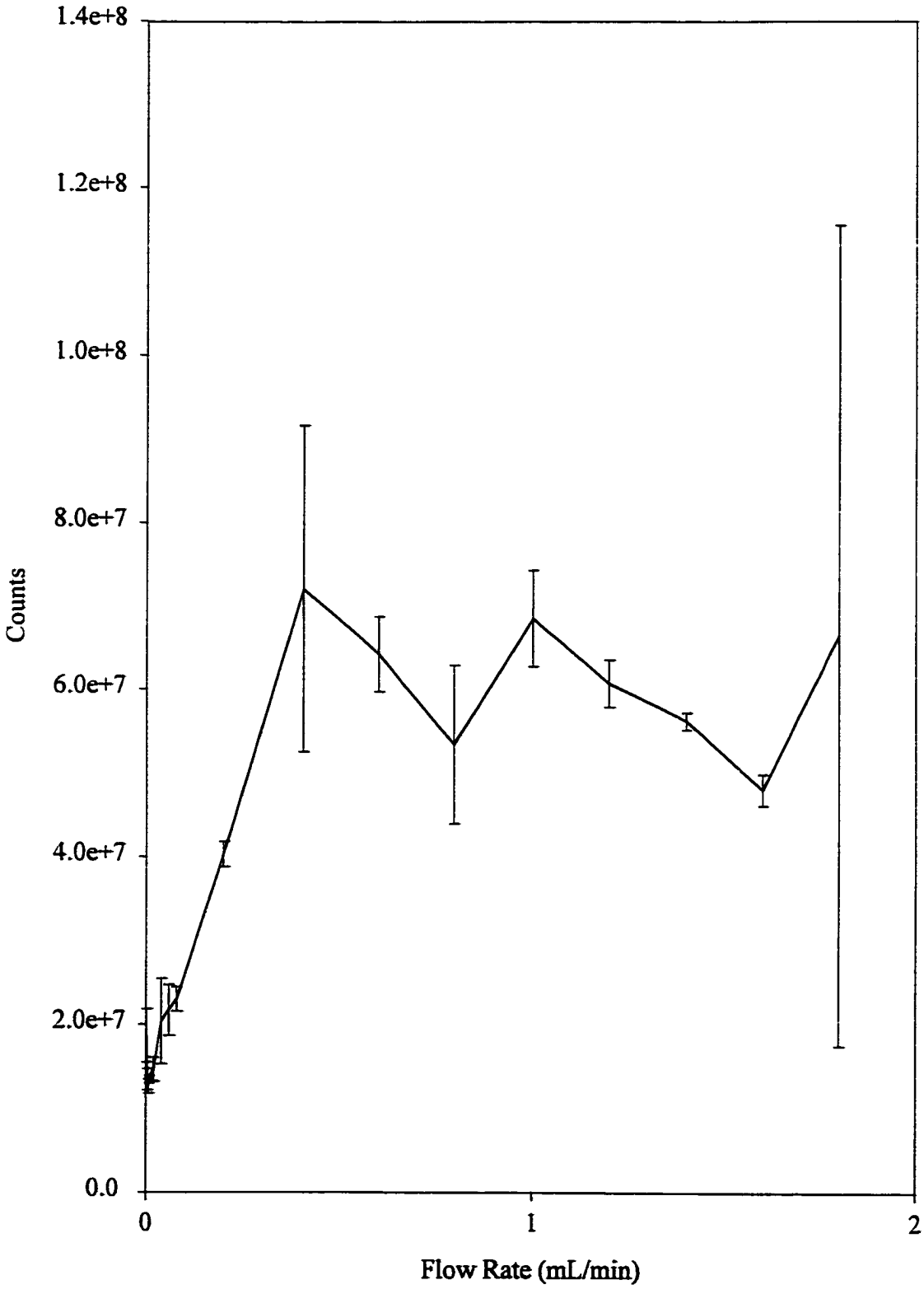

Figure 4.1. Effect of Solvent Flow Rate on Total Ions Observed in $APCI^+$ mode.

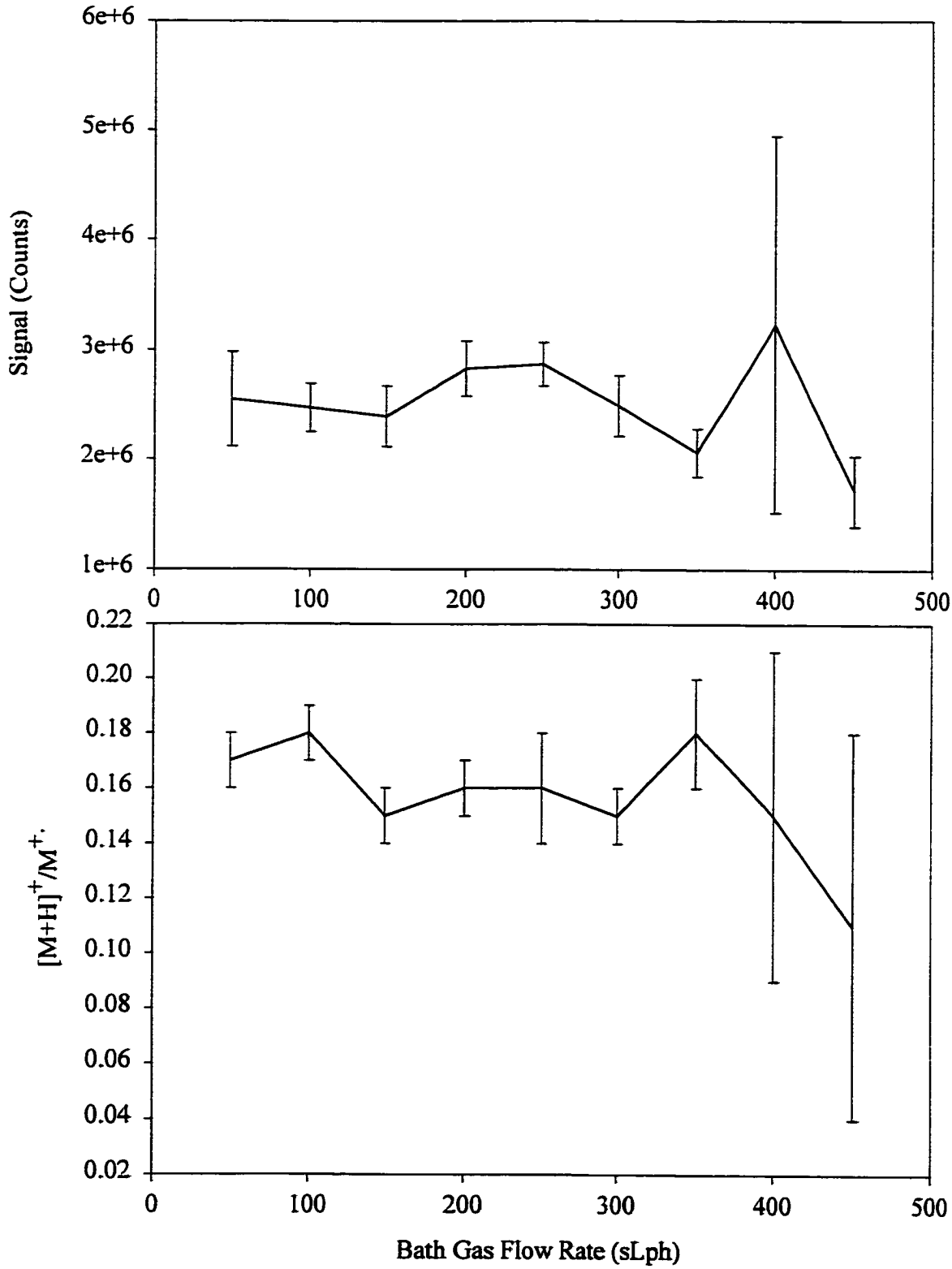

Figure 4.2. Effect of bath gas flow rate on total signal and ionisation mechanism of 0.5 mM fluorene in acetonitrile.

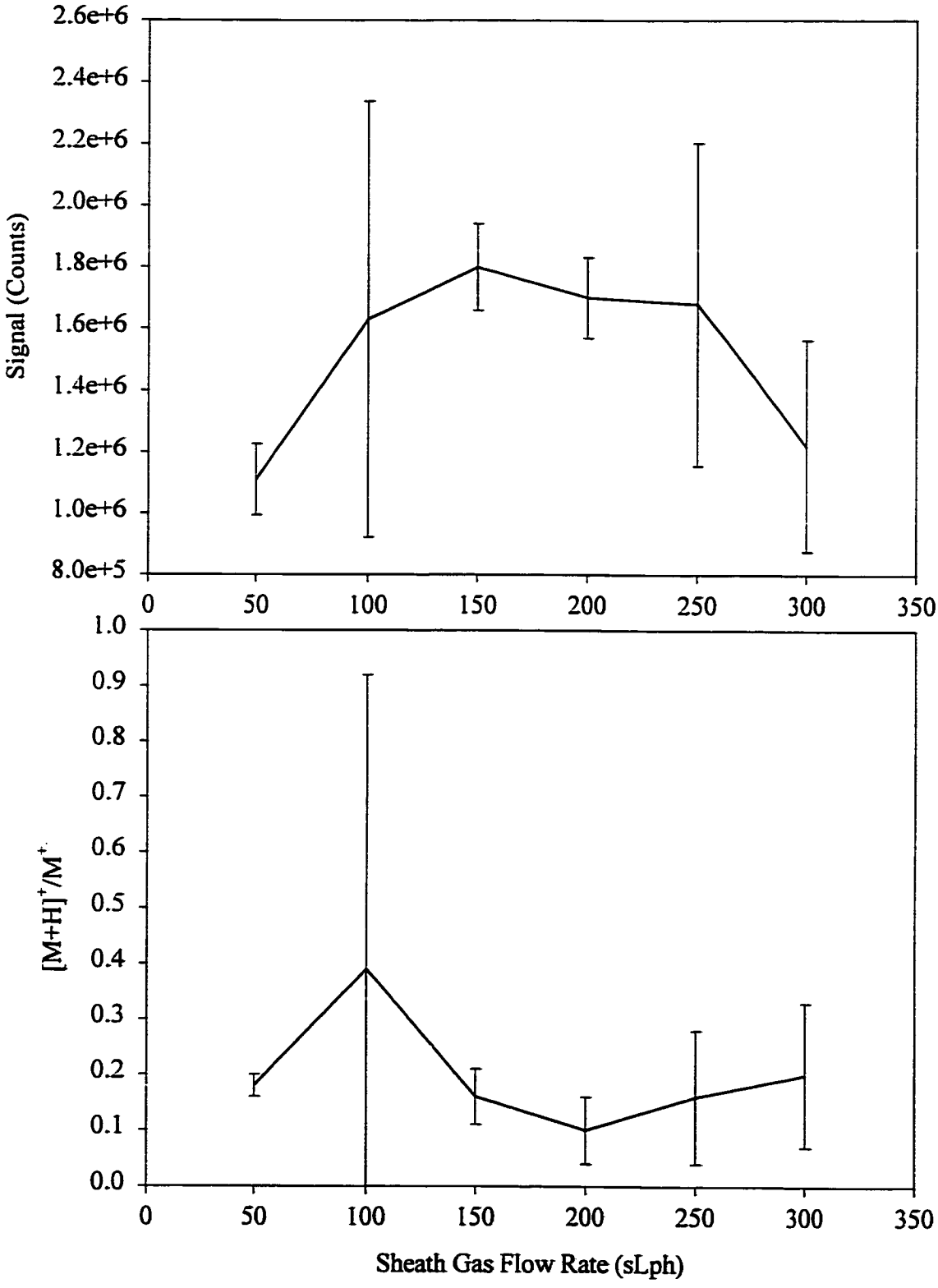

Figure 4.3. Effect of sheath gas flow rate on total signal and ionisation mechanism of 0.5 mM fluorene in acetonitrile.

4.1.4 Effect of the Bath, Sheath and Nebuliser Flow Rates (Modified Gas Box)

With the modified gas box, the bath, sheath and nebuliser gas streams were separated and the flows could be independently controlled. The effects of the flow rates of these three gases on the signal intensity, and $[M+H]^+/M^{+\bullet}$ of 5 PACs in heptane are depicted in Figures 4.4 - 4.6. These studies were performed with a continuous infusion of a 10 μM solution of naphthalene, fluorene, phenanthrene, pyrene and benzo[a]pyrene. The results indicate a regular decrease in the TIC (not depicted) as the bath gas flow rate is reduced. Reducing the bath gas flow would reduce the number of ions formed from the gas (resulting in background ions) and would make ion transmission less effective. Either one or both of these phenomena could be responsible for the decreasing TIC with decreasing bath gas flow. The response of the analyte saturates at 300 sLph and the ionisation mechanism is unaffected by bath gas flow at values equal to or less than 300 sLph, as observed with the fluorene-only standard with the original gas box. This again suggests that the bath gas is implicated in ion transmission but not in ion-molecule reactions.

The results of the sheath gas flow rate study indicate that the TIC (not depicted) is largely unaffected by the sheath gas flow, suggesting that this gas is not being ionised, the solvent is accounting for much of the background or it is not as strongly involved in ion transmission as the bath gas. Examining the individual components (Figure 4.7) suggests that naphthalene is easier to detect and exists predominantly as the molecular ion at low flow rates but the higher mass species are favoured, in terms of total signal and protonation, by higher gas flow rates.

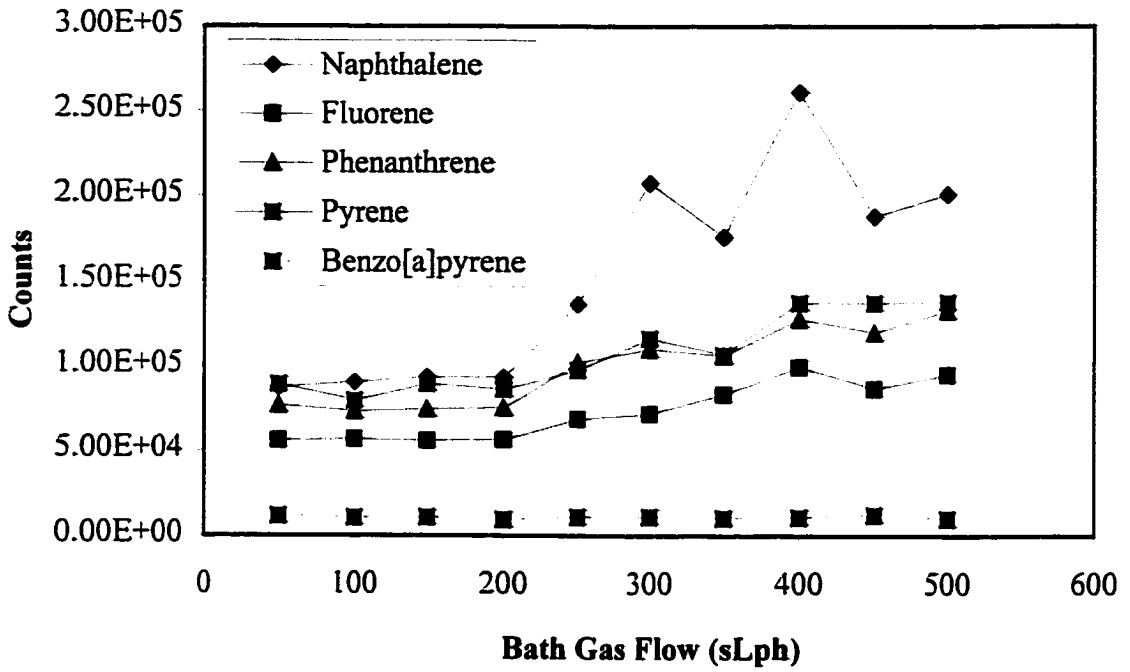

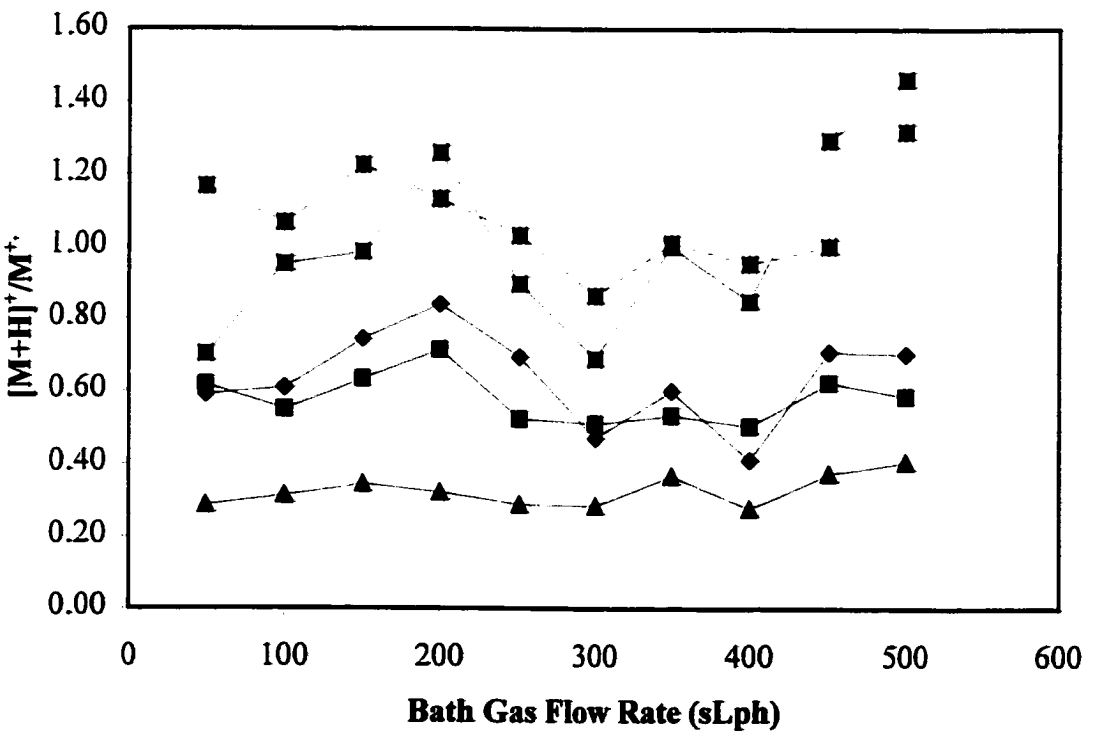

Figure 4.4. Effect of Bath Gas Flow Rate in $APCI^+$ on Total Signal and Ionisation Mechanism of PACs in Heptane.

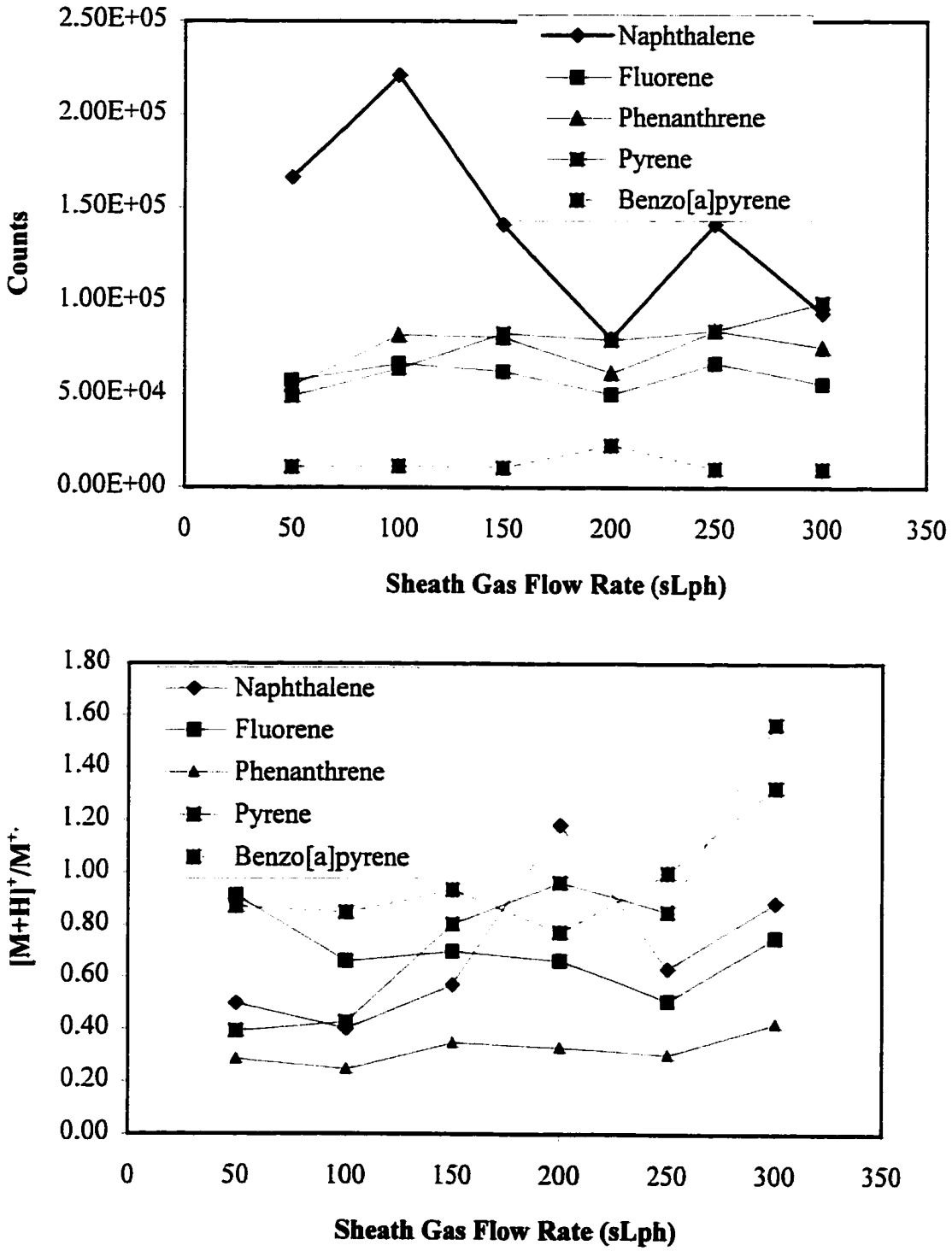

Figure 4.5. Effect of Sheath Gas Flow Rate on Total Signal and Ionisation Mechanism of PACs in Heptane.

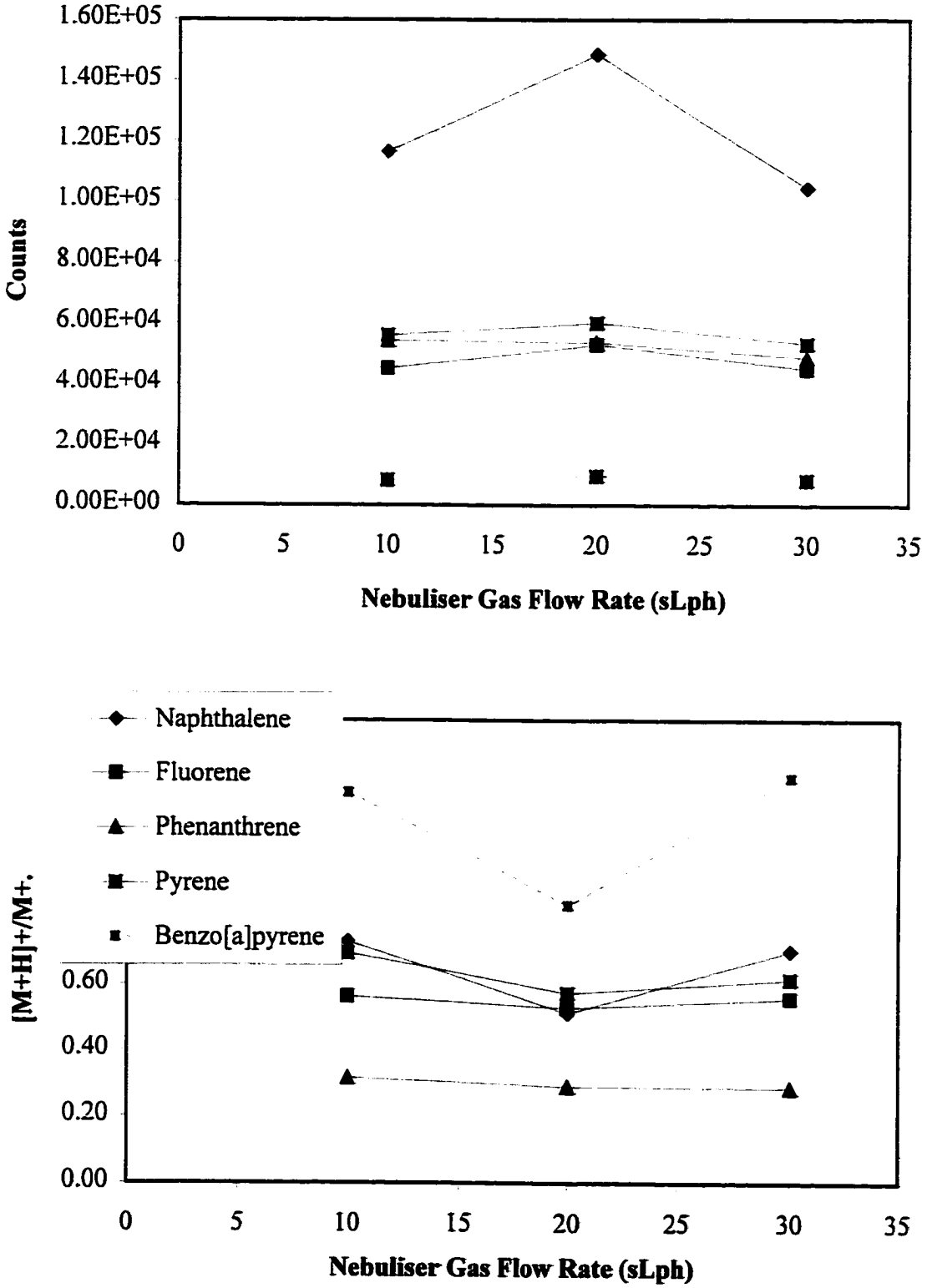

Figure 4.6. Effect of Nebuliser Gas Flow Rate on the Total Signal and Ionisation Mechanism of PACs in Heptane.

A potential means of explaining the experimental results requires making certain assumptions. Assumption 1 is that gas only background is the weighted sum of the ions due to the bath, sheath and nebuliser flow. Therefore, if the bath and nebuliser flow stay constant, reducing the sheath gas flow will reduce the number of gas ions. Assumption 2 is that the sheath gas is not directly implicated in solvent ionisation. Therefore, if the sheath gas flow rate is reduced, the yield of solvent ions should be unaffected but the ratio of solvent ions to gas ions should increase. The third assumption is that the solvent is responsible for protonation and the gas-derived ions for charge exchange. If so, the ratio of protonated molecule to molecular ion should increase with decreasing sheath gas flow as the ratio of solvent ions to gas-derived ions increases. This is not backed up by the experimental results.

If we change assumption 2 such that the sheath gas is involved in solvent ionisation, reducing the sheath gas flow will reduce the yield of solvent ions and the ratio of solvent ions to gas ions will decrease, resulting in more charge exchange as the flow rate is reduced. This concurs with the experimental results. This demonstrates that the sheath gas is strongly implicated in the ion-molecule reactions responsible for PAC analysis.

The nebuliser flow rate appears to have its optimum at 20 sLph but has no effect on ionisation mechanism. This is consistent with this gas stream being responsible only for efficient production of fine mists of droplets. Nebulisation efficiency will be influenced by solvent viscosity, with lower viscosity being associated with better nebulisation. Hence, organic solvents should spray better than water. NB: The fluorene and the 5-component heptane standards are used for all optimisation experiments, unless otherwise specified.

4.1.5 Effect of the Probe Position

How much of the solvent and gas ions introduced into the probe will be able to reach the skimmer cone will be affected by the vertical position of the probe relative to the skimmer cone orifice, this being controlled by the probe position adjustment device. Using the fluorene standard as a test solution, the probe position adjustment device was manipulated to its most downward position (defined as 0 cm) and was turned up by successive turns until reaching its most upward position (defined as +4 cm). The results, presented in Figure 4.7, indicate that the optimal position is one turn down from the most upward position (+ 3.7 cm) in terms of response, indicating that this position provides optimal entry to the analyser. The $[M+H]^+/M^{+\bullet}$ ratio is unaffected by the probe position. This is expected if it is the solvent which is most strongly implicated in the ionisation of the analyte and is transferred in the same proportion to the analyte, regardless of the probe position but the actual number of ions transmitted may change.

4.1.6 Effect of the Acquisition Mode (Scanning vs. Single Ion Recording (SIR))

The actual number of ions will affect the corresponding signal intensity. As the number of sample ions increases, the response will also increase. However, transmission of high numbers of ions, unrelated to the analyte, will result in significant chemical noise which will erode the signal-to-noise ratio. Instrumentally, this noise can be addressed by manipulating data acquisition routines - scanning vs. single ion recording (SIR) and scan range. As only the masses of interest are examined in SIR, it is generally two or more orders of magnitude more sensitive than scanning. Where unknowns must be analysed, scanning is the only option and the available means of improving response is to avoid the *m/z* regions

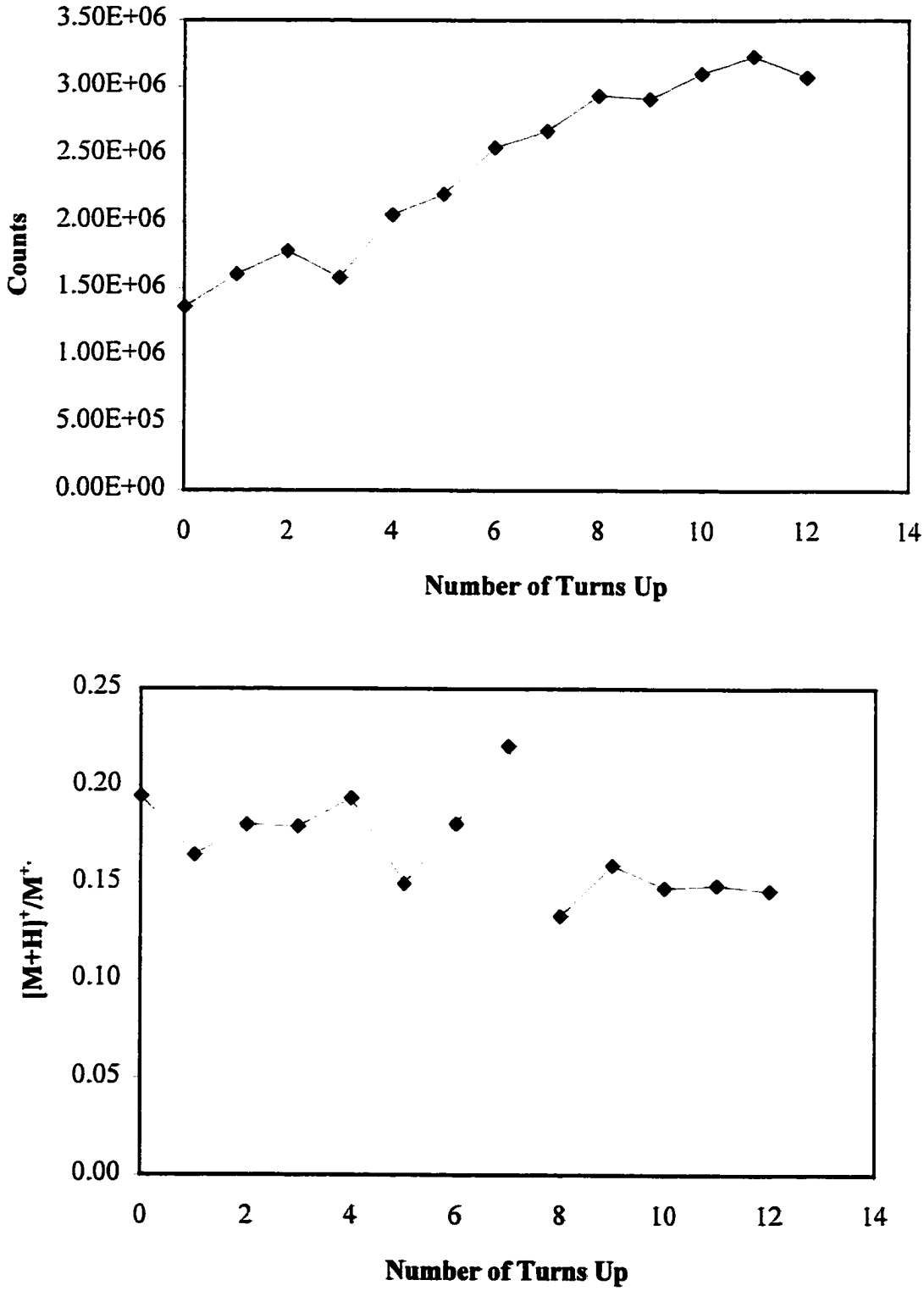

Figure 4.7. Effect of Probe Position with respect to Skimmer Cone on the Signal Intensity and Ionisation Mechanism of 0.5 mM Fluorene in Acetonitrile.

characteristic of high background (usually associated with solvent clusters) and to increase the dwell time by scanning for as long as possible over as narrow an *m/z* range as possible. This was addressed by performing a gradient LC/MS separation of LC mix - 1 thrice. In the first analysis, the *m/z* range of 70-350 was scanned every three seconds, in the second the same range was scanned in 1.50 seconds and in the third the molecular ion peaks were examined for 0.50 s/mass. The results presented in Table 4.2 indicate that increasing the dwell time in a scanning function was usually associated with better response.

The factors discussed above will be largely unaffected by the manner of liquid introduction (flow injection or chromatography) or by the nature of the solvent. The optimum corona voltage, cone voltage and source temperature were observed to be highly solvent dependent and the probe temperature was sensitive to the manner of liquid introduction.

Table 4.2. Effect of Data Acquisition Mode and Dwell Time on PAC Signal and Signal-to-background (S/B) Ratio

Compound	Scan - 3 s		Scan - 1.50 s		SIR	
	Signal	S/B	Signal	S/B	Signal	S/B
Naphthalene	2.05e4	2.32	2.17e4	1.79	5.08e3	2.70
Fluorene	3.10e4	1.90	2.15e4	1.57	2.45e3	2.14
Anthracene	6.71e4	7.80	5.61e4	4.89	6.42e3	4.97
Phenanthrene	8.23e4		6.29e4		6.72e3	
Pyrene	7.22e4	1.97	6.74e4	2.61	2.79e3	4.40
3-ethylphenanthrene	2.02e4	1.62	2.33e4	0.90	2.30e4	1.13
2-ethylphenanthrene	1.35e4		1.03e4			
1-methylpyrene	1.48e5	6.85	1.34e5	3.81	3.22e3	9.08
1-ethylpyrene	2.05e4	0.78	1.64e4	1.85	1.1e2	1.30

4.1.7 Effect of the Corona Voltage

The corona voltage ultimately determines the ion yield. A high corona discharge needle voltage may ionise even difficult to ionise compounds and may impart significant fragmentation energy to the ions, resulting in greater fragmentation, or it may just give a higher current. Figure 4.8 shows the heptane background at 2, 3.5 and 5 kV. These spectra indicate that the heptane is poorly ionised and fragmented at a corona voltage of 2.00kV, is reasonably well-ionised and fragmented at 3.5 kV (consistent with a higher input of energy) and ion yields increase further at 5.0 kV. The ionisation of the analyte is similar to that of the solvent, see Figure 4.9, which demonstrates an increasing signal intensity up to 4.5 kV. Thus, ionisation of the solvent appears to be a necessary prerequisite for the ionisation of the analyte, though the ionisation of solvent and analyte could proceed in series or in parallel. Naphthalene appears to be most affected by the increase in corona voltage, consistent with its being difficult to analyse (both charge exchange and proton transfer are energetically unfavourable). All the PACs exhibit suppressed protonation as the corona voltage is increased, perhaps this being linked to shorter residence times (the larger the voltage applied, the greater the difference in potential between the corona needle and the counter electrode, and the ions will be accelerated more), direct ionisation of the PACs or fragmentation of $[M+H]^+$ to $M^{+\bullet}$ with increasing voltage. There was no clear correlation between corona voltage and fragmentation of the analyte or solvent. Table 4.3 lists the optimal corona voltages for the most commonly used solvents. The optimal corona voltage is in the range of 4.00 to 4.50 kV, considerably higher than the manufacturer's recommendation of 3.5 kV. As the needle gets older, ion yields will be significantly decreased, as supported by

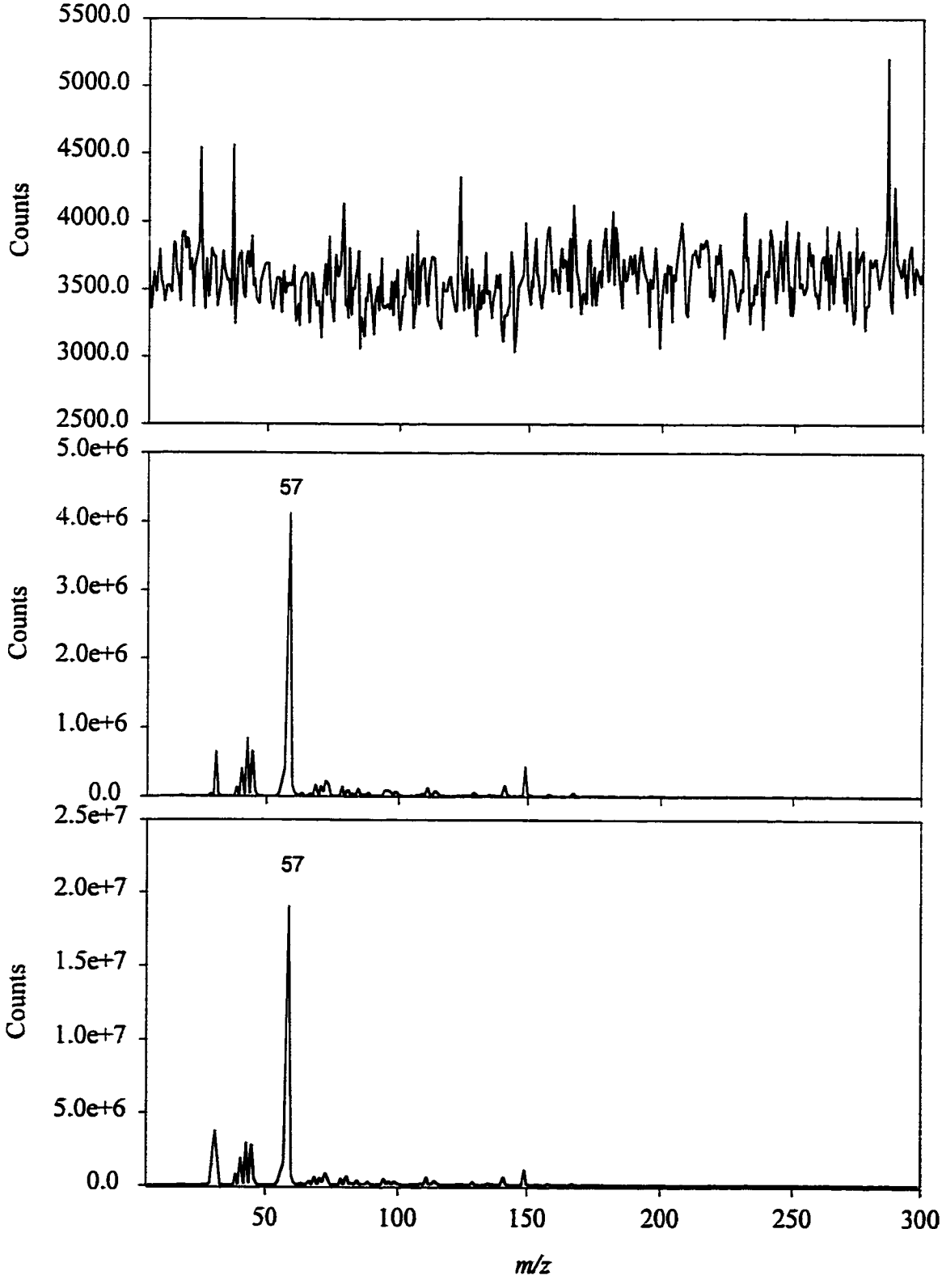

Figure 4.8. Heptane background in APCI+ mode at a corona voltage (from top to bottom) of 2.00, 3.50 and 5.00 kV.

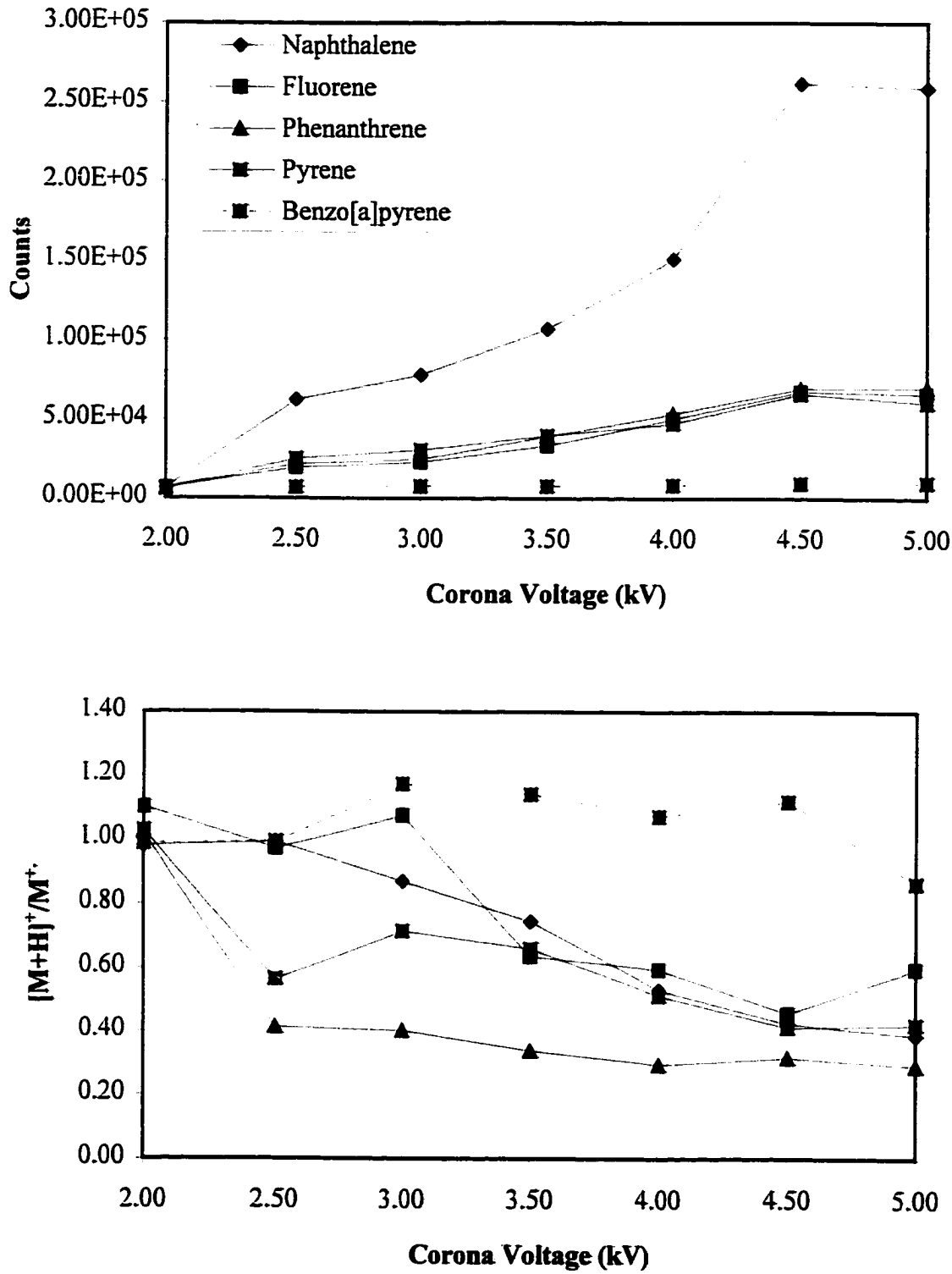

Figure 4.9. Effect of Corona Voltage on Total Signal and Ionisation Mechanism of PACs in Heptane.

experimental evidence that changing the corona needle resulted in a dramatic increase in signal intensity.

Table 4.3. Optimal Corona Voltage for Ionisation of PACs as a Function of Solvent

Compound	Optimum Corona Voltage (kV)
50:50 (v/v) acetonitrile/water	4.00
Acetonitrile	4.00
Dichloromethane	4.50
20% dichloromethane - 80% hexanes	4.00
30% dichloromethane - 70% hexanes	4.00
Hexanes	4.00
15% toluene - 85 % hexanes	4.50
15% trifluorinated toluene - 85 % hexane	4.50

4.1.8 Effect of the Cone Voltage

The cone voltage determines the degree of collisional energy input and thus, the fragmentation of the ionised species. Figure 4.10 shows the background of heptane at cone voltages of 10, 22, 40 and 100 volts. These spectra show, as expected, that as the cone voltage is increased, the solvent is more significantly fragmented. How this solvent fragmentation is reflected in the signal intensity and ionisation mechanisms of PACs is addressed in Figure 4.11. The results indicate that at low cone voltages, peak intensities are highly irreproducible, possibly due to interfering cluster ions of the same *m/z* as the analytes or a loss of analyte to clusters. An optimum is reached at 22 cone V and subsequent increases in voltage result in decreased signal intensity and increased fragmentation. *M/z* 57 ($C_4H_9^+$)

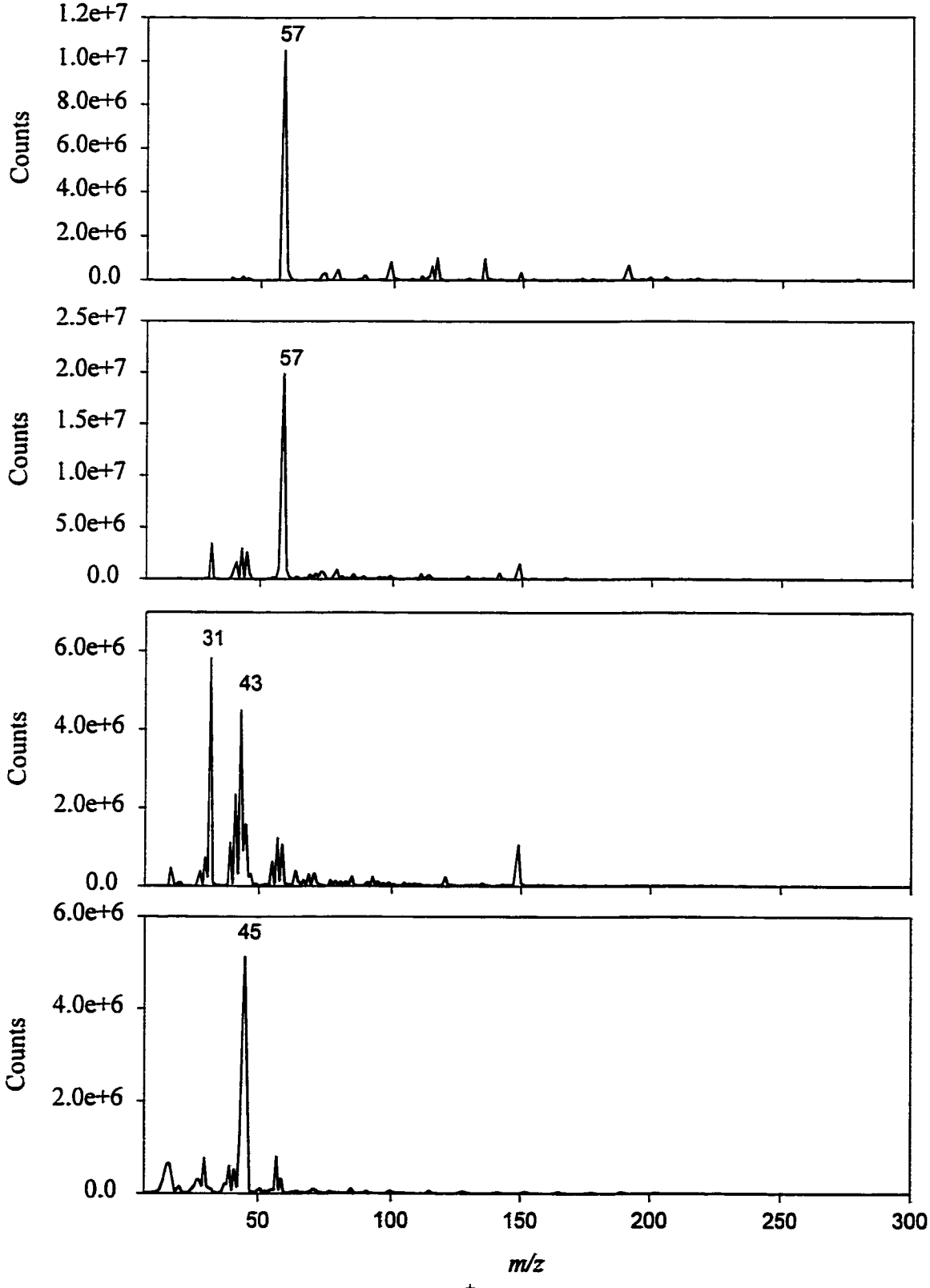

Figure 4.10. Heptane background in $APCI^+$ mode at (from top to bottom) 10, 22, 40 and 100 V cone.

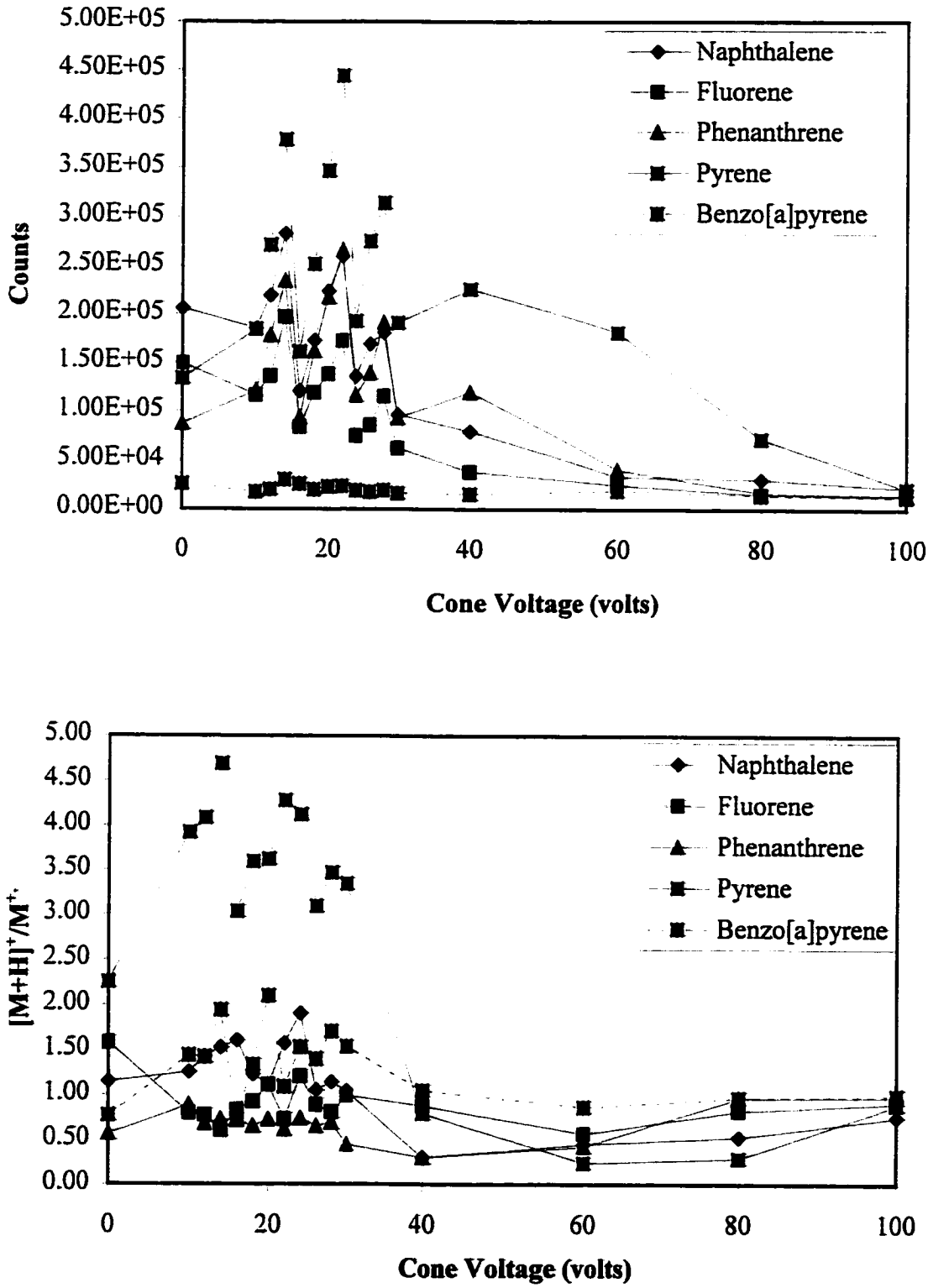

Figure 4.11. Effect of Cone Voltage on the Signal Intensity and Ionisation Mechanism of PACs in Heptane.

is the principal reagent species in the ionisation of PACs, hence where its level is high, PACs are well-protonated and response is high but where its abundance is low, PACs are poorly protonated and response is poor. Thus, where one reagent species is clearly implicated in the analyte ionisation, optimising its population should maximise analyte response. The optimal cone voltages for the other solvents are presented in Table 4.4. These results indicate that there are wide variations in the energy required to generate appropriate reagent ions with which to ionise PACs. As expected, acetonitrile with its stable triple bond is more difficult to ionise than the saturated alkane solvents.

Table 4.4. Optimal Cone Voltages For Ionisation of PACs in the Solvents Studied

Compound	Optimum Cone Voltage (V)
50:50 (v/v) acetonitrile/water	30
Acetonitrile	30
Dichloromethane	22
20% dichloromethane - 80% hexanes	30
30% dichloromethane - 70% hexanes	30
Hexanes	22
15% toluene - 85 % hexanes	22
15% trifluorinated toluene - 85 % hexane	22

4.1.9 Effect of the Source Temperature

The source temperature must be high enough to keep vapourised solvents and analytes in the gas phase, as condensation will result in dirtying of the source (leading to a decrease in sensitivity) and in smaller amounts of gas phase species available for reaction. Using heptane as the example, the TICs and the analysis of the individual components of the

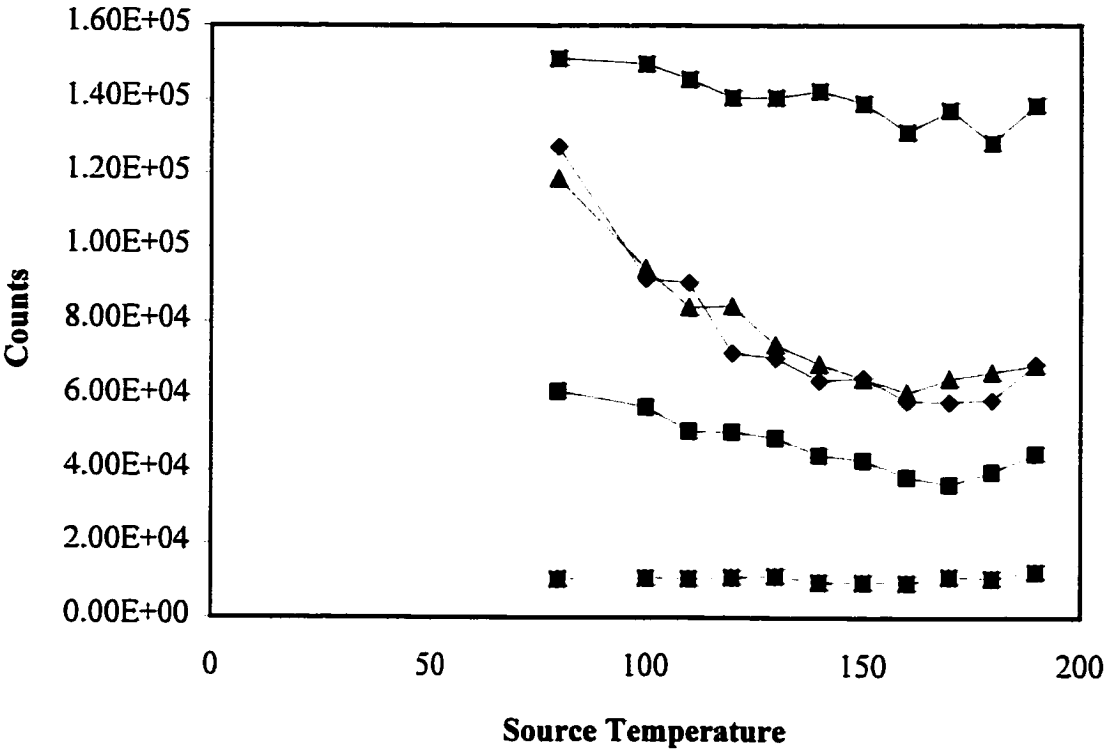

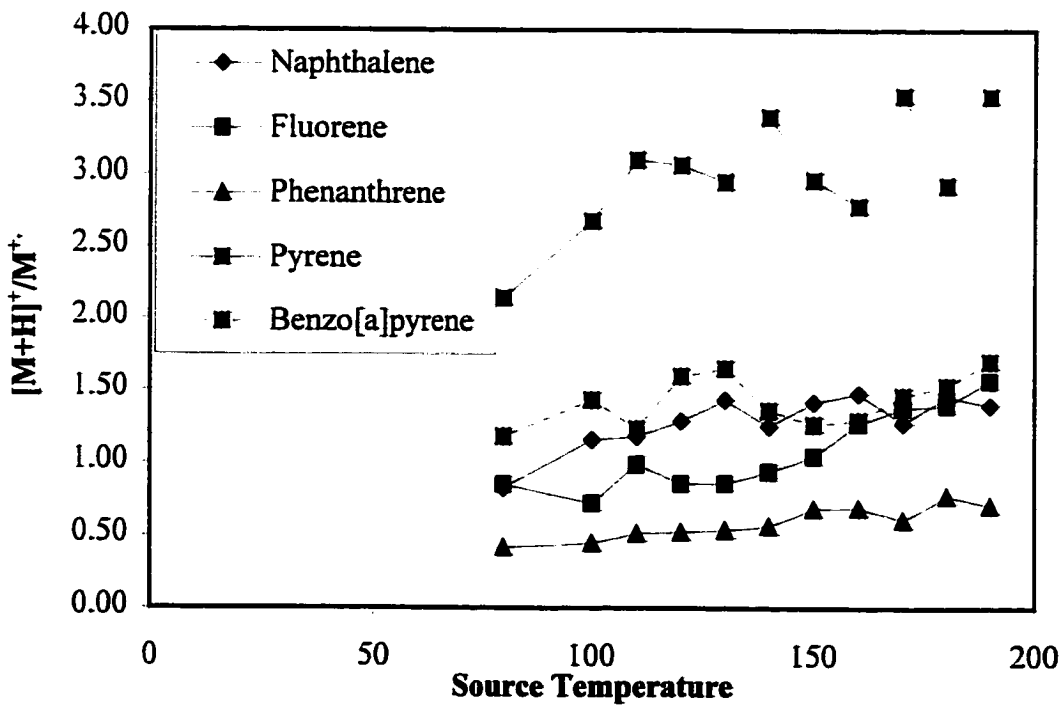

Figure 4.12. Effect of Source Temperature on Signal Intensity and Ionisation Mechanism of PACs in Heptane.

standard, see Figure 4.12, indicate that the optimum temperature is 130°C for benzo[*a*]pyrene and 80°C for the other compounds, which is above and below, respectively, the boiling point of heptane at 98°C. The source temperature has little impact on the signal intensity of benzo[*a*]pyrene, likely due to its high vapour pressure, making it difficult to maintain it in the gas phase. The source temperature has little impact on the $[M+H]^+/M^{-\bullet}$ ratio which is to be expected as it should not alter the nature of the ions present in the plasma, other than maintaining them as gas phase entities.

4.1.10 Effect of the Probe Temperature

The probe temperature must be maintained high enough to permit rapid and efficient vapourisation and desolvation of analytes. This step is a necessary precursor to ionisation of the analyte by solvent-derived ions via charge exchange or proton transfer mechanisms. Figure 4.13 demonstrates the effect of probe temperature on total signal and ionisation mechanism of PACs in heptane solvent. The results indicate that the increase of probe temperature is generally associated with a decrease in TICs and in the total signals, presumably due to declustering of background- and interference-generating species, but probe temperature had little impact on the $[M+H]^+/M^{+\bullet}$ ratio. This is to be expected as the probe temperature should not affect the energetics of the ionisation reactions. Optimal probe temperature will be affected by the liquid flow rate. With flow injection analysis, solvent is being introduced at a rate of 200 μL/min which can be efficiently vapourised at 350°C whereas in HPLC, mobile phase is introduced at 1000 μL/min for which 500°C is optimal for vapourisation.

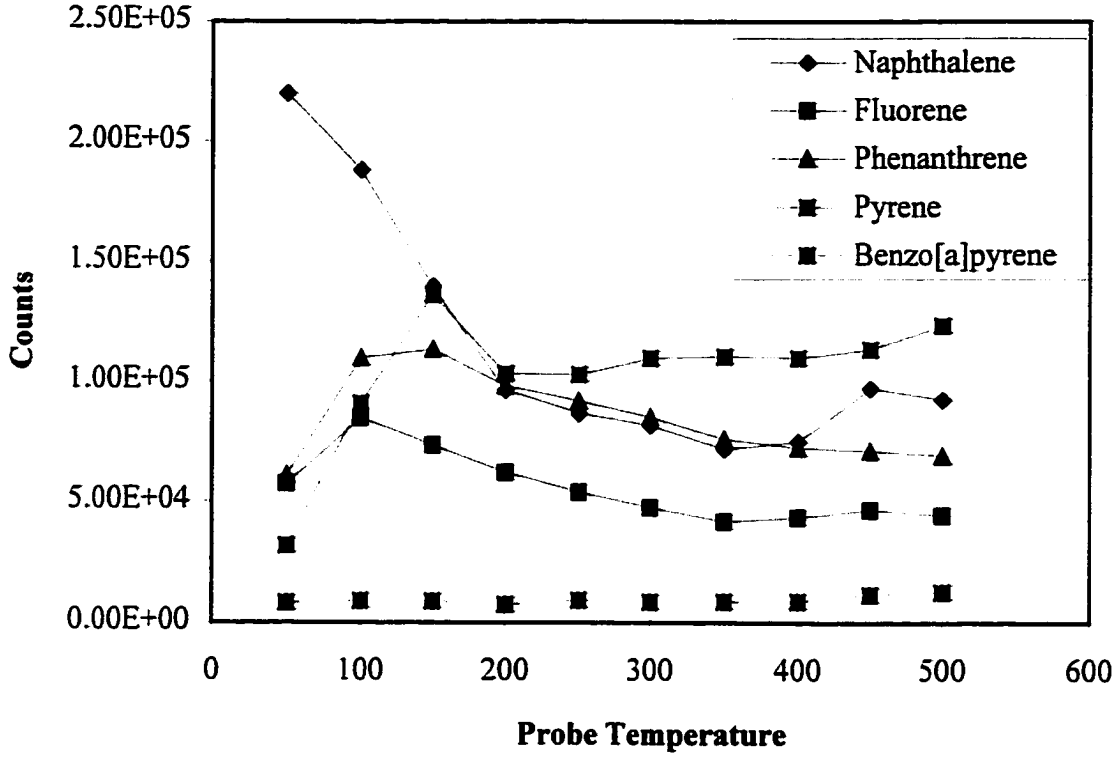

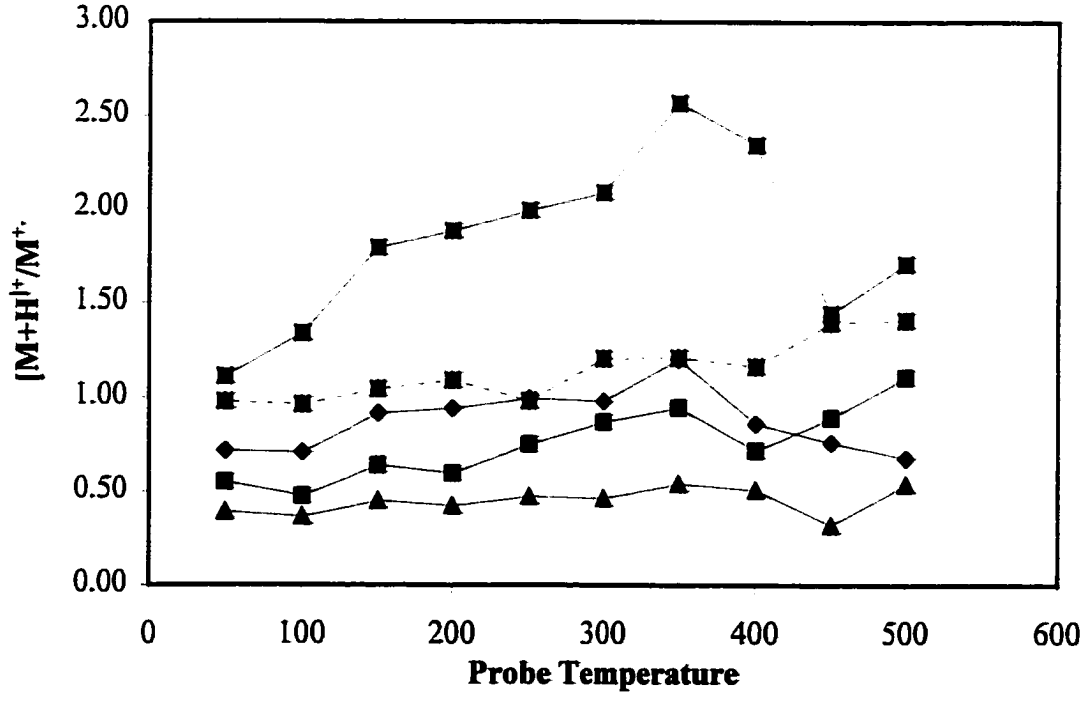

Figure 4.13. Effect of Probe Temperature on Signal Intensity and Ionisation Mechanism of PACs in Heptane.

4.1.11 Effect of the Injection Solvent vs. Mobile Phase

Flow injection analysis and particularly, gradient HPLC analysis, often involve introduction of a species in one solvent and its elution in another. The effect of injection solvent vs. the mobile phase must be considered, not only for their effect on separation efficiency but also to help understand the reactions occurring in the APCI source. To test this effect in a flow injection analysis, 0.5 mM fluorene was prepared in acetonitrile, 90:10 (v/v) acetonitrile/water, 70:30 (v/v) acetonitrile/water and 50:50 (v/v) acetonitrile/water. A 0.200 mL/min flow of acetonitrile was used as the mobile phase into which replicate injections of the fluorene standards were made. The results presented in Table 4.5 indicate that incorporating up to 10% water into the injection solvent caused a significant decrease in signal intensity and an increase in the proportion of protonated molecule to molecular ion.

Table 4.5. Effect of Injection Solvent on Signal Intensity and $[M+H]^+/M^{+\bullet}$ ratio of fluorene

Solvent	Intensity	$[M+H]^+/M^{+\bullet}$ ratio
100% acetonitrile	3.17e5	0.2286
90% acetonitrile	9.67e4	0.3773
70% acetonitrile	9.70e4	0.5710
50% acetonitrile	1.22e5	0.6549

This can be explained by the formation of protonated water clusters, which increase the background, resulting in a lower signal, and enhance the possibility of proton transfer, resulting in greater protonation. This indicates that, in this experiment, it is the injection solvent rather than the mobile phase which is most strongly implicated in the ionisation of the analyte, indicating that there is little mixing in either the transfer line or in the mass

spectrometric source of the injection solvent and the mobile phase. The effect of injection solvent is even more critical in column chromatography where compounds can have different solubilities in the solvent and in the mobile phase, thus compromising separation efficiency. LC mixes 2 and 3 were used to demonstrate the effect of injection solvent on APCI-MS response to PACs. These mixes have the same composition but 2 is in acetonitrile and 3 is in hexanes. The results presented in Figure 4.14 indicate that the concentrations of the separated species are quite low, resulting in noisy UV signal and TIC. Apart from the initial background due to elution of unretained hexanes solvent, the separation proceeds similarly. In this case, the injection solvent is rapidly excreted from the system, hence it cannot participate in ion/molecule reactions which ionise later eluting compounds. From a mass spectral point of view, the injection solvent for LC/MS is only critical in how its solubility properties differ from the mobile phase and this is important if this difference results in an initial high background due to unretained analytes.

4.1.12 Effect of the Source Gases (Original Gas Box)

As seen above, the nature of the solvents introduced and the sheath gas flow rate strongly influenced the signal intensity and ionisation mechanism. This implicated both these species in the chemical reactions in the plasma, which are responsible for the ionisation of the analytes. How the purity of the source gases with the original gas box affected the response to PACs was studied. The nature of the gas, its identity and purity, were tested with flow injection analysis and liquid chromatographic sample introduction. In the former, a 0.5 mM solution of fluorene in acetonitrile was introduced and analysed once with Dewar nitrogen and once with Extradry™ air. The results, presented in Figure 4.15, indicate that the

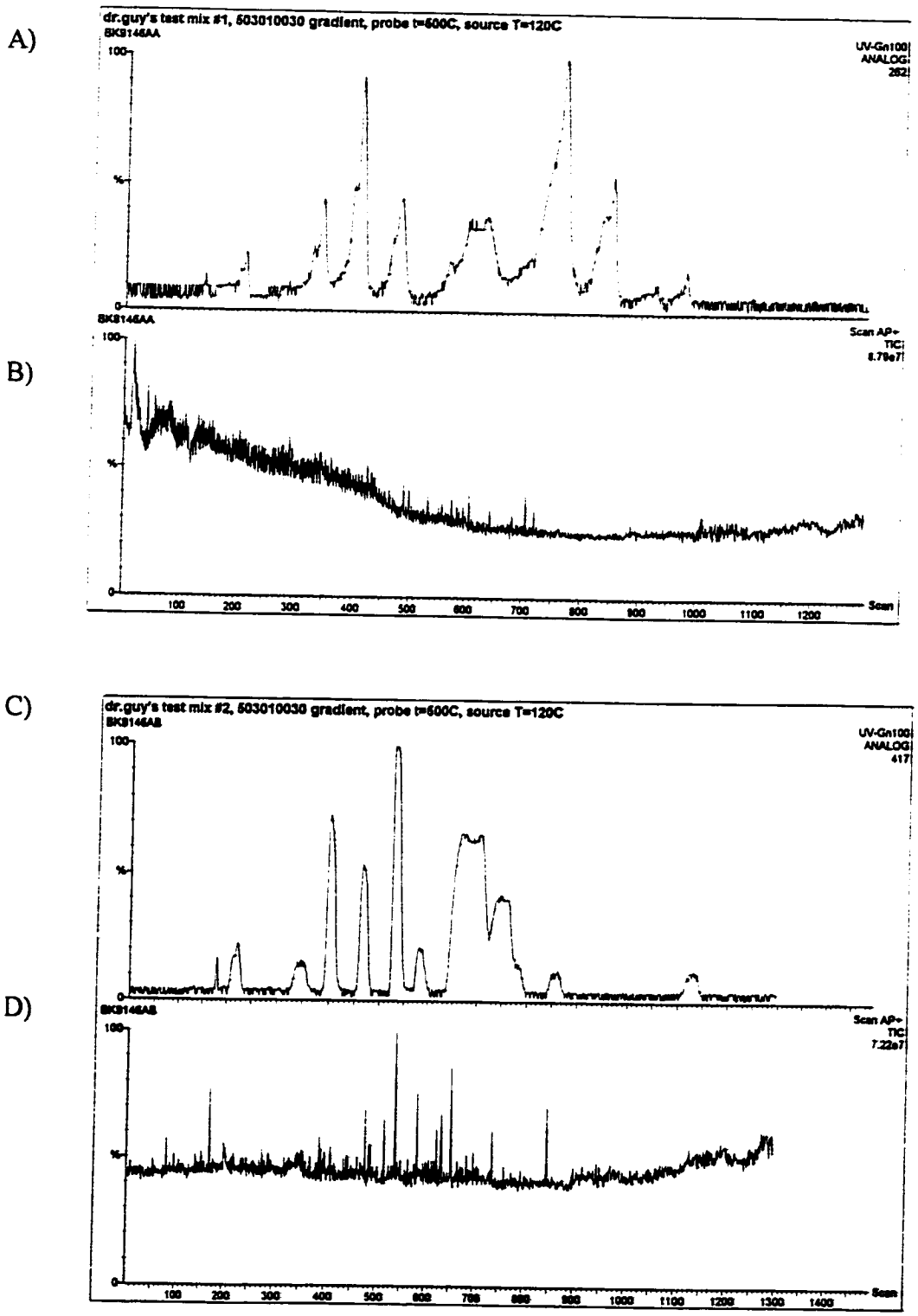

Figure 4.14. UV profiles of (A and C) at 250 nm and TIC (B and D) for reversed phase, gradient 503010030 elution of LC mixes 2 (A and B) and 3 (C and D) on a Vydac™ C_{18} column.

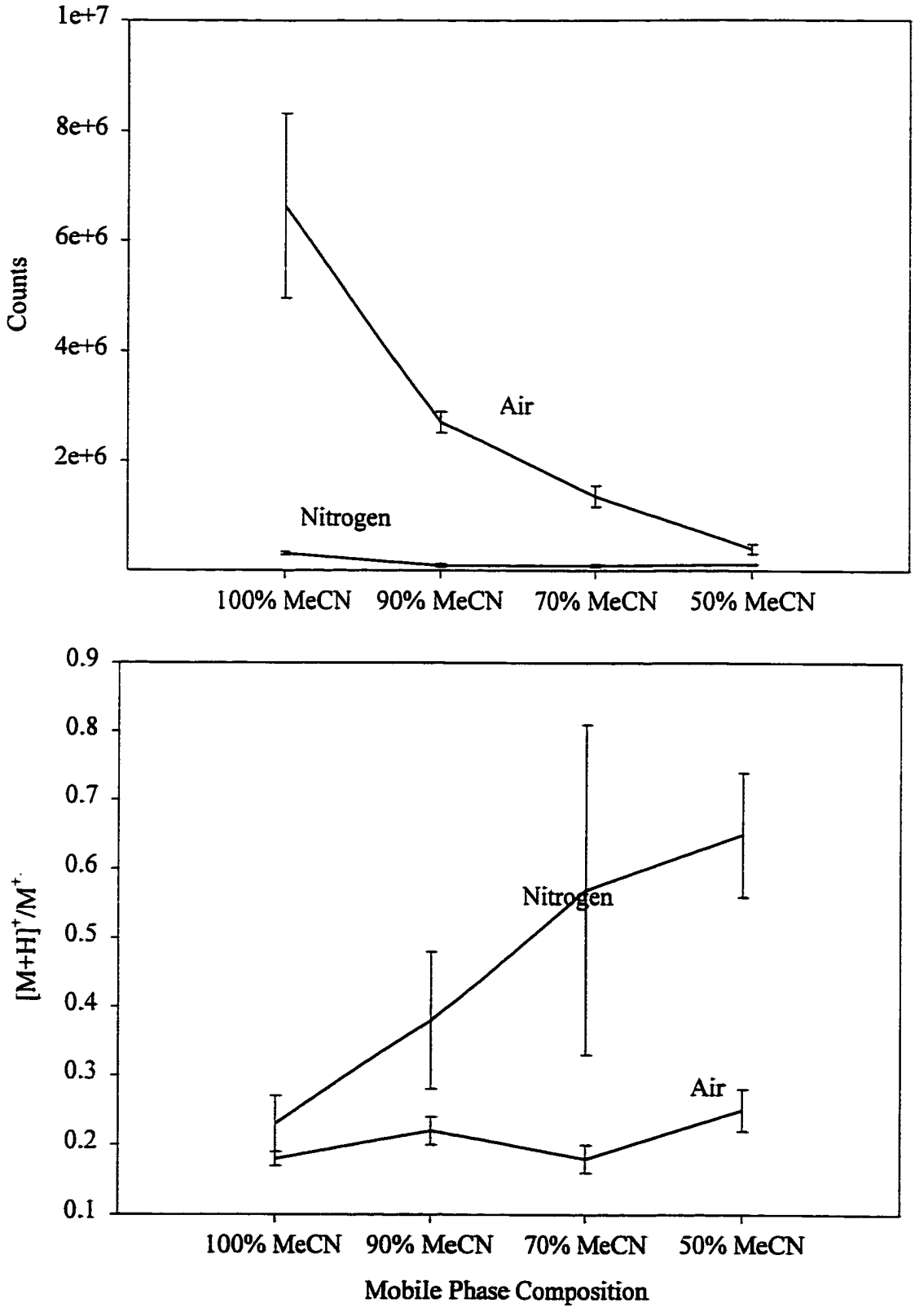

Figure 4.15. Effect of Source gas on Total Signal and Ionisation Mechanism of 0.5 mM fluorene.

use of air resulted in an almost tenfold increase in the total signal and a suppression of protonation, even when repeated with more water-rich solvents. This effect is likely due to the lower availability of water (resulting in reduced cluster formation with a corresponding decrease in background and proton transfer) and the presence of oxygen which as an electron scavenger will promote charge exchange, resulting in improved molecular ion levels. When a similar experiment with liquid chromatographic introduction of LC mix-1 was attempted once with Dewar nitrogen, once with Extradry™ air and once with industrial grade air (see Figure 4.16), the results confirmed that Extradry™ air was associated with cleaner backgrounds, improved analyte response and greater extent of charge exchange ionisation. The industrial grade air had a very high background and poor response to PACs. However, more $M^{+\bullet}$ than $[M+H]^+$ was observed. These experiments showed the importance of oxygen in the charge exchange ionisation mechanism and demonstrated the need for clean gases.

4.1.13 Effect of the Sample Concentration

The final parameter, concentration of the analytes, is not properly an instrumental parameter but does offer insight into the nature of the reactions occurring in the plasma. It is known that there is a finite quantity of reagent ions in the APCI source at any given moment in time and that exhaustion of these ions will lead to inefficient ionisation of the sample [205]. Table 4.6 presents the $[M+H]^+/M^{+\bullet}$ ratio of naphthalene, fluorene, phenanthrene, pyrene and benzo[a]pyrene in heptane as a function of concentration. These indicate that the ratio is largely unaffected by sample concentration, indicating that the reagent ions are present in large excess relative to the analyte. This is consistent with the reagent ions being derived from the solvent and source gas present, which are present in

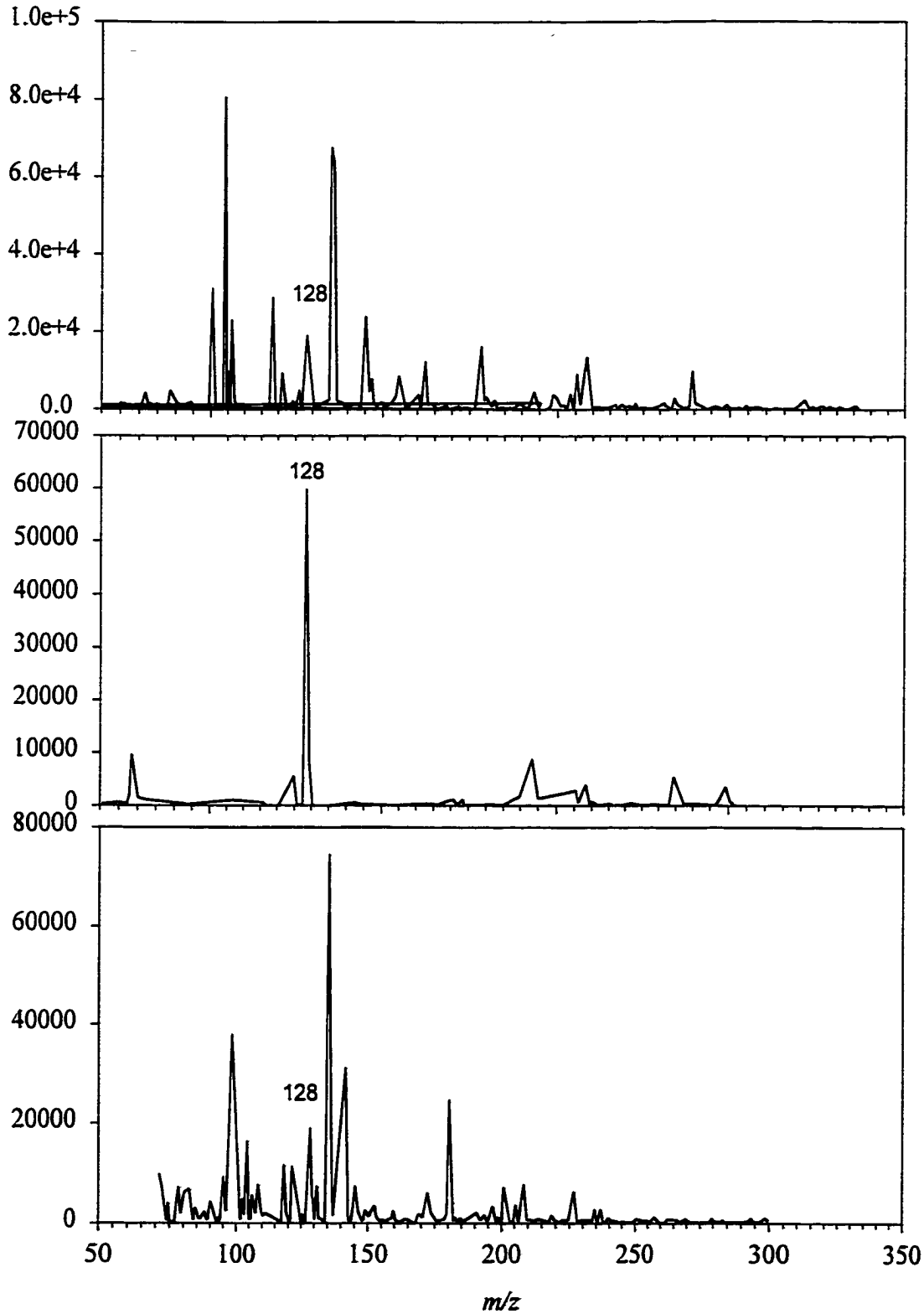

Figure 4.16. Spectra of Naphthalene (*m/z* 128) from LC mix-1 analysed by gradient with (from top to bottom) Dewar N_2, Extradry™ air and industrial grade compressed air.

large excess relative to the analyte. Based on these results, it is clear that maximising the response of the mass spectrometer to analytes is analyte, instrument and solvent-specific.

Table 4.6. Effect of Concentration on the $[M+H]^+$/ $M^{+\bullet}$ Ratio by Flow Injection

Concentration (M)	Naphthalene	Fluorene	Phenanthrene	Pyrene	Benzo[*a*]-pyrene
1e-2	2.17	0.70	0.41		0.93
1e-3	4.22	0.36	1.21	0.52	1.92
1e-4	6.65	2.48	0.96	1.35	1.64
1e-5	0.73	0.86	0.46	4.15	2.50

Table 4.7 demonstrates the detection limits of pyrene (defined as the lowest concentration of pyrene that can be reliably detected with background subtraction) studied in a variety of solvents. These results clearly indicate that aqueous mobile phases result in much poorer performance than organic solvents, mixing of solvents introduces competition amongst reagent ions and ionisation mechanisms which results in generally poorer response. For

Table 4.7. Detection Limits of Pyrene in a Variety of Solvents by Flow Injection

Solvent	Detection Limit (μM)
50:50 (v/v) acetonitrile/water	100
Acetonitrile	10.5
Dichloromethane	0.010
20% dichloromethane - 80% hexanes	10.6
30% dichloromethane - 70% hexanes	10.7
Hexanes	0.015
15% toluene - 85 % hexanes	100
15% ,αα,α-trifluorinated toluene - 85 % hexanes	10

example, hexanes and dichloromethane yield reagent ions of differing reactivity which will compete for available analytes. This competition will be deleterious to signal if one reagent ion is of much lower activity. Toluene and trifluorinated toluene have a lower ionisation energy than hexanes. They will therefore undergo charge exchange with the hexanes, yielding a radical cation and molecular hexanes. This will decrease the availability of *t*-butyl or isopropyl cations from hexanes available to react with the analyte and this will result in less efficient ionisation of analytes and a corresponding increase in detection limit. It was also observed that the cleanliness of the source has a strong effect on the spectral performance. The latter can be controlled to an extent by regular cleaning of the APCI source and by careful operation. The former two are not completely under the operator's control as proper separation of analytes frequently requires aqueous solvents and/or gradients. The limitations this places on mass spectral performance must be considered when these are required.

4.2 Applications to Real World Analysis

Having determined the optimum parameters for operation of the VG-Fisons-Micromass Quattro triple quadrupole mass spectrometer with liquid chromatographic separation, these optimised parameters (with the exception of the use of Extradry™ air due to cost and flammability considerations) were applied to the LC/MS analysis of distillation cuts of Lot #2HPP 1106 light gas oil. Figure 3.5 represents a typical UV chromatogram at 336 nm of the 90-100% distillation cut, with the identification of naphthalene and pyrene peaks 1-4 (3-ring compounds were present in too low a concentration to be identified). The plots of other fractions are similar but naphthalene peaks are more prominent.

The first step in the mass spectrometric analysis was to characterise each distillation cut (from 10-20% to 80-90%) by direct injection into the mass spectrometer. Using the observed masses and the assumption that all are derivatives of naphthalene, phenanthrene and pyrene, the composition of each distillation cut is presented in Table 4.8. As part of the identification, the masses of methyl derivatives of naphthalene, phenanthrene and pyrene were calculated and matched to the observed masses. The identification is "mass-equivalent" to a number of methyl substituents on a given PAH and does not necessarily represent a real structure (e.g. decamethylnaphthalene is probably a ring-reduced form of a higher-mass PAC). In some cases, this resulted in a greater degree of alkyl substitution than is allowed based on the PAH structure and may indicate the presence of partially reduced rings. The objective was to get an understanding of the origins of different species, not unambiguously identify them.

Up to the 40-50% cut, only naphthalene and its alkyl derivatives up to the mass equivalent of seven methyl substituents were observed. The next two cuts contain up to "nine methyl" substituents and from 60-70% onwards, one begins to see phenanthrene and pyrene derivatives. In the 80-90% fraction, up to "eleven methyl" substituents on naphthalene are observed. These assignments are somewhat ambiguous since each successive phenanthrene substitution falls 6 mass units short of naphthalene (e.g. methylphenanthrene appears at *m/z* 192 while pentamethylnaphthalene falls at *m/z* 198) and pyrene derivatives are 4 mass units below and above phenanthrene and naphthalene, respectively. For example, 1-methylpyrene has an *m/z* value of 216, trimethylphenanthrene a value of 220 and hexamethylnaphthalene, 212. These are well-resolved enough to be distinguishable. With real samples, ions are

Table 4.8. Mass composition of each of the distillation fractions injected into the MS and analysed by scanning APCI$^+$.

Fraction	POSTULATED COMPOUNDS
10-20 %	naphthalene + up to 7 Me ($C_{10}H_8$ to "$C_{10}H(CH_3)_7$")
20-30 %	naphthalene + up to 7 Me ($C_{10}H_8$ to "$C_{10}H(CH_3)_7$")
30-40 %	naphthalene + up to 7 Me ($C_{10}H_8$ to "$C_{10}H(CH_3)_7$")
40-50 %	naphthalene + up to 9 Me ($C_{10}H_8$ to "$C_{10}(CH_3)_9$")
50-60 %	naphthalene + up to 9 Me ($C_{10}H_8$ to "$C_{10}(CH_3)_9$")
60-70 %	naphthalene + up to 9 Me ($C_{10}H_8$ to "$C_{10}(CH_3)_9$") phenanthrene/anthracene ($C_{14}H_{10}$) pyrene (unmod, Me, di-Me) ($C_{16}H_{10}$ - $C_{16}H_8(CH_3)_2$)
70-80 %	naphthalene + up to 9 Me ($C_{10}H_8$ to "$C_{10}(CH_3)_9$") phenanthrene/anthracene ($C_{14}H_{10}$) pyrene (unmod, Me, di-Me) ($C_{16}H_{10}$ - $C_{16}H_8(CH_3)_2$)
80-90 %	naphthalene + up to 11 Me ($C_{10}H_8$ to "$C_{10}(CH_3)_{11}$") phenanthrene/anthracene ($C_{14}H_{10}$) pyrene (unmod, Me, di-Me) ($C_{16}H_{10}$ - $C_{16}H_8(CH_3)_2$)

observed as groups of 4-10 *m/z* values, complicating identification. Thus, alkylated phenanthrenes are likely present but cannot be specifically identified. It is also possible that there are partially reduced ring structures present in the fractions which fall within observed mass ranges that have been assigned as alkylated naphthalenes, phenanthrenes or pyrenes. For example, 1,2,3,4-tetrahydroanthracene has an *m/z* value of 182, 9,10-dihydroanthracene has an *m/z* value of 180 and tetramethylnaphthalene, 184.

The sheer number of possible components in any given distillation fraction is overwhelming. To address this problem, the 80-90% distillation fraction was separated on the silica column and a 200 μL cut at the top of the naphthalene peak was directed into the

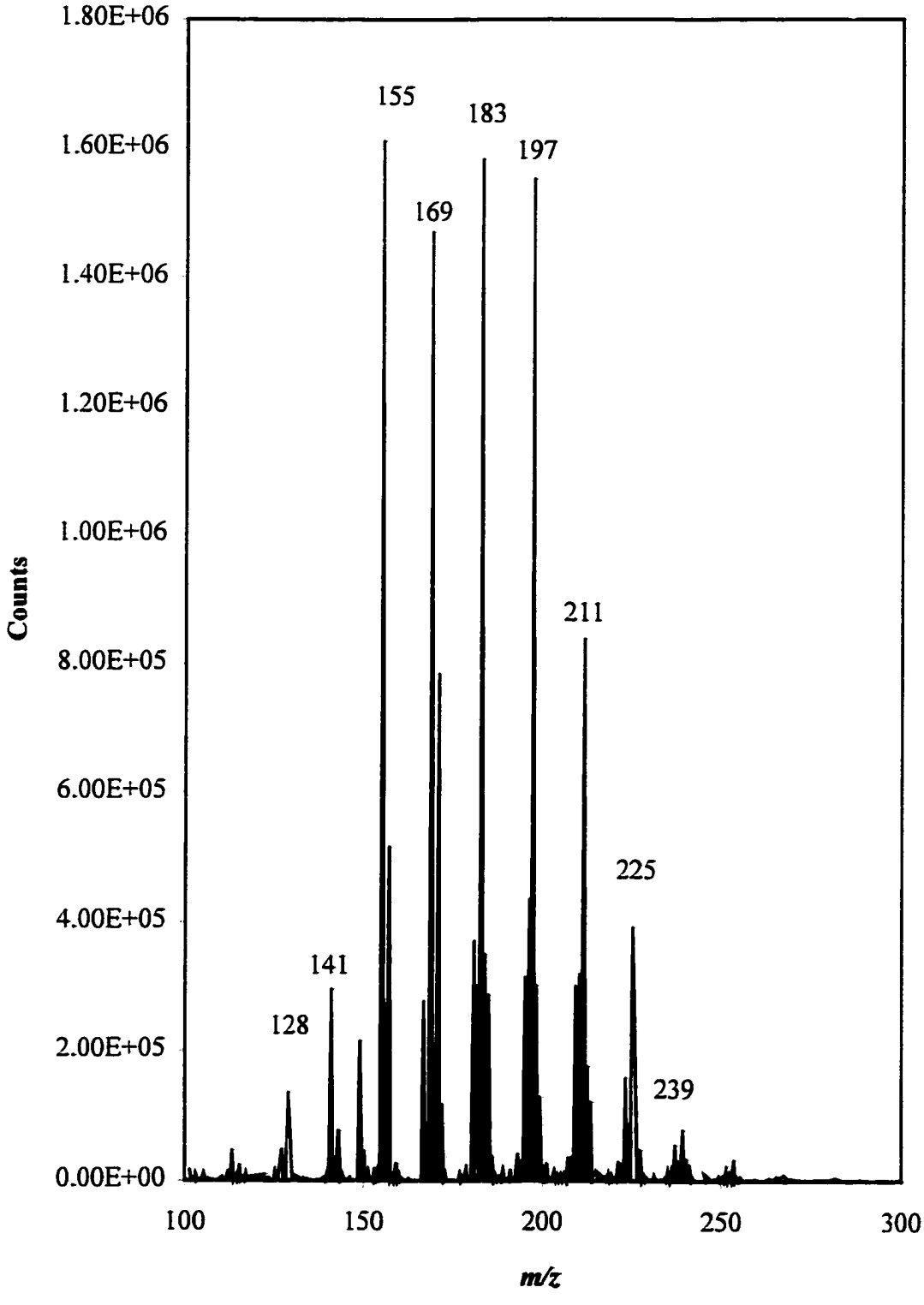

Figure 4.17. Background-subtracted mass profile of the naphthalene peak of the 80 - 90% distillation cut.

mass spectrometer. The observed mass spectrum, presented in Figure 4.17, indicates that the parent naphthalenes are not present but all the deprotonated peaks $[M-H]^+$ of mass equivalents of mono- to decamethylnaphthalene are visible. These highly substituted naphthalenes are likely larger PACs with reduced rings. This deprotonation is typical of alkylated naphthalenes in $APCI^-$ and these results are in good agreement with the results presented in Table 4.8. Intermediate masses from *m/z* 155-197 are enriched relative to the other masses, which may indicate that these are the predominant forms of alkylated naphthalenes in this fraction and/or that higher mass materials are breaking down or are not as easily vapourised and detected. It is not possible to determine which of these phenomena are occurring without appropriate standards. Chromatographic separation of these species in the second dimension was unsuccessful with a normal phase separation and although the reversed phase separation with UV and fluorescence detection was successful, the concentrations of the species were too low to permit detection by APCI-MS either by full scan or by SIR.

The focus shifted to the analysis of pyrene peaks by the fractionation of a 20 μL injection of the 80-90% distillation cut on the silica column and a 500 μL cut onto the TCP column. The TICs, and the fluorescence and mass chromatograms of pyrene peaks 1 through 3 are presented in Figures 4.18 through 4.20. These results revealed that pyrene peak 1 is dominated by pyrene, pyrene peak 2 has two out of three possible methylpyrenes, implying either the non-existence of one isomer or co-elution of isomers, and peak 3 displayed three dimethyl peaks, out of a possible fifteen isomers, again implying co-elution or non-existence of some peaks. Not all peaks could be assigned and in later experiments with laser

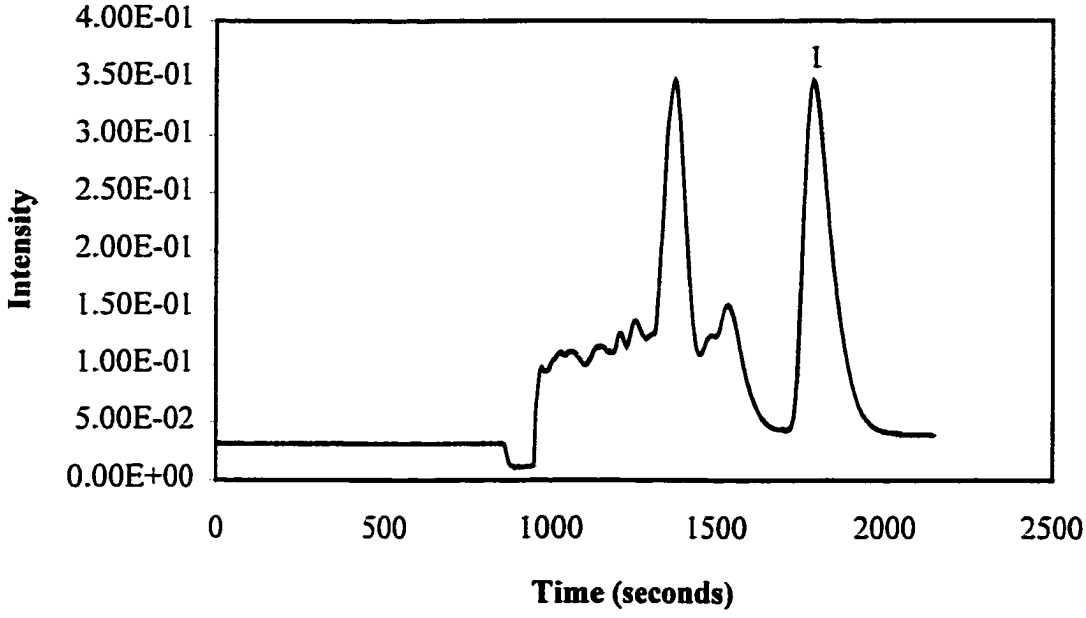

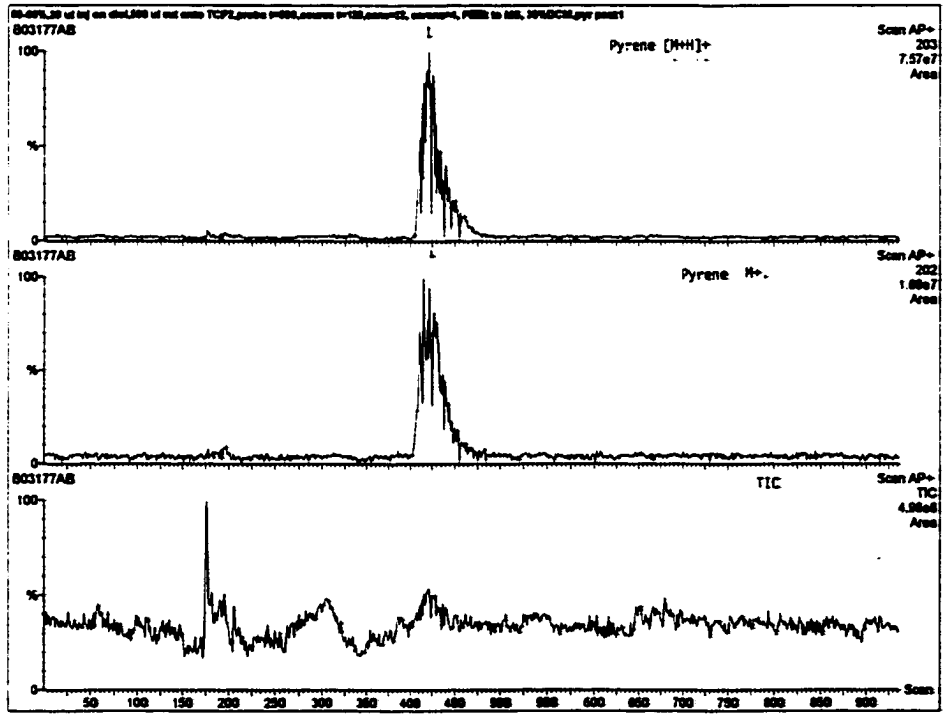

Figure 4.18. Fluorescence (λex = 230 nm, λem = 380 nm) , and mass chromatograms of pyrene peak 1 of the 80 - 90% distillation fraction.

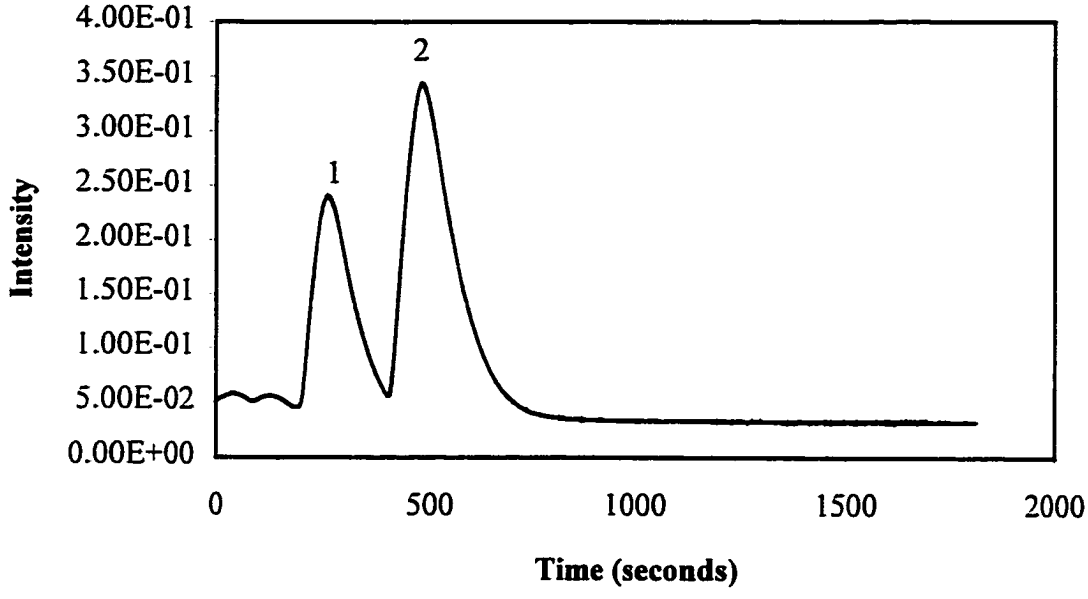

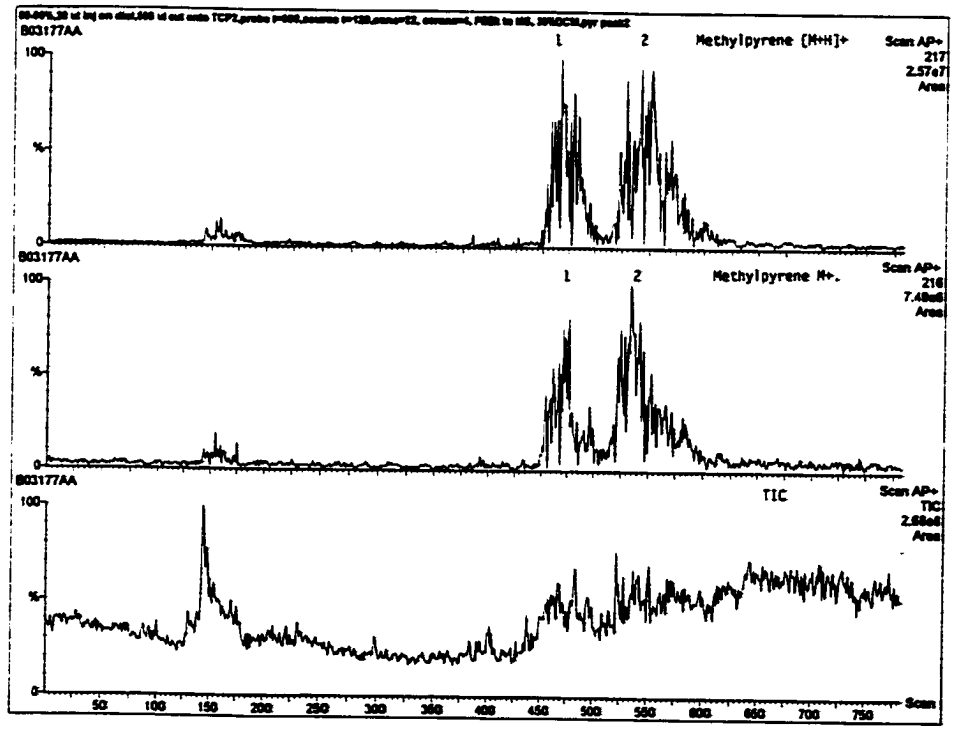

Figure 4.19. Fluorescence (λex = 230 nm, λem = 380 nm) and mass chromatograms of pyrene peak 2 of the 80 - 90% distillation fraction.

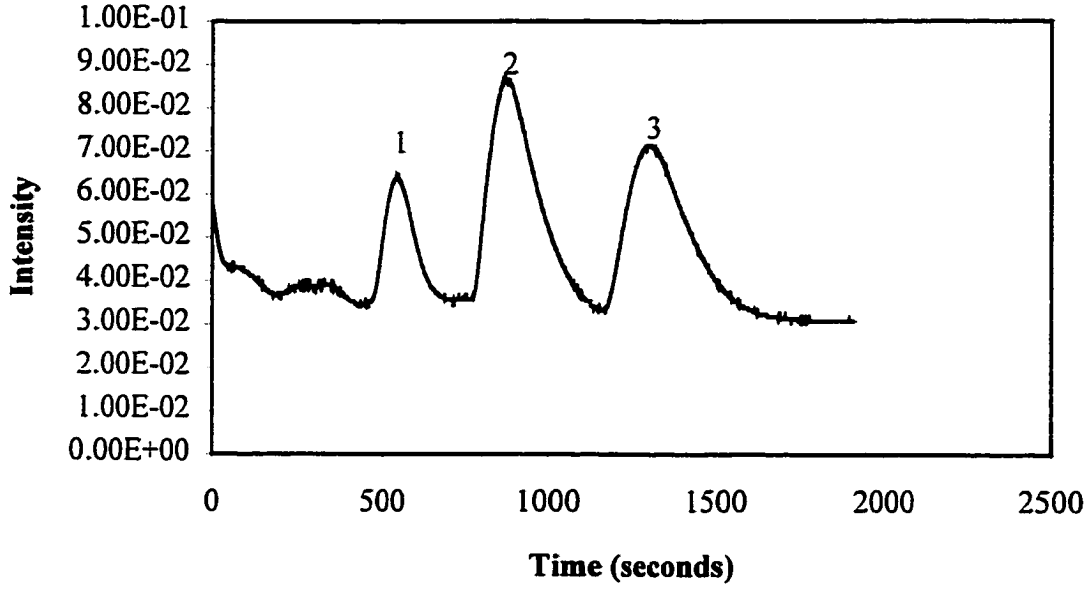

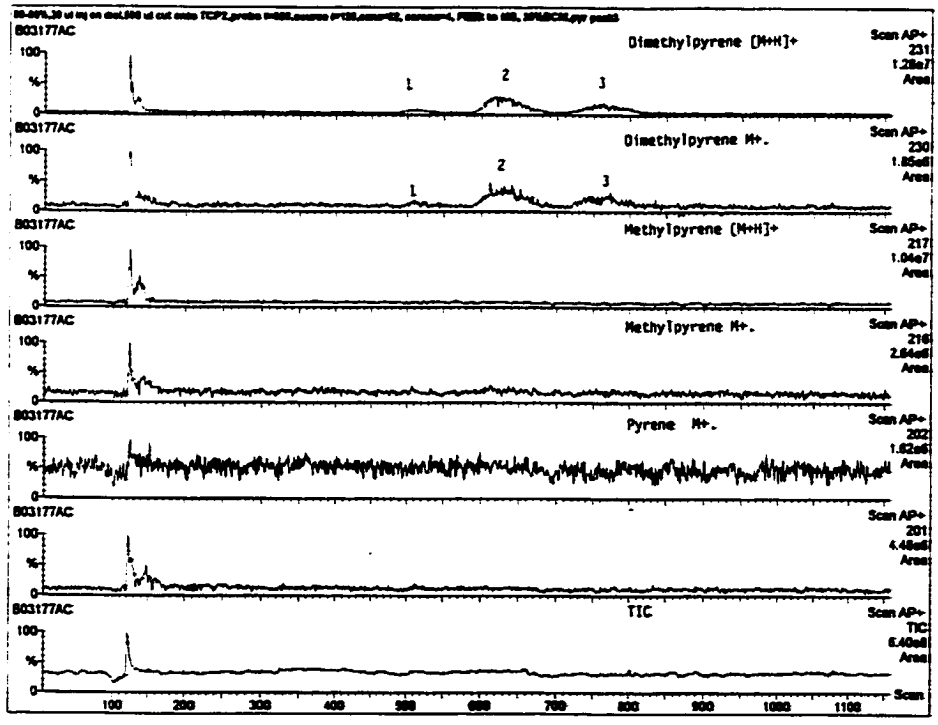

Figure 4.20. Fluorescence (λex = 230 nm, λem = 380 nm) and mass chromatograms of pyrene peak 3 of the 80 - 90% distillation fraction.

fluorescence detection and other chromatographic conditions revealed the presence of alkylated naphthalenes and phenanthrenes in these fractions, which agrees with the direct injection results.

The 90-100% fraction was analysed in a similar fashion. The TICs, and the fluorescence and mass chromatograms of pyrene peaks 1 through 4 are presented in Figures 4.21 through 4.24. This fraction was visibly darker, contained more particulate matter and exhibited much richer spectra at each peak. Thus, pyrene peak 1 had a methylpyrene peak, pyrene peak 2 exhibited two dimethylpyrene peaks, pyrene peak 3 exhibited three tetramethylpyrene peaks and peak 4, one pentamethylpyrene peak. These are higher mass materials than those observed with the 80-90% fraction. This is consistent with the higher boiling point of this fraction, making for considerably higher mass compounds than that observed with the 80-90% fraction.

The results of the analysis of these fractions and of the pyrene peaks indicates the existence of some components, relatively low in concentration, which are being masked by the larger peaks and which are not being reliably detected. Fluorescence detection demonstrated that these fractions were far more complex than the mass spectral response suggested but the sensitivity of the mass spectrometer, even in single ion recording mode, was insufficient for characterisation. This sparked an interest in understanding the nature of the reactions in the plasma in an effort to better optimise the mass spectral response to PACs. This is discussed more fully in Chapter 6.

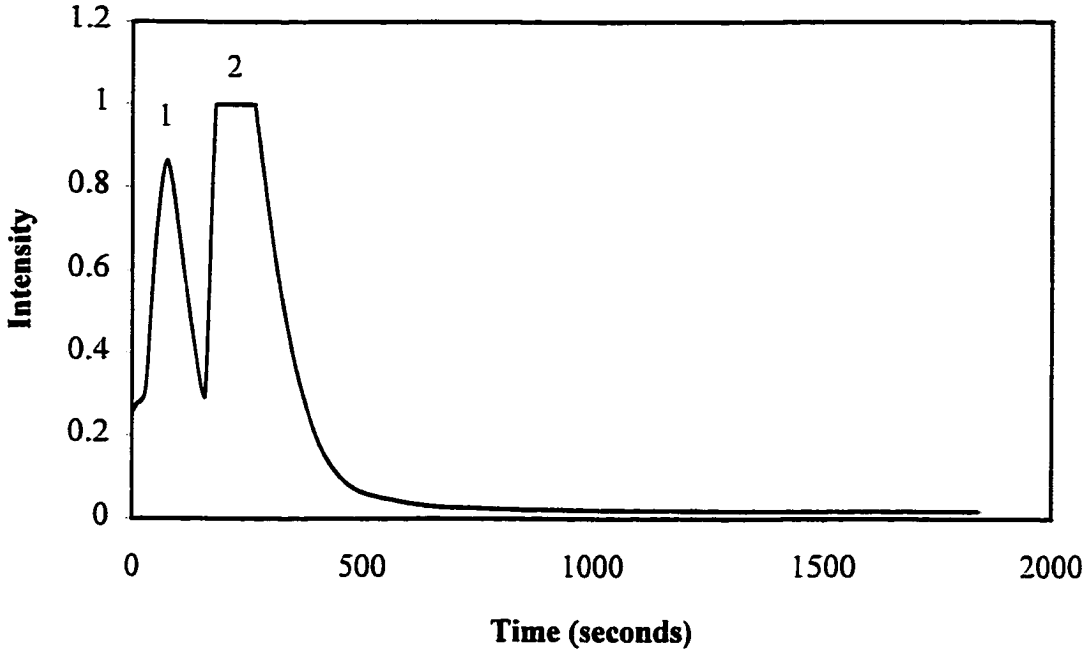

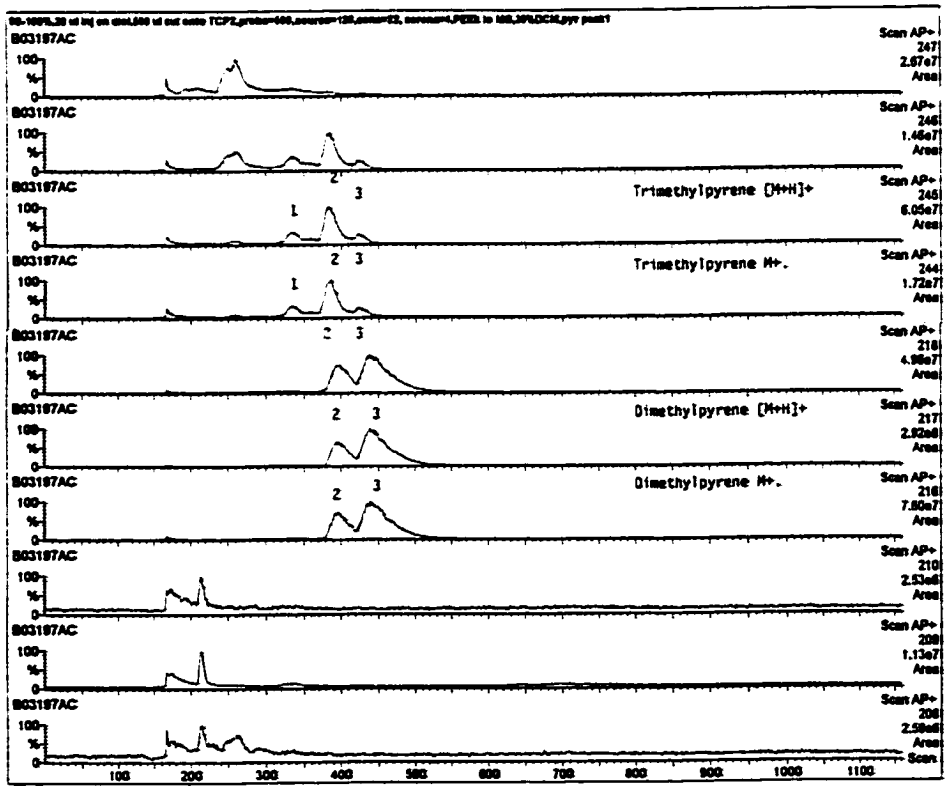

Figure 4.21. Fluorescence (λex = 230 nm, λem = 380 nm) and mass chromatograms of pyrene peak I of the 90 - 100 % distillation fraction.

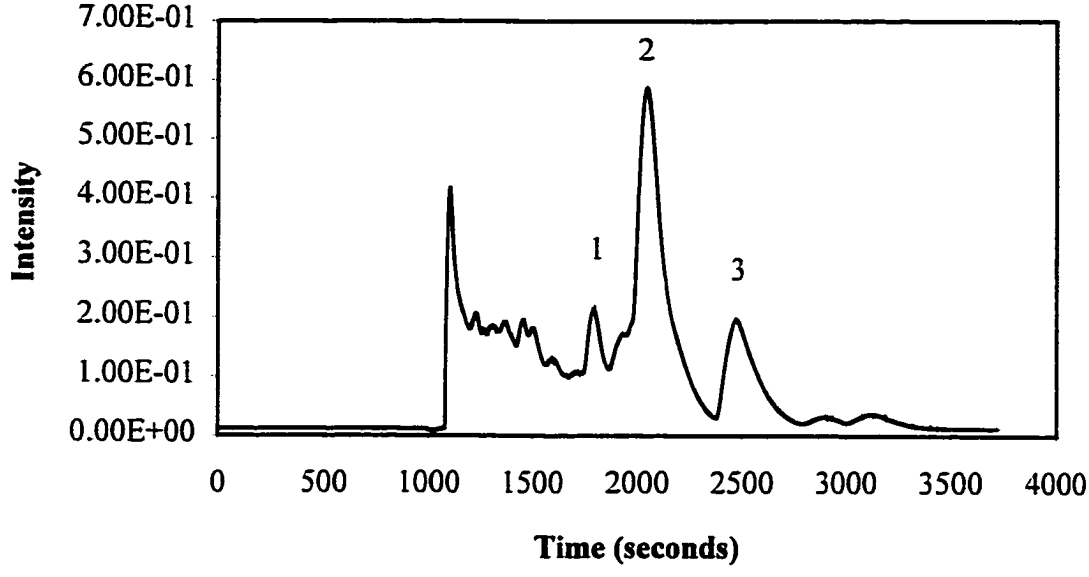

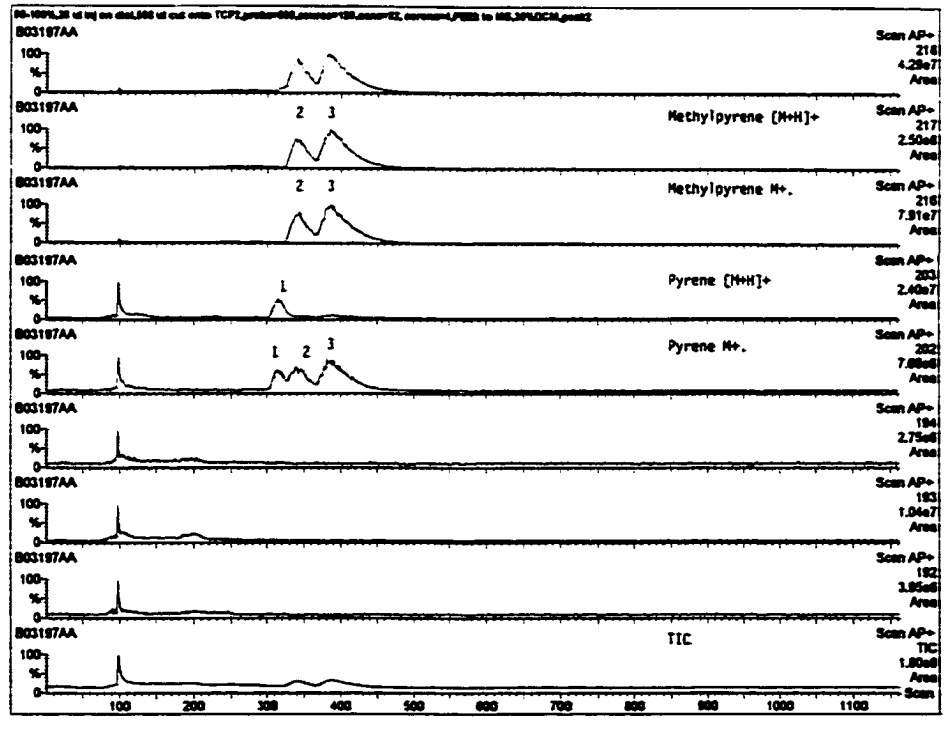

Figure 4.22. Fluorescence (λex = 230 nm, λem = 380 nm) and mass chromatograms of pyrene peak 2 of the 90 -100 % distillation fraction.

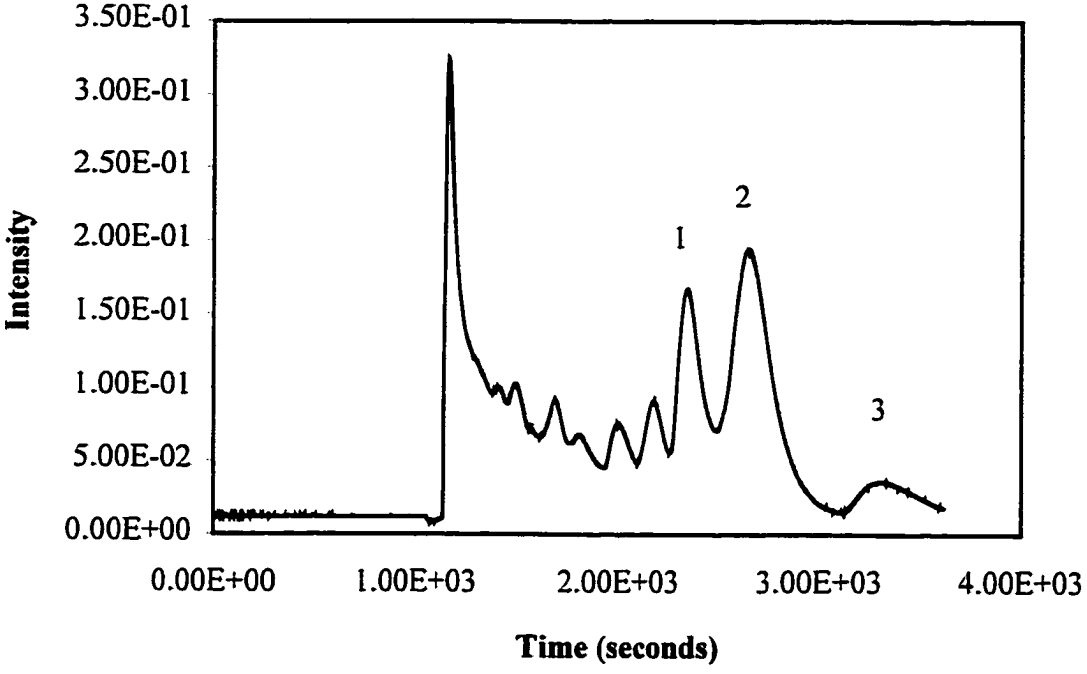

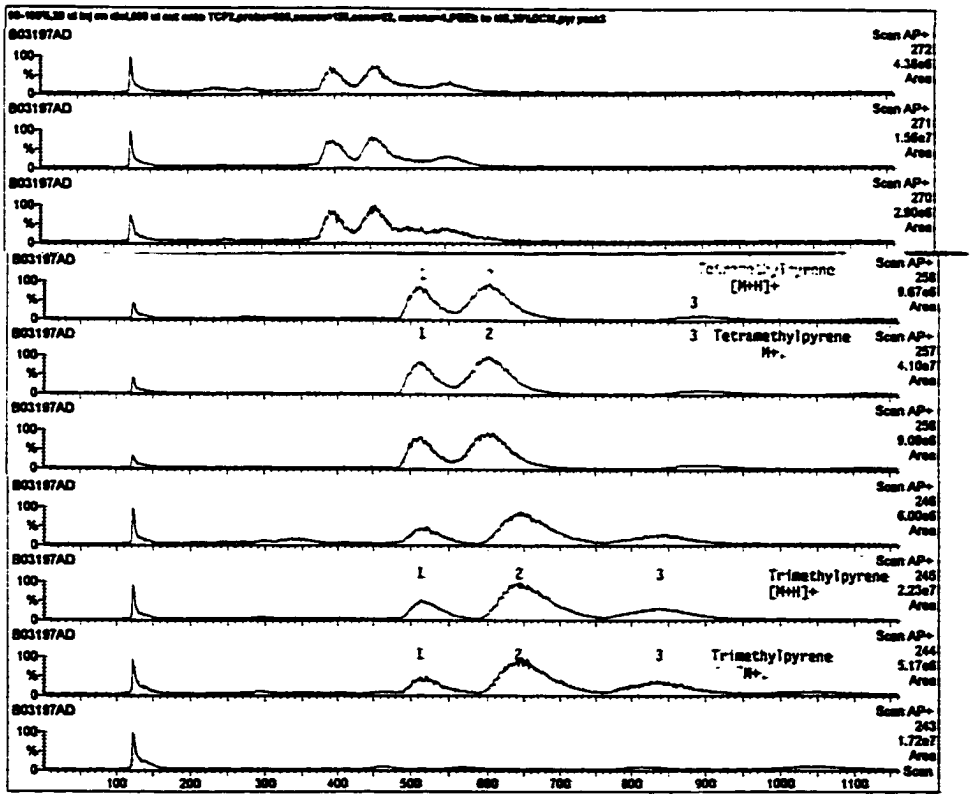

Figure 4.23. Fluorescence (λex = 230 nm, λem = 380 nm) and mass chromatograms of pyrene peak 3 of the 90 -100% distillation fraction.

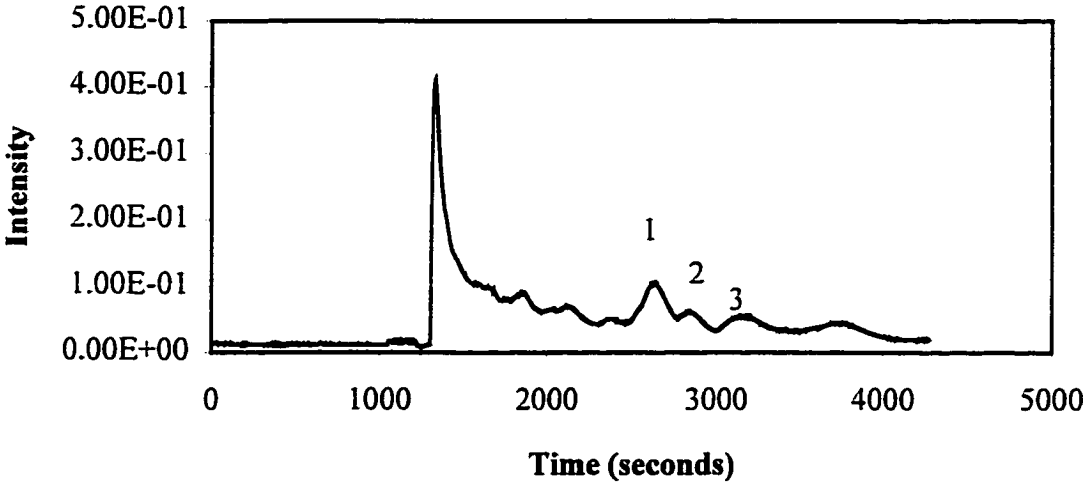

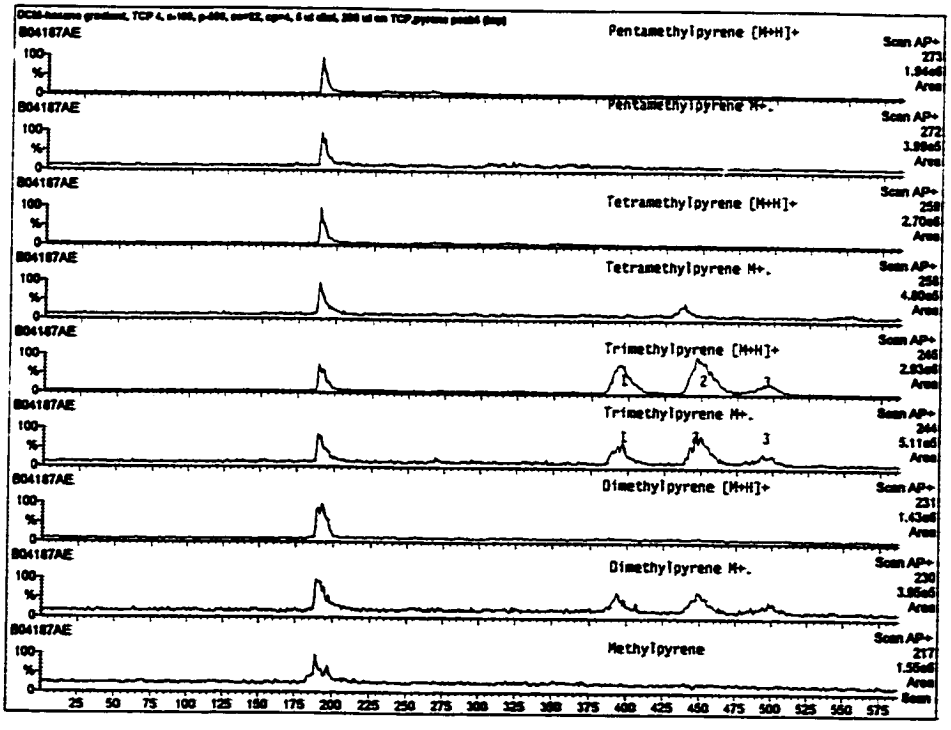

Figure 4.24. Fluorescence (λex = 230 nm, λem = 380 nm) and mass chromatograms of pyrene peak 4 of the 90 -100% distillation fraction.

Chapter 5

Solvent Effects

5.1 Introduction

Liquid chromatography is a widely used separation technique, as the plethora of available stationary and mobile phases enables the efficient separation of a broad spectrum of compounds, especially the involatile and thermally labile compounds unamenable to gas chromatographic analysis. It provides retention time, molecular weight, number of aromatic rings and some insight into substitution. However, structure elucidation is not always possible from chromatographic data alone. This information is all that is required in routine work but not for the qualitative analysis of unknowns. By coupling LC separation to a mass spectrometer, structural information can be obtained [163]. Some examples of the successful application of LC/APCI-MS has been successfully applied to the analysis of carbamate pesticides [188], sulfadiazine residues [177], renin inhibitor [189], cholecystokinin receptor [190], fullerenes [191], heterocyclic amine carcinogens [181], hydroxy polycyclic aromatic hydrocarbons [192], polyaromatic sulfur heterocycles [176] and flame-generated polycyclic aromatic hydrocarbons [193].

In optimising these methodologies, the mobile phase composition was selected for its chromatographic rather than its mass spectral properties, with the caveat that inorganic modifiers and buffers be avoided or minimised to prevent high backgrounds [171], despite the observations of other authors that the solvent composition impacted the signal intensity and ion structure (fragment, adduct, molecular ion, deprotonated molecular ion, protonated molecular ion) of the analyte. Shaefer and Dixon [195] demonstrated that the sensitivity of

APCI was greatest in aprotic mobile phases. In fact, if the analyte molecule had an acidic group of weaker acidity than any of the acidic additives added to mobile phase, analyte ionisation was suppressed or quenched. If the analyte was more acidic than the additive, its ionisation efficiency was unaltered. These differences could be correlated to the acidity/basicity of the gas-phase reagent ions. Preliminary studies by Horning [80] and Carroll [196] indicated that solvents ionised by different mechanisms in an APCI source and that this had an impact on analyte ionisation. Thus, alcohols formed proton-bound clusters, which transfer protons or protonated alcohols to the analyte. Benzene formed predominantly $C_6H_6^{+\bullet}$, providing a mechanism for charge exchange ionisation of analytes. Iso-octane and hexane fragment to $C_4H_9^+$ which can transfer a proton to polycyclic aromatic compounds to give the protonated molecular ion.

As observed in Chapter 4, the detection limit is significantly affected by the choice of solvent. In this chapter, a more systematic approach to the effects of solvent on PAC response, both signal intensity and ionisation mechanism, will be undertaken.

5.2 Effect of Solvent Identity

Polycyclic aromatic compounds typically exist as complex mixtures in challenging matrices. Due to the complexity of the sample, multi-dimensional chromatography is often required for sample characterisation. This generally involves an initial normal phase separation with hexanes on a silica column to group the PACs by aromatic ring number. Subsequent steps, in normal or reversed phase, then separate the components of a given ring size with some combination of aqueous acetonitrile, acetonitrile, hexanes and dichloromethane. These solvents were selected for the initial study to determine the effect

of solvent, if any, on mass spectral response.

Figures 5.1 and 5.2 demonstrate the total signal and the ratio of protonated molecular ion to molecular ion, respectively, of the 5 or 7 components in the Imperial standards (see Table 3.2) of single injections (no statistical data available). These results indicate that the organic solvents are preferred to aqueous solvents for overall signal intensity which concurs with the manufacturer's suggested operating conditions [54] and that dichloromethane offers the best signal intensity. The reasons for this may lie in the solubility of PACs, the solvent boiling point and/or the solvent purity. As PACs are highly soluble in dichloromethane, the boiling point of dichloromethane is low and the solvent is freshly distilled before use, the observed signal optimum may be the result of solvent purity or the best nebulisation. HPLC grade acetonitrile should be purer than freshly distilled reagent grade dichloromethane or hexanes yet the total signal intensity is lower, indicating that it may be an effect of sample transfer or ionisation efficiency. Hexanes have a lower boiling point and a lower PAC solubility than acetonitrile, indicating that these physical parameters are not sufficient explanation for the behaviour in the plasma. The lowest signal intensity was associated with aqueous acetonitrile. Although protonated water or solvent clusters are the major means of proton transfer to the analyte, the solvent is present in large excess relative to the analyte. The greater the population of protonated water clusters relative to the analyte molecules, the greater will be the excess of reagent ions, and the corresponding background. Water at a concentration of 10 ppm was sufficient to form protonated water clusters which would protonate PACs [92, 93], so a greater water concentration is unnecessary and deleterious. When examining the degree of protonation, acetonitrile/water is associated with high levels,

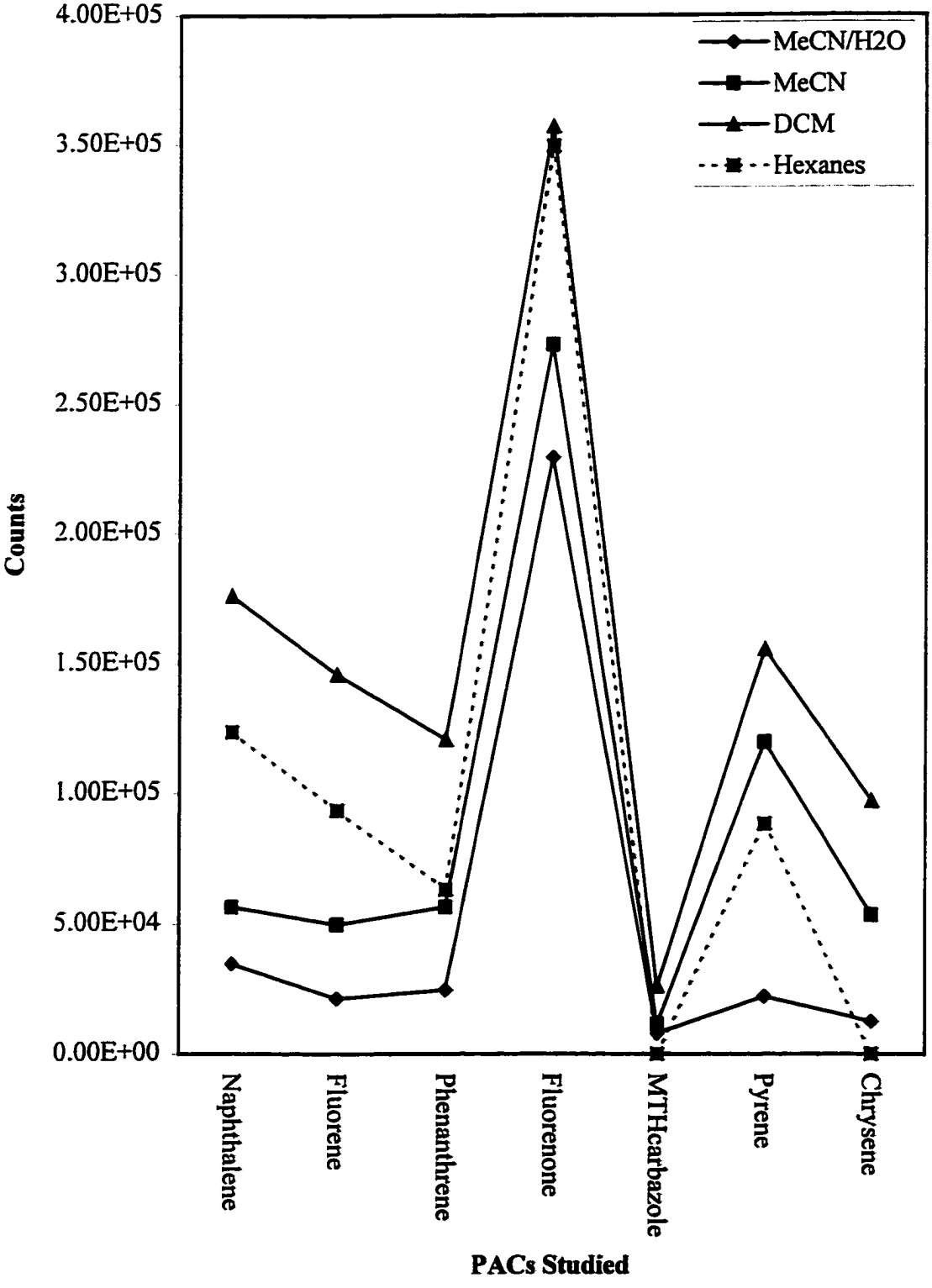

Figure 5.1. Total Signal (sum of protonated molecule and molecular ion response) for PAC components of Imperial standards as a function of solvent.

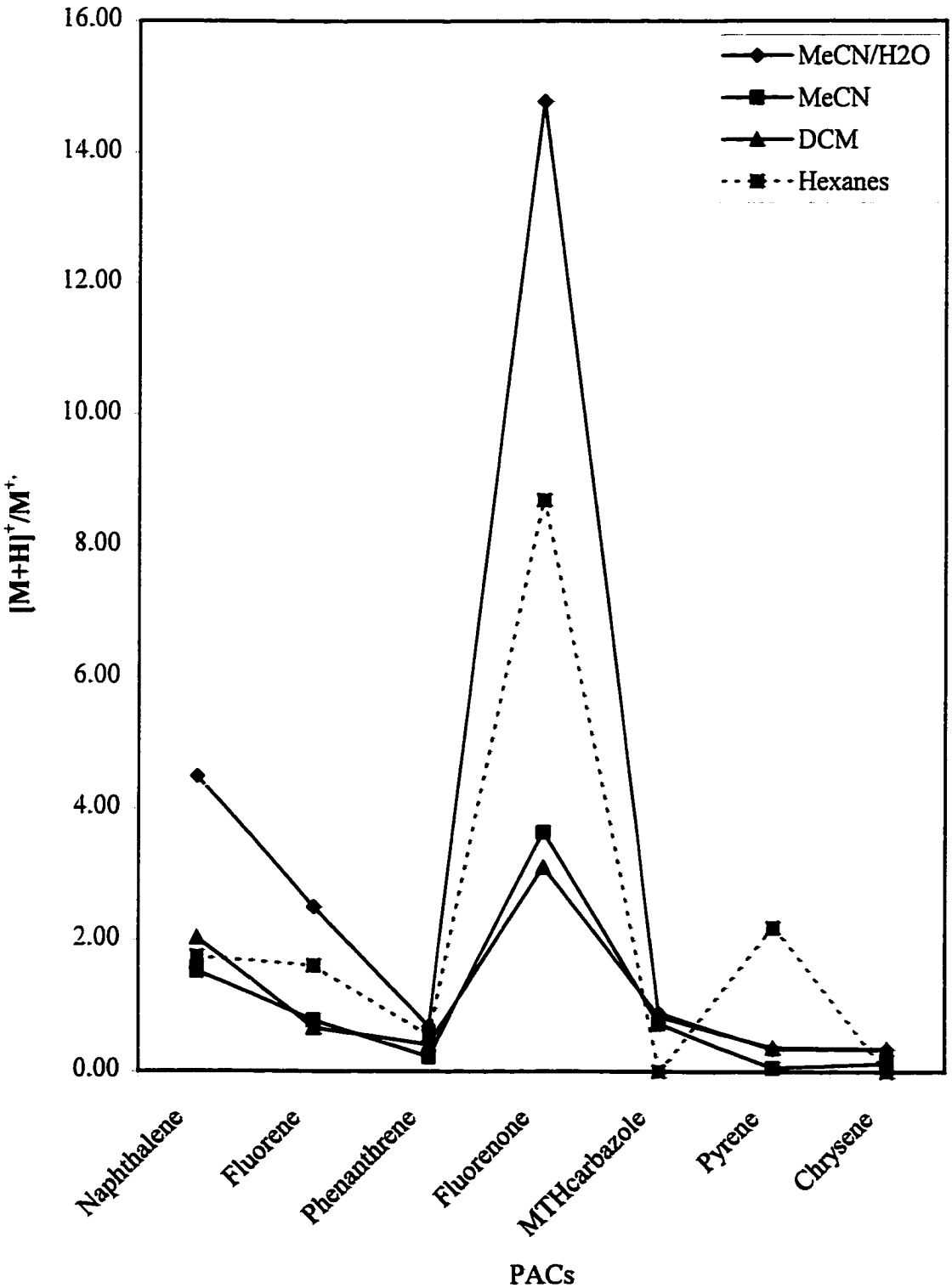

Figure 5.2. Protonation vs. charge exchange ionisation of the components of Imperial standards as a function of solvent.

hexanes with intermediate levels and acetonitrile and dichloromethane with low levels. Both $H_3O^+(H_2O)_n$ and $C_4H_9^+$ species have been correlated with high degrees of protonation. The poorly acidic, dry acetonitrile (though it is impossible to remove all traces of water) and dichloromethane are not expected to be associated with high degrees of protonation, as was observed. Dichloromethane with its two electronegative chlorine atoms is likely to have a relatively high electron affinity, thus promoting charge exchange. There is no observable positive or negative correlation of signal response to degree of protonation.

When performing isocratic separations, a single solvent can be selected for optimal LC and MS performance for a given analyte. Gradient separations require mixing at least two solvents which will result in a range of cluster and reagent ions of differing reactivity to PACs. How these will impact on the ionisation mechanism of a typical PAH, naphthalene, was examined by preparing naphthalene solutions ranging from 100% aqueous to 100% organic. The results of these studies are presented in Figure 5.3. These indicate that protonation falls off dramatically with organic contents of ≥5%. The solvent, and resulting reagent ions, are in a large excess relative to the analyte so this is not the result of reagent ion depletion with increasing organic content. Rather, the nature and abundances of the reagent ions in the plasma is being altered (may see water clusters, solvent clusters, water-solvent clusters, solvent impurities), which introduces reagent ions of differing reactivity, which then compete for the analyte molecules. This results in lower protonation efficiency. It should also be noted that the $[M+H]^+/M^{+\bullet}$ ratios are higher in the presence of methanol than in the presence of acetonitrile. Methanol is a poorer gas phase base than acetonitrile (gas phase basicity (methanol) = 724.5 kJ/mol, gas phase basicity (acetonitrile) = 748 kJ/mol) making

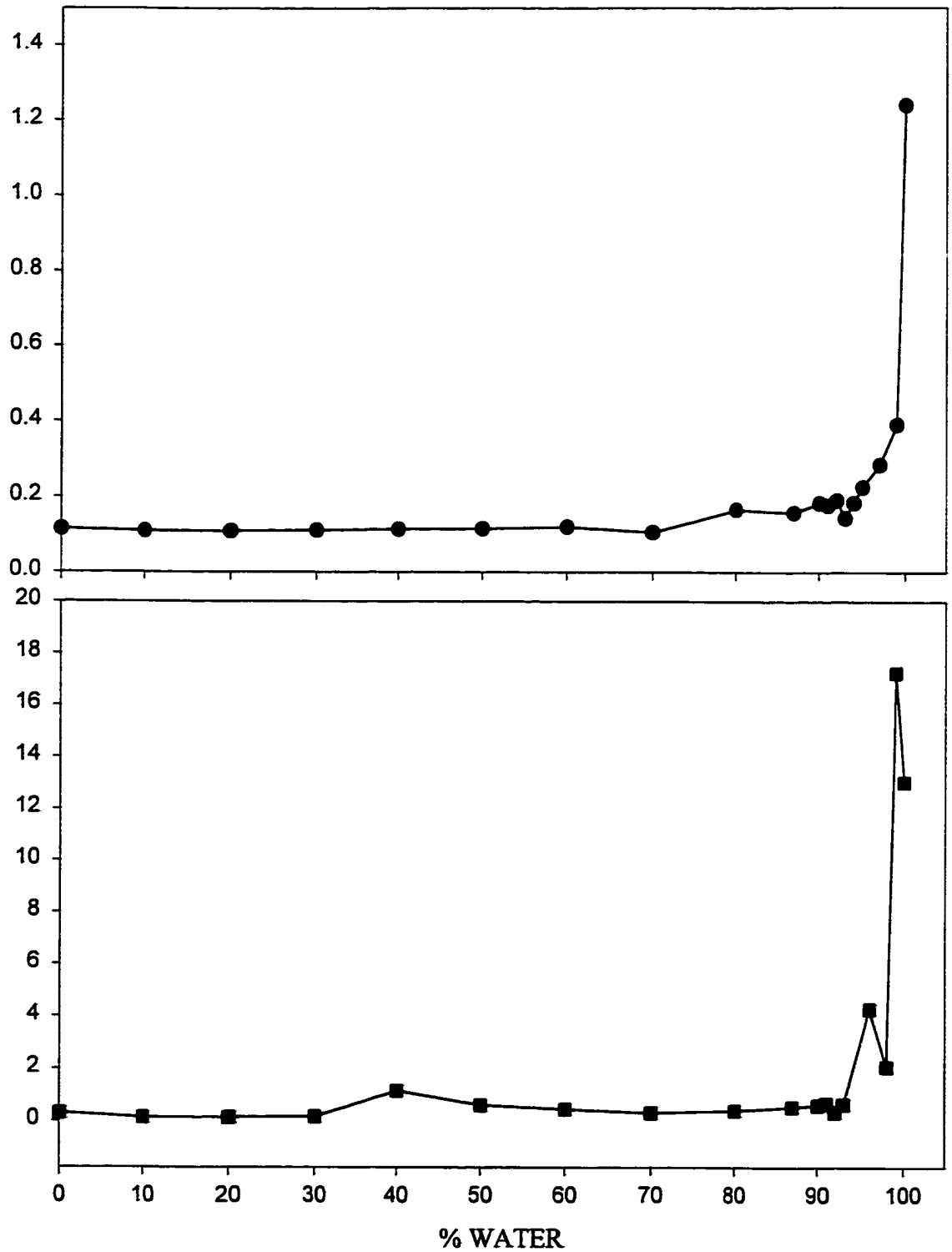

Figure 5.3. $[M+H]^+/M^{+\cdot}$ of naphthalene as a function of %water with acetonitrile (upper trace) and with methanol (lower trace).

it more energetically favourable to abstract a proton from methanol than from acetonitrile.

The high degree of protonation and high signal strength obtained with hexanes prompted an examination of other alkane solvents which would be expected to have similar solubility and chromatographic properties but might offer enhanced signal response. The background spectra of *n*-pentane, hexanes, *n*-hexane, *n*-heptane, *n*-octane, iso-octane, *n*-nonane and cyclohexane are presented in Figure 5.4. All of the alkane solvents fragmented in an expected fashion, with predominantly *m/z* 43 ($C_3H_7^+$) forming. In the case of pentane, the alkane dissociates first to *m/z* 71({M-H]$^+$ ion) which then loses ethene to yield a propyl cation (*m/z* 43). Heptane appears to lose predominantly a C_3H_7 radical or propene and a hydrogen radical to yield predominantly a butyl cation (*m/z* 57). The ion at *m/z* 57 ($C_4H_9^+$), the predominant ion in the spectra reported by Carroll [196], was present in high levels in heptane, octane, iso-octane and nonane. These solvents were associated with high signal intensities but relatively low levels of protonation (see Figures 5.5 and 5.6), indicating that proton transfer occurs more readily from *m/z* 43 than from *m/z* 57, which concurs with CI results. Pyrene was observed to be the most highly responsive and highly protonated, however there was no observable positive or negative correlation of signal intensity with ionisation mechanism. Based on these results, the use of octane, heptane or iso-octane would be preferable from a mass spectral point of view to the use of hexanes. The neurotoxic properties of *n*-hexane make it undesirable as an alternative to hexanes.

The results with the various solvents indicate that even in the absence of benzene, the nature of the solvent profoundly influences the total response and ionisation mechanism of PACs. Dichloromethane appears to be the solvent of choice for maximum sensitivity and

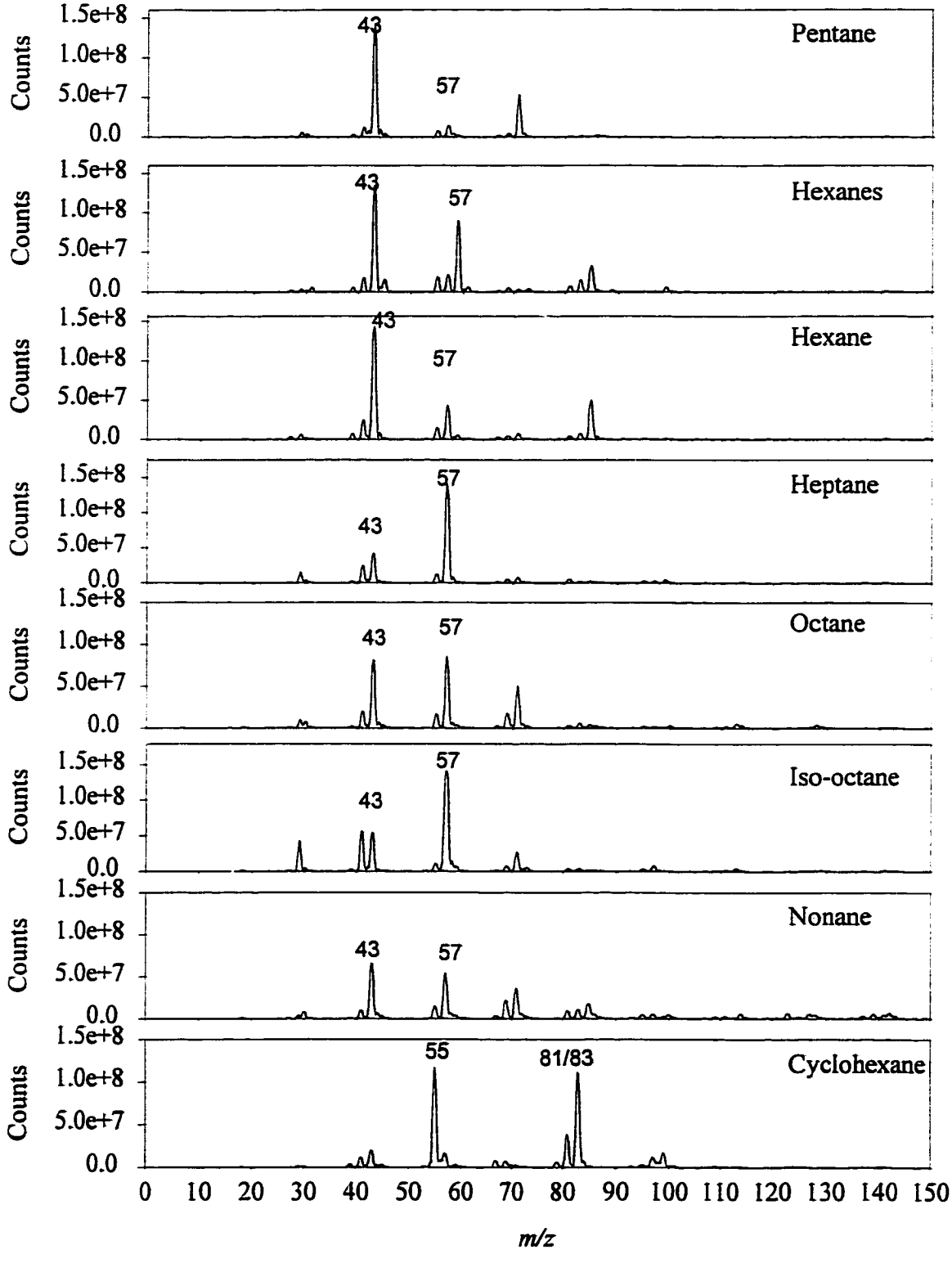

Figure 5.4. Background (from top to bottom) of *n*-pentane, hexanes, *n*-hexane, *n*-heptane, *n*-octane, iso-octane, *n*-nonane and cyclohexane.

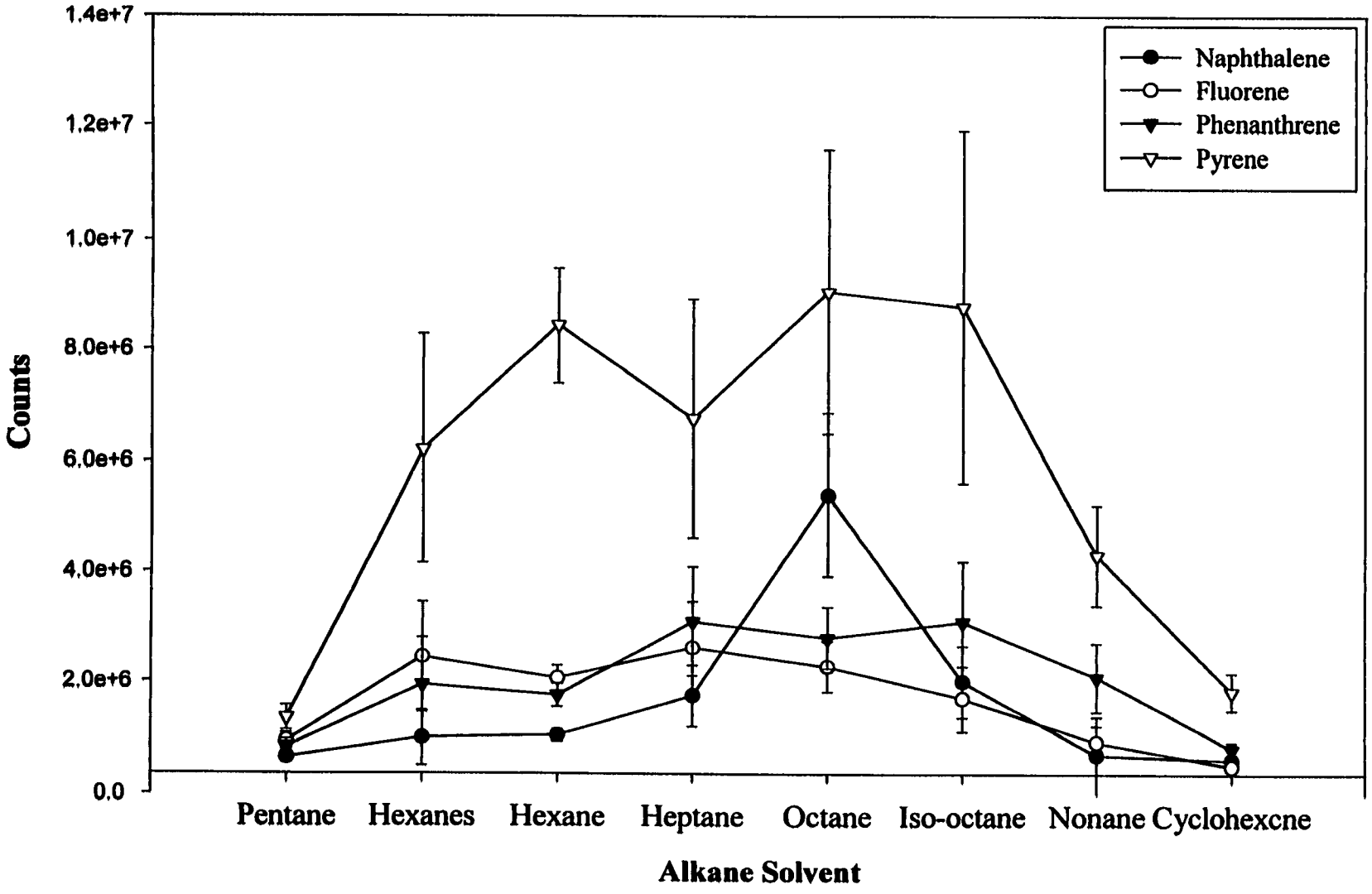

Figure 5.5. Total signal of select PAHs (0.0200 M) as a function of alkane solvent.

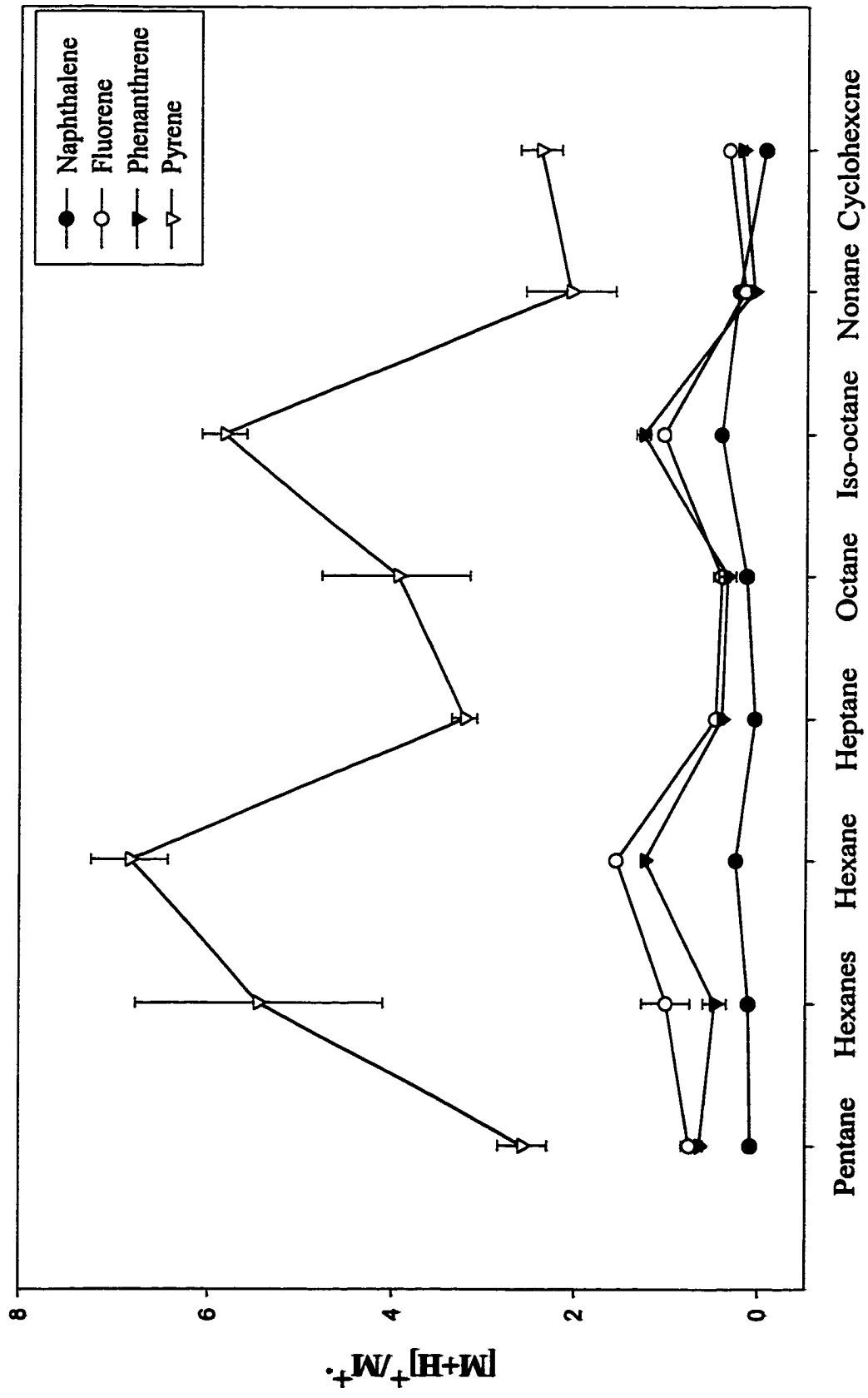

Figure 5.6. Protonation vs. charge exchange of select PAHs as a function of alkane solvent.

aqueous solvents are to be avoided. This may require the manipulation of chromatographic separations to avoid the use of aqueous solvents.

5.3 Effect of Solvent Purity

5.3.1. Distilled vs. Milli-Q water

The results with 50:50 (v/v) acetonitrile/water reported above clearly indicate that a high water content is correlated with poor signal-to-noise ratio. Whether some of this background was attributable to impurities in the water was addressed by performing an isocratic separation of LC-1 with 70:30 (v/v) acetonitrile/Milli-Q water and with 70:30 (v/v) acetonitrile/distilled water. The Milli-Q water is passed through a system of filters which de-ionise the water and remove organic impurities. The total ion chromatograms (TICs) and the naphthalene mass spectrum are depicted in Figure 5.7. The results indicate that the TIC is quieter, the background lower and the naphthalene signal higher with Milli-Q water than with distilled water. This confirms that impurities in the distilled water are responsible for some of the background. The use of Milli-Q water taken directly from the purification system to minimise contact with phthalate-containing plastics was instituted for all further experiments. Despite these precautions, the response of PACs with neat acetonitrile was significantly better than that of aqueous acetonitrile, indicating that even clean water will generate significant background.

5.3.2. Purification of Hexanes by Adsorption on Alumina

The switch to the use of solvent-dedicated tubing and glassware and skimmer Cone C resulted in alteration of the hexanes background (see Figure 5.8). The ion at *m/z* 43 ($C_3H_7^+$) did not dominate the spectra, rather *m/z* 59 ($C_3H_7O^+$) was the dominant ion. This ion could

A)

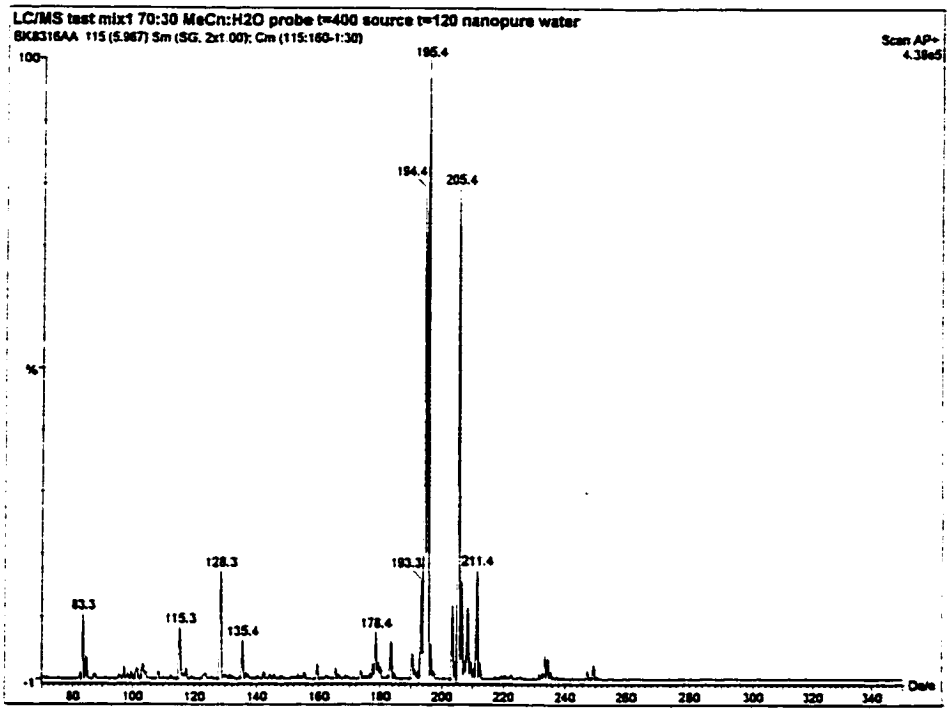

B)

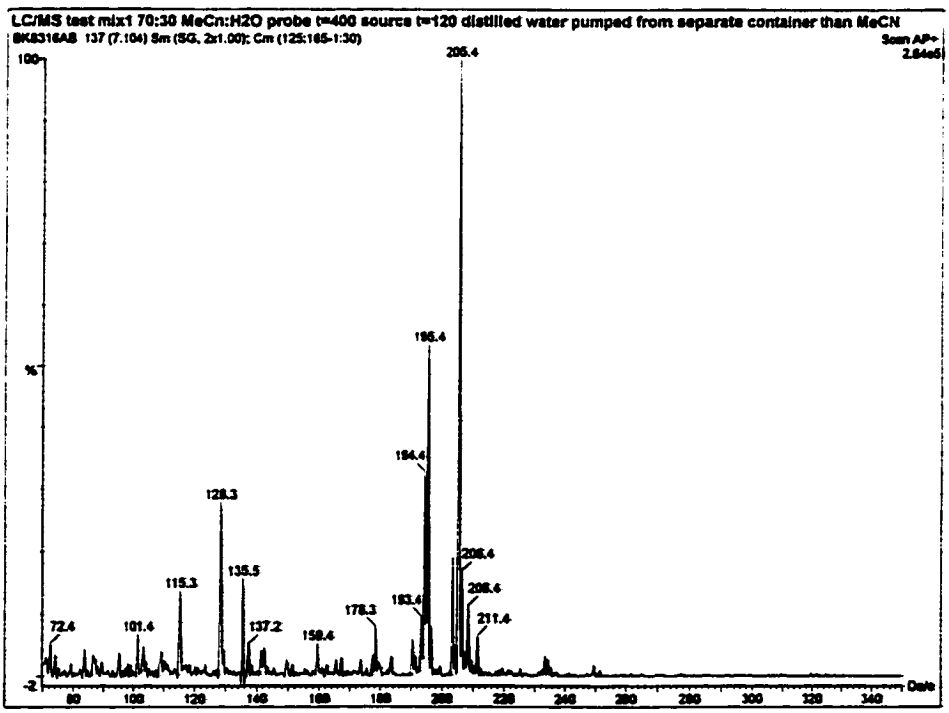

Figure 5.7. Spectra of naphthalene obtained with Milli-Q (A) and distilled (B) water in the mobile phase for RP-HPLC/APCI-MS analysis.

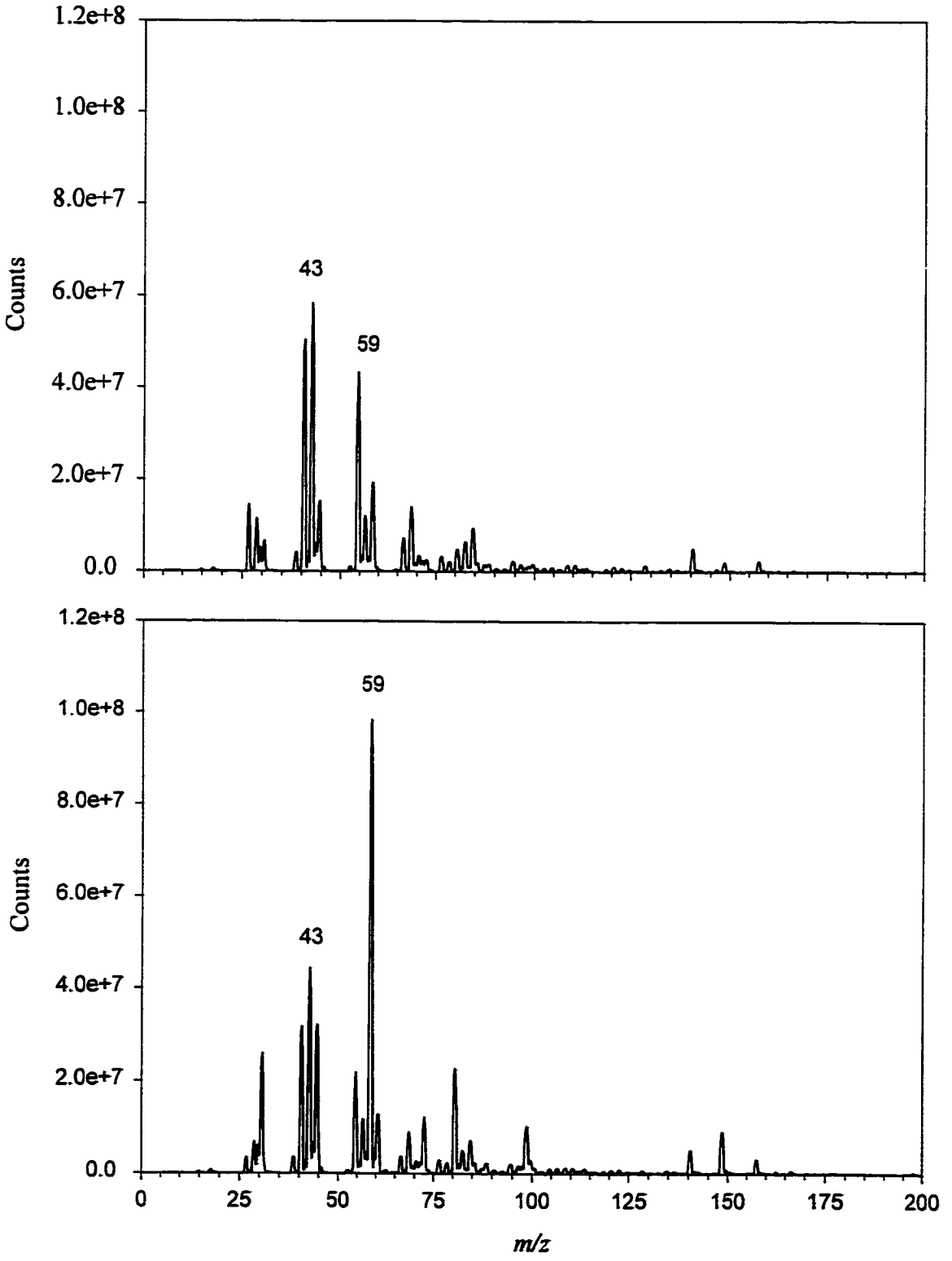

Figure 5.8. Background of hexanes purified (upper trace) by adsorption on alumina and unpurified solvent (lower trace)

be gas- or solvent-derived. The former possibility was tested by examining the solvent background with Dewar nitrogen and with tank nitrogen, the latter being of much higher purity. The nature of the gas used in the mass spectrometer had no impact on the spectral appearance, indicating that *m/z* 59 was not originating from the gas line. The latter supposition was then tested by passing the hexanes through a dry alumina column which should remove the polar, especially oxygen-containing compounds from the solvent. The backgrounds of filtered and unfiltered hexanes indicates that after filtration, the *m/z* 59 peak was substantially reduced., indicating that it was derived from a solvent impurity.

Whether the nature of the ions in the background had any effect on the response or $[M+H]^+/M^{+\bullet}$ of PACS in hexanes was determined by analysing a 1/1000th dilution of Imperial-2 standard with purified and unpurified hexanes (injection solvent = mobile phase) by APCI-MS. The results presented in Table 5.1 indicate that the impurity, although clearly dominating the background spectrum, had little impact either on the signal intensity. This indicates that the PACs are still being ionised. The higher degrees of protonation with less of the impurity indicates that it is more competitive for the available protons than the PACS, consistent with its being a better gas phase base.

Table 5.1 Effect of Purification of Hexanes on Total Signal and $[M+H]^+/M^{+\bullet}$ of PACs

Compound	Purified Hexanes - Response	Unpurified Hexanes - Response	Purified Hexanes - $[M+H]^+/M^{+\bullet}$	Unpurified Hexanes - $[M+H]^+/M^{+\bullet}$
Naphthalene	6.87e4	6.59e4		1.88
Fluorene	3.93e4	1.08e4	1.24	
Phenanthrene	2.64e4	2.23e4	1.87	0.65
Pyrene	6.33e4	5.57e4	2.83	1.83

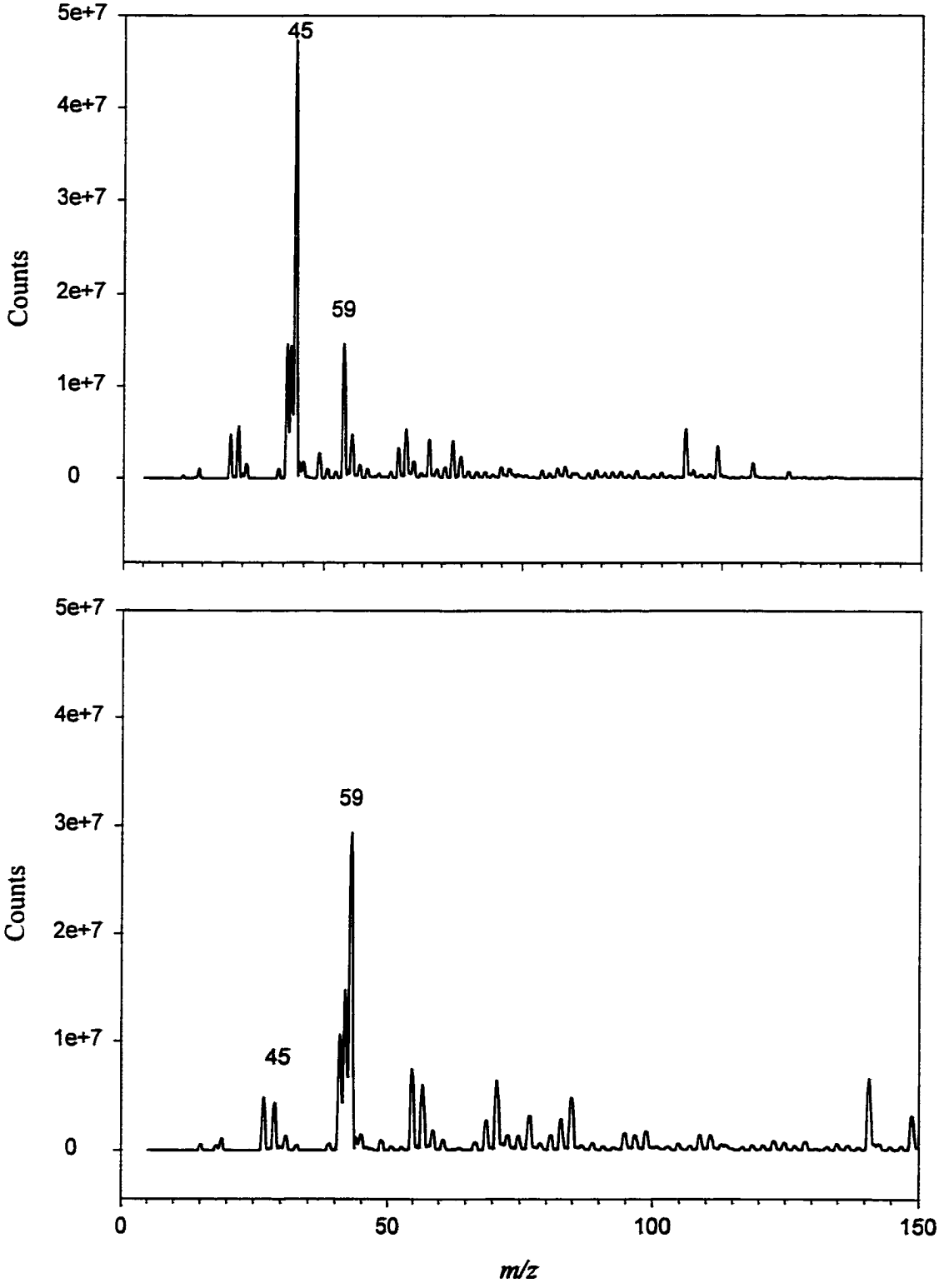

Figure 5.9. Background of dichloromethane purified by adsorption on alumina (upper trace) and unpurified dichloromethane (lower trace).

5.3.3 Purification of Dichloromethane (DCM) by Adsorption on Alumina

An examination of the dichloromethane background also indicated a strong *m/z* 59 ion. The solvent was passed through alumina to remove polar contaminants and the solvent background compared to unfiltered dichloromethane (see Figure 5.9). In this case as well, the peak decreased upon filtration of the sample, though to a lesser extent.

Whether *m/z 59* or the other oxygen-containing species in the dichloromethane background had any impact on the response of PACS was tested by preparing a 1/100th dilution of Imperial-3 with purified and unpurified dichloromethane and analysing by APCI-MS(injection solvent = mobile phase) in single ion recording (SIR) mode. The results, presented in Table 5.2 indicate that the signal intensity and the ionisation mechanism of the smaller PACs are the most affected by the removal of solvent impurities. Unlike the case of hexanes, removal of the impurity actually decreased the protonation, running contrary to the behaviour expected of carbon and oxygen bases. This may indicate that other impurities in the dichloromethane solvent are actually assisting protonation.

Table 5.2. Effect of Purification of DCM on Total Signal and $[M+H]^+/M^{+\bullet}$ of PACs

Compound	Purified DCM - Response	Unpurified DCM - Response	Purified DCM - $[M+H]^+/M^{+\bullet}$	Unpurified DCM - $[M+H]^+/M^{+\bullet}$
Naphthalene	5.48e4	3.91e4	2.41	8.54
Fluorene	1.26e5	2.81e5	6.77	39.97
Phenanthrene	7.47e4	3.99e4	4.39	3.69
Pyrene	8.03e4	7.30e4	2.78	2.92

The commonality of *m/z* 59 in the backgrounds of hexanes and dichloromethane suggests a common origin for this contaminant. It may be originating from the distillation

apparatus used in distilling these two solvents, which is not used for either water or acetonitrile or may be related to the new solvent bottles. The purified solvents were originally placed in graduate cylinders, due to the small volumes involved while the unpurified solvent was taken from the solvent bottle. The ion at *m/z* 59 may not be turning up in the spectrum of acetonitrile because of the dominance of the protonated acetonitrile in the background spectrum.

5.4 Solvent Additives

A number of solvent additives were tested as a means of breaking up the water clusters to reduce the chemical noise due to protonated water clusters. These included ethylene glycol monomethyl ether, ethylene glycol monoethyl ether, trifluorotoluene and methanol. These were added to a total concentration of 2% to 50:50 (v/v) acetonitrile/water. The aqueous acetonitrile backgrounds with and without additives were obtained by scanning the range from *m/z* 70 to 300. The addition of additives did not reduce the abundance of *m/z* 73 (probalywater cluster) but did increase the total background by up to a factor of twenty (see Figure 5.10). The effect of the addition of these additives on the signal intensity for the components of PAC mix-1 is indicated in Table 5.3. The results suggest that the trifluorinated toluene results in signal enhancement for almost all species but no change in ion form (data not shown), which cannot be explained as a decrease in background but may be the result of somewhat improved solubility or better ionisation efficiency of the PACs or better transport efficiency than the other solvents are capable of. The fact that some, but not all, of the PACs are enhanced by a given additive may indicate an interfering peak near that of the PAC.

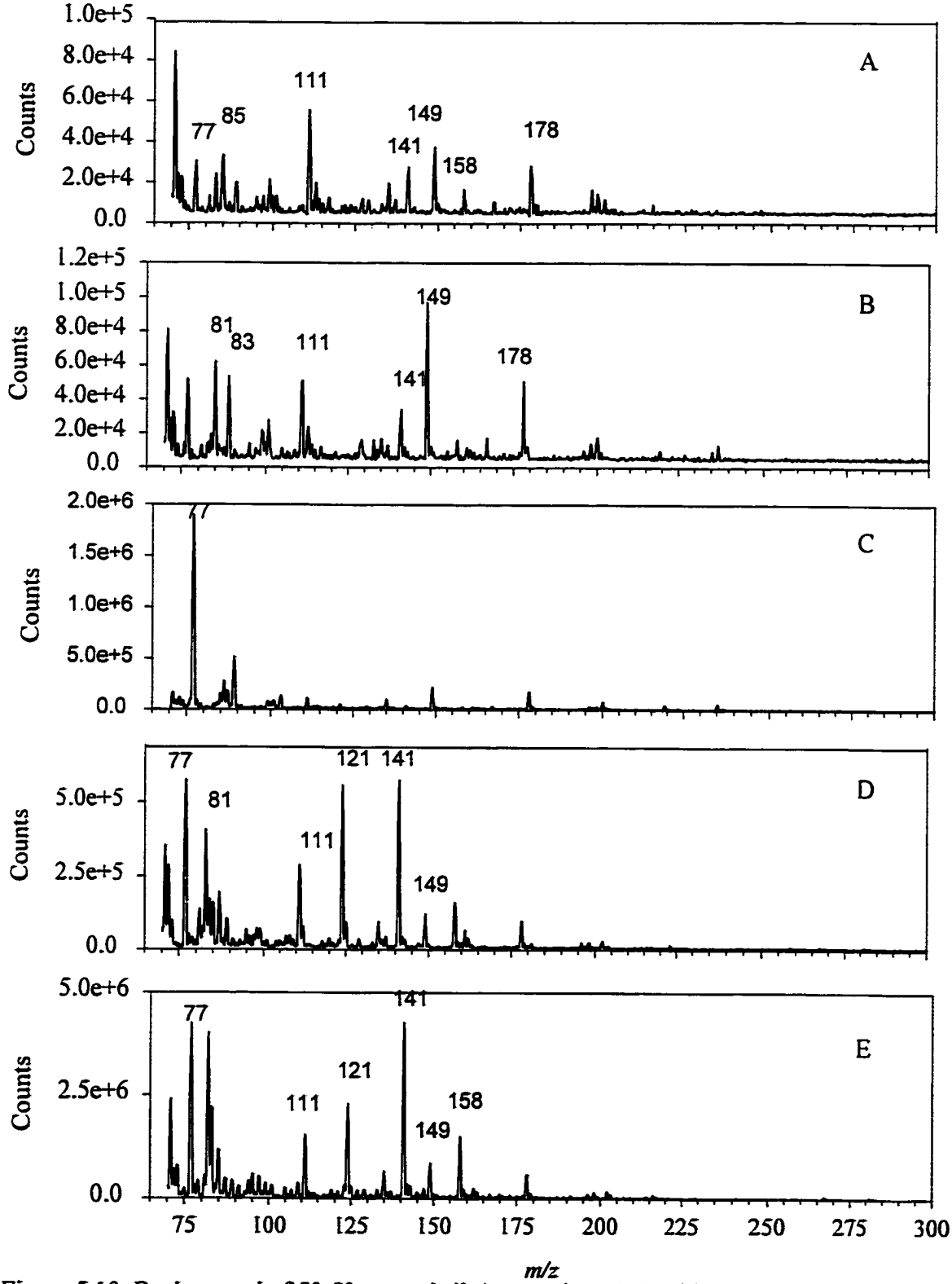

Figure 5.10. Background of 50:50 acetonitrile/water alone (A), with 2% ethylene glycol monomethyl ether (B), with 2% ethylene glycol monoethyl ether (C), with 2% trifluoro-toluene (D) and with 2 % methanol (E).

The use of acidic (acetic, trifluoroacetic and formic acids) or chlorine-containing (chloroform) additives was attempted in the hope that introducing a stronger gas phase acid would lead to greater protonation and a corresponding better signal-to-noise ratio. The backgrounds of unmodified 50:50 (v/v/) MeCN/H_2O and with 2% additive are presented in Figure 5.11. This figure indicates that the addition of a stronger gas phase acid or chloroform resulted in a decrease of *m/z* 19 and an increase of *m/z* 42 which is consistent with acetonitrile being a better gas phase base than water, and an overall increase in the background. The effect that these additives had on total signal intensity and ionisation mechanism of the components of PAC mix-1 is outlined in Tables 5.4 and 5.5.

The results indicate that, in general, the addition of the acetic acid and TFA degraded the signal intensity, the addition of formic acid improved it and that of chloroform had no impact. The results are not explicable by relative acidities. The chloroform results concur

Table 5.3 Signal Intensity of PACs with/without solvent additives

Compound	No additive	EG mono-methyl	EG Monoethyl	Trifluoro-toluene	Methanol
Benzene	7.7e3	3.7e3	6.7e3	not detected	4.4e4
Naph-thalene	9.4e3	1.0e4	2.1e4	4.3e4	1.7e4
Tetralin	3.1e3	8.0e3	1.9e4	2.1e4	2.2e4
Biphenyl	3.6e3	2.6e3	not detected	1.9e4	1.1e4
Fluorene	1.4e4	1.1e4	1.6e4	1.3e5	3.8e3
Anthracene	1.3e4	2.0e4	1.7e4	6.9e4	6.0e3
Pyrene	3.8e3	2.3e3	1.2e4	3.6e4	2.1e4
Chrysene	1.1e3	1.5e3	not detected	not detected	2.8e3
Perylene	not detected	not detected	not detected	1.1e4	5.6e3

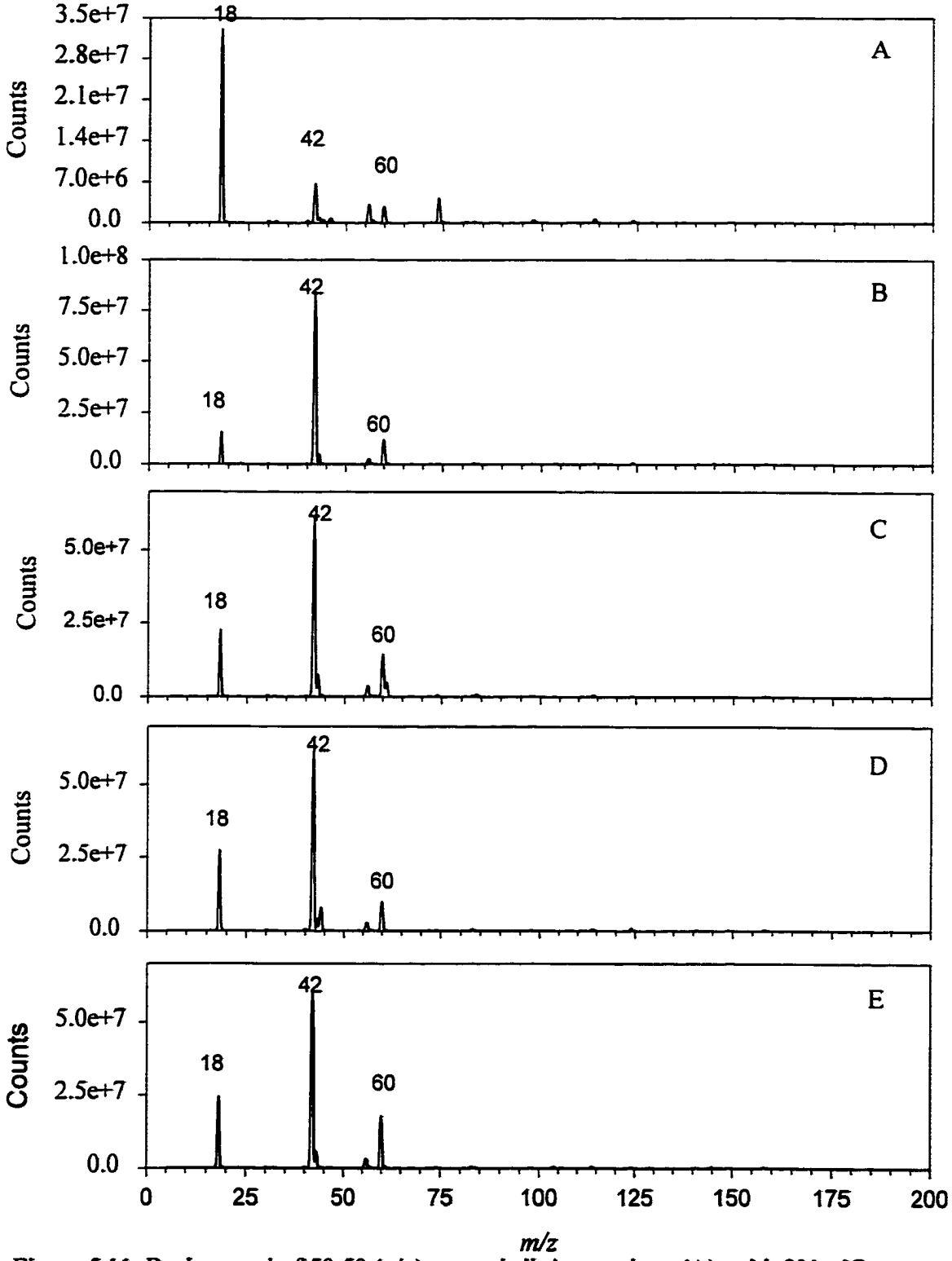

Figure 5.11. Background of 50:50 (v/v) acetonitrile/water alone (A), with 2% trifluoro-acetic acid (B), with 2% acetic acid (C), with 2% formic acid (D) and with 2% chloroform (E).

Table 5.4. Effect of Additives on Signal Intensity of PACs

Compound	None	Acetic acid	TFA	Formic acid	Chloroform
Benzene	5.7e3	5.3e3	6.1e3	5.5e3	5.9e3
Naphthalene	4.1e4	2.5e4	2.9e4	5.6e4	3.6e4
Tetralin	1.3e4	1.7e4	3.7e4	1.5e4	6.0e4
Biphenyl	2.9e4	1.8e4	2.3e4	4.3e4	2.2e4
Fluorene	4.0e4	2.8e4	2.6e4	5.3e4	3.7e4
Anthracene	8.2e4	5.2e4	8.9e4	7.3e4	7.5e4
Pyrene	9.5e4	6.6e4	6.6e4	1.0e5	8.9e4
Chrysene	1.3e4	9.8e4	1.2e4	1.7e4	2.0e4
Perylene	2.0e4	1.54	1.6e4	4.7e4	2.3e4

with its inability to ionise in the positive ion mode. The lack of any effect on protonation was surprising as stronger gas phase acids were being introduced. Thus, the equilibria of PAC protonations were not being perturbed by the addition of these additives.

Table 5.5. Effect of additives on $[M+H]^+/M^{+\bullet}$ of PACs

Compound	None	Acetic acid	TFA	Formic acid	Chloroform
Benzene	2.0	1.4	1.7	0.47	1.7
Naphthalene	0.4	0.55	0.35	1.1	0.37
Tetralin	2.3	2.0	0.40	0.33	6.6
Biphenyl	0.4	0.33	0.29	0.30	0.31
Fluorene	0.35	0.33	0.29	0.23	0.38
Anthracene	0.24	0.28	0.21	0.21	0.28
Pyrene	0.18	0.21	0.20	0.36	0.18
Chrysene	0.31	0.08	0.47	2.8	0.65
Perylene	0.29	0.37	0.35		0.31

Chapter 6

Characterisation of APCI Plasma

6.1 Understanding the Nature of the APCI Plasma

An atmospheric pressure chemical ionisation plasma is generated by the application of a high voltage to the tip of a corona needle. This corona discharge will ionise solvent, gas and sample molecules and the resulting ions will then be analysed in the mass analyser. It is to be expected that changing the solvent or gas composition should produce a change in the nature of the plasma and that this would have an effect on the degree of ionisation and the species present in the mass spectrum. A constant sample composition, in this case, a mixture of polycyclic aromatic compounds will be used to probe the nature of the plasma.

6.1.1. Comparison of APCI with Classical Chemical Ionisation (CI)

One manner of understanding the nature of the APCI plasma is to contrast it with conventional chemical ionisation (CI) mass spectrometry. The most commonly used reagents for CI are methane, isobutane, ammonia and hydrogen. A review of the methane plasma composition was undertaken by Grabner, Poppe and Budzikiewicz in 1990 [56]. Methane will undergo reaction by inelastic collisions with electrons. The products of these collision and the amount of energy transferred will depend on the energy of the impacting electrons. If the electron energy is 50 eV or higher, ions and neutrals will be generated at an almost equal rate. At higher energies, more ions than neutrals are generated but at low energies bonds will be broken but no charge separation will occur. In positive ion mode, the primary ion products formed from methane are the result of ionisation, dissociative ionisation, dissociation and electronic excitation with subsequent dissociation of CH_4 or $CH_3^{\bullet}$ while

neutrals are formed by dissociation reactions. Specifically, the following ions: H^+, $H_2^{+\bullet}$, $C^{+\bullet}$,CH^+, $CH_2^{+\bullet}$, CH_3^+, $CH_4^{+\bullet}$ and neutrals: $H^\bullet$, H_2, C, $CH^\bullet$, $:CH_2$, $CH_3^\bullet$ are observed. The primary ions, in the confined space of the CI source and with sufficient gas pressure, will be able to undergo fast ion/molecule reactions. A primary ion is likely to collide with fewer than 100 times, therefore only those reactions with small energy barriers will be observed. These correspond to reactions with rate constants in the area of 10^{-9} cm^3/s and exothermic or slightly endothermic reactions (see table 6.1 for physical properties of observed reactions).

Table 6.1. Reactions, standard enthalpies of formation, product distribution (relative product abundance in the plasma), and rate constants of 2° and 3° reactions [56]

Reaction	ΔH_R (eV)	Product Distribution	Rate constant (x 10^{-9} cm^3/s)
$H^+ + CH_4 \rightarrow CH_4^{+\bullet} + H^\bullet$	-0.99	0.18	4.5
$\rightarrow CH_3^+ + H_2$	-3.80	0.82	
$H_2^{+\bullet} + CH_4 \rightarrow CH_5^+ + H^\bullet$	-2.95	≤0.03	3.8
$\rightarrow CH_4^{+\bullet} + H_2$	-2.82	0.37	
$\rightarrow CH_3^+ + H_2 + H^\bullet$	-1.15	0.60	
$C^+ + CH_4 \rightarrow C_2H_2^{+\bullet} + H_2$	-4.19	0.25	1.3
$\rightarrow C_2H_2^{+\bullet} + H_2$	-4.04	0.75	0.75
$CH^+ + CH_4 \rightarrow C_2H_4^{+\bullet} + H^\bullet$	-2.71	0.05	
$\rightarrow C_2H_3^+ + H_2$	-4.43	0.84	
$\rightarrow C_2H_2^{+\bullet} + H_2 + H^\bullet$	-0.08	0.11	
$CH_2^{+\bullet} + CH_4 \rightarrow C_2H_5^+ + H^\bullet$	-1.95	0.23	1.2
$\rightarrow C_2H_4^{+\bullet} + H_2$	-2.65	0.42	
$\rightarrow C_2H_3^+ + H_2 + H^\bullet$	+0.11	0.22	
$\rightarrow C_2H_2^{+\bullet} + 2\,H_2$	-0.04	0.13	
$CH_3^+ + CH_4 \rightarrow C_2H_5^+ + H_2$	-1.07	1.00	1.2

$CH_4^{+\bullet} + CH_4 \rightarrow CH_5^+ + CH_3$	-0.17	1.00	1.5
$CH_5^+ + CH_4 \rightarrow$ isotope exchange		1.00	3.0
$C_2H_2^{+\bullet} + CH_4 \rightarrow C_3H_4^{+\bullet} + H_2$	-3.25	0.21	8.4
$\rightarrow C_3H_5^+ + H^\bullet$	-0.93	0.79	
$C_2H_3^+ + CH_4 \rightarrow C_3H_5^+ + H_2$	-1.17	1.00	2.0
$C_2H_4^{+\bullet} + CH_4 \rightarrow$ no reaction			≤1.0
$C_2H_5^+ + CH_4 \rightarrow C_3H_7^+ + H_2$	-0.44	1.00	1.0
$C_2H_5^+ + O_2 \rightarrow$ no reaction			≤2.0
$CH_5^+ + O_2 \rightarrow$ no reaction			≤5.0
$CH_4^{+\bullet} + O_2 \rightarrow O_2^{+\bullet} + CH_4$	-0.54	1.00	4.4
$CH_5^+ + H_2O \rightarrow H_3O^+ + CH_4$	-1.87	1.00	3.7
$C_2H_5^+ + H_2O \rightarrow H_3O^+ + C_2H_4$	-0.45	1.00	1.4
$CH_5^+ + CO \rightarrow HCO^+ + CH_4$	-0.62	1.00	9.9
$CH_4^{+\bullet} + CO_2 \rightarrow HCO_2^+ + CH_3^\bullet$	-0.13	1.00	1.2
$CH_5^+ + CO_2 \rightarrow HCO_2^+ + CH_4$	< 0.01	1.00	3.2
$HCO_2^+ + CH_4 \rightarrow CH_5^+ + CO_2$	> -0.01	1.00	7.8

The actual yields of primary, secondary and tertiary reactions in the methane plasma will depend on experimental values. As the methane pressure is increased, the number of collisions between primary ions and methane will increase, such that the yield of secondary ions will increase with increasing methane pressure, until it reaches a maximum and then decreases again (due to greater formation of tertiary ions or decomposition). As the temperature is increased at constant pressure, the number of secondary and tertiary reactions will decrease while kinetic energy increases. An increase in the repeller potential will

increase the acceleration of ions toward the exit slit, reduce residence time in the source and this will reduce the number of collisions. However, the kinetic energy will be increased, causing more energy to be transferred on collision with neutral molecules and this allows endothermic reactions to take place. An increased repeller potential will reduce the amount of CH_5^+ and $C_2H_5^+$. The electron energy will also have a strong impact on the yields of primary, secondary and tertiary ions. The electron energy and the electric field gradient in the region of ion formation will determine the residence time of the ions, the largest effects being observed from 20 to 50 eV. The levels of CH_5^+ are considerably lower at 20 eV than at 50eV. Regardless of the experimental conditions, only 10-20% of ions will survive until the analyser, the others being lost by dissociative recombination. Under typical conditions, the methane plasma will consist of 32.6% CH_5^+, 11.2% $C_2H_3^+$ and 39% $C_2H_5^+$ [56].

With an understanding of the typical reaction conditions in a methane CI source it is possible to use this knowledge to rationalise the response of PACs. Simonsick and Hites in 1984 used a 15% mixture of methane in argon to ionise polycyclic aromatic compounds. The methane would promote a proton transfer medium, yielding predominantly the protonated molecules by reaction of the analyte with $C_2H_5^+$. The argon atmosphere, on the other hand, promotes charge transfer, yielding predominantly the molecular ion, by reaction of the analyte with $Ar^{+\bullet}$. The ratio of $[M+H]^+$ to $M^{+\bullet}$ would provide a means of distinguishing the isomeric forms of PACs, such as differentiating between pyrene and fluoranthene. This ratio was also observed to be sensitive to experimental conditions, such as source temperature, pressure, and cleanliness. Thus, an increase in source temperature was correlated with a decrease in this ratio due to the decrease in ion residence time, which

selectively extracts $Ar^{+\bullet}$ and prevents the formation of $C_2H_5^+$, enhancing the amount of $Ar^{+\bullet}$ available and the subsequent increase in charge transfer. Increasing the source pressure will increase the residence time, selectively enriching the plasma with $C_2H_5^+$ in relation to $Ar^{+\bullet}$ with consequent increase in the degree of protonation. As the source gets dirtier, the ratio also increases as the result of the generation of a thin film on the lenses which also increases ion residence time. Hence, instrumental parameters which increase the residence time of ions will cause an increase in protonation relative to charge exchange. A correlation exists between the ionisation energy (IE) of PACs and the ratio of protonated molecule to molecular ion. This can be expressed as:

$$[M+H]^+/M^{+\bullet} = 1.601\ (IE) - 11.049 \qquad (r^2 = 0.947) \qquad \text{eq. 6.1 [196]}$$

Brotherton and Gulick in 1986 [159] examined PACs by positive and negative ion CI coupled with gas chromatographic separation as an alternative to electron ionisation. They also observed a competition between charge exchange and proton transfer which could be exploited for isomer differentiation. They examined the response of PACs in positive ion CI with methane, isobutane doped with oxygen, argon doped with methane, hydrogen, and nitrogen doped with nitrous oxide as reagent gases. They calculated and compared the response factors (totals counts per nanogram of compound injected) of selected PACs with these different reagent gases and with EI. The results are presented in the Table 6.2. Methane spectra of the PACs included $M^{+\bullet}$, $[M+H]^+$, $[M + 29\ (C_2H_5)]^+$ and $[M+41\ (C_3H_5)]^+$ ions. The results with isobutane/oxygen were similar but an additional peak at $[M + 57(C_4H_9)]^+$ was observed. The 95% argon - 5% methane plasma yielded the molecular ion as the base peak. Nitrogen/nitrous oxide acts as a charge-exchange medium, thereby

Table 6.2. Positive ion response (total counts excluding plasma ions/ng of compound) of PACs

Compound	EI	CH_4	Ar/CH_4	C_4H_{10}/ O_2	H_2	N_2/ N_2O
Phenanthrene	21	8.0	22	10	25	38
Anthracene	18	8.0	20	50	14	18
Fluoranthene	17	5.0	13	24	19	13
Pyrene	22	4.5	16	9.0	20	22
Benz[*a*]anthracene	15	3.0	9.0	28	13	11
Chrysene	19	2.0	8.0	6.0	16	12
Triphenylene	12	0.5	10	14	10	6.0
Tetracene	10	1.0	1.5	3.0	0.1	0.8
Benzo[*b*]fluoranthene	4.0	5.0	8.0	8.0	36	4.0
Benzo[*k*]fluoranthene	12	2.0	5.0	3.0	37	3.0
Benzo[*e*]pyrene	10	0.5	6.0	10	14	5.0
Benzo[*a*]pyrene	2.0	4.0	5.0	6.0	31	1.4
Perylene	25	1.3	2.0	4.0	2.0	2.0

favouring molecular ion formation and disfavouring addition products. The level of protonated molecule could be increased slightly by transfer from hydronium ion where water is a trace impurity. The use of hydrogen gave the best sensitivity and the best overall isomer discrimination. It will form H_3^+ which has a low proton affinity and can act as both a Brønsted acid and a charge-exchange reagent.

Negative ion CI was also carried out in with the same reagent gases and in carbon dioxide, carbon monoxide and nitrogen/carbonyl sulfide. The observed spectra could be rationalised by dividing the PACs into three classes. Class 1 PACs included anthracene,

fluoranthene, benz[*a*]anthracene, tetracene and perylene which exhibited mainly molecular anion, and other characteristic ions. Phenanthrene, pyrene, chrysene, triphenylene and benzo[*e*]pyrene formed Class 2 and were more diverse. A predominant molecular anion was observed for pyrene only with carbon monoxide or dioxide and benzo[*e*]pyrene in methane but $[M-H]^-$ was predominant for all others. Class 3 included the benzofuoranthenes and the benzo[a]pyrene which yielded only molecular anion and isotope peaks.

Ions at $[M+14]^-$ and $[M+15]^-$ occurred frequently and were ascribed to $[M-2H+O]^-$ or $[M-CH_2^+]^-$ and $[M-H+O]^-$. $[M+14]^-$ occurs most frequently in argon/methane or in methane plasmas while $[M+15]^-$ predominated when oxygen is present. In the hydrogen plasma, there is some OH^- and H^- which can either abstract a proton or form adducts, hence $[M-H]^-$ and $[M+H]^-$ can be observed, especially with Class 2 PACs. In the case of nitrogen/nitrous oxide, both O^- and NO^- are present. The former is the stronger base, hence some PACs will form $[M-H+O]^-$. PACs in CO_2 and CO yielded similar spectra but these were distinct from the spectra with other gases. Class 1 compounds gave molecular anion base peaks with some formation of $[M-H+O]^-$ and $[M-2H+20]^-$. Class 2 ions gave predominantly $[M+2H]^-$ along with $[M+44]^-$, $[M+43]^-$ and $[M+42]^-$ from the addition of carbon dioxide with the loss of 0-2 hydrogens. The carbon dioxide plasma itself contained ions at *m/z* 60 (CO_3^-), 68 and 112 while carbon monoxide yielded *m/z* 126 and 148. Carbonyl sulfide mixed with nitrogen gave a plasma containing polysulfide anions, CO^- and COS^-. Only the molecular anion was observed with any class of PACs studied. These sulfur-containing species have high electron affinities so they deplete the supply of electrons available to ionise PACs and thereby, reduce their response [159].

In 1988, Hazel, Bowen and Jennings investigated the mechanisms by which the molecular ion forms in methane chemical ionisation of polymethylbenzenes. The three mechanisms which they considered were: 1) loss of $H^{\bullet}$ from $[M+H]^{+}$, 2) charge transfer from reagent gas and 3) residual electron ionisation in the CI source. The first was rejected based on the energetics involved which would suggest that methyl loss from the protonated molecule is more likely. As this did not occur, hydrogen loss is even less likely. The energetics of the second mechanism would require CH_5^{+} to capture an electron and reform methane and hydrogen radical, liberating only 765 kJ/mol of energy which would be insufficient to ionise any PAC. Thus, the only plausible mechanism left is residual EI in the source and this is confirmed by the presence of peaks originating from methyl loss from the molecular ion (typical of EI) [66].

Daishima *et al.* in 1992 examined the methane negative ion CI of PACs. They observed that the most common base peaks were $[M-H]^{-}$, $M^{-\bullet}$ and $[M+H]^{-}$. Which of these peaks was the base peak could be rationalised on the basis of their structure and on the ratio of the base peak counts in negative ion (N) and positive ion (P) modes (N/P). Hence, $[M-H]^{-}$ predominated where the molecule had an aliphatic chain and N/P <1. Where $M^{-\bullet}$ was the predominant ion, the electron affinity and the N/P were high. Where $[M+H]^{-}$ predominated, the base peak structure included a phenyl group and the observed N/P < 1. If the N/P ratio > 5, the compounds were determined with good sensitivity but if below 5, sensitivity was poor. Thus, this ratio could be used as a predictor of sensitivity [70].

Canton and Grimalt applied GC/MS to the analysis of PACS in coastal sediments. The origin of the PAC could be traced from the observed species. Hence, pyrolytic sources

contained high concentrations of catacondensed structures and nonalkylated PAC structures, urban sources were rich in cyclopenta[*cd*]pyrene and a high ratio of benzo[*a*]pyrene to benzo[*e*]pyrene. Crude oil contamination shows enhanced fluoranthene vs. pyrene and equal proportions of benzo[*ghi*]perylene and indeno[1,2,3-*cd*]pyrene. High mass materials are most readily analysed by negative ion CI as opposed to EI and FID detection [158].

A CI source is typically operated at 1 Torr and hence, each ion or molecule introduced will undergo about 100 collisions with other species before leaving the source [56]. These collisions ensure that only long-lived species will be detected.

An APCI source, by contrast, operates at 760 Torr and if CI is used as a model, any molecule or ion formed will be subject to 76 000 collisions assuming the same residence time in both modes. This will further reduce the likelihood of observing short-lived or unstable species.

The current understanding of the nature of the APCI plasma is based on experiments by Professor Kebarle [92]. The instrumental design of the APCI source used is presented in Figure 6.1 and it was operated in a moist air environment.

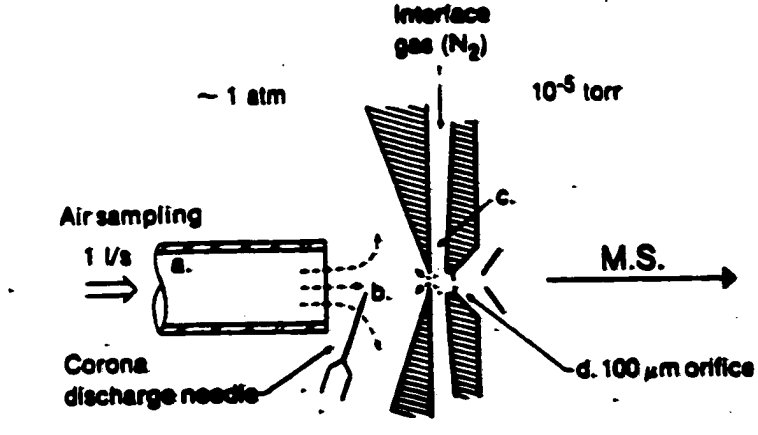

Figure 6.1. Instrument used for Determining APCI mechanisms [92]

The understanding of the reaction chemistry of moist air in an APCI plasma is summarised in the following series of reactions:

$$e^- + N_2 \rightarrow N_2^{+\bullet} + N_2 \rightarrow N_4^{+\bullet} + O_2 \rightarrow O_2^{+\bullet}$$

$$e^- + O_2 \rightarrow O_2^{+\bullet} \rightarrow O_4^{+\bullet}$$

$$O_2^{+\bullet}, O_n^{+\bullet} + H_2O \rightarrow O_2^{+\bullet}(H_2O)$$

$$O_2^{+\bullet}(H_2O) + H_2O \rightarrow O_2^{+\bullet}(H_2O)_2 \rightarrow H_3O^+(OH^\bullet) + O_2$$

$$H_3O^+(OH^\bullet) + H_2O \rightarrow H_3O^+(H_2O) + OH^\bullet$$

$$H_3O^+(H_2O) + H_2O \rightarrow H_3O^+(H_2O)_2$$

$$H_3O^+(H_2O)_n + H_2O \rightarrow H_3O^+(H_2O)_{n+1}$$

Typically, there will be three to eight water molecules clustered about the hydronium ion. These hydrated ions are the main reagent ions in this type of APCI (without a solvent). When they undergo ion-molecule reactions with species whose gas phase basicity exceeds that of water, there will be observed protonation, as in the following equation:

$$H_3O^+(H_2O)_h + B \rightarrow BH^+(H_2O)_b + (h+1-b)\ H_2O$$

In the instrumental setup used in this original study, a dry nitrogen source was used as an interface gas between the source and analyser. This gas keeps the vacuum chamber and quadrupole rods clean and thermally declusters ions. This declustering occurs as the result of a gas jet formation at the orifice. This formation converts thermal energy to kinetic energy which leads to a significant cooling effect. The lower the effective temperature in the gas stream, the higher the degree of clustering. These may not be observed at the detector because ions will be lost in the curtain gas and in the gas jet and the quadrupoles will

discriminate against high-mass ions [92].

This was applied to the analysis of sample molecules introduced as gases into the mass spectrometer source. Analytes with a gas phase basicity (free energy of the reaction: $B + H \rightarrow BH^+$) greater than or equal to 837 kJ/mol have high and almost uniform sensitivity. These were defined as group K analytes and were typically nitrogenous bases. Group T compounds (oxygen-containing bases) have a gas phase basicity below 837 kJ/mol and exhibit a lower overall sensitivity less than group K analytes. Their sensitivity increases with increasing gas phase basicity. Group L compounds are particularly insensitive compounds, lower even than would be predicted based on their gas phase basicity. Into this latter class fall the polycyclic aromatic compounds [92].

To understand what occurs in the APCI plasma, it is important to understand the events that occur near the corona needle where the ions are generated and what happens along their path to the detector. The voltage drop near the corona needle is greatest at its tip. The positive ions generated near the corona needle will leave the ionisation region and drift towards the orifice. This drift region is where all the ion/molecule reactions will take place. The ion drift time determines the ion residence time, which determines how many collisions an ion will undergo. As the distance between the needle and the analyser region increases, the ion residence time increases, fewer ions enter the source and the number of hydronium ion reagent ions decreases. Actual ion yields are subject to both kinetic and thermodynamic control. Kinetic control, in this case, means that the intensity of the BH^+ is determined by the rate of proton transfer from the reagent ions to the analytes. This applies for the group K analytes and an increase in residence time will result in higher observed protonation.

Residence time can be increased by increasing the distance (lengthening the drift region), and/or by decreasing the corona voltage. For the less reactive Group T and L compounds, thermodynamic control of reaction is operative [92].

This was explained by Kebarle *et al.* [92] on the basis of free-energy arguments. The free energy change of the proton transfer reaction is mainly determined by enthalpic considerations as there is little change in entropy, and will largely depend on the gas phase basicities and hydration energies of the species involved. For the proton transfer to be energetically favourable, the gas phase basicity difference must be large enough to overcome the unfavourable energetics of proton transfer. The Group K analytes have a gas phase basicity so high relative to hydrated hydronium ion that the reaction is exothermic and proton transfer occurs readily. Group T and L bases have gas phase basicities that are lower, making the reaction endothermic and hence energetically less favourable. To get uniform sensitivity for all compounds, one can either decrease the hydration of the hydronium ion by water removal from air or by the use of higher operating temperatures in the source [92].

The system used in the present study is the Fisons-VG-Micromass™ depicted in Figure 2.4b. In this system, a minimum of 200 μL/min flow of solvent and dissolved analyte is being introduced into the plasma. The APCI plasma will thus consist of source gases, solvent and analyte molecules interacting with each other. It was clear from Chapter 5 that the solvent had a large impact on the signal intensity and degree of protonation of the PACs. There are several possible explanations for this. One is that protonated water clusters are being formed but are primarily ionising the solvent, which in turn ionises the analytes. Another is that analyte ions are interacting both with the protonated water clusters and the

solvent, the reactions being competitive. The third possibility is that no water clusters are being formed and it is only the ionisation of the solvent or its impurities which subsequently ionises the analytes. The fourth possibility is that source gas ions are directly ionising the analyte. The fifth is that the analyte may ionise directly in the field of the corona needle, without the co-operation of the gas or solvent. To elucidate which of these five possibilities is most likely, experiments were carried out with selected PACs in 50:50 (v/v) acetonitrile/water, acetonitrile, dichloromethane and hexanes with a number of different gases, both alone and in combination. Both the signal intensity and the predominant ions of these PACs were compared as a function of source gas composition. The gas alone and the gas plus solvent backgrounds were obtained to demonstrate the impact of the gas on solvent ionisation and fragmentation. An attempt to explain these behaviours based on the physical properties, as detailed in Table 6.3, was then attempted.

Based on these values, ionisation should decrease in the following order: perylene, pyrene, carbazole, chrysene, triphenylene, phenanthrene, fluoranthene, naphthalene, fluorenone, and dibenzothiophene. Protonation should decrease in the order: perylene, pyrene, chrysene, fluorene, fluoranthene, phenanthrene, triphenylene and naphthalene. Based on IE and equation 6.1, we would therefore expect the following ratios of protonated molecule to molecular ion for the PACs if gas and/or solvent have no impact (see Table 6.4).

Table 6.3. Physical properties of gases, solvents and analytes used [201 - 204].

Species	Ionisation energy (eV)	Proton Affinity (kJ/mol)	Gas Phase Basicity (kJ/mol)
N_2	15.581	493.8	464.5
O_2	12.0697	421	396.3
CO_2	13.777	540.5	515.8
CO	14.014	594, 426.3	562.8, 402.2
CH_4	12.61	543.5	520.6
H_2	15.42593	422.3	394.7
H_2O	12.621	691	660
MeCN	12.20	779.2	748
Dichloromethane	11.33		
Hexanes*	10.13		
Naphthalene	8.144	802.9	779.4
Fluorene	7.91	831.5	803.8
Phenanthrene	7.891	825.7	795.0
Fluorenone	8.29		
Pyrene	7.426	869.2	840.1
Chrysene	7.60	840.9	810.1
MTC			
Dibenzothiophene	8.44		
9-Phenanthrol			
Carbazole	7.57		
Triphenylene	7.87	819.2	791.2
Fluoranthene	7.90	828.6	800.9
Perylene	6.960	888.6	859.6

* Solvent is actually a mixture of alkanes, with *n*-hexane being the predominant species

Table 6.4. Predicted $[M+H]^+/M^{+\bullet}$ Ratios for PACs

Compound	$[M+H]^+/M^{+\bullet}$
Naphthalene	1.99
Fluorene	1.62
Phenanthrene	1.58
Fluorenone	1.20
Pyrene	0.84
Chrysene	1.12
MTC	
Dibenzothiophene	2.46
9-Phenanthrol	
Carbazole	1.07
Triphenylene	1.55
Fluoranthene	1.60
Perylene	0.09

6.1.2. Comparison of APCI Plasma with Glow Discharge Plasmas

Studies of the components of mixed-gas plasmas, similar to those studied in this study, have been undertaken with glow discharge devices. For example, a 99% nitrogen - 1% methane plasma will contain N^+, $N_2^{+\bullet}$, N_2H^+, NO^+, OH^+, $H_2O^{+\bullet}$ at greater than 10% abundance with trace amounts (< 10%) of $C^{+\bullet}$, CH^+, CH_3^+, $CH_4^{+\bullet}$, H_3O^+, CN^+, CNH^+ and $O_2^{+\bullet}$ [197]. A 97% carbon dioxide - 3% nitrogen plasma will contain NO^+, $O_2^{+\cdot}$ and $CO_2^{+\cdot}$ in greater than 5% abundance and $O^{+\bullet}$, $N_2^{+\bullet}$, $CO^{+\bullet}$, COH^+, CO_2H^+, NO_2^+, $H_2O^{+\bullet}$, H_3O^+, $C^{+\bullet}$ and CN^+ [197]. A nitrogen-oxygen plasma will exhibit N^+ (10% abundance) and NO^+, $O_2^{+\cdot}$, $N_2^{+\bullet}$, $O^{+\bullet}$ and $Ar^{+\bullet}$ in less than 2% abundance [198]. Several types of reactions occur in a

nitrogen plasma [199]. These include dissociative reactions, charge exchange reactions, associative ionisation, and electron ionisation to yield N, N^+ and $N_2^{+\bullet}$. An air plasma will exhibit N^+, $O^{+\bullet}$, $N_2^{+\bullet}$, NO^+, $O_2^{+\bullet}$, and $N_2O^{+\bullet}$ as ions and $H^\bullet$, H_2, N, O, OH, H_2O, N_2, NO, O_2 and N_2O as neutrals due to the neutral exchange reactions, associative ionisation/dissociation recombination reactions, electron ionisation/recombination reactions and charge transfer reactions in the plasma among the air constituents [200].

6.2 Results with Skimmer Cone A

These results represent preliminary experiments with one, two and three gas experiments, as described in Table 3.4 , with each of the four solvents as an attempt to evaluate the gas and solvent effects on PAC response. These experiments are considered preliminary because later experiments showed that cone A was faulty and that the solvent delivery systems were subject to considerable memory and carryover effects. However, the trends in PAC response gave important insights into the APCI plasma chemistry. All these experiments were performed as single measurements and statistical data is unavailable.

6.2.1 One Gas Systems

One gas experiments were performed with a single gas in the bath (B), sheath (S) and nebuliser (N) streams. The gases studied included Dewar N_2, tank N_2, O_2, building air, Extradry™ air, carbon dioxide, carbon monoxide, methane and hydrogen. Air and oxygen were not used with hexanes due to the risk of combustion.

The total signal intensity (protonated and unprotonated molecule response) and the ratio of protonated molecule to molecular ion for PACs in Imperial-3 standard prepared in dichloromethane are presented in Figures 6.2 and 6.3. Dichloromethane was selected as it

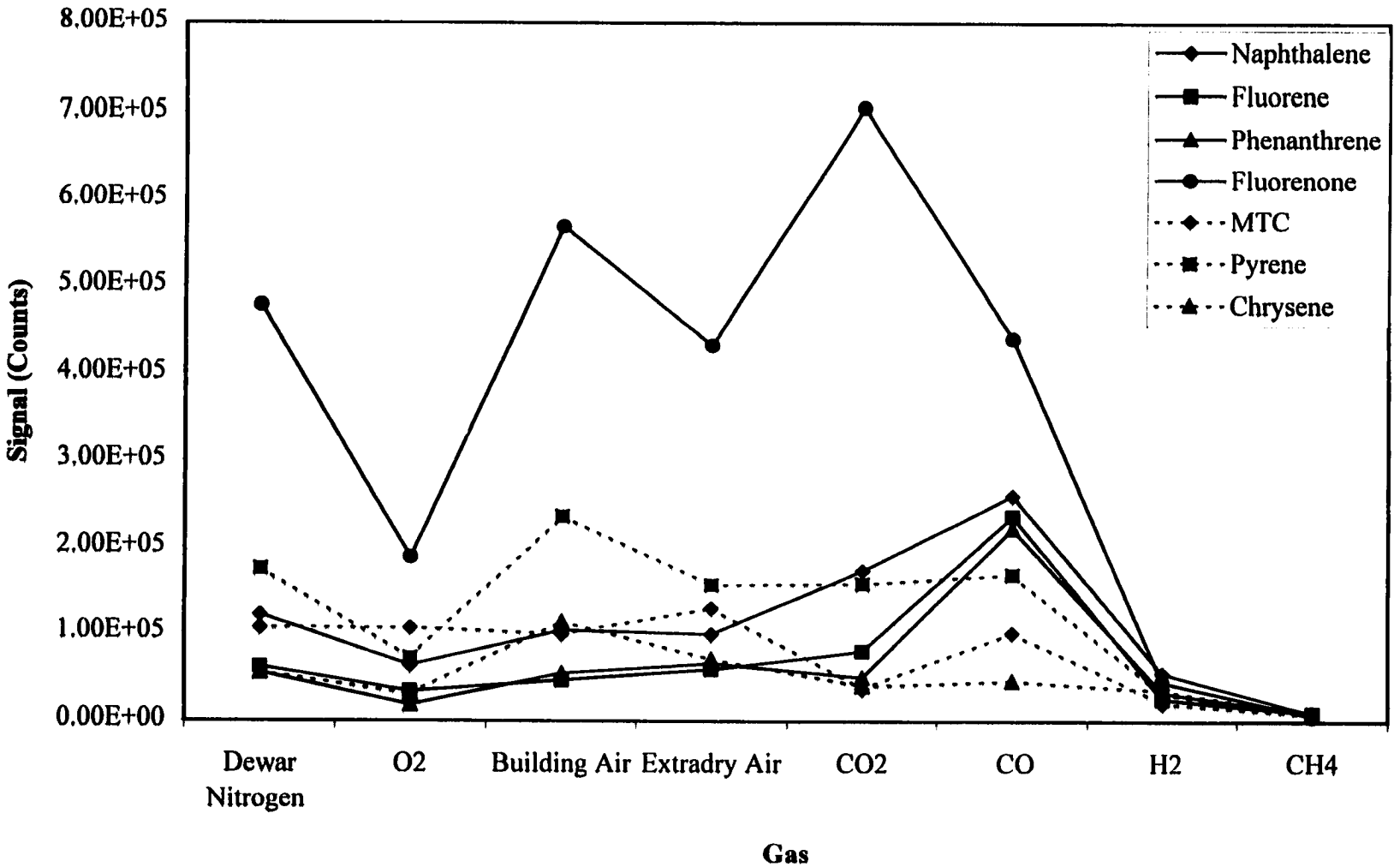

Figure 6.2. Total signal (protonated and charge exchanged) of a 1/100 dilution of Imperial-3 in dichloromethane with dichloromethane as the mobile phase as a function of gas (skimmer cone A).

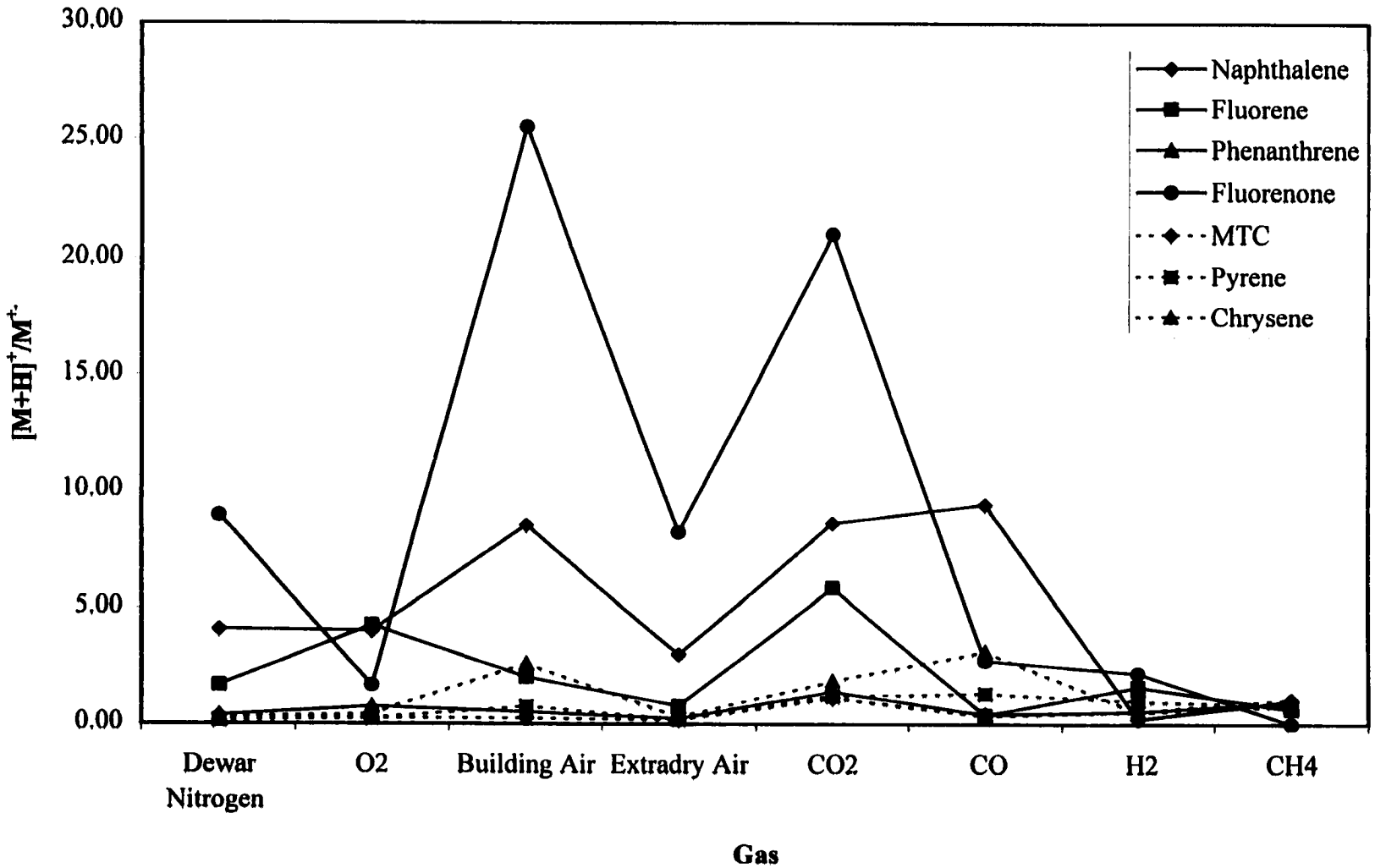

Figure 6.3. Ratio of protonated molecule to molecular ion of a 1/100 dilution of Imperial-3 with dichloromethane woth dichloromethane as the mobile phase as a function of gas (skimmer cone A).

is suitable both for reversed and normal phase chromatography. Similar plots were made for the other solvent systems studied.

These figures illustrate that the nature of the source gas and the analyte impact strongly on the observed signal intensity and the predominant ion form of the analyte. Dewar nitrogen, as the gas commonly used as the source gas in the Quattro instrument, will be used as a reference point. 1) With 50:50 (v/v) acetonitrile/water and in reference to Dewar nitrogen, both types of air result in a factor of 1.5 improvement in PAC signal, carbon monoxide offers no improvement, carbon dioxide and oxygen result in a small decrease, while hydrogen and methane offer an almost tenfold drop in signal intensity. Clearly, fluorenone is the most readily observed of all the PAC components, with the other PACs being present at much lower levels. In fact, the others decrease in the order: pyrene, naphthalene, fluorene, phenanthrene, MTC and chrysene. 2) With acetonitrile, there is a suppression of fluorenone signal for all gases studied relative to Dewar nitrogen, all other PACs show optimal signal with Extradry™ air and to a lesser extent carbon dioxide and there is no observable impact on MTC. 3) The dichloromethane results are less clear cut. The fluorenone signal does predominate over all other PACs, building air and carbon dioxide offer an improvement over Dewar nitrogen for fluorenone but the improvement for the other components is quite small, if any with other gases. Fluorene, naphthalene, and phenanthrene signals are enhanced by the use of carbon monoxide. Methane and hydrogen are associated with strong signal suppression. 4) With hexanes, carbon monoxide offers an improvement over Dewar nitrogen for all compounds of the mixture, especially for naphthalene. Fluorenone dominates the spectra with Dewar nitrogen but to a lesser extent than with all the

other gas combinations. The use of hydrogen and methane resulted in almost an order of magnitude drop in sensitivity.

When comparing protonation levels of PACs, in 50:50 (v/v) acetonitrile/water, fluorenone is the most readily protonated. All gases, except Extradry™ air and carbon dioxide, result in increased protonation of fluorenone, with the highest degree of protonation being observed in building air. There are drastically different levels of protonation of fluorenone with the two types of air, yet the signal intensities are virtually identical. With fluorene, the highest level of protonation and the highest level of signal coincide in carbon monoxide. For all other PACs, protonation is either suppressed or largely unaffected by the gas combination used. 2) With acetonitrile, fluorenone protonation is enhanced relative to Dewar nitrogen by the use of building air, carbon dioxide or carbon monoxide and hydrogen. There is a very weak correlation between the extent of protonation and the fluorenone signal intensity. Of the remaining PACs, naphthalene shows the most dramatic change in ion form, peaking in carbon dioxide and carbon monoxide. There is no correlation between this behaviour and the observed signal intensity. 3) With dichloromethane, the order of fluorenone signal is reflected by fluorenone protonation. For the other PACs, no such correlation exists. Fluorene is most easily protonated with oxygen and carbon dioxide, contrary to most other PACs. For most others, the presence of oxygen, alone or as a component of air, is associated with a decrease in protonation (building air is an exception to this, likely due to the presence of a number of contaminants that alter the plasma chemistry) which is consistent with its charge exchange properties and its ability to act as an

electron scavenger. 4) With hexanes, an increase in protonation efficiency is mirrored by an increase in the signal of the PACs studied, with the exception of MTC.

These results confirm that the nature of the gases and solvents used does significantly impact on both the signal intensity and the ion form of the PAC analytes. It was observed that species could be ionised by both proton transfer and charge exchange but that optimal signal intensity was not associated with either mechanism. Which mechanism predominated depended on the solvent, gas and analytes present. Hence, 9-fluorenone was readily observed and protonated, irregardless of the solvent or gas used, though to an extent that was influenced by the solvent and gas used. This is to be expected for a ketonic species with a high ionisation energy, making proton transfer more energetically favourable than charge exchange. MTC with its heterocyclic nitrogen involved in resonance is expected to have a high ionisation energy, a low proton affinity and a low gas phase basicity. Thus, as expected, it was associated with a low signal intensity and poor protonation. Among the PAHs, naphthalene, fluorene and phenanthrene have high ionisation energies and low proton affinities/gas phase basicities. Based on equation 6.1 [196] which considers only ionisation energies, protonation should decrease in the order: naphthalene, fluorene and phenanthrene. On the basis of proton affinities or gas phase basicities alone, protonation should be in the order: fluorene > phenanthrene > naphthalene. None of the physical parameters mentioned (ionisation energy, proton affinity or gas phase basicity) on their own is sufficient to explain the experimental results. Pyrene has the lowest ionisation energy and the highest proton affinity/gas phase basicity. It is, thus, expected to be the best barometer of the APCI plasma composition as both ionisation mechanisms are strongly competitive. Protonation increases

from acetonitrile to acetonitrile/water to dichloromethane to hexanes. Assuming that the principal reagent ions are derived from the solvent and not any impurities, this is counterintuitive as the ionisation energy of these solvents increases in the order: hexane (mainly *n*-hexane) < dichloromethane < acetonitrile < acetonitrile/water, making it more plausible that charge exchange would be favoured with hexanes rather than acetonitrile/water. This behaviour might be explicable on the basis of gas phase basicity (GB) which is the free energy of the protonation of a base. Acetonitrile does have a higher GB value than water, making it more energetically favourable for water to transfer a proton to the analyte. Dichloromethane with its two electron withdrawing chlorines and hexanes (a carbon base) are expected to be poor gas phase bases so would readily transfer a proton to another species or cannot compete as effectively with analytes for available protons as acetonitrile or water can. Examining the intrasolvent results indicates that there is a general trend of a high signal strength being correlated with a low level of protonation.

The ionisation energies of the gases, assuming the principal gas ionises and the ions formed are not destabilised by reaction with gas impurities, increase in the order of oxygen, methane, carbon dioxide, carbon monoxide, hydrogen and nitrogen. Based on this, charge transfer to the solvent or analyte should decrease in that order. Oxygen does indeed promote charge exchange, consistent with its electron scavenging behaviour. Charge exchange should be almost equally favourable in the presence of nitrogen and hydrogen, which is not observed for any solvent. Looking at the gas phase basicities, they increase in the order of hydrogen, oxygen, carbon monoxide (at the C), nitrogen, carbon dioxide, methane and carbon monoxide (at the oxygen). This may explain why hydrogen seems to promote proton transfer

to pyrene while nitrogen promotes charge exchange. CO and CO_2 have intermediate ionisation energies and gas phase basicities, and thus may be expected to promote both ionisation mechanisms. The signal intensities and level of protonation with hydrogen and methane were very low. An analysis of the gas only background of these gases revealed that H_3^+ and CH_5^+ (typical CI reagent ions of these gases) did not appear to form, thus providing no means for proton transfer. Theses gases also did not appear to form a useful radical cation, thereby eliminating the possibility for charge exchange ionisation. This provides no mean by which the PACs or solvents can be ionised by the gas and indicates that reactions in the APCI plasma are different from those in a CI plasma.

6.2.2 Two Gas Systems

For all of these experiments, the bath gas is introduced at 300 standard litres per hour (sLph), the sheath gas at 300 sLph and the nebuliser gas at 30 sLph. The two gas experiments fall into two categories, type I and type II. In type I, gas 1 is used as the bath (B) and sheath (S) gas while gas 2 is used as the nebuliser (N) gas. The resulting mixture, based on the flow rates of the bath, sheath and nebuliser gas streams, is 95% gas 1 and 5% gas 2. Unless gas 2 is more reactive than gas 1, the gas background spectrum should be dominated by gas 1. In a type II experiment, gas 1 is the bath gas while gas 2 is the sheath and nebuliser gas. The resulting gas mixture, based on the flow rates of the bath, sheath and nebuliser gas streams, will be 47.5% gas 1 - 52.5% gas 2.

Figures 6.4 and 6.5 represent the total signal intensity for type I and type II systems, respectively while Figures 6.6 and 6.7 represent the $[M+H]^+/M^{+\bullet}$ ratios for these experiments with PACs in dichloromethane as a representative of the other systems.

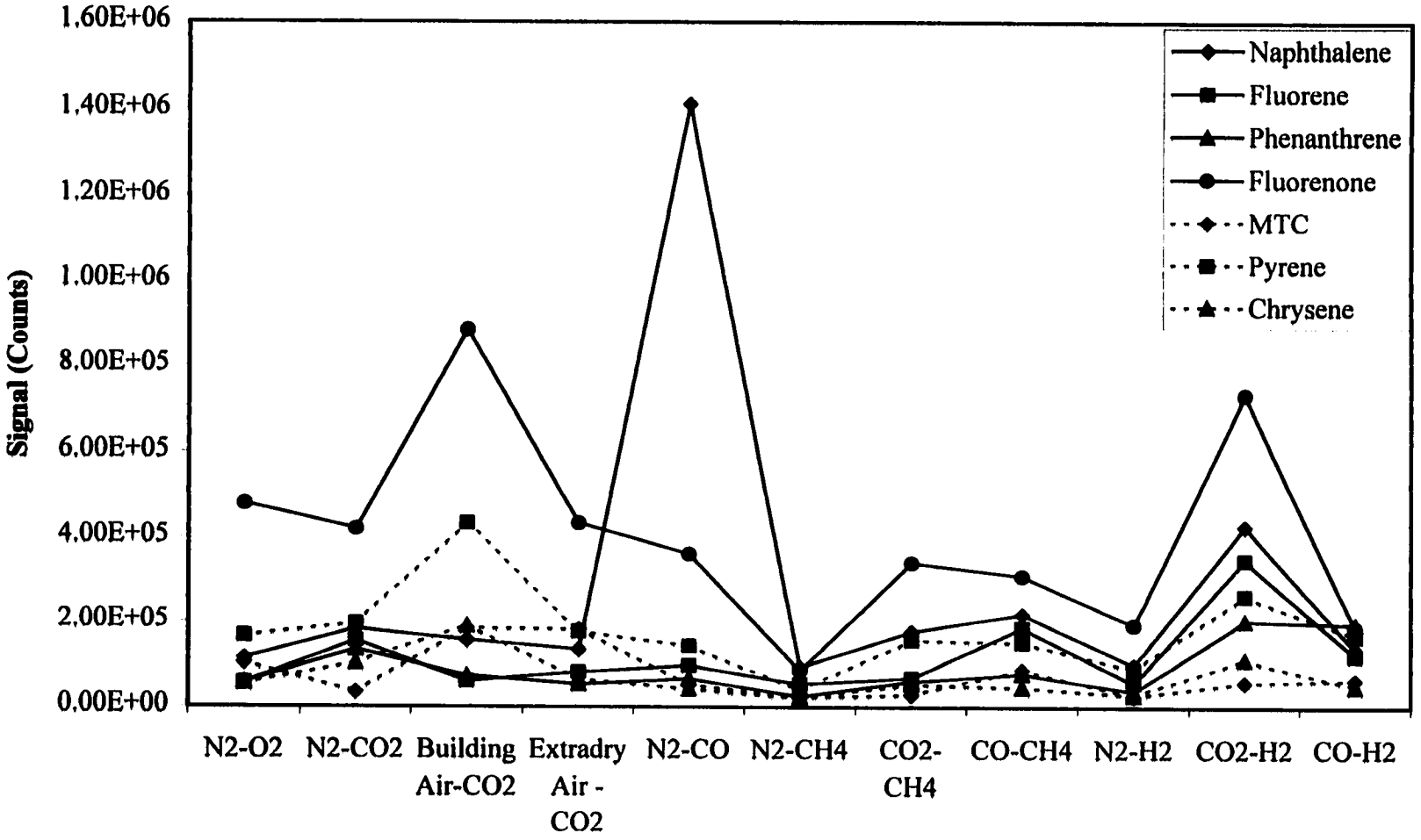

Figure 6.4. Total signal (protonated and charge exchanged) of a 1/100 dilution of Imperial-3 with dichloromethane as solvent and mobile phase as a function of gas in two gas, Type 1 experiments.

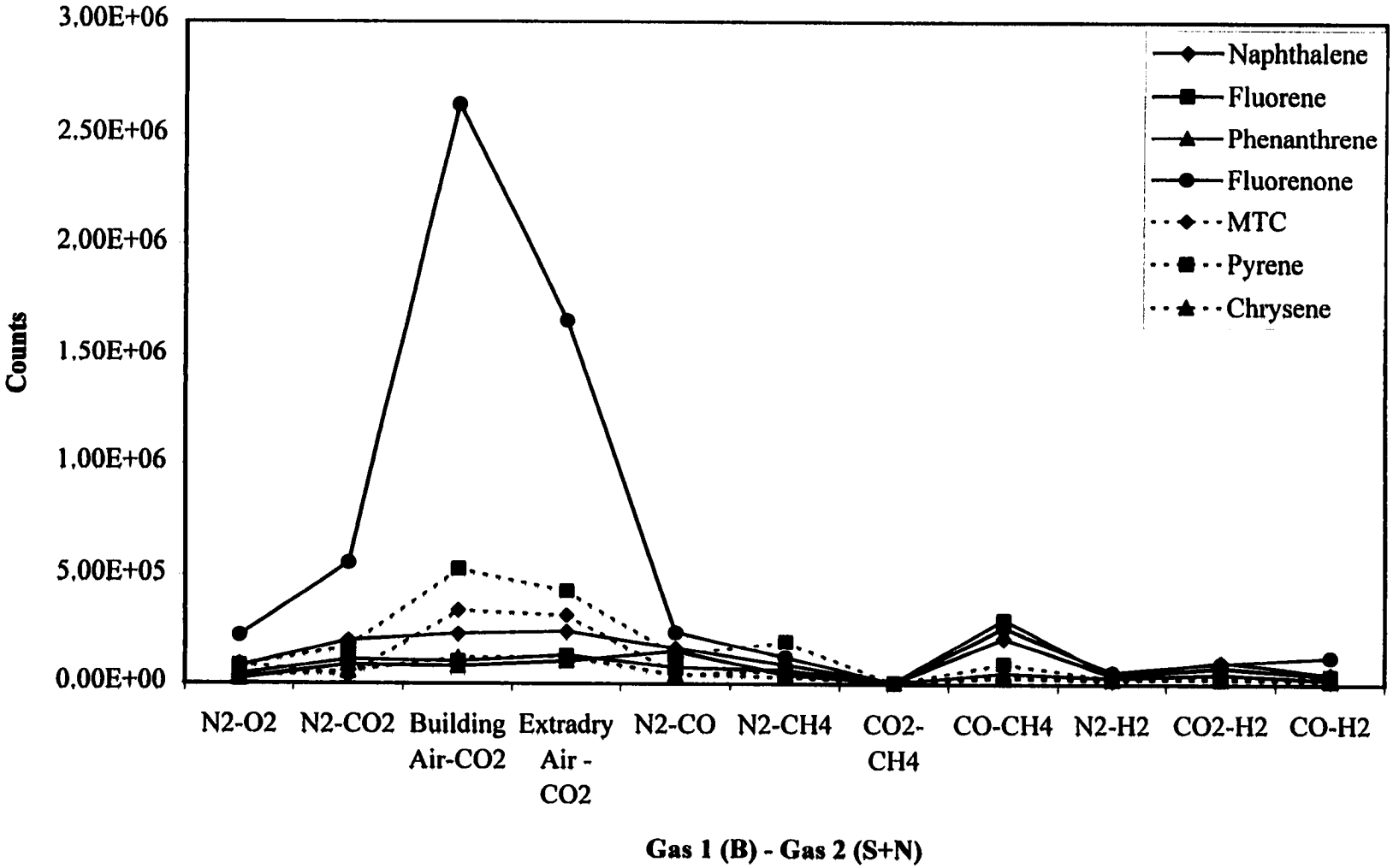

Figure 6.5. Total signal (protonated and charge exchanged) of a 1/100 dilution of Imperial-3 with dichloromethane as solvent and mobile phase as a function of gas in two gas, Type II experiments.

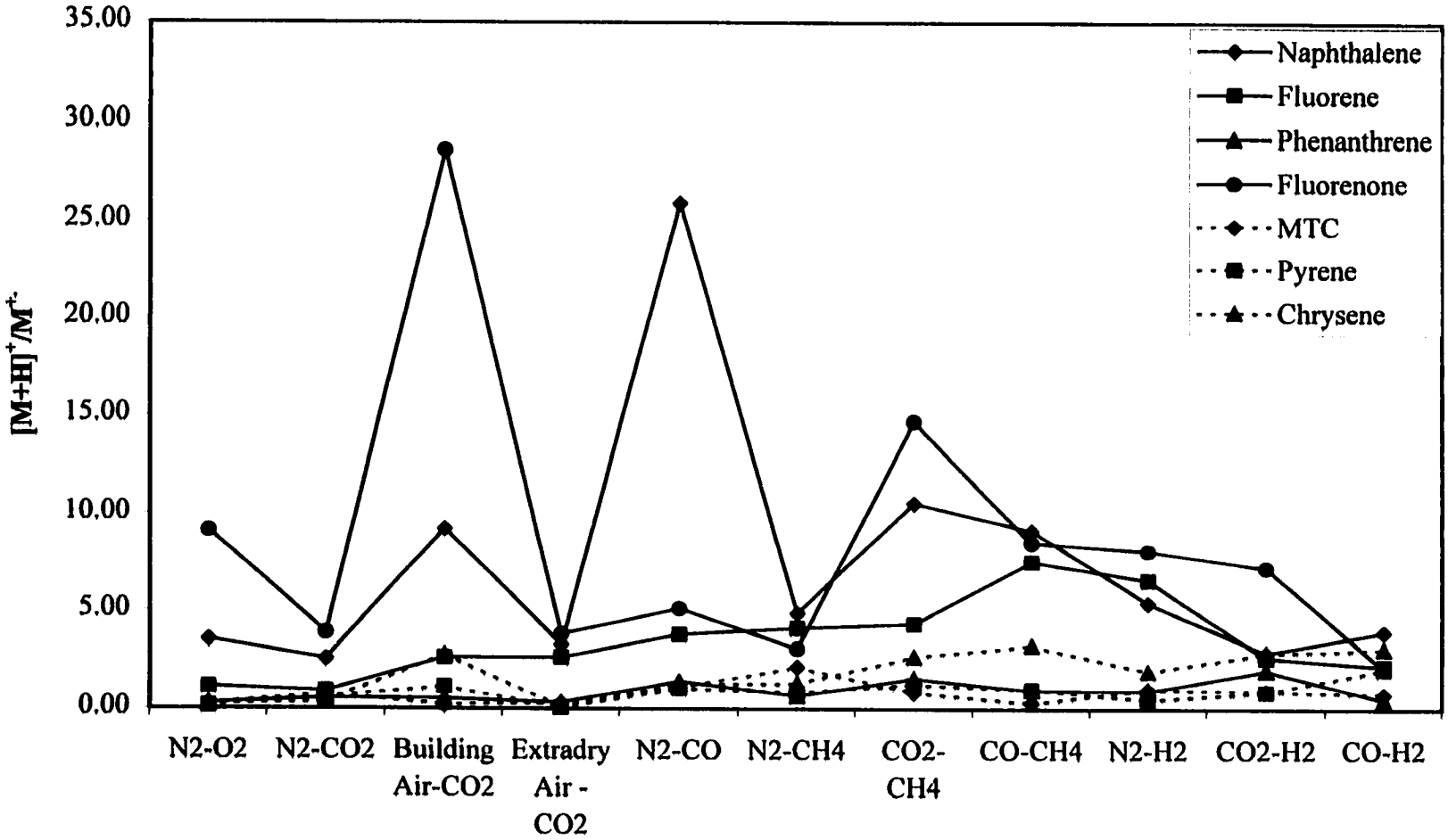

Figure 6.6. Ratio of protonated molecule to molecular ion of a 1/100 dilution of Imperial-3 with dichloromethane as solvent and mobile phase as a function of gas in a two gas, Type I experiments.

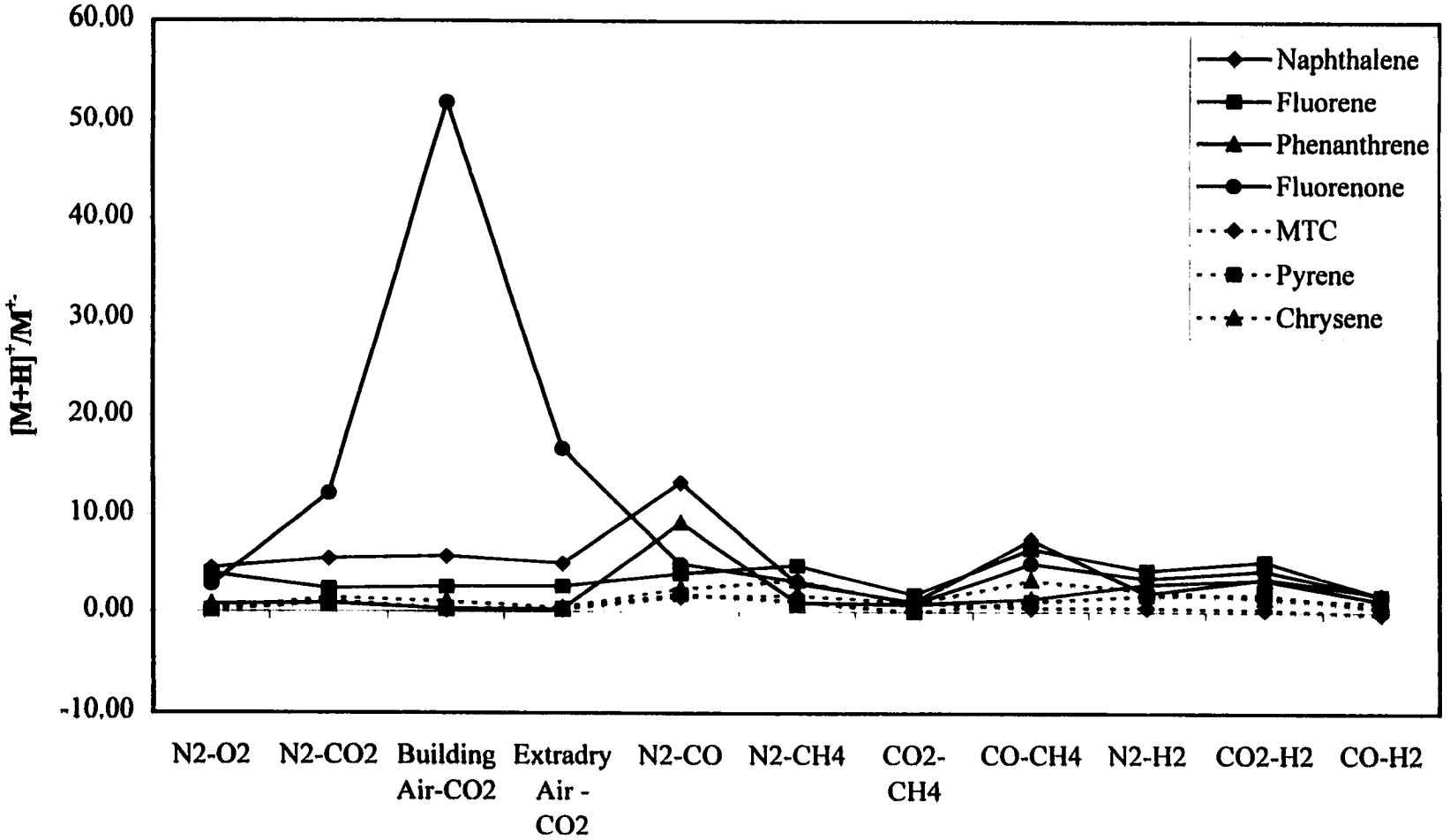

Figure 6.7. Ratio of protonated molecule to molecular ion of a 1/100 dilution of Imperial-3 with dicdichloromethane as solvent and mobile phase as a function of gas in two gas, Type II experiments.

The results with 50:50 (v/v) acetonitrile/water indicate that fluorenone is the most readily detected PAC though pyrene and naphthalene follow closely, especially with air-carbon dioxide mixtures. Improvement in signal intensity relative to the one gas system is greatest with nitrogen-oxygen (only for fluorenone) and Extradry™ air-carbon dioxide, particularly when carbon dioxide is used as both the sheath and the nebuliser gas. The other gas combinations show no improvement or a decrease. Thus, the carbon monoxide-methane combination appears as a large signal in the two gas combinations but is actually similar in magnitude to the observed one gas system with carbon monoxide. In terms of ionisation mechanism, the plots of protonated molecule to molecular ion ratios reveal that fluorenone is the most easily protonated, as expected. The protonation levels of fluorenone and the other PACs, for the most part, can be predicted based on the results with single gas systems. Thus, fluorenone protonation was high in the presence of building air and low in the presence of carbon dioxide. Therefore, as the proportion of carbon dioxide in the source increases, it is expected and was observed that the protonation of fluorenone would decrease. There was no observable correlation between solvent ion intensity, PAC signal and PAC protonation, as was previously observed.

With acetonitrile, fluorenone typically dominates the mass spectrum of the standard, though it is followed closely by pyrene and naphthalene, especially with air-carbon dioxide mixtures. The results indicate that in type I systems, the nitrogen-oxygen, Extradry™ air-carbon dioxide, and carbon monoxide-methane systems offer a two fold improvement in total signal over the respective one gas systems. In a type II experiment, only Extradry™ air-carbon dioxide and building air offer an improvement (twofold) over the type I system.

Thus, the combination of Extradry™ air-carbon dioxide offers a fourfold improvement over the case where only Extradry™ air is used and almost a tenfold improvement over Dewar nitrogen alone. Although Extradry™ air-carbon dioxide has the highest signal intensity and the lowest degree of protonation, no other correlation between total signal and ion form can be made.

In dichloromethane, there is an anomalous result for naphthalene in the type I, nitrogen-carbon monoxide case. These systems and particularly this cone are subject to sudden spikes which interfere with the *m/z* ranges of interest, in this case naphthalene, though fluorenone dominates the spectrum. In the type I experiments, building air-carbon dioxide, Extradry™ air-carbon dioxide and carbon dioxide-hydrogen offer a 1.5 to 2 fold improvement in signal intensity over the pure gas case (see Figure 6.8). In the Type II system, only the air-carbon dioxide systems were associated with a sizeable improvement in total signal, especially for fluorenone. This represents a two to five fold improvement over nitrogen or air plasmas. The plots of ratio of protonated molecule to molecular ion as a function of gas combination reveal the same anomalous behaviour of naphthalene in a Type I, nitrogen-carbon monoxide plasma. The highest protonation is observed with building air-carbon dioxide and carbon dioxide-methane in a type I system, and building air-carbon dioxide, nitrogen-carbon monoxide and carbon monoxide-methane in a type II system. Both Extradry™ air and building air with carbon dioxide were associated with high signal intensity but represented intermediate and high levels of protonation, respectively, confirming that there is a poor correlation between ionisation mechanism and overall sensitivity.

With hexanes, there is no two gas combination which outperforms the one gas, carbon monoxide system. However, the type I carbon dioxide-hydrogen system does provide an improvement over the all carbon dioxide case but this improvement is lost in a type I system. The Type I and II nitrogen-carbon dioxide system offers a two fold improvement over all nitrogen. As expected, there is an increase in protonation with the incorporation of carbon monoxide, though increasing the proportion of carbon monoxide does not necessarily lead to higher levels of protonation. This is contrary to the results with the other solvents.

6.2.3 Three Gas Systems

The three gas experiments involve using Dewar nitrogen as the bath gas, with one of four (carbon dioxide, carbon monoxide, hydrogen and methane) as sheath gas and one of the remaining three as the nebuliser gas. Based on the results of the one and two gas systems, it is expected that the sheath gas will have the predominant effect on the backgrounds and ion intensities and distributions.

Figures 6.8 and 6.9 depict the total ion intensity vs. gas combination and the $[M+H]^+/M^{+\bullet}$ ratio vs. gas combination, respectively, for PACs in dichloromethane. Similar plots were prepared for the other three solvents but are not presented.

The results with aqueous acetonitrile indicate that the nitrogen-methane-carbon dioxide combination is optimal for PAC detection while nitrogen-carbon monoxide-hydrogen is the best overall system for PAC detection in acetonitrile, both offering a two to three fold improvement over the appropriate two gas cases. These improvements are insufficient, however, to outperform the Extradry™ air-carbon dioxide system for either of these solvents. The best gas combination with dichloromethane in terms of total signal is

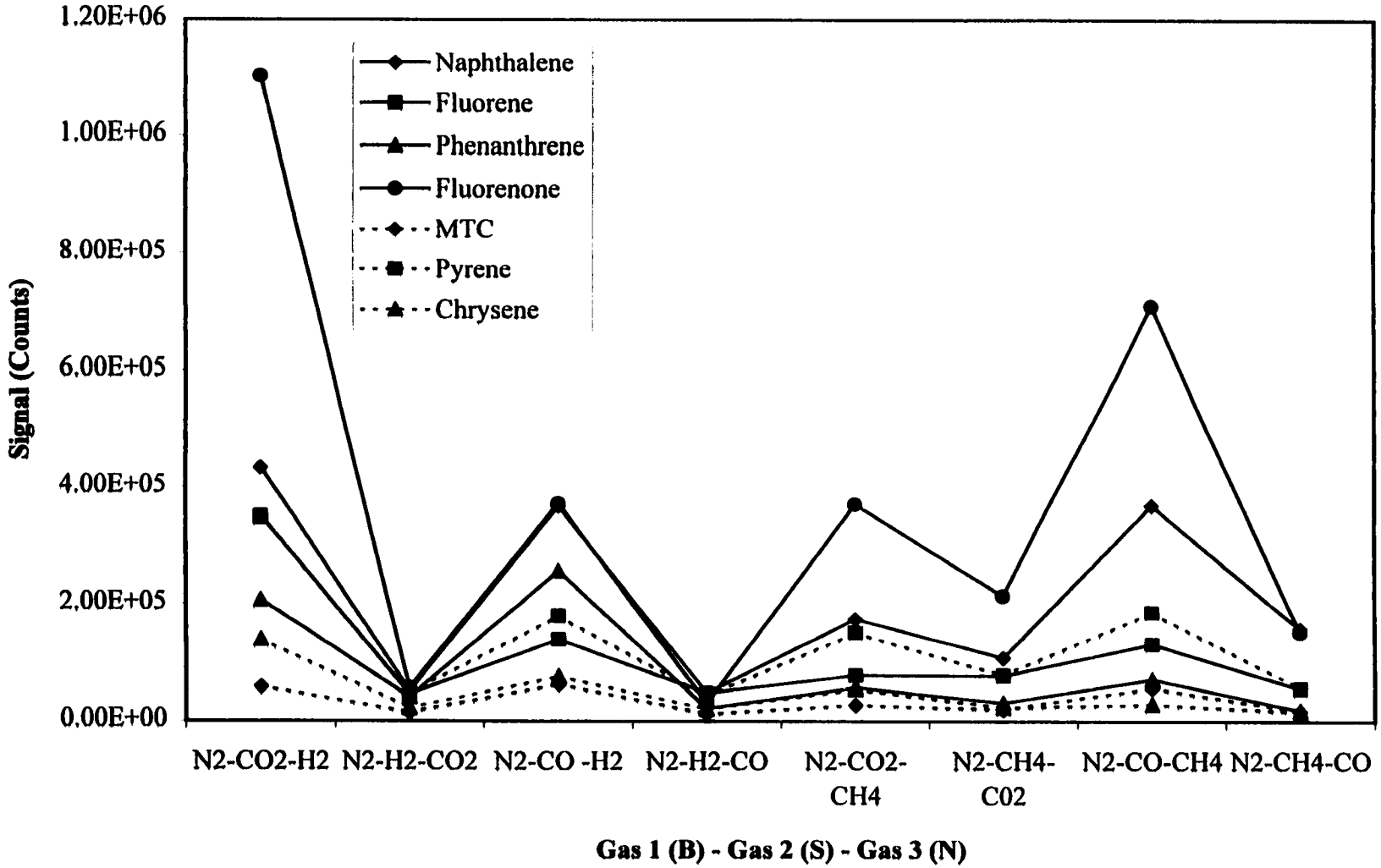

Figure 6.8. Total signal (protonated and charge exchanged) of a 1/100 dilution of Imperial-3 with dichloromethane as solvent and mobile phase as a function of gas in three gas experiments.

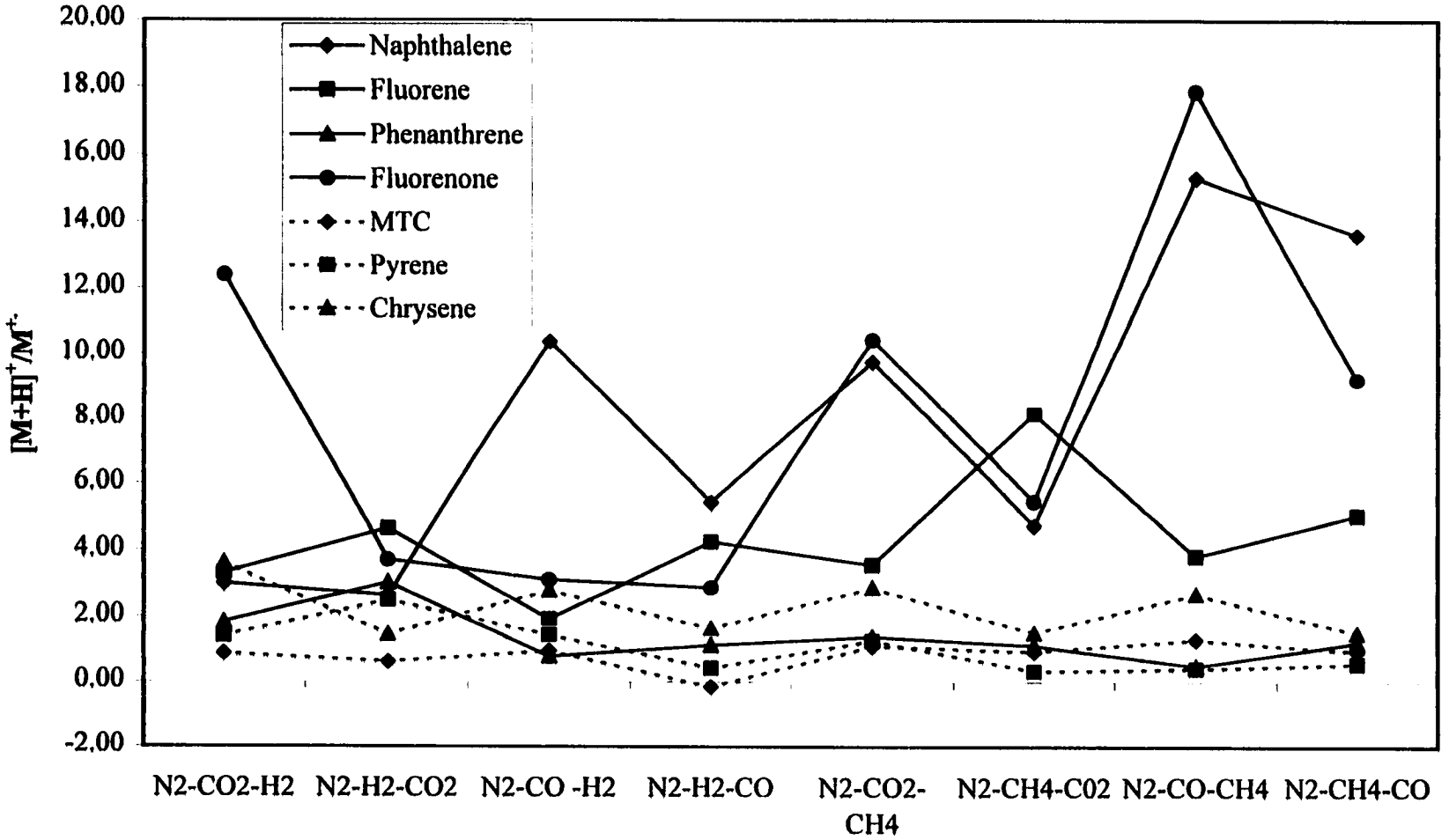

Figure 6.9. Ratio of protonated molecule to molecular ion of a 1/100 dilution of Imperial-3 with dichloromethane as solvent and mobile phase as a function of gas in three gas experiments.

nitrogen-carbon monoxide-methane but it offers no significant improvement over the two gas case and is less efficient for PAC analysis than an air-carbon dioxide system. With hexanes, the best system appears to be a nitrogen-carbon dioxide-hydrogen system, offering a twofold improvement over the two gas case. These results indicate that all gases are participating to a measurable extent in the ionisation of PACs.

Protonation of fluorenone in aqueous acetonitrile mirrors its signal intensity trends, indicating that for this species, increased protonation is associated with better sensitivity. The other PACs do not exhibit this trend nor is there any observable correlation between the abundance of *m/z* 42 in the solvent background of aqueous acetonitrile and the protonation of the analyte. With acetonitrile, the intensities of the PAC signals and the degree of protonation somewhat mirror each other, indicating that in this solvent system, sensitivity is improved if protonation occurs. Similar behaviour is reported for hexanes and dichloromethane.

The predominant ionisation mechanisms observed were poorly correlated with ionisation energy, proton affinity or gas phase basicity. In fact, the plasma seems to support a number of consecutive and competitive reactions which ultimately result in a mix of species. If from Kebarle's work [92], a gas phase basicity of at least 837 kJ/mol was required for proton transfer from hydronium water clusters to be kinetically controlled. As the gas phase basicity of water is 660 kJ/mol, it can be predicted that at least a 177 kJ/mol difference in gas phase basicity between the analyte and the water cluster is necessary for protonation to be kinetically controlled. In this case, few of the solvents or analytes studied here are basic enough to extract protons under kinetic control conditions. This implies that

thermodynamic, equilibrium conditions will predominate which according to the results of Kebarle *et al.* [92] should result in low degrees of protonation and low sensitivity.

For subsequent studies, it was decided to abandon research with carbon monoxide, methane and hydrogen. These gases pose explosion and/or health risks, offer no particular advantage for PAC analysis and are quite expensive, in relation to the other gases studied. Hydrogen was also associated with probe cooling, source heating and reduced lifetime of the corona needle.

6.2.4 Conclusions from the work with Skimmer Cone A

These studies were undertaken with the goal of evaluating the effects of gases and solvents on the analysis of PACs and understanding how the nature of these gases and solvents affects APCI plasma chemistry. In the course of these studies a number of things were learned. These included the fact that this instrument demonstrated severe memory and carryover effects, a sensitivity to contamination of gases and solvents,even if present in trace amounts, and frequent signal spiking was observed. This was addressed by using dedicated glassware and tubing to prevent carryover from previous analyses, distilling or filtering solvents where appropriate, source and probe heating to remove adhered substances, frequent cleaning of the source, performing all studies where possible in a single day with a single lot of solvents and gases, and performing replicate analyses. It was observed that altering the source gases dramatically impacted the nature of the chemical background, solvent fragmentation and analyte ionisation, with the sheath gas being of pre-eminent importance. However, despite expectations from the literature [92], hydronium ion-water clusters were not readily observed nor were they of pre-eminent importance in solvent or analyte

ionisation, the latter being strongly structure-dependent. Hence, ketonic species were much more readily protonated and detected than aromatic hydrocarbons or heterocycles. It was possible to semi-quantitatively predict the abundance of solvent ions in two and three gas systems based on their relative abundances in one gas systems, but these abundances were not strongly correlated either with analyte signal or protonation. In fact, the extent of charge exchange or proton transfer of gases, solvents and analytes could not be reliably predicted on the basis of ionisation energies, proton affinities or gas phase basicities. From an analytical perspective, PACs in acetonitrile-water, acetonitrile or dichloromethane are best analysed with Extradry™ air as the bath gas and carbon dioxide as the sheath and nebuliser gas while PACs in hexane are best analysed in all carbon monoxide or nitrogen-carbon dioxide systems. A number of gases (CO, CH_4 and H_2) could be discarded based on their toxic or analytical properties. There is no particular advantage to either charge exchange or proton transfer for the analysis of PACs. Therefore, where possible, source conditions should be manipulated for best overall signal intensity, irregardless of the dominant mechanism.

6.3. Studies with Skimmer Cone B

6.3.1 Effect of Orifice Size

Having used three skimmer cones with different orifice sizes over the course of this work, it was interesting to study the effect orifice size made on the analysis of PACs. Skimmer Cone A was the skimmer cone purchased with the instrument. Skimmer cone B was formed when skimmer cone A was dropped, the orifice collapsed and an attempt was made to drill out a new hole. A misalignment and the use of an incorrectly sized drill bit resulted in a larger hole cut at 20° to the normal. Skimmer cone C was a cone purchased new

from Micromass in November of 1998. To assess the effect of orifice size, a 1 μM solution of pyrene was prepared in hexanes. With skimmer cone A, this was at the limit of detection for this material. Dewar nitrogen was used in all cases and standard flow injection analysis conditions were used to analyse this sample with cones B and C. A similar preparation had been analysed one year earlier with cone A and the results are presented in Table 6.5.

Table 6.5. Comparison of Three Skimmer Cones

Cone	Total Signal	$[M+H]^+/M^{+\bullet}$
A	4.16E5	3.65
B	1.76E5	1.67
C	1.49E6	3.57

These results indicate that skimmer cone C is almost fourfold better than skimmer cone A and almost ninefold better than skimmer cone B. The orifice of B is bigger than either of the two others but it is at an angle so ion transmission is likely not as inefficient. Its larger orifice size was also correlated with a higher source and analyser pressure, which may result in more ion-molecule collisions, causing a decrease in protonation.

6.3.2 Interactions among sample components

The above ratios of $[M+H]^+/M^{+\bullet}$ are higher than those observed with the 7 component mixtures described in the skimmer cone A results. This seems to indicate either that pyrene is less effective at competing for protons when a stronger base, like fluorenone is present, or that the sample components actually interact with each other. Using the eight solutions described in Table 3.5, which are combinations of pyrene with poor gas phase bases, the amount and type of response was examined. Figure 6.10 presents the total signal

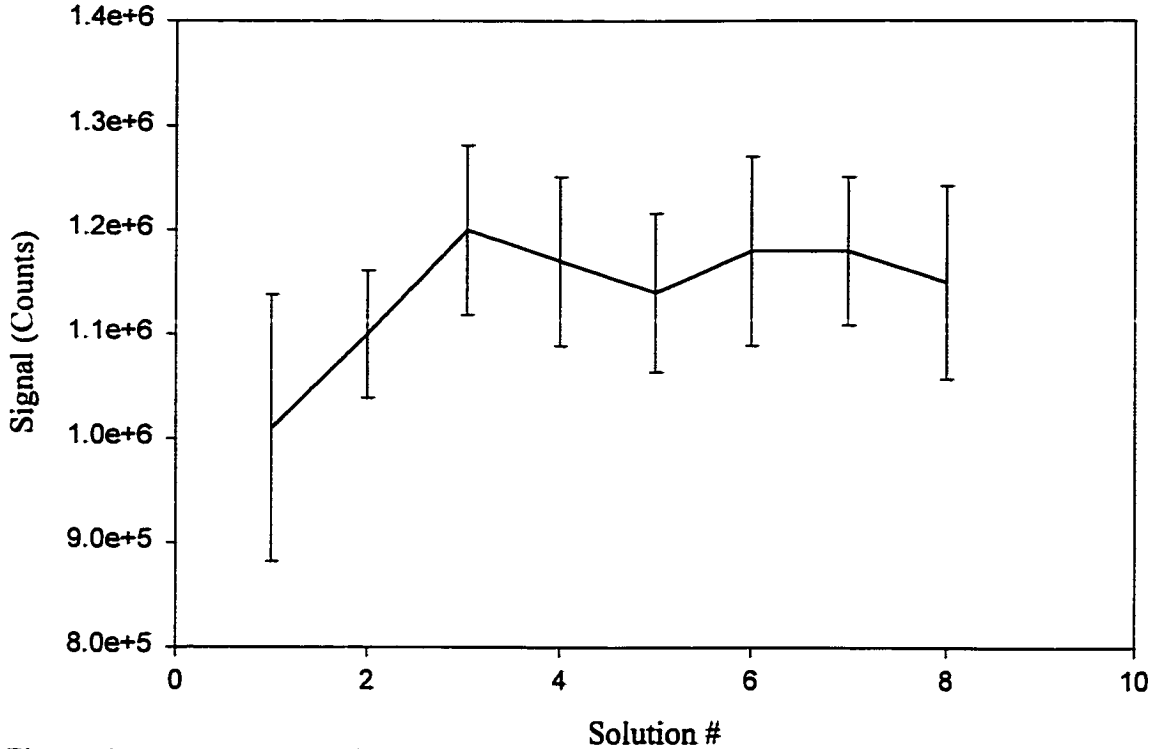

Figure 6.10. Total signal of pyrene as a function of solution composition (see Table 3.5) with skimmer cone C.

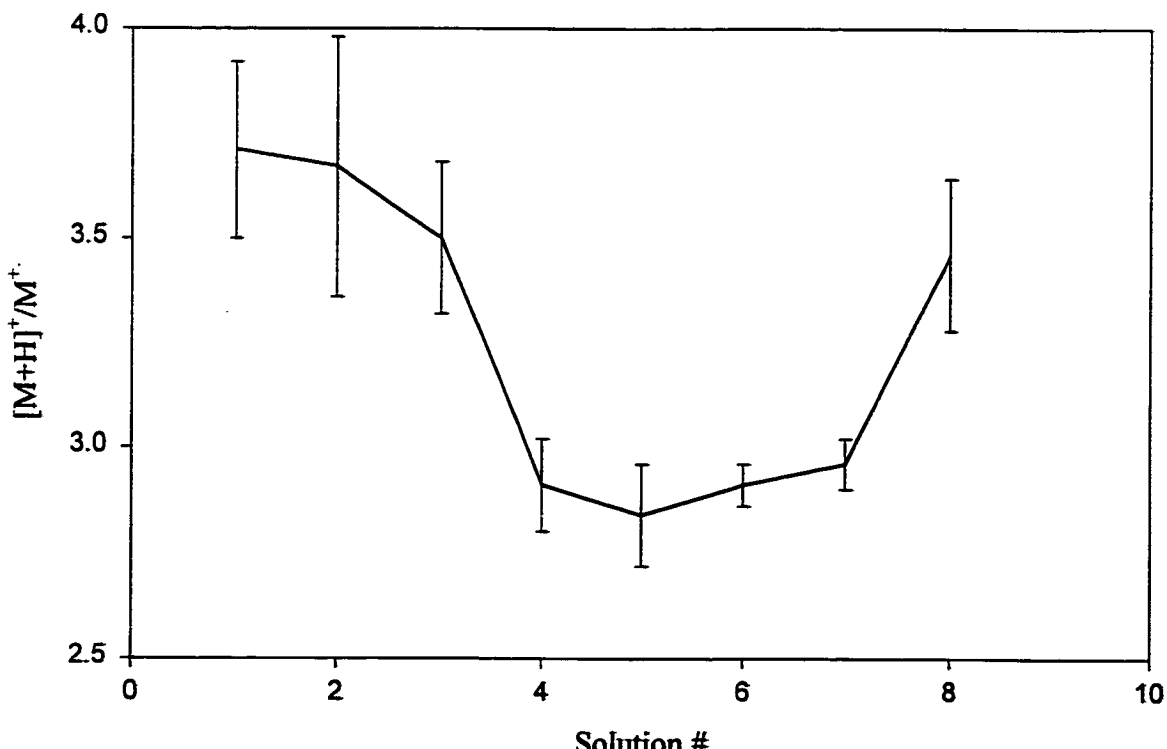

Figure 6.11. Ratio of protonated molecule to molecular ion of pyrene as a function of solution composition (see Table 3.5) with skimmer cone C.

due to pyrene as a function of solution composition. These results indicate that in the absence of fluorenone, the pyrene signal is not significantly affected by other sample components. Figure 6.11 presents the ratio of the protonated molecule to molecular ion and it is not significantly affected by the nature of the other sample components. This indicates that if competition is occurring, pyrene is not at a disadvantage relative to the others.

6.4 Studies with Skimmer Cone C

6.4.1 Comparison to Skimmer Cone A Results with Imperial Standards

Having discovered that the orifice size and the signal intensities of a pyrene standard were substantially different for skimmer cones A and C, the response with skimmer cone C to Imperial standards 1 through 3 was tested with the appropriate solvents using dedicated glassware and tubing and compared to cone A. Figure 6.12 and 6.13 depict the total signal and the ratio of protonated molecule to molecular ion, respectively, as a function of solvent, gas combination and cone for pyrene. Comparing these indicates that for the most part, the same trends are observed though the signal intensities and protonation are higher with skimmer cone C. Thus, sheath gas was the most important, fluorenone was most readily observed and protonated, MTC was poorly responsive and poorly protonated and the other PAHs did not behave as predicted on the basis of their physical parameters. Where discrepancies occur, it is derived from the fact that the results with cone A were obtained over several weeks, with different batches of gases and solvents, and three corona needles. Those obtained with skimmer cone C were obtained in one day per solvent, with a single corona needle and one batch of solvents and gases. Due to the loss of cone A, it was not possible to repeat the studies to address the source of irreproducible results.

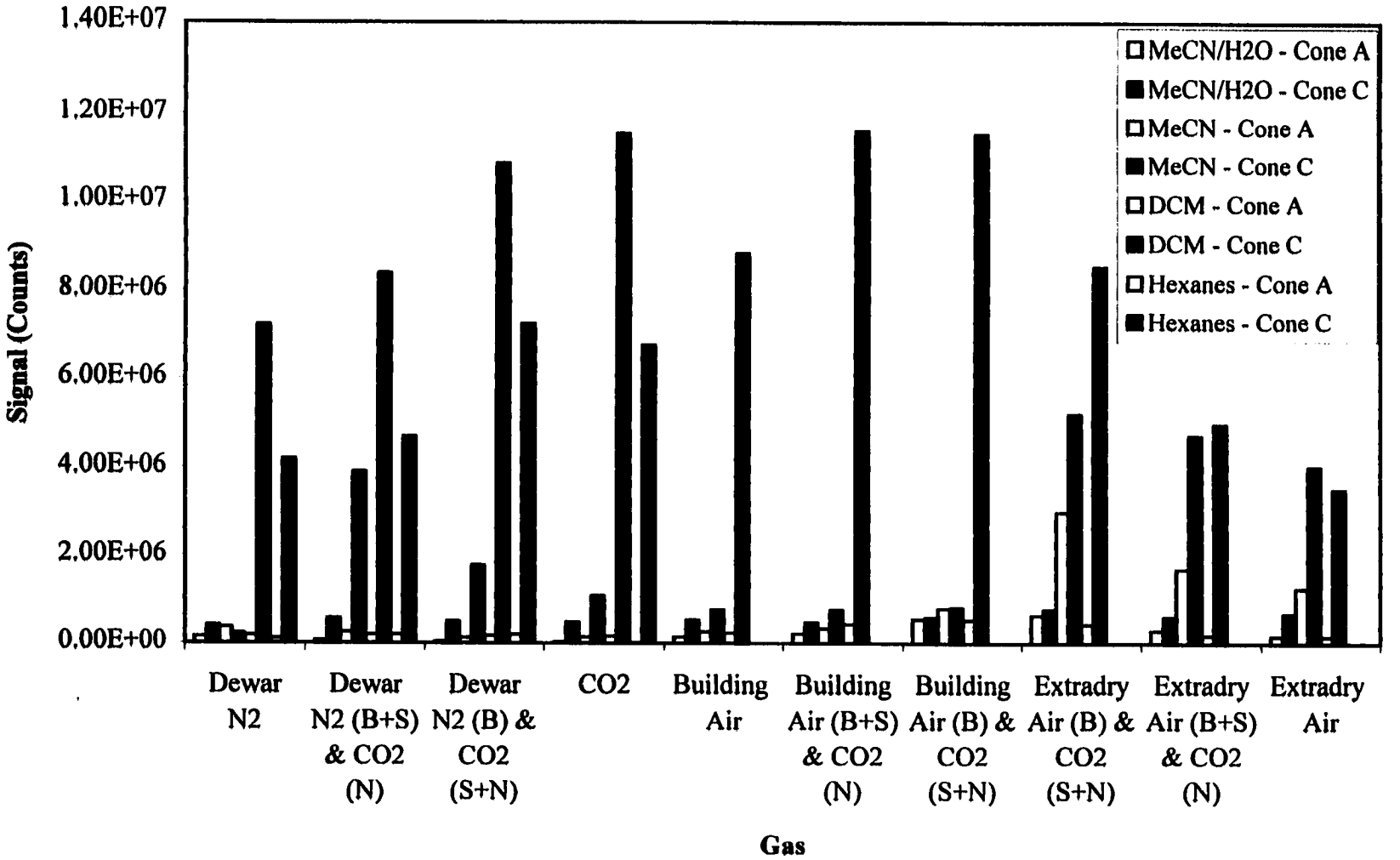

Figure 6.12. Comparison of skimmer cones A and C for pyrene detection in all solvents.

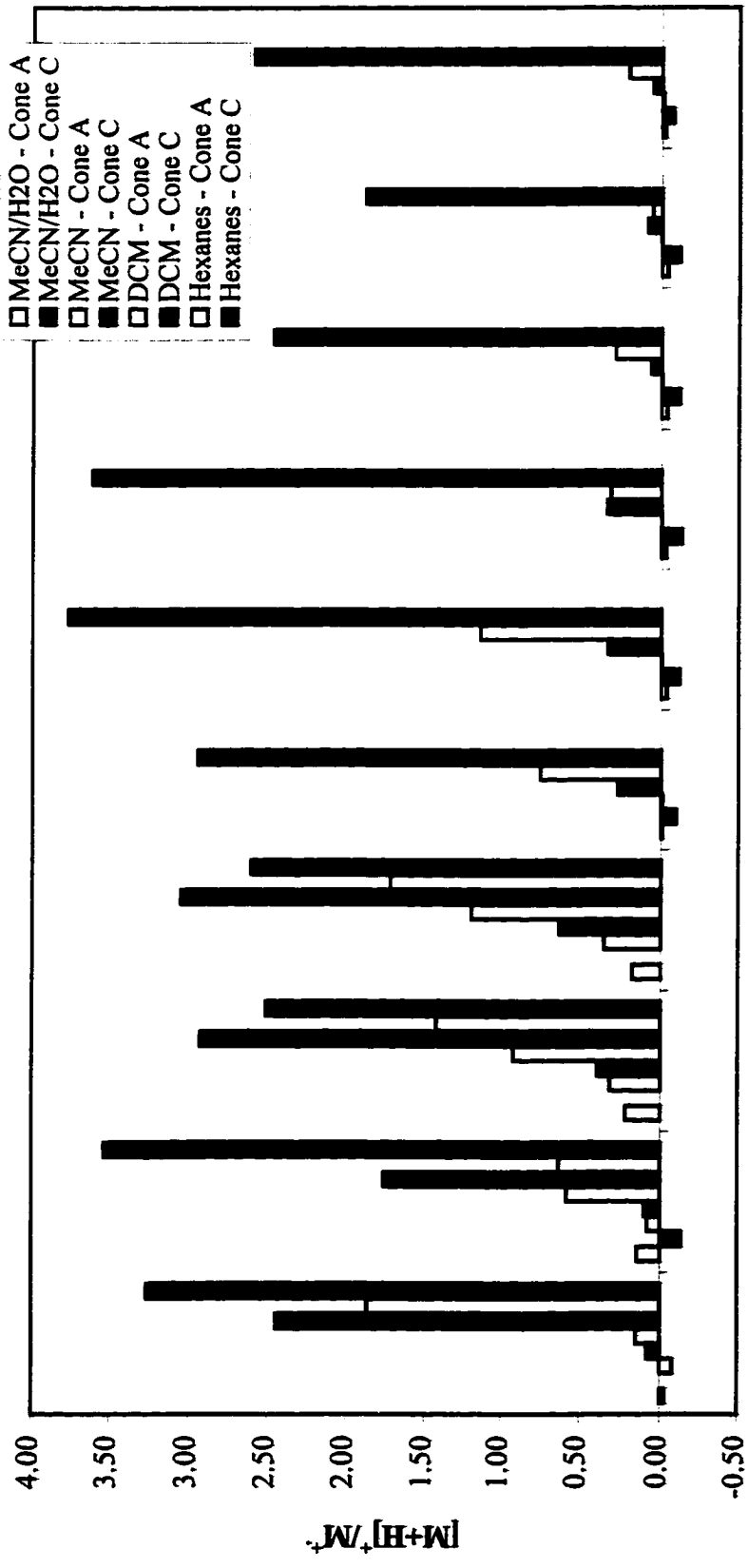

Figure 6.13. Comparison of skimmer cones A and C for pyrene protonation ina ll solvents.

NB: All analyses were performed in triplicate for these studies. Due to the large number of graphs on a page, statistical data is not presented. The calculated relative standard deviations ranged from 5 to 20% (within reasonable experimental error for mass spectrometric measurements.

6.4.2 Studies of IO standards

Cone C was then used to probe the nature of the APCI plasma and its effect on the response of new standard solutions. The gas backgrounds of Dewar nitrogen, tank nitrogen, building air, Extradry™ air, and carbon dioxide are presented in Figure 6. and the assigned structures (based on cone voltage studies and MS/MS results) are presented in Table 6.6.

Table 6.6. *M/z* and structures of gas and gas + acetonitrile-containing solvent background ions

	Gas Only		Gas + MeCN/H_2O		Gas + MeCN	
Gas	***m/z***	**Ion**	***m/z***	**Ion**	***m/z***	**Ion**
Dewar N_2	19 30 37 42 42.6	H_3O^+ NO^+ $H_3O(H_2O)^+$ N_3^+	37 42 60	$H_3O^+(H_2O)$ $CH_3CN \bullet H^+$ $CH_3CN \bullet H_3O^+$	42 83 124	CH_3CNH^+ $(CH_3CN)_2H^+$ $(CH_3CN)_3H^+$
Tank N_2	19 37 42 57	H_3O^+ $H_3O(H_2O)^+$ N_3^+	19 37 42 60	H_3O^+ $H_3O^+(H_2O)$ CH_3CNH^+ $(CH_3CN)H_3O^+$	42	CH_3CNH^+
Extradry™ air	59	$C_3H_7O^+$ $H_5C_3O_2^+$	37 42 59 60	$H_3O^+(H_2O)$ CH_3CNH^+ $C_3H_7O^+$ $H_5C_3O_2^+$ $CH_3CN(H_3O^+)$	42 82 124	CH_3CNH^+ $(CH_3CN)_2H^+$ $C(CH_3CN)_3H^+$

CO_2	19 33 45	H_3O^+ O_2H^+ HCO_2^-	41.9 59.9	CH_3CNH^+ $CH_3CN^+(H_3O^+)$	42	CH_3CNH^+
Building Air	18 19 37 43 45 55 59 73 74 101 111 114 129	NH_4^+ H_3O^+ $H_3O^+(H_2O)$ CH_3CO^+, $C_3H_7^+$ CO_2H^+, $C_2H_5^+$ $H_3O^+(H_2O)_2$ $C_3H_7O^+$ $H_5C_3O_2^+$ $C_4H_9O^+$ $H_5C_3O_2^+$ $H_3O^+(H_2O)_2$ $C_4H_{12}N^+$ $C_5H_{11}O^+$ $C_6H_{13}O^+$ $C_7H_{15}O^+$ $C_8H_{17}O^+$	18 42 60 114	NH_4^+ CH_3CNH^+ $CH_3CN(H_3O^+)$ $CH_3CNH_9O_4^+$	42	CH_3CNH^+

These results indicate that the spectrum of Dewar N_2 is dominated by *m/z* 19, tank N_2 is dominated by *m/z* 37, both airs by *m/z* 59 (though the Extradry™ air spectrum is much cleaner than building air) and CO_2 by *m/z* 45. These spectra are distinct from those observed with skimmer cone A and it is not known why. Possible explanations include: 1) with the larger orifice size more ions are transmitted and 2) an improvement in technique (greater rigour in preventing carryover and contamination). As a carbon dioxide tank emptied or sat for long periods of time, *m/z* 47 ($CO_2H_3^+$) was observed to form. Monitoring the gas background was a useful means of monitoring gas quality. Examining the gas backgrounds

indicates that building air is the dirtiest gas, Extradry™ air the cleanest with Dewar N_2, tank N_2 and CO_2 making up the middle. Thus, assuming that the gas species and not its impurities are responsible for ionising the solvent and consequently the analyte, it can be predicted that the cleaner the gas, the more ionisation of the solvent will occur, causing solvent ion intensity and signal to noise ratios for PAC analysis to improve in the order: building air, Dewar N_2, tank N_2, CO_2 and Extradry™ air.

Whether this is so can be determining by examining the solvent backgrounds as a function of gas (see Figures 6.15 through 6.18). The ion structures, where known, are presented in Tables 6.6 and 6.7. The predominant species in the 50:50 (v/v) acetonitrile/water spectra with all gases studied were *m/z* 42 and 60, corresponding to protonated acetonitrile and a proton bound acetonitrile-water cluster, respectively. The prediction that solvent ions (*m/z* 42 and 60) would increase in the order: building air, Dewar N_2, tank N_2, CO_2 and Extradry™ air was not quite valid. The two nitrogen sources were almost equivalent and carbon dioxide was much poorer than expected. The acetonitrile spectra were dominated by *m/z* 42 which was expected to increase in the order: building air, Dewar N_2, tank N_2, CO_2 and Extradry™ air. This expectation was not valid as Extradry™ air produced the lowest degree of *m/z* 42. Hence, for both solvents, a simple examination of the gas background was insufficient to predict the nature of the solvent-derived species in the plasma. However, the nature of the gas did impact on the clustering of acetonitrile. Only Extradry™ air and Dewar N_2 were associated with solvent clustering.

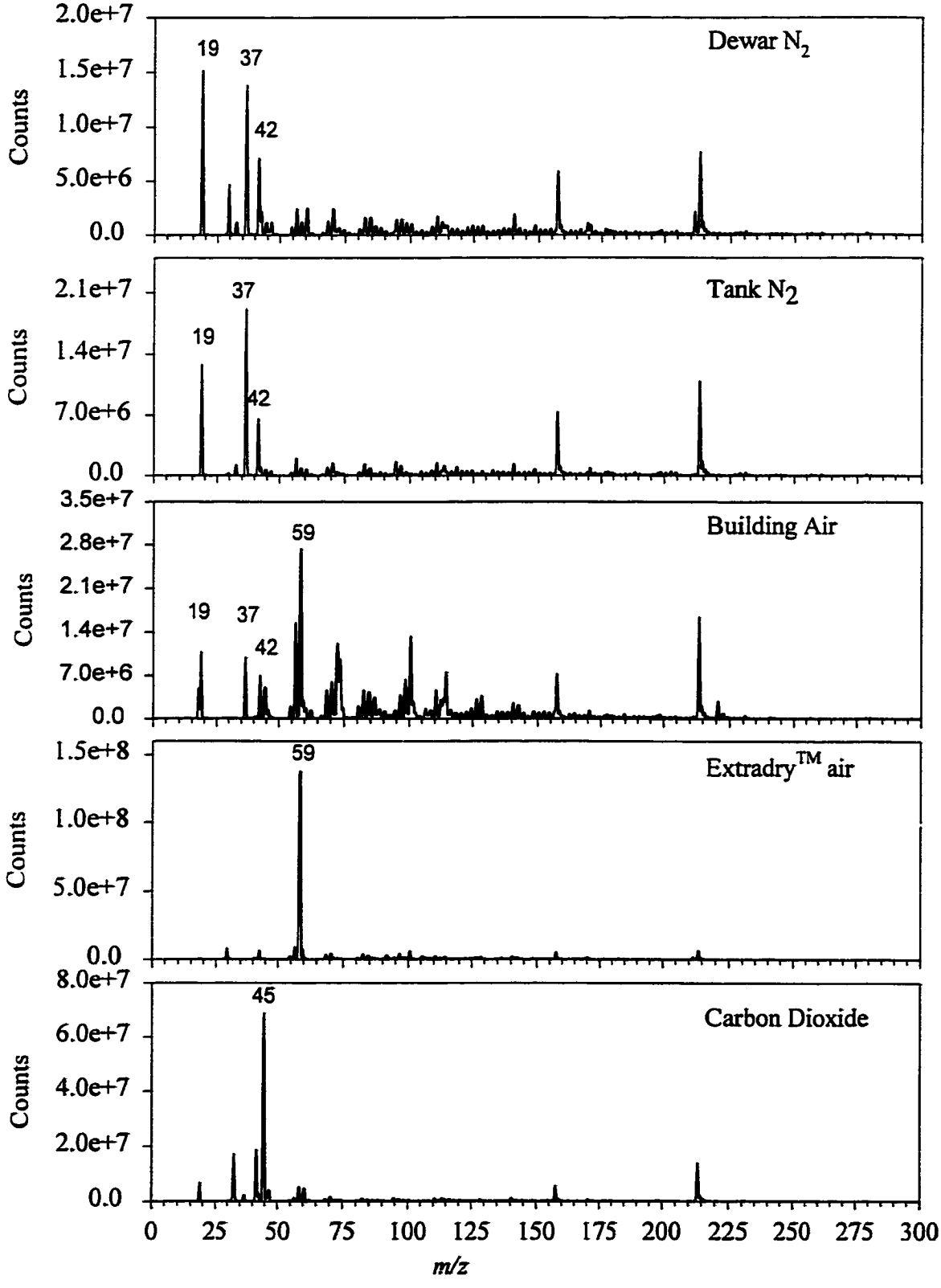

Figure 6.14. Background of Dewar N_2, tank N_2, building air, Extradry™ air and CO_2.

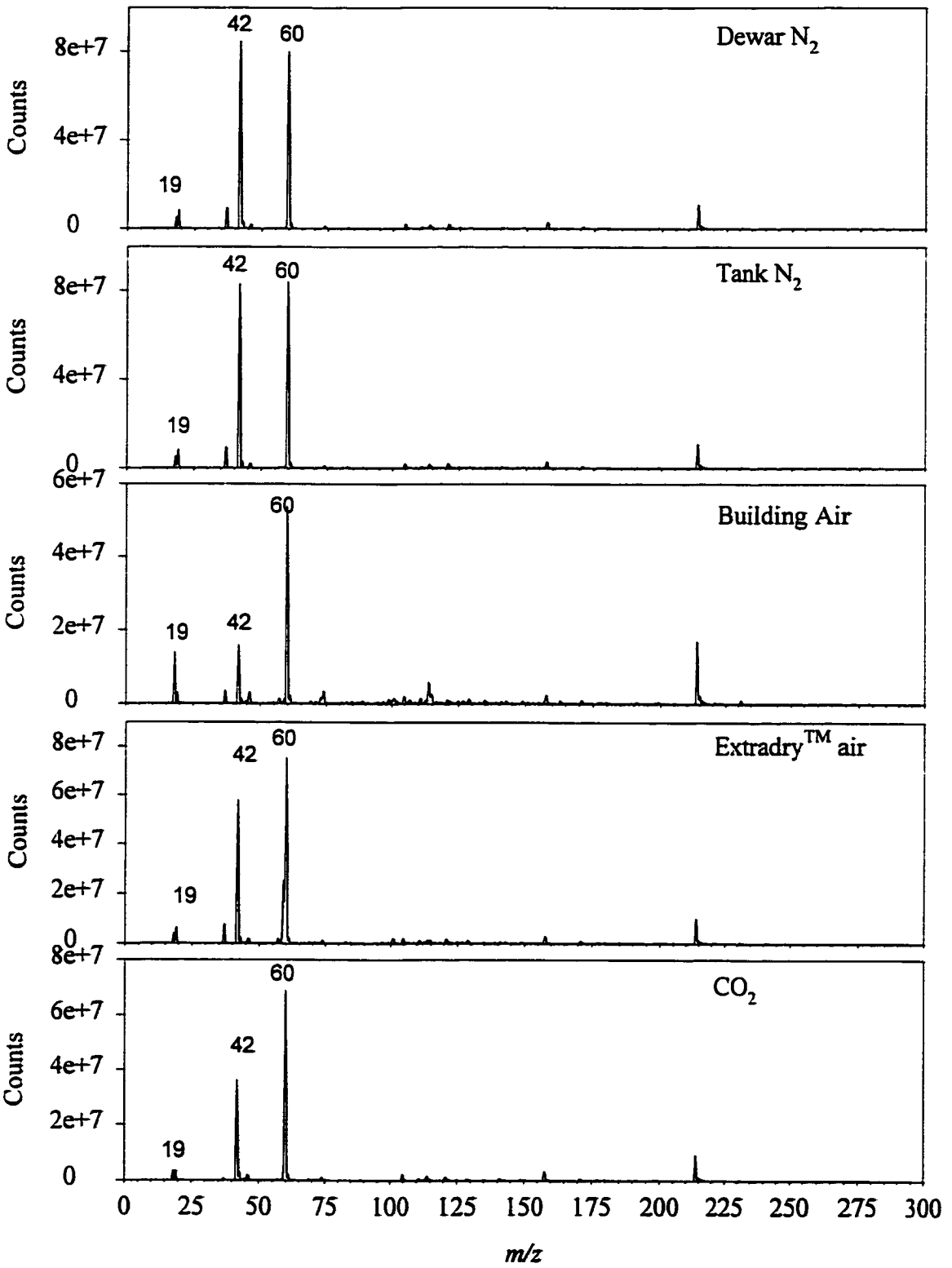

Figure 6.15. Background of 50:50 (v/v) acetonitrile/water with Dewar N_2, tank N_2, building air, Extradry™ air and CO_2.

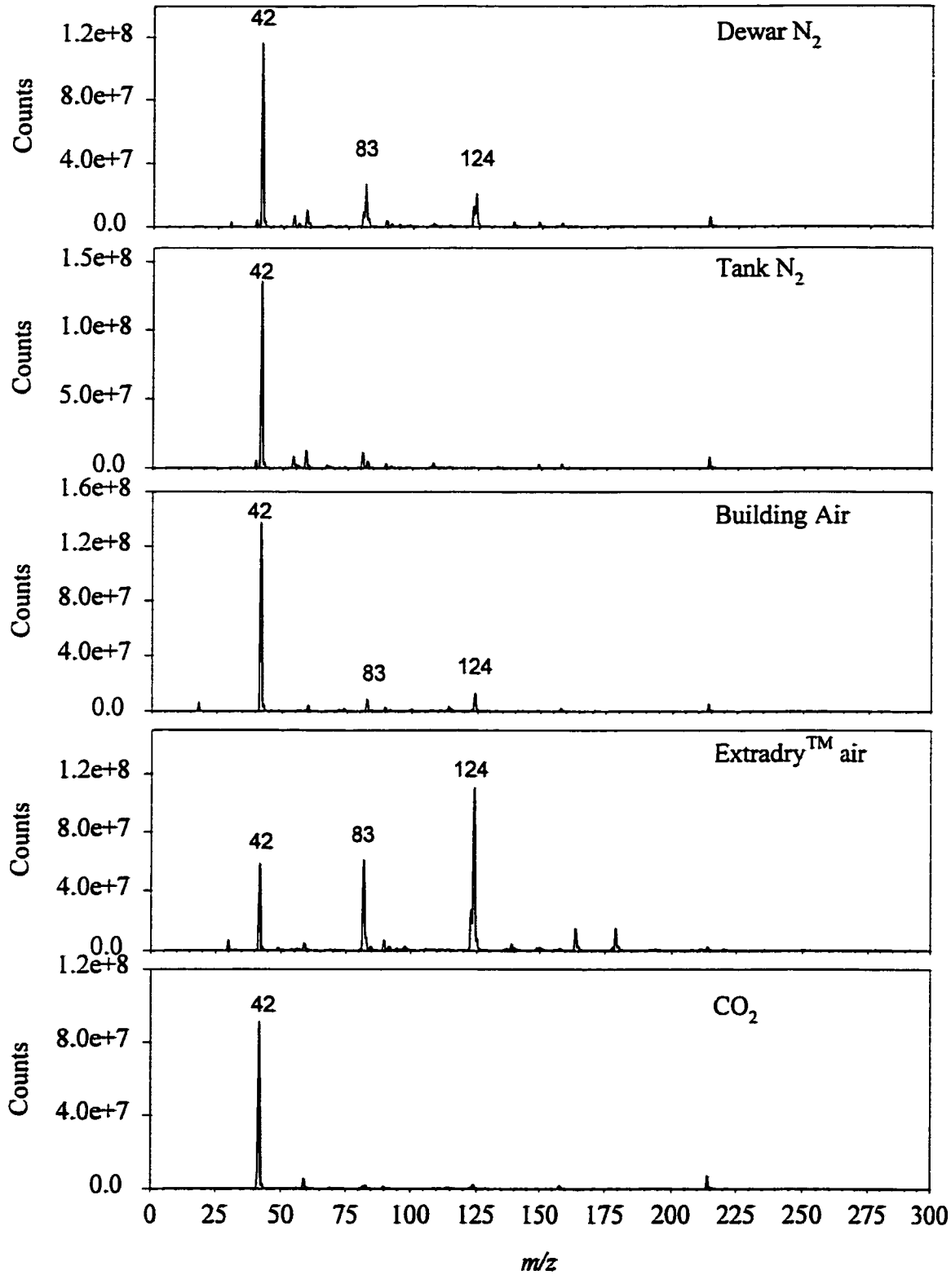

Figure 6.16. Acetonitrile background with Dewar N_2, tank N_2, building air, Extradry™ air and CO_2.

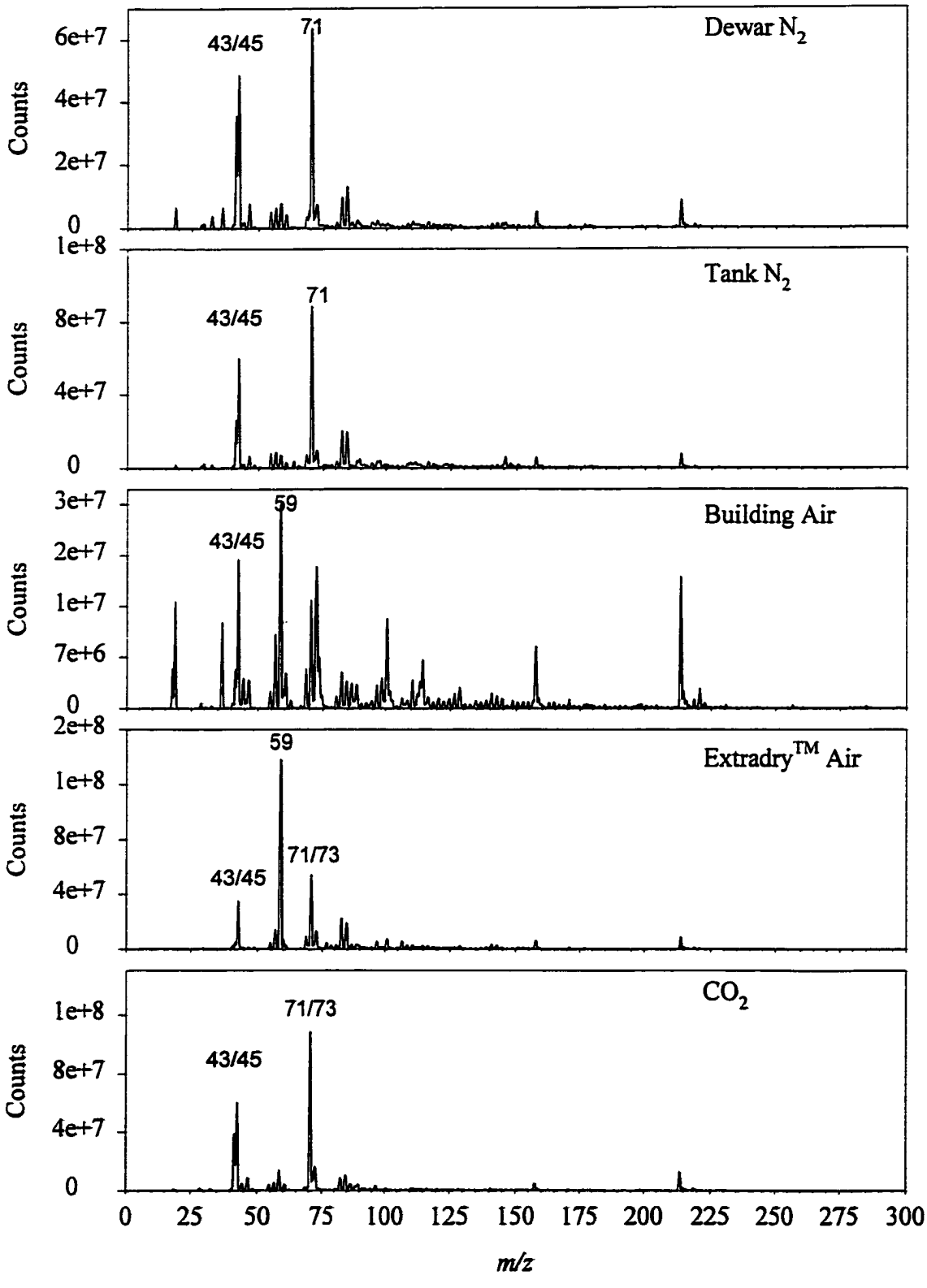

Figure 6.17. Dichloromethane background with Dewar N_2, tank N_2, building air, Extradry™ air and CO_2.

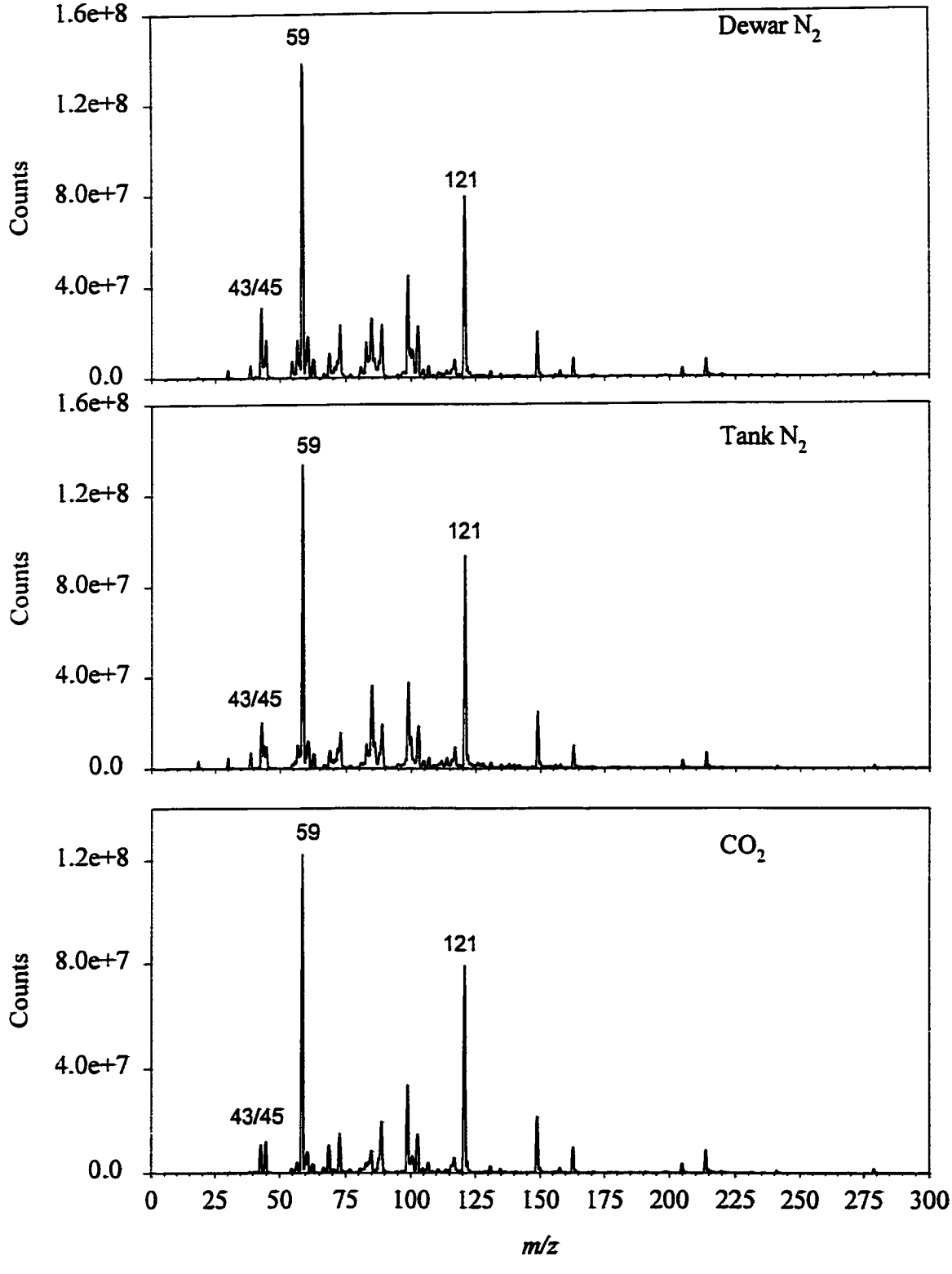

Figure 6.18. Hexanes background with Dewar N_2, tank N_2 and CO_2.

Table 6.7. Background of gas only, DCM and hexanes as a function of gas combination with Skimmer Cone C

	Gas Only		Gas + DCM		Gas + Hexanes	
Gas	***m/z***	**Structure**	***m/z***	**Structure**	***m/z***	**Structure**
Dewar N_2	19 30 37 42	H_3O^+ NO^+ $H_3O(H_2O)^+$ N_3^+	42 73 83 85	$C_2H_4N^+$ $H_9O_4^+$ CH_2Cl^+ CH_2Cl^+	43 45 57 73 83 85	$HNCO^+$, $C_3H_7^+$ $C_4H_9^+$ $C_5H_{13}^+$ $C_4H_9O^+$ $H_5C_3O_2^+$ $C_6H_{11}^+$ $C_6H_{13}^+$
Tank N_2	19 37 42	H_3O^+ $H_3O(H_2O)^+$ N_3^+	83 85	CH_2Cl^+ CH_2Cl^+	43 59 73 85	$HNCO^+$, $C_3H_7^+$ $C_3H_7O^+$ $H_5C_3O_2^+$ $C_5H_{13}^+$ $C_4H_9O^+$ $H_5C_3O_2^+$ $C_6H_{13}^+$
Extradry™ air	59	$C_3H_7O^+$ $H_5C_3O_2^+$	83 85	CH_2Cl^+ CH_2Cl^+		
CO_2	19 33 45	H_3O^+ O_2H^+ HCO_2^+			59 73	$C_3H_7O^+$ $H_5C_3O_2^+$ $C_5H_{13}^+$ $C_4H_9O^+$ $H_5C_3O_2^+$

Building Air	18	NH_4^+	18	NH_4^+		
	19	H_3O^+	19	H_3O^+		
	37	$H_3O^+(H_2O)$	37	$H_3O(H_2O)^+$		
	43	CH_3CO^+, $C_3H_7^+$	43	CH_3CO^+ $C_3H_7^+$		
	45	CO_2H^+, $C_2H_5^+$	45	CO_2H^+ $C_2H_5^+$		
	55	$H_3O^+(H_2O)_2$	83	CH_2Cl^+		
	59	$C_3H_7O^+$ $H_5C_3O_2^+$	85	CH_2Cl^+		
	73	$C_4H_9O^+$ $H_5C_3O_2^+$ $H_3O^+(H_2O)_2$				
	74	$C_4H_{12}N^+$				
	101	$C_5H_{11}O^+$				
	111	$C_6H_{13}O^+$				
	114	$C_7H_{15}O^+$				
	129	$C_8H_{17}O^+$				

For dichloromethane, an examination of the masses indicates that *m/z* 83/85 are derived from dichloromethane, though the isotope intensities are not quite correct, indicating interfering peaks. Only carbon dioxide is not associated with any dichloromethane-derived peaks. In all cases, the hexanes background is dominated by *m/z* 59, probably arising from an oxygen-containing impurity in the solvent. There is no significant difference in its intensity from gas to gas. Since the gas had little influence on solvent ionisation, it should have little impact on the signal intensity or ionisation mechanism for the PACs.

The total signal intensity of the components of IO standards 1-6 in their appropriate solvents are presented in Figures 6.19 through 6.26. There is an anomalously high result for naphthalene in Figure 6.19 which should be disregarded. In 50:50 (v/v) acetonitrile/water and IO standard 1, all PACs are observed with good signal intensity, no one species is

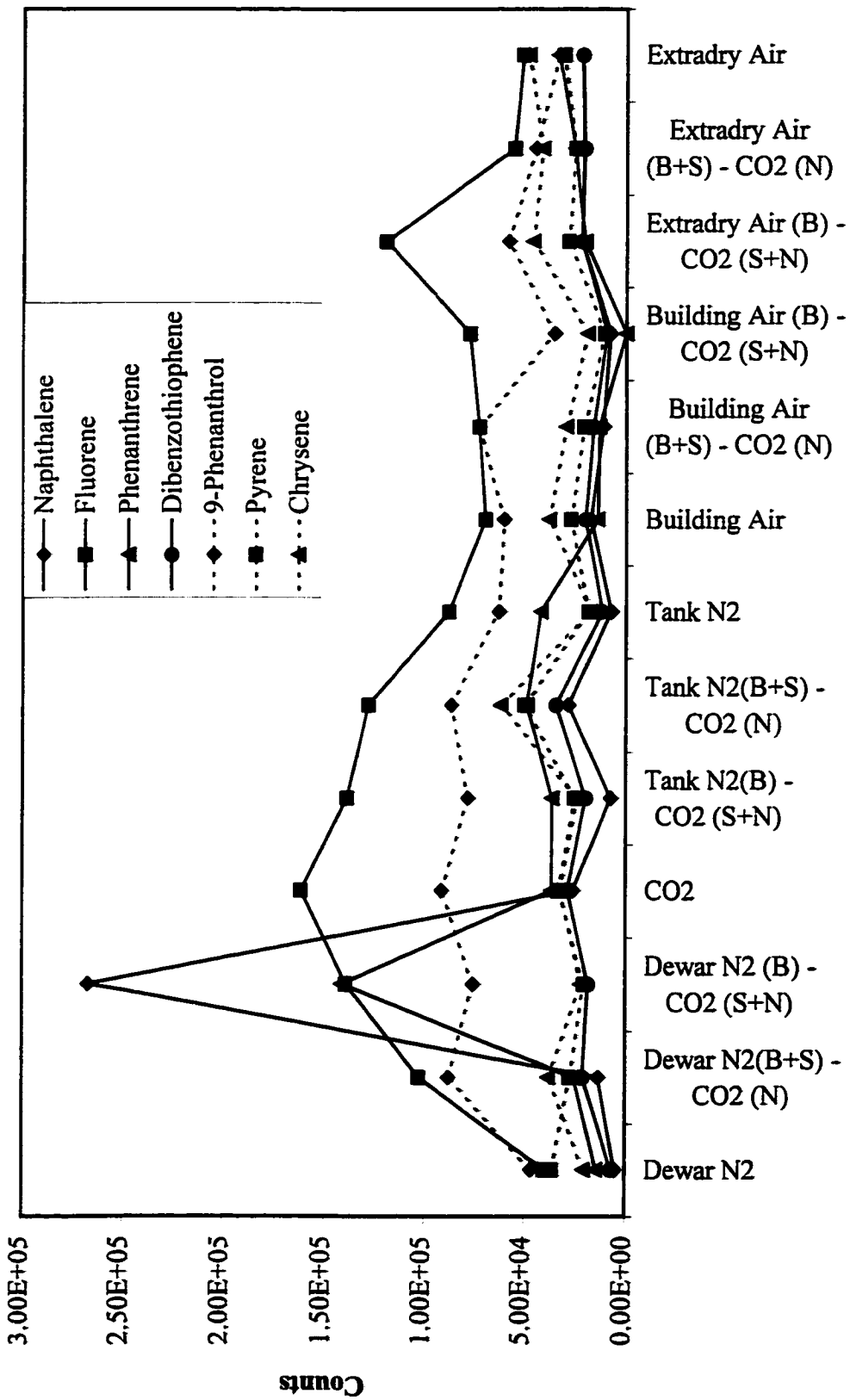

Figure 6.19. Total Signal of a 1/100 dilution of IO-1 standard with 50:50 (v/v) acetonitrile/water as a function of gas combination with skimmer cone C.

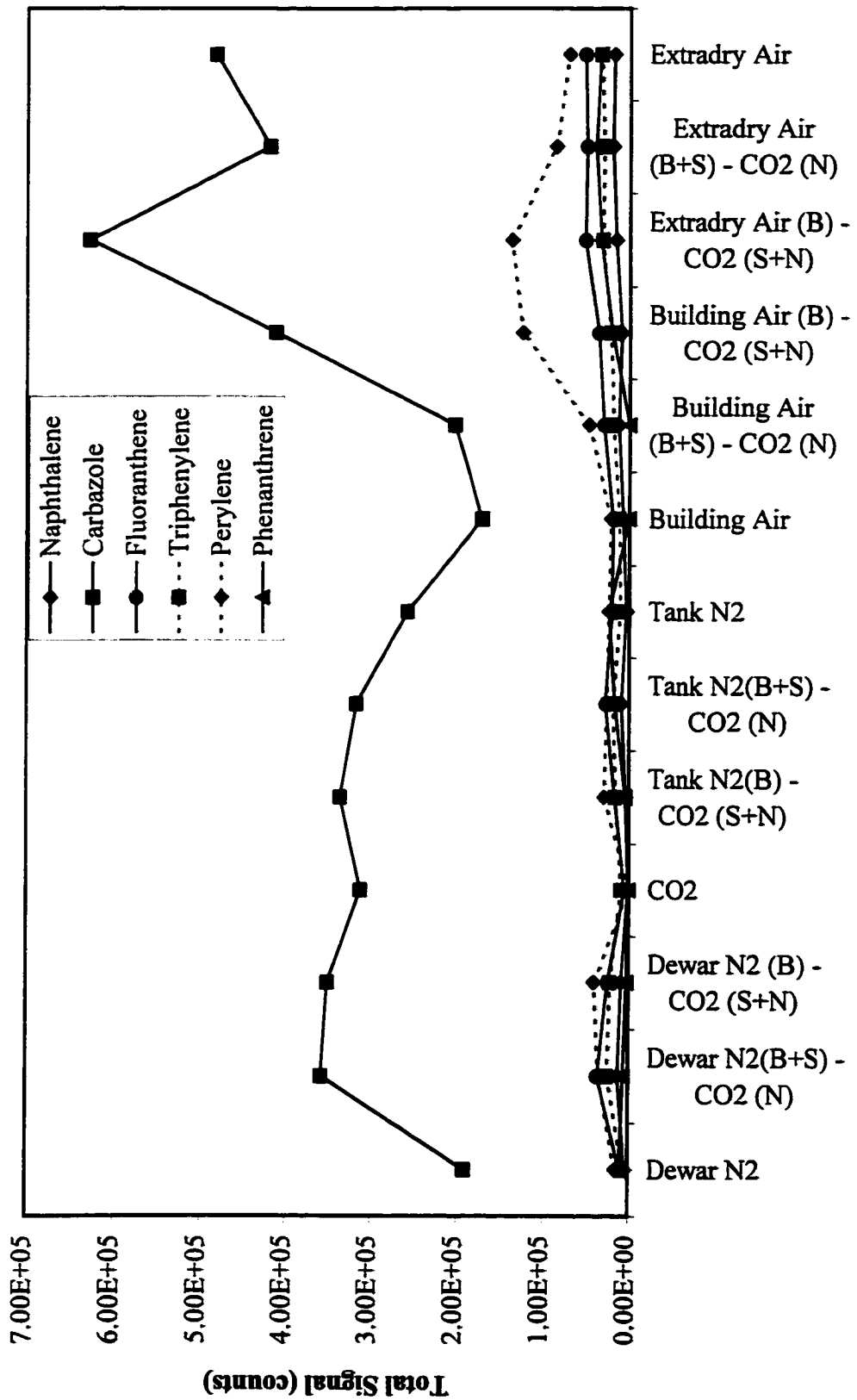

Figure 6.20. Total Signal of of a 1/100 dilution of IO-2 standard with 50:50 (v/v) acetonitrile/water as a function of gas combination with skimmer cone C.

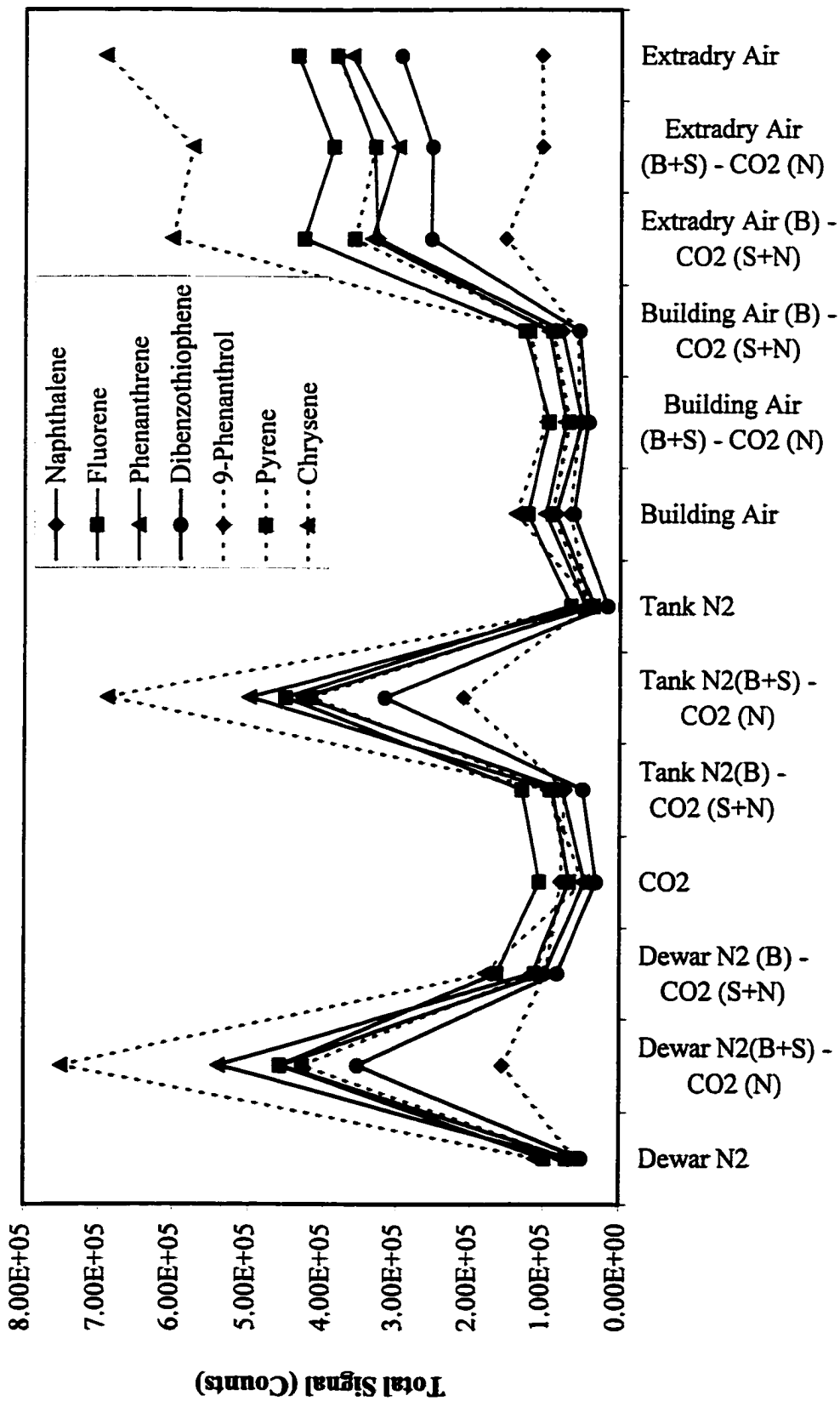

Figure 6.21. Total Signal of a 1/100 dilution of IO-1 standard with acetonitrile as a function of gas combination with skimmer cone C.

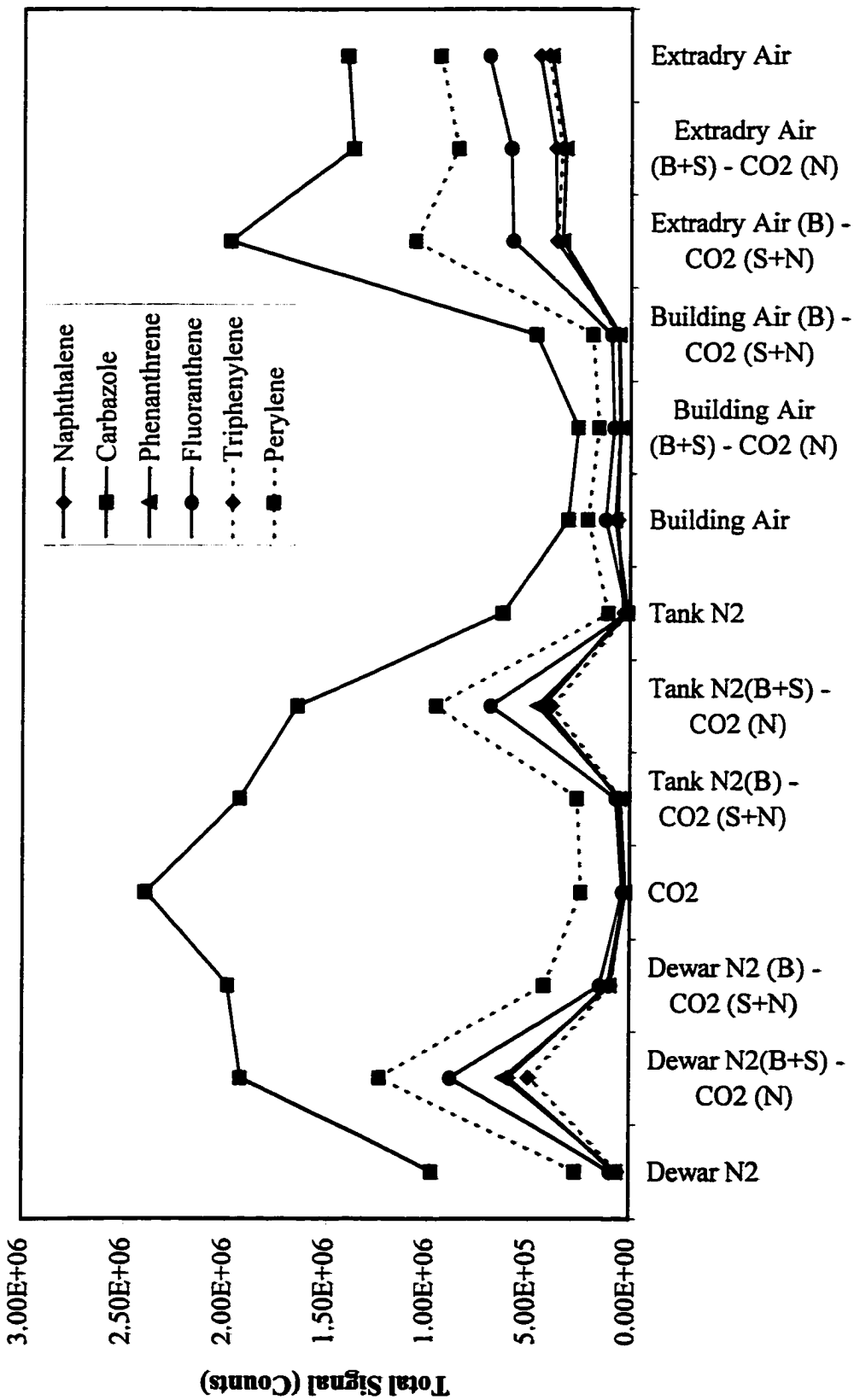

Figure 6.22. Total Signal of a 1/100 dilution of IO-2 standard with acetonitrile as a function of gas combination with skimmer cone C.

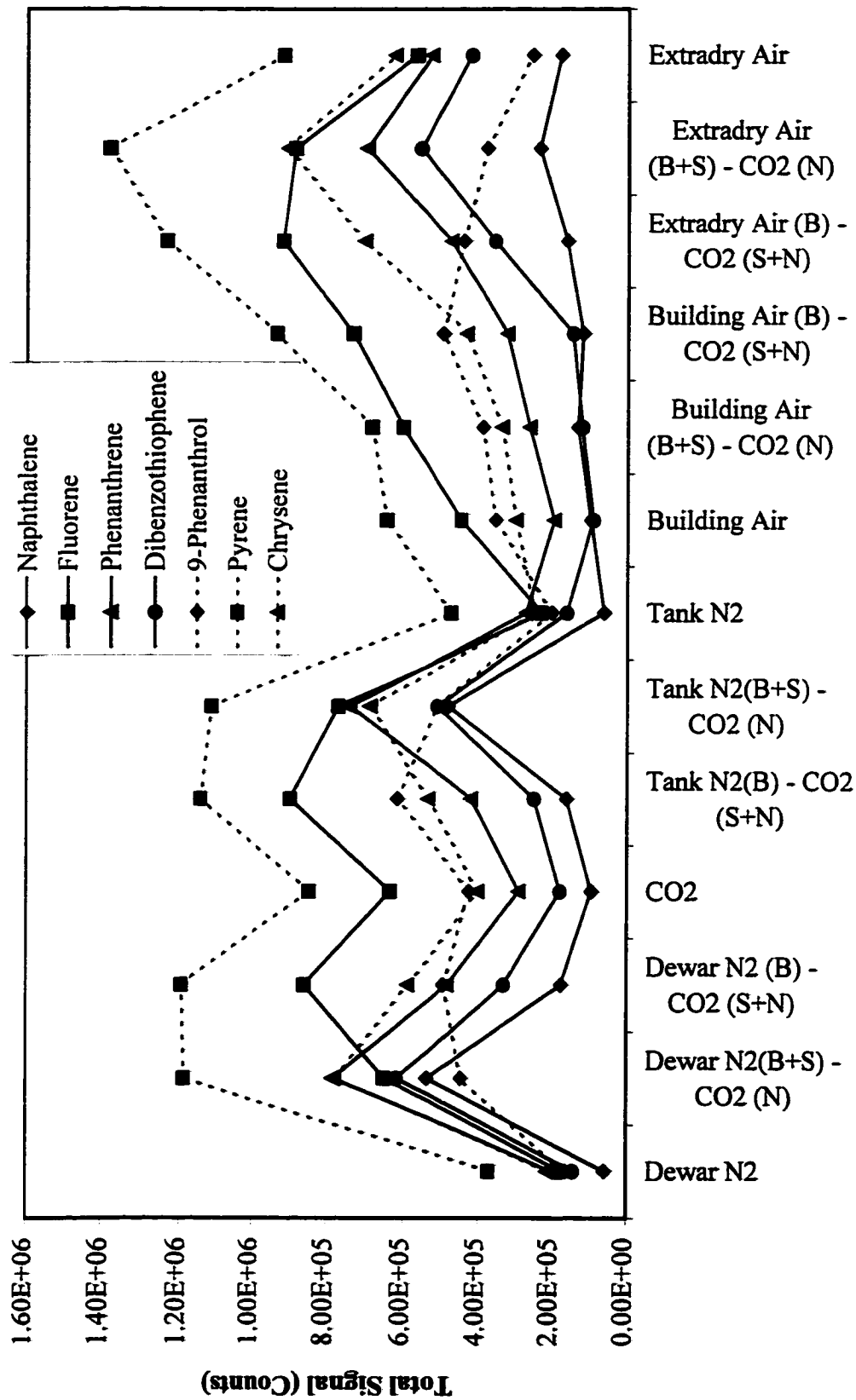

Figure 6.23. Total Signal of a 1/100 dilution of IO-3 standard with dichloromethane as a function of gas combination with skimmer cone C.

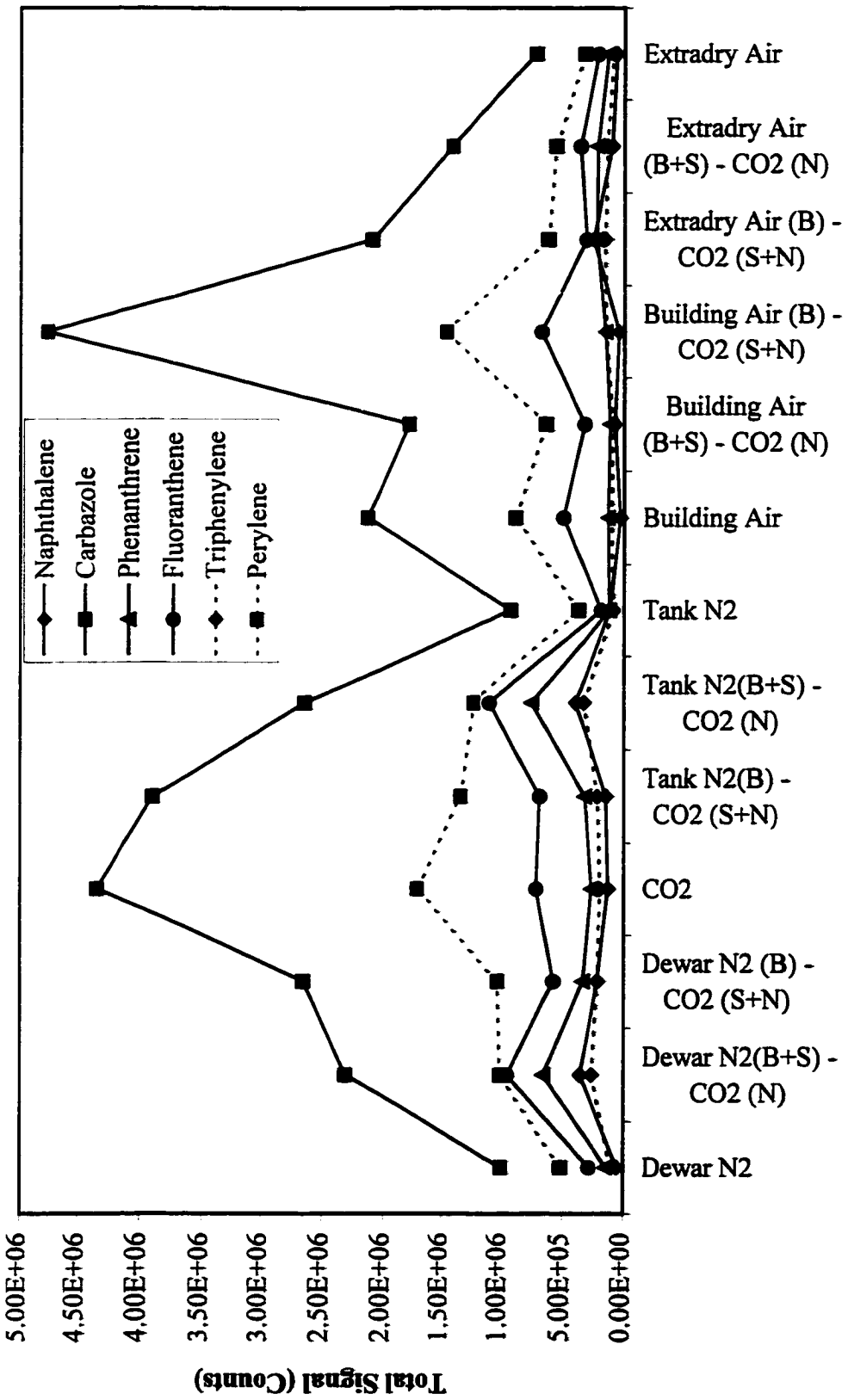

Figure 6.24. Total signal of a 1/100 dilution of IO-4 standard with dichloromethane as a function of gas combination with skimmer cone C.

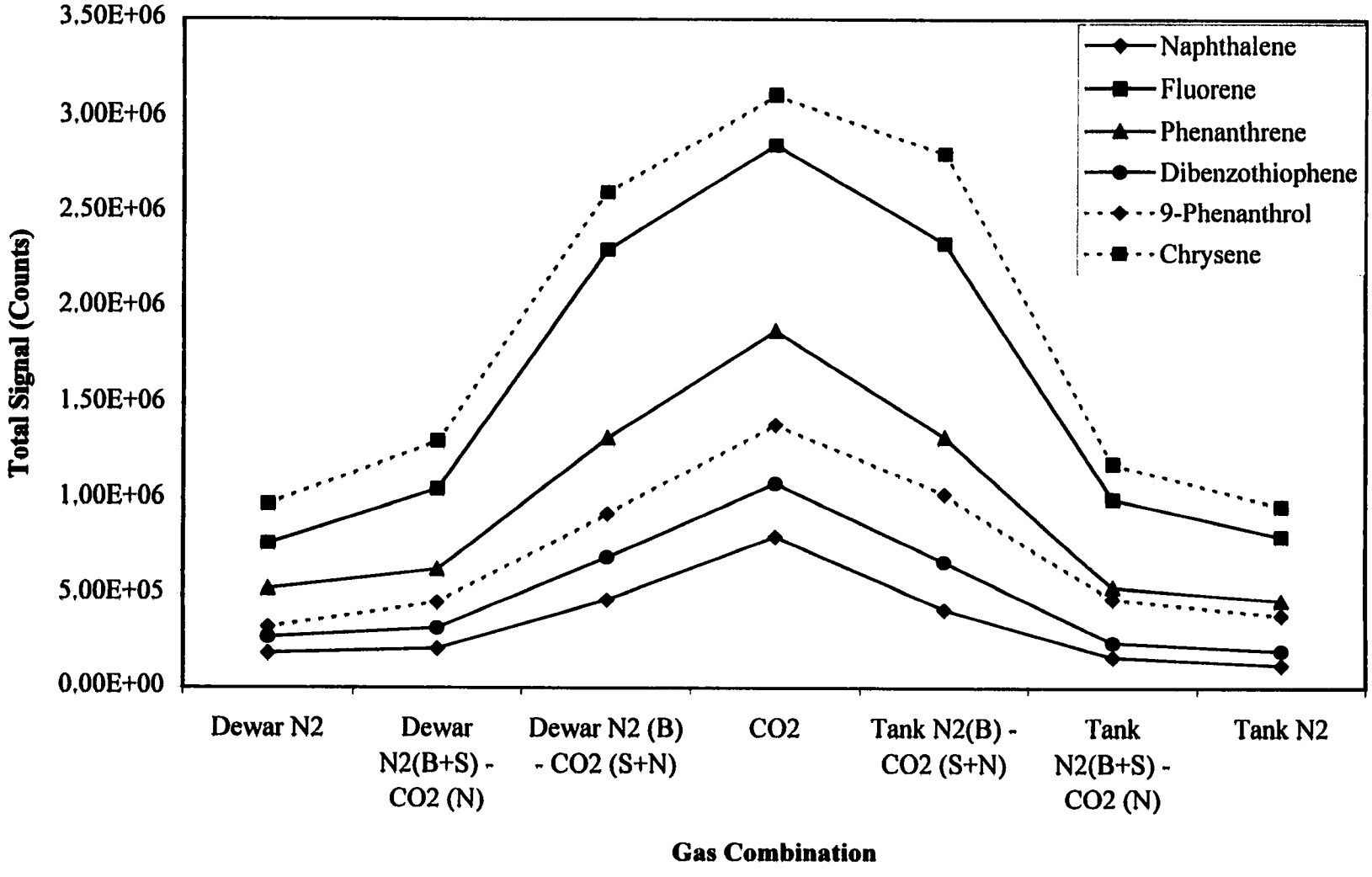

Figure 6.25. Total Signal of a 1/100 dilution of IO-5 standard with hexanes as a function of gas combination with skimmer cone C.

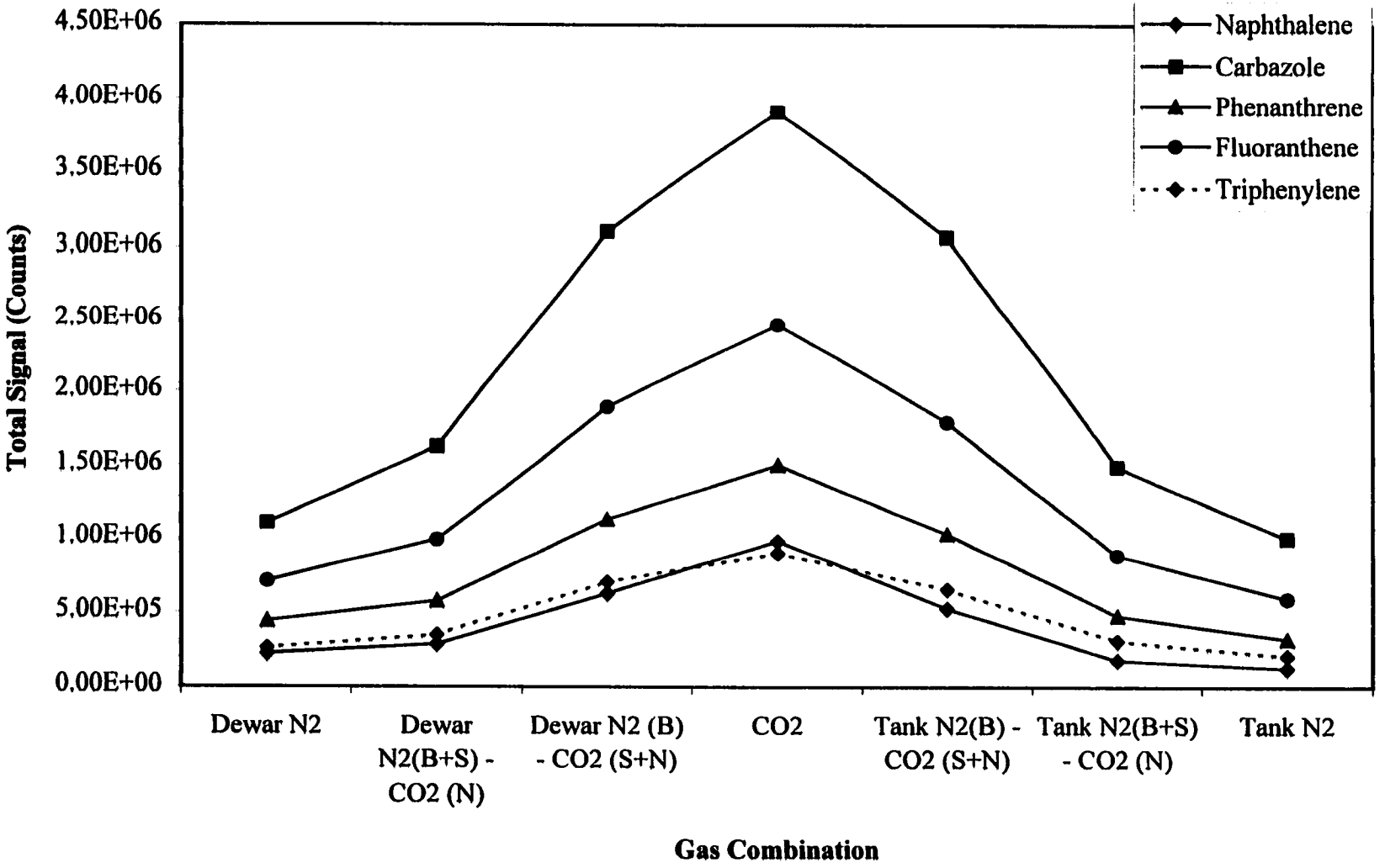

Figure 6.26. Total Signal of a 1/100 dilution of IO-6 standard with hexanes as a function of gas combination with skimmer cone C.

dominating over the other (despite the presence of an oxygen-containing species which on the basis of the results with fluorenone should have been dominating the spectrum). This latter observation indicates that exocyclic heteroatoms, especially oxygen, are not a predictor of sensitivity in APCI. A combination of air or nitrogen as the bath and sheath gas and carbon dioxide as the nebuliser gas is associated with higher signal intensity for most PACs, except fluorene. With IO standard 2, carbazole is clearly dominating the spectrum, its abundance peaking with the Extradry™ air (bath gas)-carbon dioxide (sheath gas). For the other PACs in the mixture, carbon dioxide in the nebuliser gas is sufficient to improve the signal and making it the sheath gas generates no significant increase in signal. With acetonitrile and IO standard 1, there is an almost eight-fold improvement in signal strength over the case of aqueous acetonitrile, all PACs are observed with high signal efficiency and chrysene is detected with highest sensitivity. Clear and similar optima with Extradry™ air alone, nitrogen as bath and sheath gas with carbon dioxide as nebuliser gas are observed. A similar behaviour is noted with IO standard 2, except that carbazole dominates over the other forms and is better detected as the proportion of carbon dioxide in the source rises. With dichloromethane as solvent, the best signal intensities were observed with Extradry™ air in all streams or nitrogen (from either source) as the bath and sheath gas and carbon dioxide as the nebuliser gas. Increasing the carbon dioxide content did not improve signal strength for relatively small PACs. However, enriching the source with carbon dioxide assisted in the observation of higher mass PACs and carbazole. These results were also observed with aqueous and pure acetonitrile. With hexanes as the solvent, there is a clear optimum with carbon dioxide in all streams, regardless of the sample composition. This is interesting as

nothing in the solvent spectra led us to believe that there should be a difference. However, the carbon dioxide spectrum was cleaner than either nitrogen source, so we may be observing an effect of decreased background noise rather than an improvement in actual signal.

Figures 6.27 through 6.34 represent the plots of the ratio of protonated molecule to molecular ion for the standards. For aqueous acetonitrile, carbazole and fluorene are almost equally well-protonated, with protonation of all PACs peaking in carbon dioxide. This behaviour does not correlate with the abundances of the solvent peaks. For neat acetonitrile, protonation is lower than with aqueous acetonitrile and peaks in carbon dioxide and tank nitrogen, which corresponded to low levels of solvent clustering. This seems to indicate that proton transfer does indeed occur from the solvent and is more difficult if the proton is solvated. For dichloromethane, protonation is observed to increase with an increase in the carbon dioxide content. Thus, a decrease in the dichloromethane peaks (greater fragmentation of the solvent) is associated with higher protonation, perhaps indicating that the protons are derived from dichloromethane. With hexanes, protonation levels maximise with tank nitrogen, a positive correlation between the abundance of *m/z* 43 and protonation being observed.

The results again indicate that a high level of protonation is not necessarily correlated with high signal intensities. When performing mass spectral analyses with APCI mode, it is therefore suggested that the operator seek the best possible conditions for observing the total signal of PACs, rather than trying to manipulate the solvent or gas to give predominant protonation in the hope that this will generate optimal signal strength.

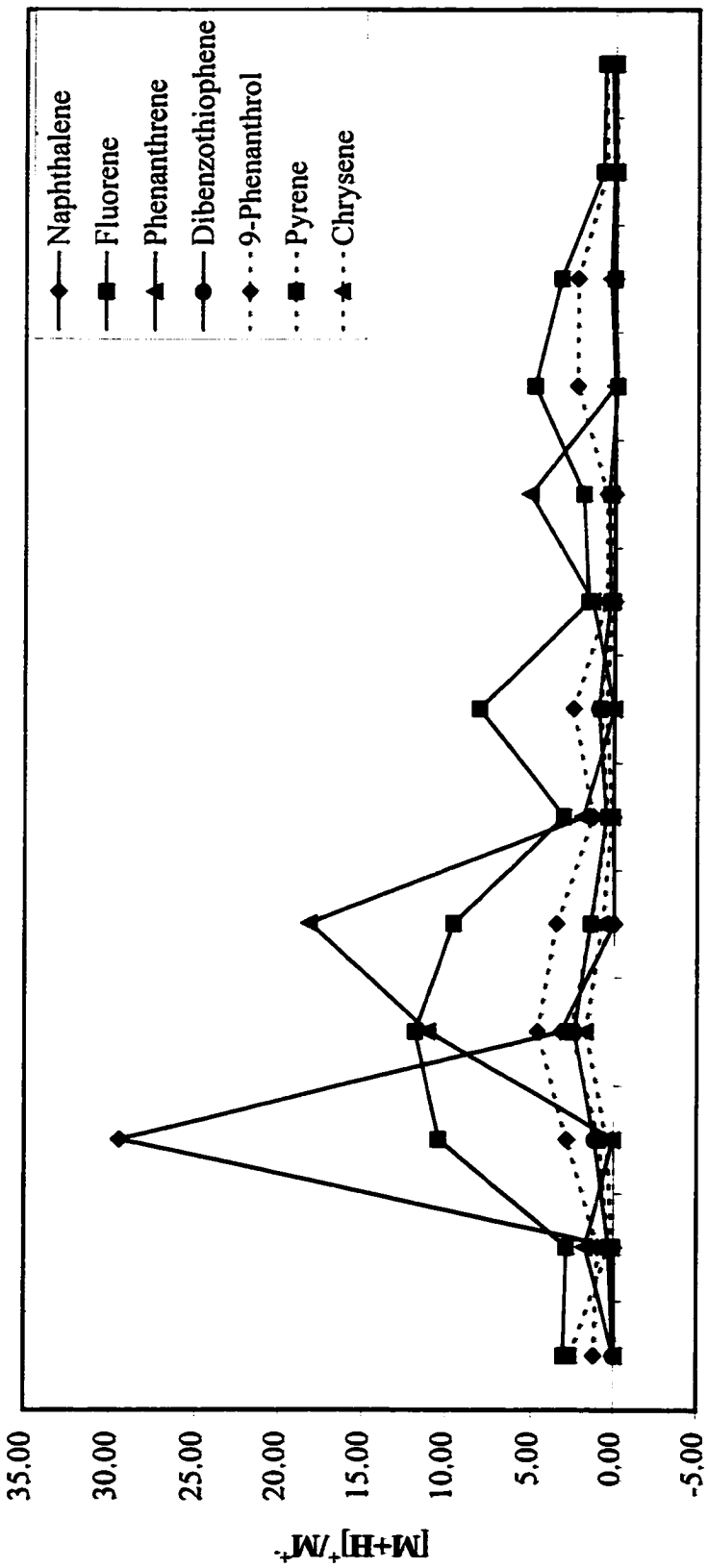

Figure 6.27. Ratio of protonated molecule and molecular ion of a 1/100 dilution of IO-1 standard with 50:50 (v/v) acetonitrile/water as a function of gas combination with skimmer cone C.

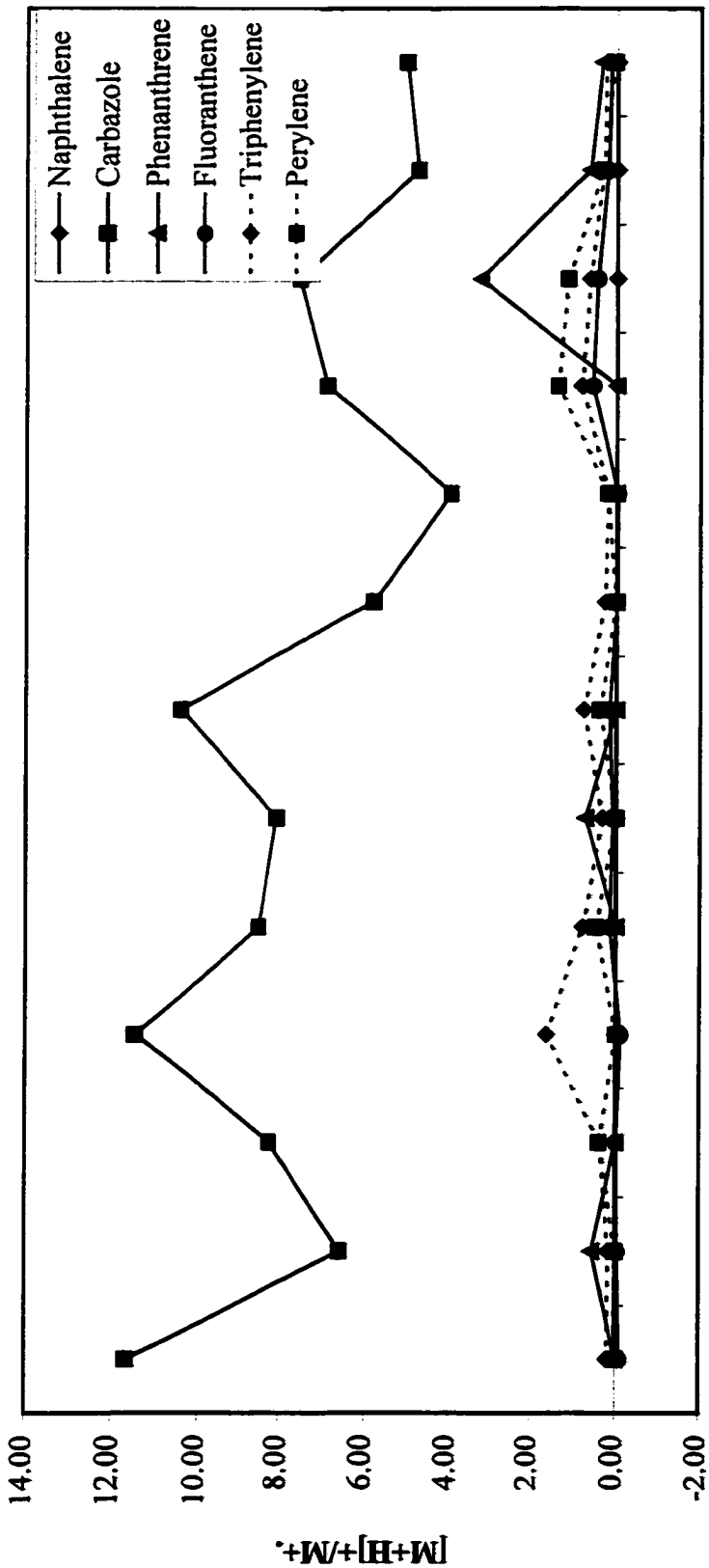

Figure 6.28. Ratio of protonated molecule to molecular ion of a 1/100 dilution of IO-2 standard with 50:50 (v/v) acetonitrile/water as a function of gas combination with skimmer cone C.

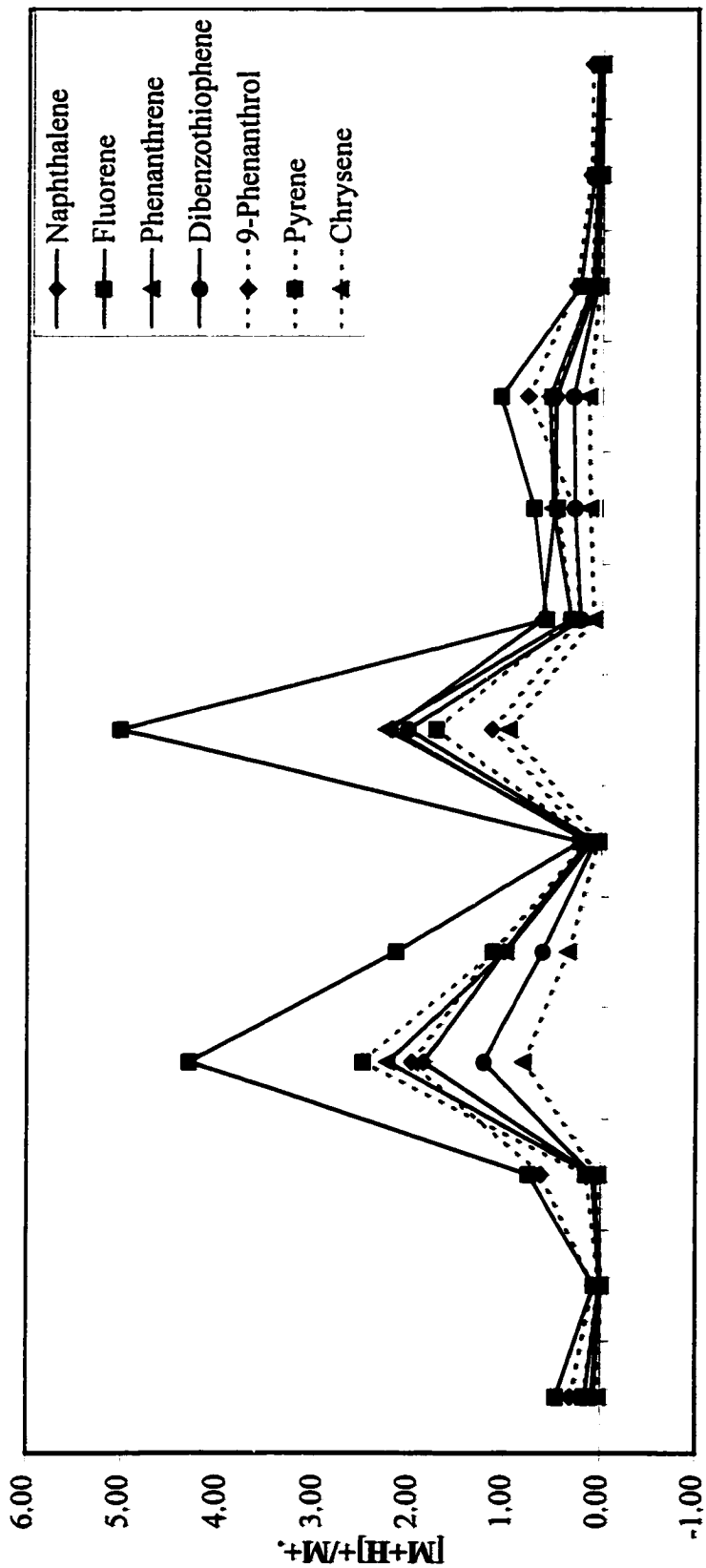

Figure 6.29. Ratio of protonated molecule to molecular ion of a 1/100 dilution of IO-1 standard with acetonitrile as a function of gas combination with skimmer cone C.

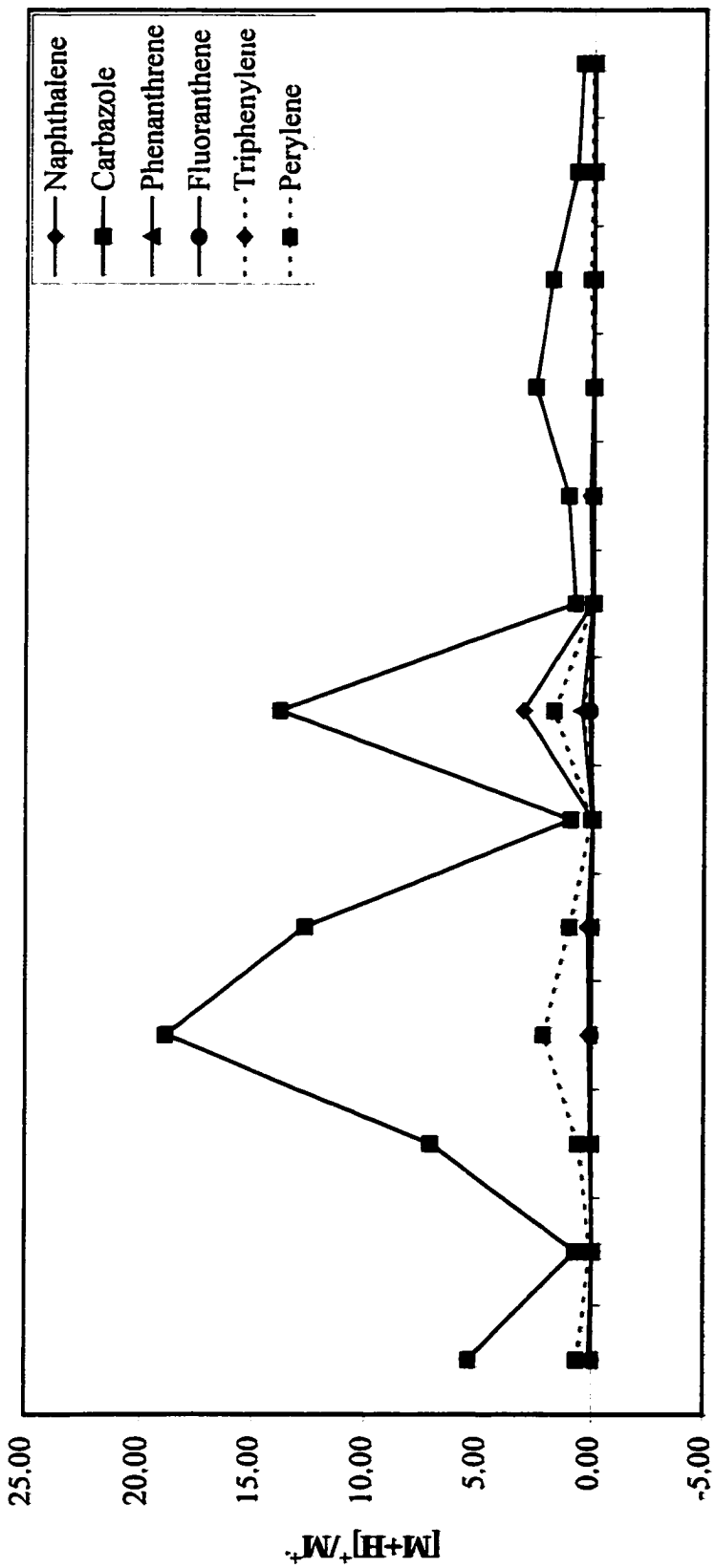

Figure 6.30. Ratio of protonated molecule to molecular ion of a 1/100 dilution of IO-2 standard with acetonitrile as a function of gas combination with skimmer cone C.

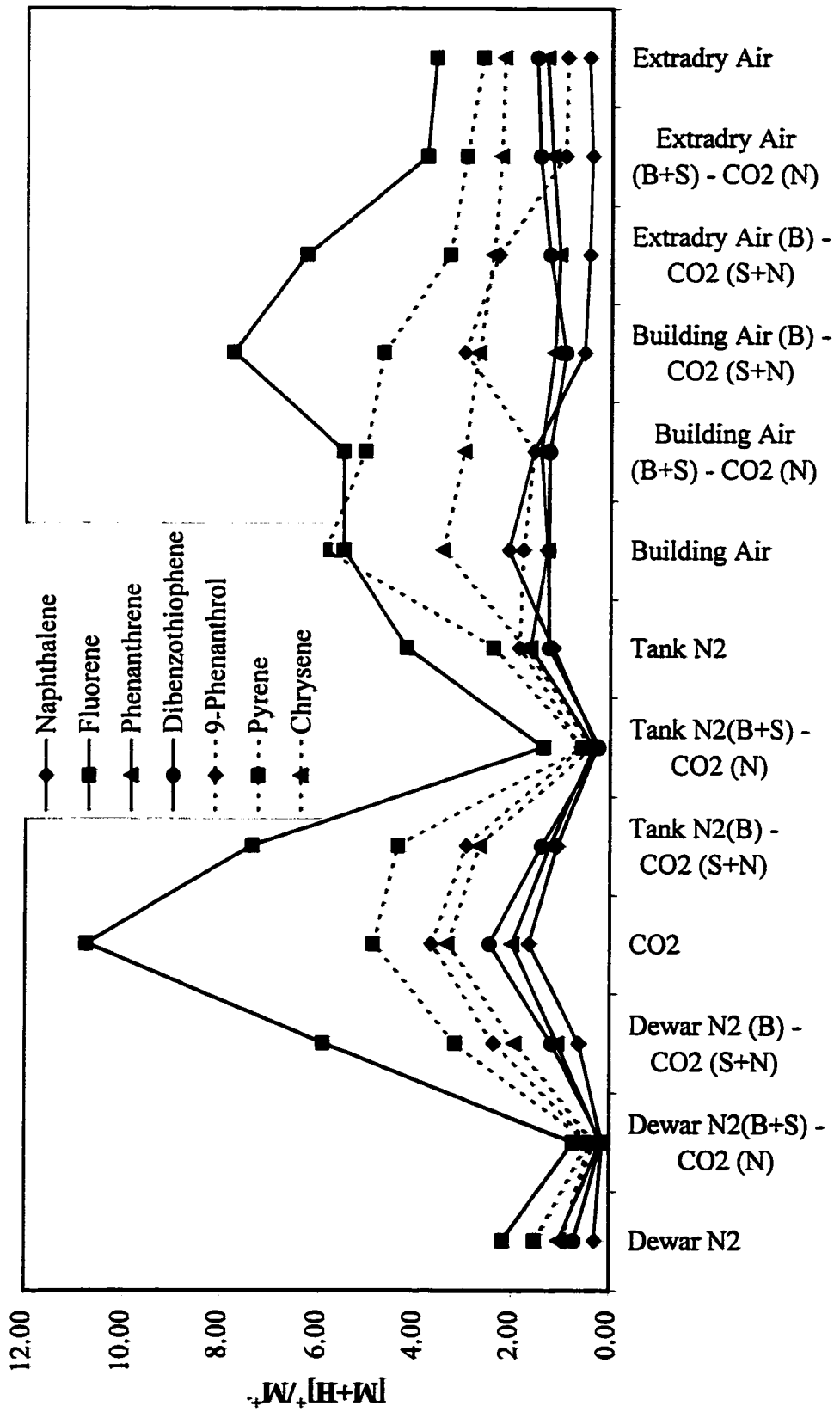

Figure 6.31. Ratio of protonated molecule to molecular ion of a 1/100 dilution of IO-3 standard with dichloromethane as a function of gas combination with skimmer cone C.

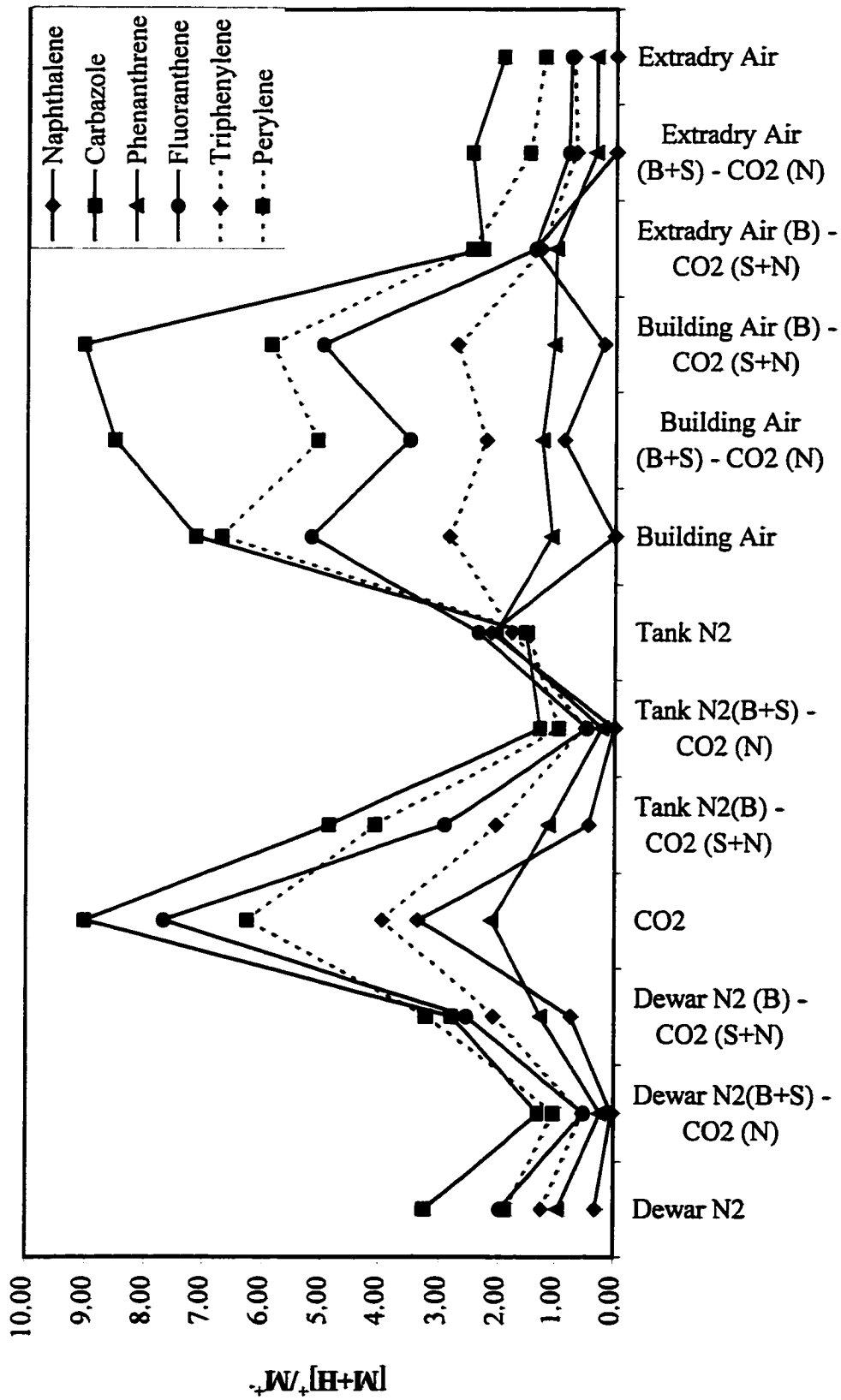

Figure 6.32. Ratio of protonated molecule to molecular ion of a 1/100 dilution of IO-4 standard with dichloromethane as a function of gas combination with skimmer cone C.

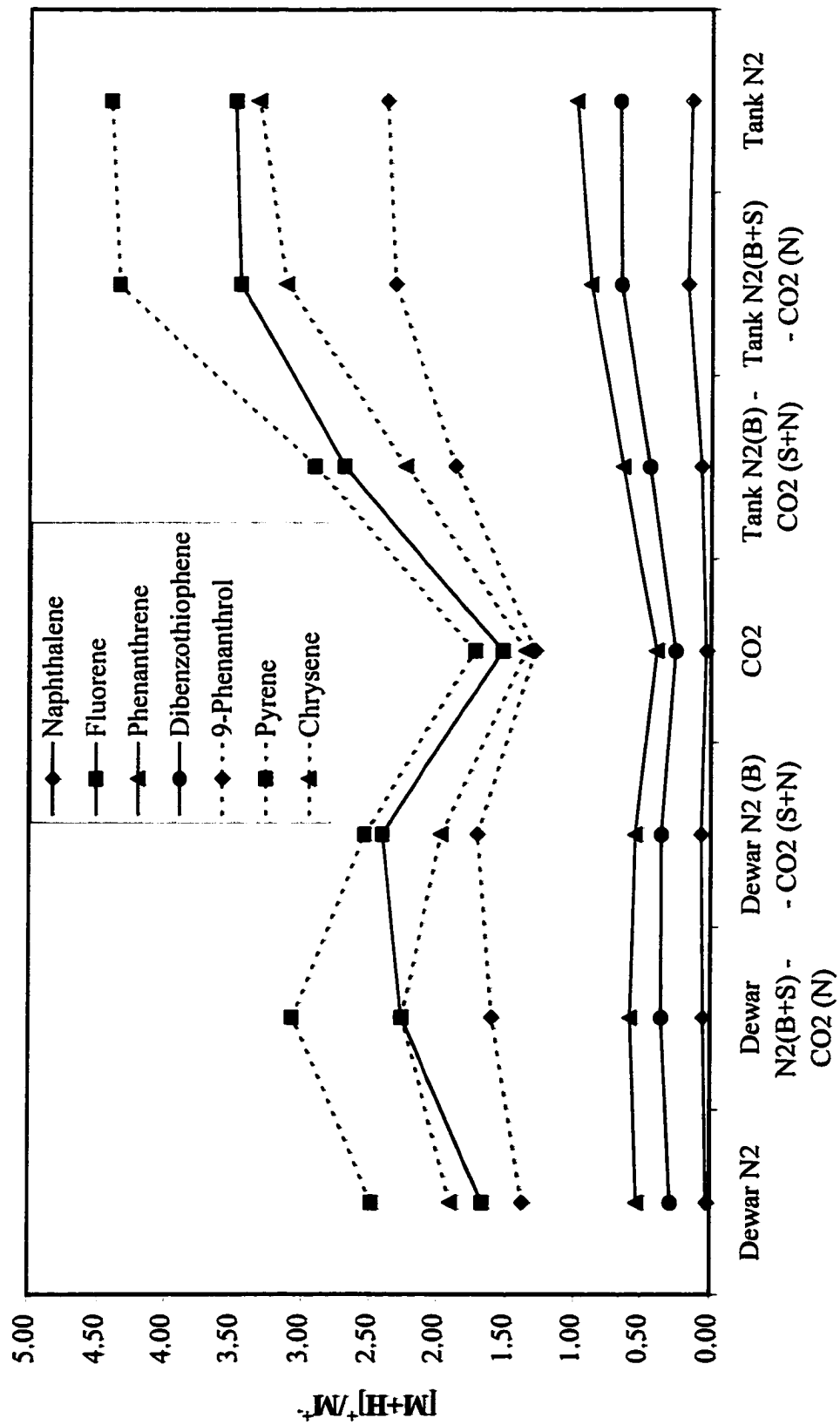

Figure 6.33. Ratio of protonated molecule to molecular ion of a 1/100 dilution of IO-5 standard with hexanes as a function of gas combination with skimmer cone C.

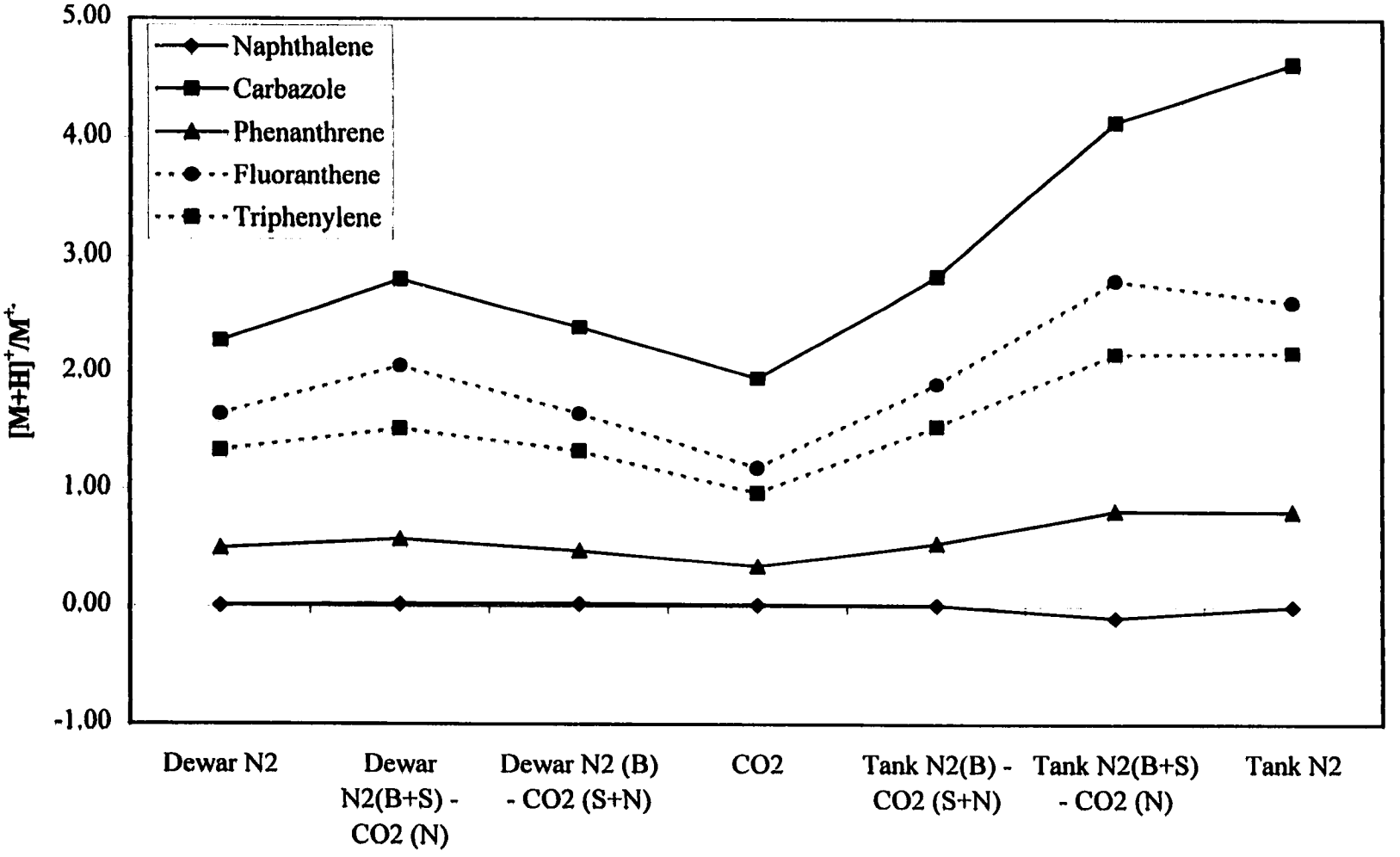

Figure 6.34. Ratio of protonated molecule to molecular ion of a 1/100 dilution of IO-6 standard with hexanes as a function of gas combination with skimmer cone C.

Aqueous solvents should be eschewed in favour of organic solvents. Where feasible, hexanes should be used as the solvent. If this is not feasible, dichloromethane is preferable to acetonitrile or to aqueous acetonitrile. To improve signal intensity and minimise operating costs, analyses with aqueous acetonitrile, acetonitrile or dichloromethane as solvent should be performed with nitrogen as the bath and sheath gas and carbon dioxide as the nebuliser gas while analyses with hexanes should be performed with all carbon dioxide in the source (this carbon dioxide should be periodically checked as to whether the predominant ion is *m/z* 45 or *m/z* 47 as this is an indicator of gas purity).

6.5 Application to Real World Analysis

From the studies reported in section 6.4, there is an advantage in PAC analysis in acetonitrile to the use of Extradry™ air. This would be rather expensive for routine operation but a combination of nitrogen in the bath and sheath gas stream with carbon dioxide in the nebuliser stream is almost as beneficial but far more economical.

A Syncrude light gas oil (MB13C) was separated on a silica column, giving the characteristic naphthalene peak and 3-4 pyrene peaks (see Figure 3.5). A sample of the chromatographic eluent between the end of the elution of pyrene peak 2 and the start of the elution of pyrene peak 3 was collected to characterise the PACs in this previously unexamined region. It was evaporated to dryness and reconstituted in 1 mL of acetonitrile. Cold column chromatography was used to separate a 300 μL injection of sample with acetonitrile as the mobile phase. Cold column chromatography allows water to be avoided, but maintains PAC separability. The separation was monitored with a UV detector at 336 nm and the mass spectrometer in APCI mode operating in tandem. Mass spectral analysis was

performed with single ion monitoring at *m/z* 216, 217, 220, 221, 230-233, 242, 243, 256, and 257 (0.2 sec at each mass at each cone voltage) with the following mass spectral parameters: corona voltage = 4.00 kV, source temperature = 120°C, probe temperature = 350°C, cone voltage = 15, 30, 50, bath and sheath flows of 300 sLph and nebuliser flows of 50 sLph.

In the first run, Dewar nitrogen was used in all streams. In the second run, Dewar nitrogen was used as the bath and sheath gas and carbon dioxide as the nebuliser gas. Figure 6.35 shows the total ion chromatograms for these runs at 30 V cone. It indicates that the signal in the presence of carbon dioxide is three times better and the noise is substantially reduced.

Table 6.8. $[M+H]^+/M^{+\bullet}$ Ratio as a Function of Gas

m/z	PAC	$[M+H]^+/M^{+\bullet}$ Dewar N_2 (B+S+N)	$[M+H]^+/M^{+\bullet}$ Dewar N_2 (B+S) - CO_2 (N)
216/217	Methylpyrene	1.61	0.62
220/221	Trimethylphenanthrene	0.35	0.19
230/231	Dimethylpyrene	2.87	1.65
232/233	Tetramethyldihydo-phenanthrene or dimethyldihydropyrene	1.45	0.36
242/243	Trimethyldihydro-pyrene and/or methylchrysene or methylbenzanthracene	1.20	0.70
256/257	Tetramethyldihydro-pyrene and/or dimethylchrysene or dimethylbenzanthracene	1.03	0.50

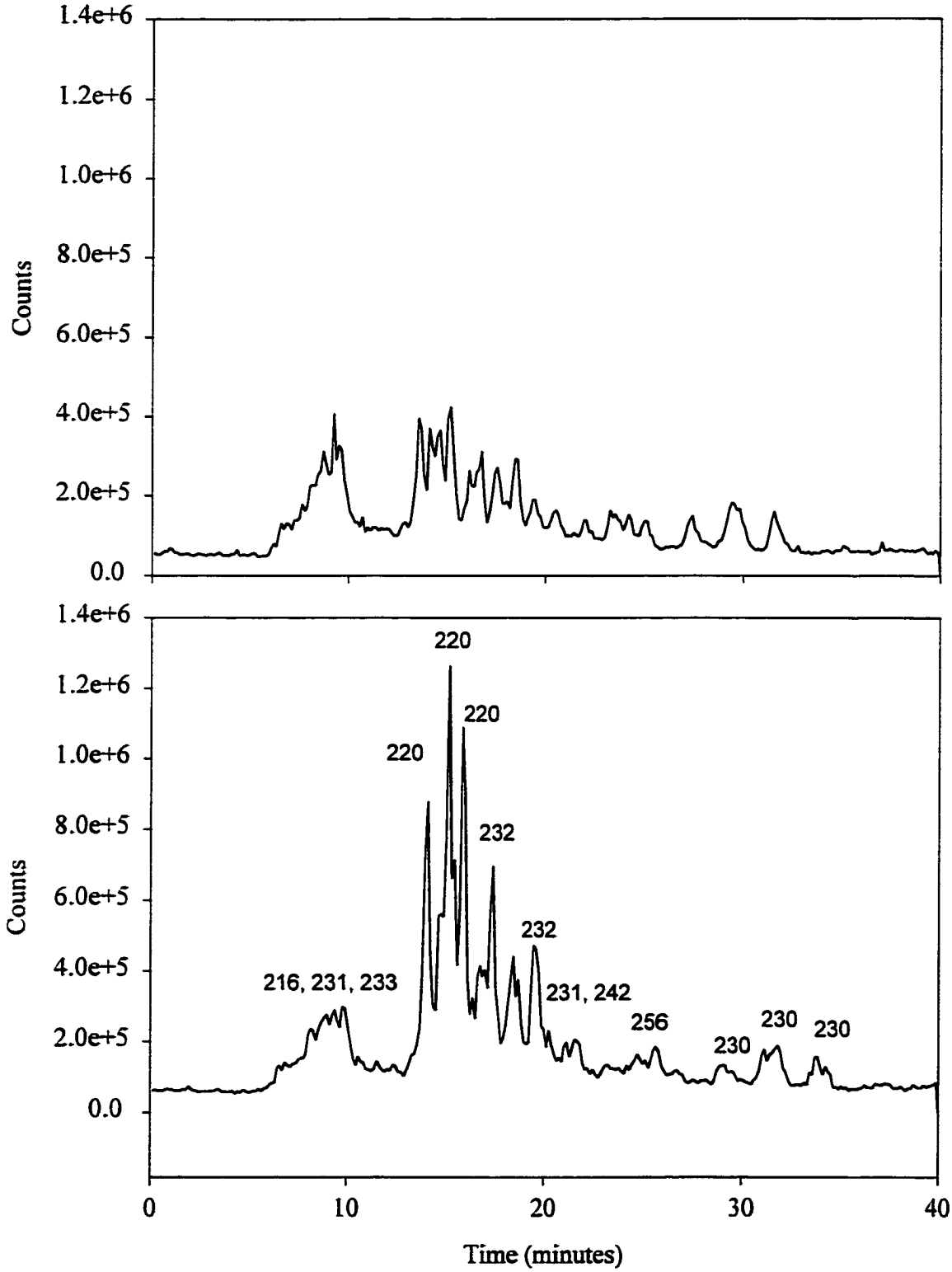

Figure 6.35. TICs of gap between pyrene peaks 2 and 3 with a) Dewar N_2 in all streams and b) Dewar N_2 as bath and sheath gas, CO_2 as nebuliser gas with skimmer cone C.

Table 6.8 lists the components identified and the ratio of the protonated molecule to the molecular ion at 30 V cone. These results indicate that a variety of PACs are better detected by the use of carbon dioxide in conjunction with Dewar nitrogen, than with nitrogen alone and that the enhancement is similar to that observed for standards introduced via flow injection analysis at a much lower flow rate. Thus, flow rate does not appear to have an impact on total signal intensity. This indicates that protonation will decrease with the incorporation of carbon dioxide but the signal intensity will improve. More significantly, this strategy can be employed to improve identification of trace analytes in samples.

Chapter 7

ESI vs. APCI

7.1 Introduction

Electrospray (ESI) and atmospheric pressure chemical ionisation (APCI) are liquid introduction atmospheric pressure ionisation techniques used in mass spectrometry, frequently in conjunction with prior HPLC (high performance liquid chromatography) separation of sample components. These techniques were evaluated as methods for the identification of polycyclic aromatic compounds (PACs) by LC/MS.

7.1.1 Atmospheric Pressure Chemical Ionisation

The APCI technique is widely used for coupling of HPLC separation and mass spectral detection because of 1) its high flow rate tolerance (up to 2 mL/min), 2) its lack of solvent preference (functions with aqueous or organic solvents), 3) its ability to ionise a broad range of compounds, 4) its softness as an ionisation technique, yielding predominantly protonated molecular ions ($[M+H]^+$) and/or molecular ions ($M^{+\bullet}$), and 5) its ability to effect sample fragmentation by the manipulation of the cone voltage.

A sequence of steps occurs in $APCI^+$ with liquid introduction [54]. Liquid from a flow injection device or an LC column enters the heated probe and encounters the nebuliser gas, which converts the liquid into very fine droplets at the probe tip. Hot sheath and bath gases vaporise these droplets and transport both sample and solvent molecules into the path of the corona discharge needle. This needle, when operated from 2 to 5 kilovolts (kV), will ionise nitrogen or oxygen in the gas stream [92], initiating a series of reactions ultimately leading to the formation of hydronium ion – water clusters. Solvent and analyte molecules

are ionised in subsequent steps in a series of ion-molecule reactions in the region between the corona needle and the skimmer cone. The ions flow through the counter electrode or "pepper pot", the extraction and skimmer cones and into the quadrupole analyser. A radiofrequency (rf) lens prevents the loss of ions due to path deviations [54]. Other systems employ a thin foil of ^{63}Ni, a β emitter, which emits electrons with a wide range of energies with an approximate mean energy of 20 keV. This broad distribution of energies will result in a wide variation in energy transfer to analytes, resulting in irreproducible ionisation and fragmentation levels. A corona needle yields a more reproducible ionisation. However, the spectra generated with these devices are very similar though the linear dynamic range for analytical applications is better with the corona discharge needle [195].

Two dominant mechanisms operate in APCI-MS are proton transfer and charge exchange [195]. The ease with which a compound undergoes charge exchange or proton transfer is reflected by the observed ratio of protonated molecular ion to molecular ion ($[M+H]^+/M^{+\bullet}$). It has been suggested that this ratio is dependent both on the physical properties of the analyte (ionisation energy, proton affinity and gas phase basicity) and source conditions, in particular laboratory humidity and source cleanliness [196, 205]. Both a high laboratory humidity and a dirty source [95] were associated with higher levels of protonated molecular ion. In terms of physical properties, there is a general tendency for the proton affinity to increase and the ionisation energy to decrease with an increasing number of aromatic rings. PAHs are weak gas phase bases, so should be observed as $[M+H]^+$ [80]. In fact, the analysis of high-mass PACs (*m/z* 400-2000, C_{36} and larger) after prior LC separation yielded protonated molecular ions and molecular ions with little fragmentation.

Compounds with more than 100 carbons gave only a protonated molecular ion while those with fewer than 100 carbons gave both $[M+H]^+$ and $M^{+\bullet}$, with a preponderance of molecular ion. Part of the reason for the discrepancy may be enhanced M^{+2} formation with the larger compounds. Given that low-mass PACs have high ionisation energies and low proton affinities, there is more of an energetic driving force for charge exchange, especially in the presence of benzene. The high-mass PACs with their low ionisation energies and high proton affinities, will form high-energy molecular ions on collision with charge exchange species, yielding significant fragmentation. Proton transfer is very energetically favourable, so it is not surprising that high levels of protonation are observed. Regardless of the compound identity, protonation tends to be more sensitive than charge exchange because the energetics are more favourable and this tends to have less interference from other compounds. Alkylation of PAHs was not observed to affect the $[M+H]^+/M^{+\bullet}$ ratio in $APCI^+$ mode but was sufficiently variable in the $APCI^-$ mode to permit isomer discrimination [195].

More recent work by Mansoori [182] casts doubt on the predictive use of proton affinities and ionisation energies to determine $[M+H]^+/M^{+\bullet}$ ratios of PACs. He observed that charge exchange was dominant for PAHs of mass less than 200 Da while those with mass greater than 200 yielded predominantly protonated molecular ion.

7.1.2 Electrospray Ionisation (ESI)

Coupling of non-pneumatically assisted electrospray ionisation to HPLC is more problematic than APCI because of its low flow rate tolerance (1-40μL/min), requiring splitting of the column effluent, and its more rigorous solvent demands (50:50 acetonitrile/water or methanol/water with 1% acetic or formic acids with no buffer salts is

considered ideal [54]). Another limitation is that ionisation is usually more efficient in solution than in the gas phase or within the ESI interface. Its ability to detect very high molecular weight materials by multiple charging has gained it wide acceptance for bioanalytical, biochemical and polymer applications.

Electrospray is most efficient with ions preformed in solution by acid/base chemistry, electrochemistry or adduct formation of small ions to non-ionic compounds. The sample is introduced in a liquid stream into the ESI probe. The application of a high voltage on the ESI capillary will produce a fine mist of electrically charged droplets, which takes on the appearance of a cone, the Taylor cone. The high voltage on the capillary and source heating, if applicable, helps to desolvate the ions, until bare ions are generated, passed through the lenses and detected. A nebuliser gas stream can be used in conjunction with the high voltage on the capillary to assist in droplet production and desolvation.

Low mass compounds tend to form protonated species in positive mode and deprotonated species in negative ion mode [54]. Polycyclic aromatic compounds are not readily ionised in solution, which hampers their detection in electrospray. To overcome this limitation, PACs may be electrochemically converted to radical cations either in solution or prior to detection. One means of doing so is provided by the stainless steel capillary inside an electrospray probe to which a high voltage (2 to 5 keV) can be applied. Van Berkel and Zhou [206] in 1995 suggested that the electrospray ion source is a constant-current device where the size of the current depends on the rate of droplet production (or flow rate). When operated, charge builds up, thereby generating a field that counters the externally applied field and prevents ion migration in the source. To restore charge balance, electrochemical

reactions must occur at the capillary. Thus, the electrospray source becomes an electrochemical device, which may be capable of ionising samples. To enhance this electrochemical reaction, Van Berkel et al [207] infused a chemical electron transfer reagent, 2,3-dichloro-5,6-dicyano-1,4-benzoquinone (DDQ) at 56μM concentration with a 46 μM solution of 2,3-benzanthracene analyte dissolved in 50:50 (v/v) dichloromethane/methanol and obtained a 400 fold increase in the response of the analyte.

In a later paper, it was demonstrated that the choice of solvent was critical to the success of the experiment as it must dissolve the analyte, spray properly and stabilise the radical cations. Combinations of acetonitrile, methanol and/or water with acidic or basic additives are commonly used for ESI because of their solubility properties, their stable sprays, and the ability to ionise analytes by acid/base chemistry. However, the analyte ions once formed in solution must be stabilised to prevent their consumption in nucleophilic reactions with solvents or solvent additives. Dry, non-nucleophilic solvents such as dichloromethane and acetonitrile (though all water cannot be removed) and particularly, trifluoroacetic acid (TFA), appear to stabilise the radical cations. In the latter case, the CF_3 group of TFA interacts with the cation, yielding a radical cation-TFA adduct that is sterically hindered, thus preventing nucleophilic attack. Methanol tends to add to the radical cation but is easier to spray than dichloromethane. When the performance with CH_2Cl_2/MeOH (90:10 (v/v)), in the presence and absence of TFA was compared, the addition of TFA enhanced the electrochemical reaction [208]. This group then showed that the addition of 0.1% SbF_5 to CH_2Cl_2/0.1%TFA was a sensitive and selective means of ionising highly conjugated, aromatic compounds [209]. Xu, Lu and Cole [210] boosted the sensitivity of ESI by

constructing an electrochemical cell in the ESI probe. Upon comparison with other solvents, dichloromethane was observed to stabilise radical cations, sprayed reasonably well and had a wide enough anodic range to permit oxidation of PAHs in the electrochemical cell with the generation of radical cations. The stability of these radical cations was structure-dependent. In fact, the radical cations could be separated into three groups. Group 1 species encompassed anthracene, phenanthrene and pyrene underwent rapid, irreversible reactions with solvents and hence could not be detected. Group 2 species (9,10-dihydroanthracene, perylene and rubrene) produced relatively stable radical cations which could be observed without electrochemical mediation. Group 3 comprised 9-methylanthracene, chrysene and benzo[*a*]pyrene. These species gave radical cations of intermediate stability though only upon electrochemical oxidation. It was suggested that the reactive sites in these radical cations were blocked by their substitution patterns.

Another option is to form charge transfer complexes as was used in the CE separation of PAHs upon complexation with tropylium ion and 2,4,6-triphenylpyrylium ion (TPP) [211]. The results of this study indicated that the larger the PAH, the greater its ability to interact with the cation and the greater was the observed positive charge on the PAH. Triphenylpyrylium ion complexed more efficiently than tropylium ion, resulting in greater selectivity. The explanation of the sterically influenced binding of these cations to PAHs may be the result of electrostatic forces in the cation-π interactions (the greater the accessibility of the electronegative ring centre, the more improved is cation binding) and/or degree of overlap between the PAH and cation (tropylium interacts better with pericondensed than catacondensed structures).

How applicable these techniques are was explored by Anacleto et al. [212] in 1992 and by Moriwaki et al. [213] in 1999. The former showed that the use of DDQ for the analysis of fullerenes in ESI^+ mode was associated with high background and very poor signal-to-noise ratios. The latter group was able to demonstrate 100 μM detection of pyrene, benzo[*a*]pyrene and coronene with complexation to 1 mM tropylium cation in acetonitrile by ESI with prior LC separation of components.

7.2 Optimisation of Electrospray Ionisation (ESI)

Electrospray normally requires the preformation of ions in solution, their nebulisation, desolvation and detection as bare ions. The instrumental parameters which affect these processes include mobile phase flow rate, mobile phase composition, the bath gas and nebuliser gas flow rates (no sheath gas is used), capillary voltage, cone voltage, source temperature and vertical position angle of the probe relative to the skimmer cone. No statistical data is available for these studies.

7.2.1. Effect of Mobile Phase Flow Rate on ESI

The mobile phase flow rate controls the rate of introduction of solvent and sample, and hence the number of ions present in the source. An overabundance of background ions will result in high background, resulting in poor signal-to-noise ratios. High flow rates will also overwhelm the desolvation capabilities of the ESI probe, resulting in poor ion yields. Biphenyl in 99% MeCN + 1% acetic acid was used for optimising the mobile phase flow rate (see Figure 7.1). The optimal flow rate appeared to be 2.5 mL/h, which likely represents the most reliable pumping and best desolvation. This parameter had no impact on the degree of protonation, indicating that most ionising reactions were occurring in solution.

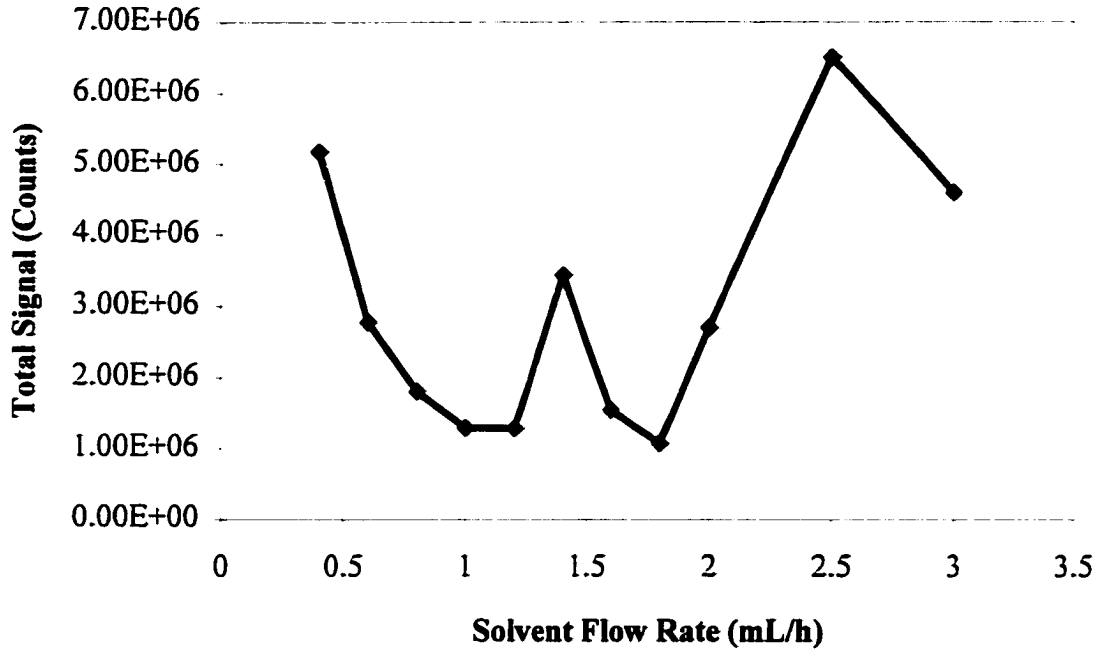

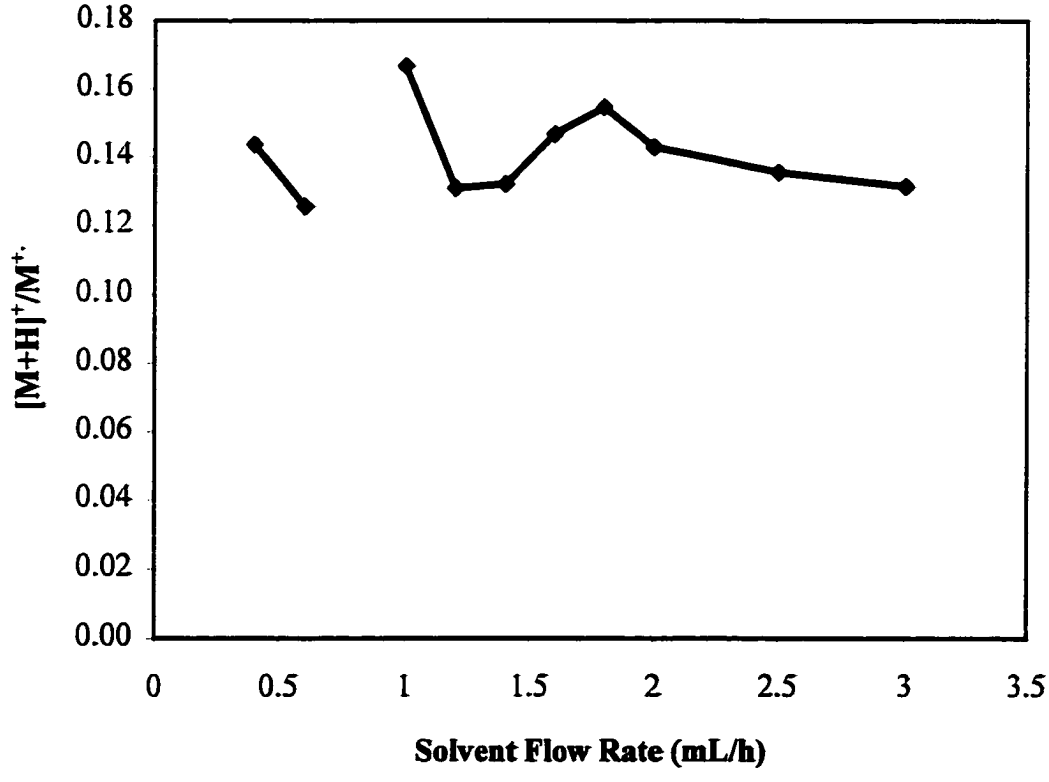

Figure 7.1. Optimisation of the Solvent Flow Rate using biphenylene in 99% acetonitrile + 1 % acetic acid.

7.2.2 Effect of Bath Gas Flow Rate

The purpose of the bath gas is to prevent ion loss through collisions with source walls. The response and $[M+H]^+/M^{+\bullet}$ ratios as a function of bath gas flow rate are plotted in Figure 7.2. These graphs demonstrate that the molecular ion is preferentially formed and that there is no significant impact on the ionisation mechanism of the PAC with changes in the flow rate, consistent with solution phase ionisation and the purpose of the bath gas. A bath gas flow rate of 400 sLph was optimal, indicating that a relatively high gas flow rate is required for proper ion transmission. This value is considerably higher than the Micromass recommendation of 200 sLph and is likely the result of analyte properties or its interaction with the solvent.

7.2.3 Effect of Nebuliser Gas Flow Rate

The nebuliser gas is responsible for assisting the conversion of liquid sample into a fine mist of charged droplets. Ideally, the larger the nebuliser flow rate, the finer will be the droplets, resulting in better ion transmission and hence, response. The results in Figure 7.3 are consistent with this supposition, the response increasing with nebuliser flow rate. The $[M+H]^+/M^{+\bullet}$ ratio is expected to be unaffected by the nebuliser flow but this is clearly not the case. At low nebuliser flow, protonation is quite high and decreases to a minium at 10-20 sLph. At low nebuliser flow, the sample is not efficiently nebulised, resulting in large droplets (high noise) and the formation of cluster ions will be reduced. With higher nebuliser flows, droplets should be smaller, resulting in smaller noise and cluster ions will be discriminated against.

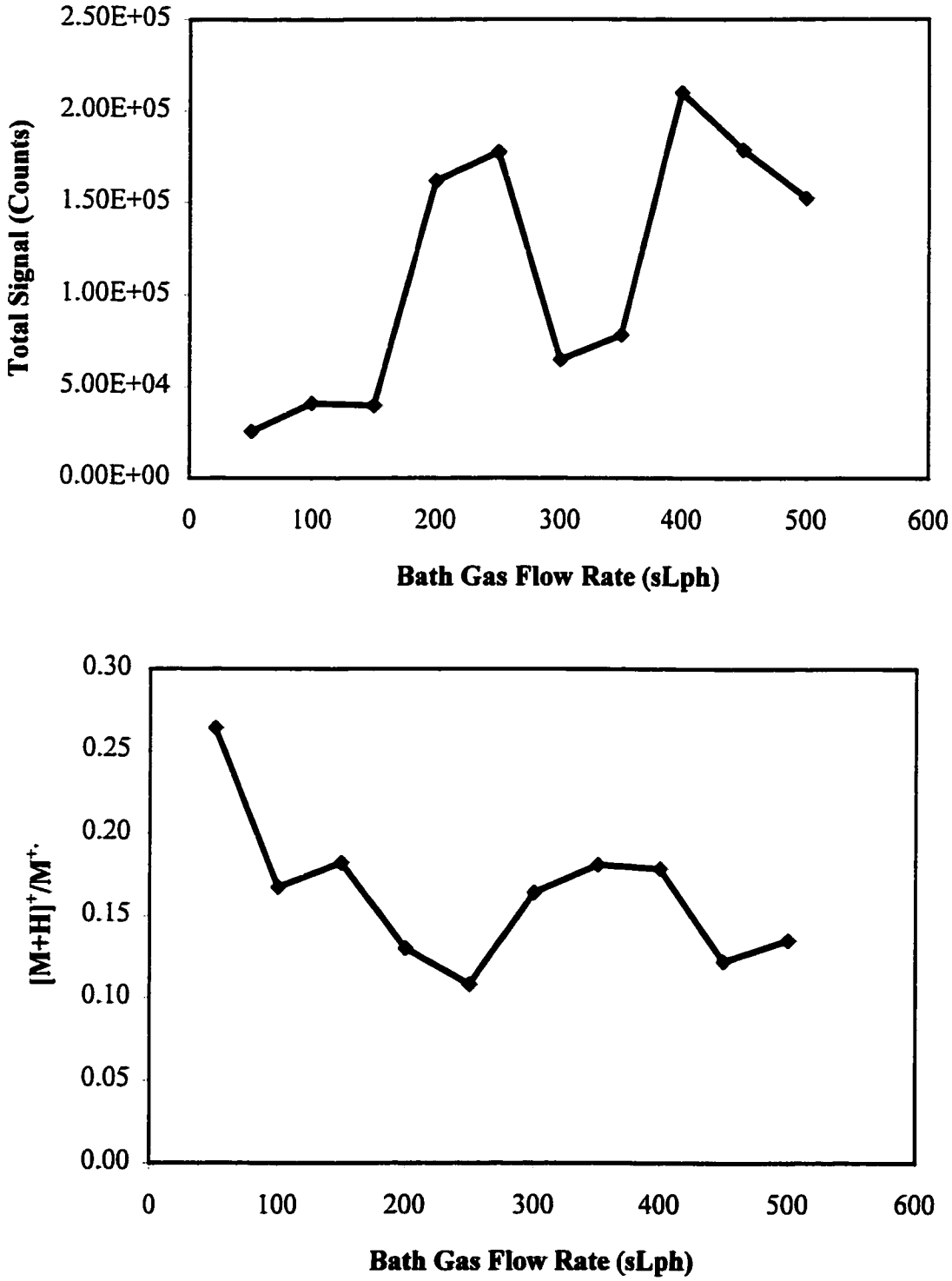

Figure 7.2. Optimisation of Bath Gas Flow Rate for ESI^+ dection of biphenyl in 99% acetonitrile + 1 % acetic acid.

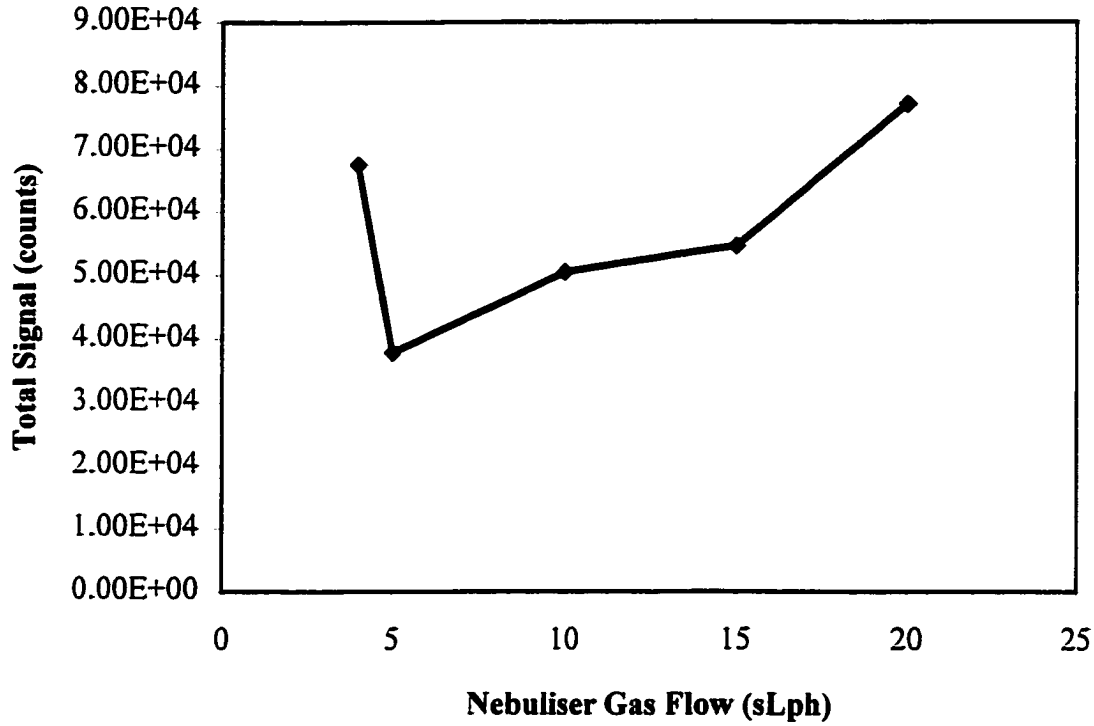

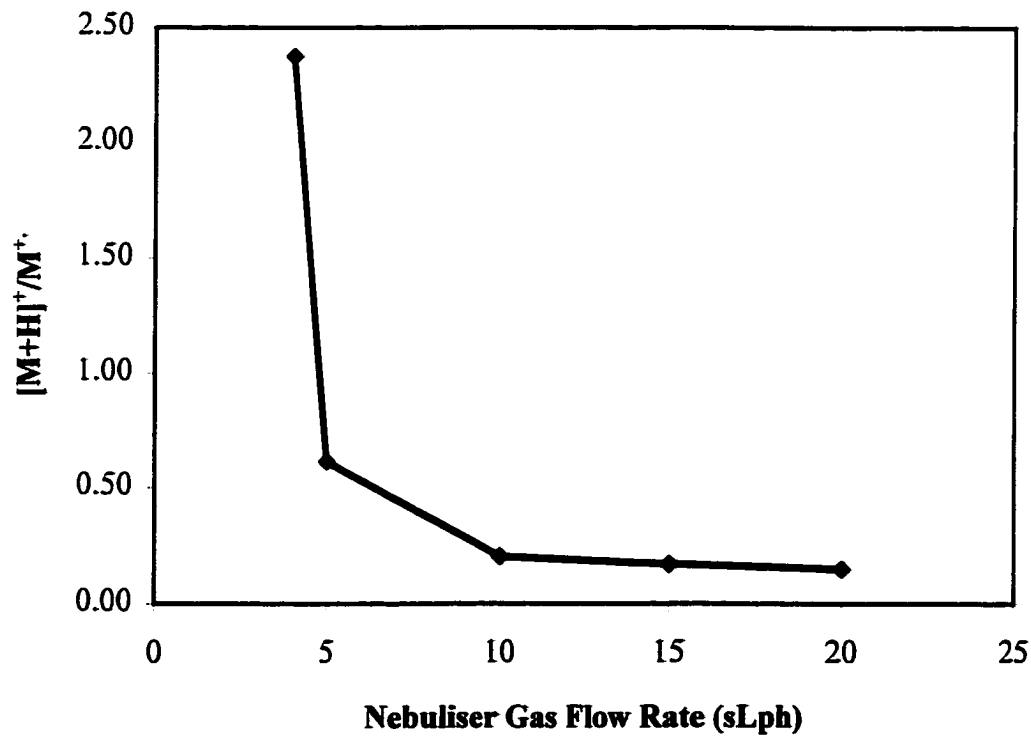

Figure 7.3. Effect of Nebuliser Gas Flow Rate on Total Signal and Ionisation Mechanism of biphenyl in 99 % acetonitrile + 1 % acetic acid in ESI^+ mode.

7.2.4 Effect of Capillary Voltage

The capillary voltage is strongly implicated in the desolvation efficiency of the ESI source and its potential ability to electrochemically ionise the analyte. A high voltage will ensure good desolvation and possibly electrochemical generation of a radical cation species but too high a voltage will initiate sample fragmentation due to the deposition of excess energy and other undesirable side reactions. Figure 7.4 demonstrated that the optimal voltage is 3.5 kV, consistent with the manufacturers guidelines, and that it does not affect the ionisation mechanism, consistent with solution phase ionisation and capillary-mediated radical cation formation.

7.2.5 Effect of Cone Voltage

The cone voltage determines the rate of acceleration of the ions from the source to the analyser and the degree of declustering/fragmentation (see Figure 7.5). At low cone voltages, cluster formation is highly favoured, leading to significant background while at high cone voltages, sample fragmentation is a problem. The optimal cone voltage is likely to be species-dependent but with a solution of biphenyl in 99% acetonitrile + 1 % acetic acid, an optimum cone voltage of 22 V was observed. An increase in cone voltage was associated with an increase in $[M+H]^+/M^{+\bullet}$ which is inconsistent with expectations. This may indicate formation of an isobaric ion which is interfering with the signal for the protonated molecular ion - an increase in deprotonation would be more explicable.

7.2.6 Effect of Source Temperature

The source temperature assists in maintaining species in the gas phase and it must be set high enough to vapourise the solvent and analyte and assist in desolvation. It is, therefore,

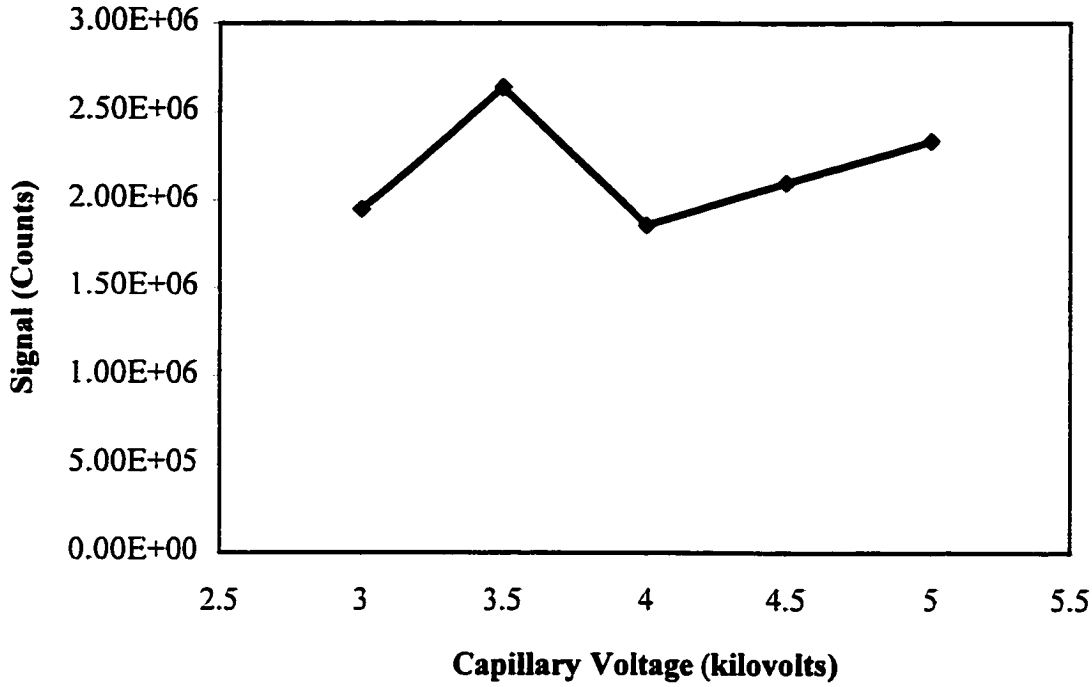

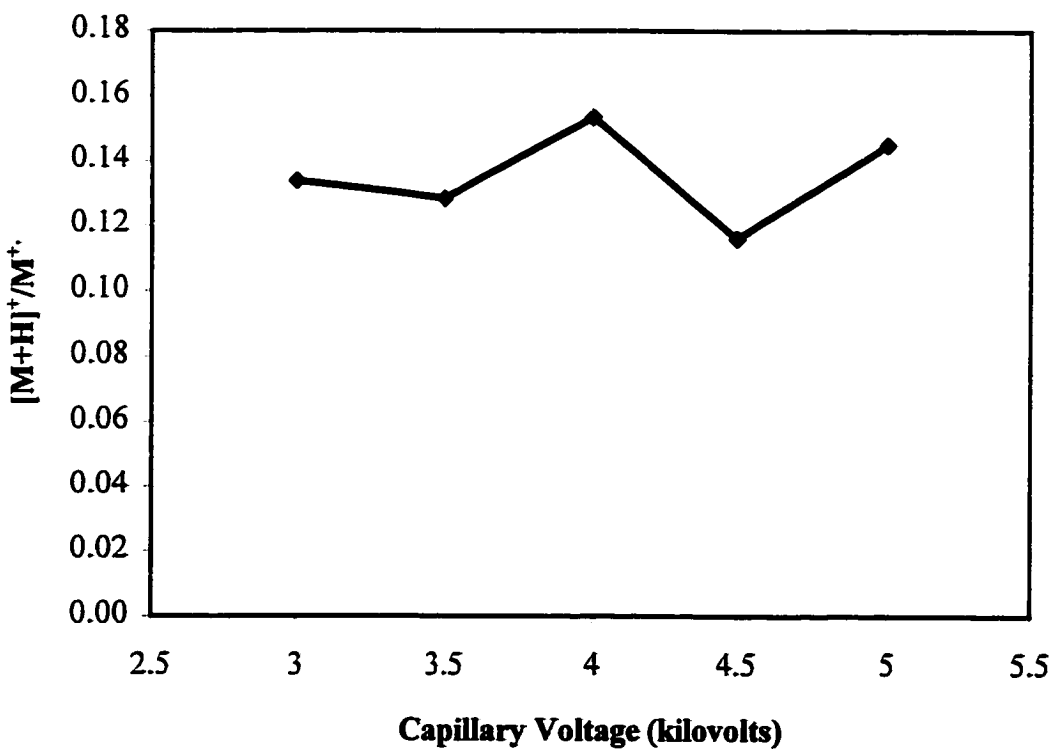

Figure 7.4. Effect of Capillary Voltage on Total Signal and Ionisation Mechanism of biphenyl in 99% acetonitrile + 1% acetic acid in ESI^+ mode.

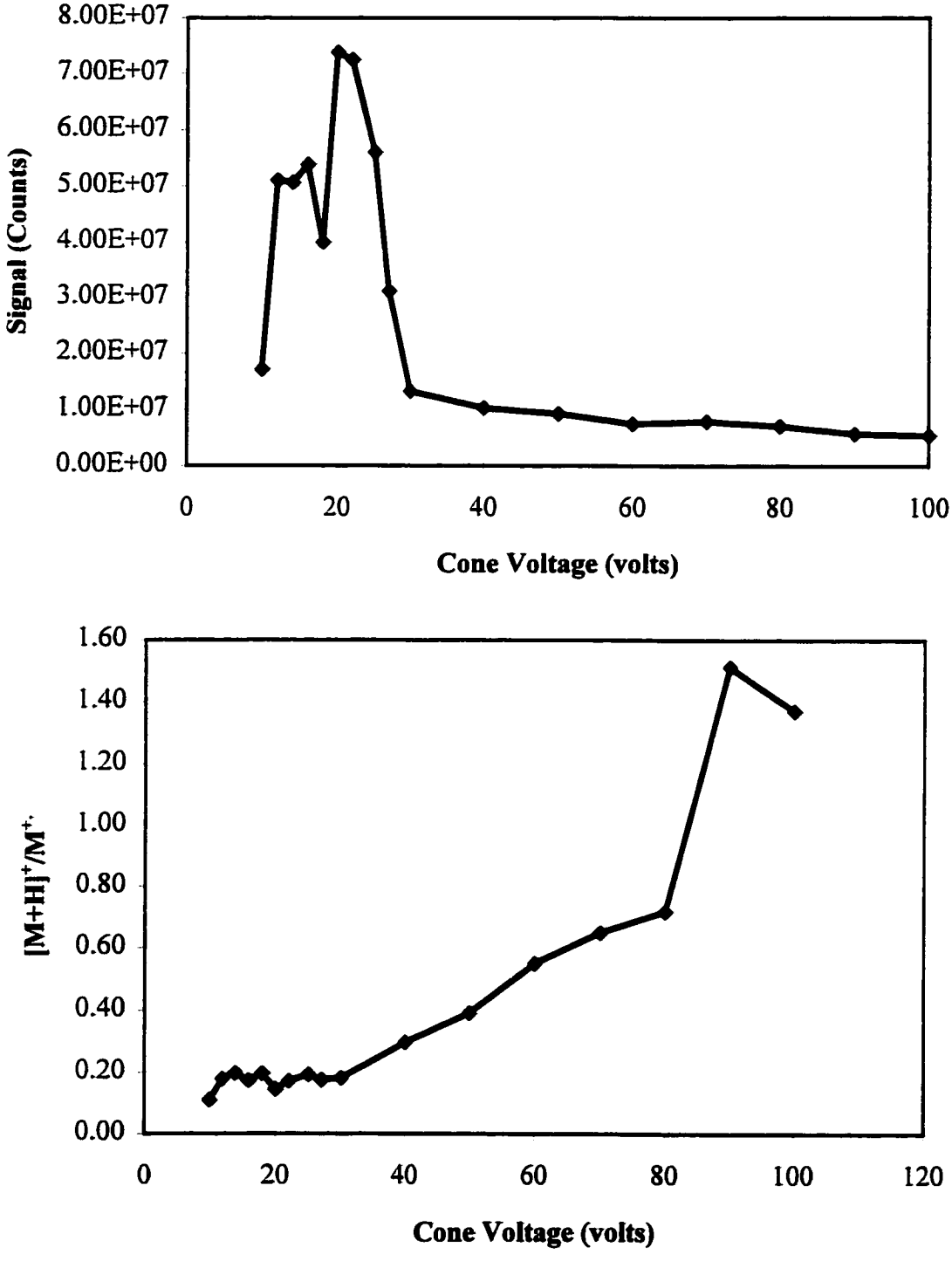

Figure 7.5. Effect of Cone Voltage on the Signal Intensity and Ionisation Mechanism of Biphenyl in 99% acetonitrile + 1 % acetic acid in ESI^+ mode.

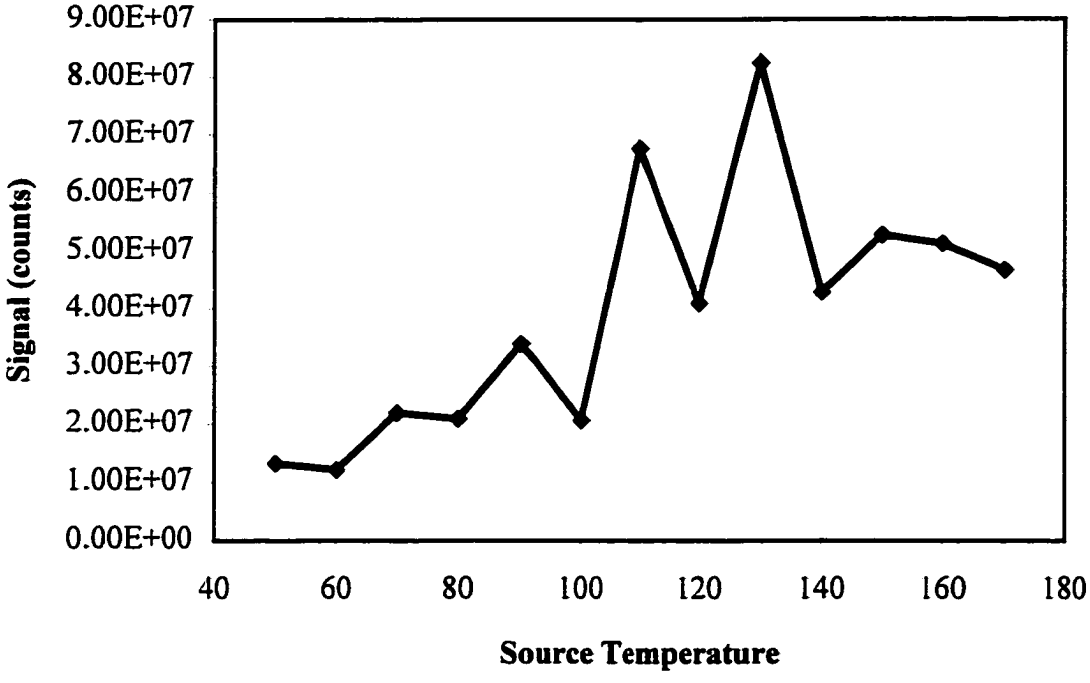

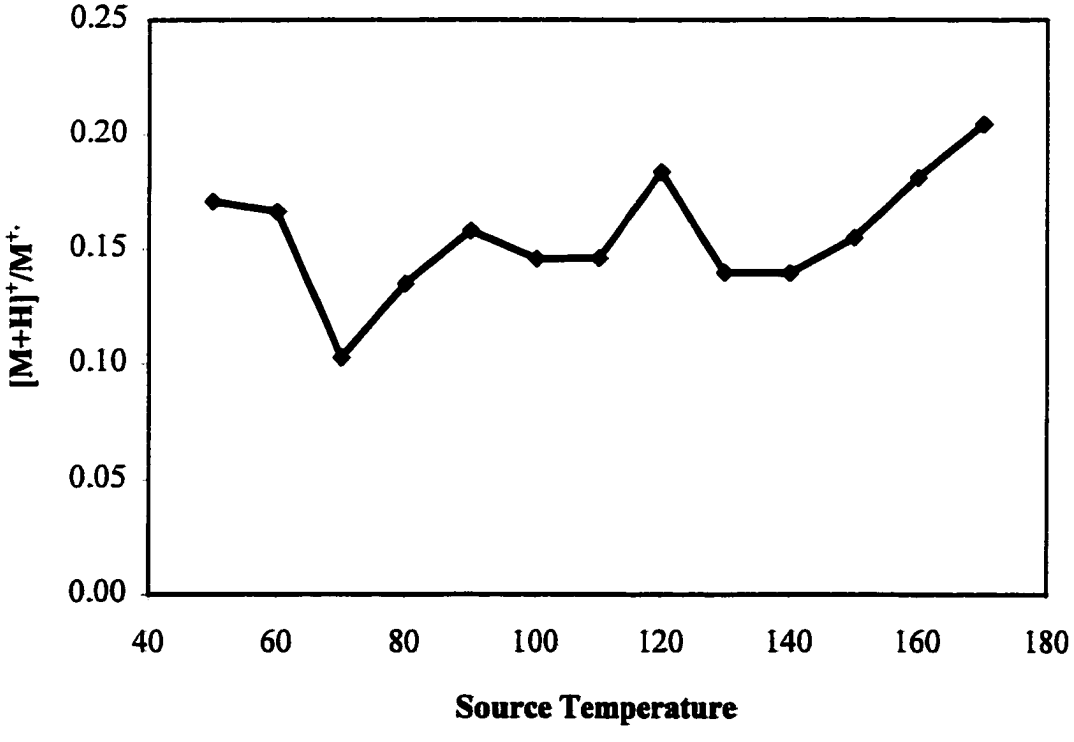

Figure 7.6. Effect of Source Temperature on the Signal Intensity and Ionisation Mechanism of Biphenyl in 99% acetonitrile + 1% acetic acid in ESI^+ mode.

expected to have little effect on the form (protonated molecular ion, molecular ion, deprotonated molecular ion) of the analyte. With acetonitrile-acetic acid, an optimal source temperature was 130°C (far removed from Micromass' recommendation of 65-70°C) and no effect on ion form was noted (see Figure 7.6).

7.2.7 Effect of Probe Position

The probe position was optimised with respect to the vertical position of the probe relative to the skimmer cone. The behaviour was similar to that observed with APCI (data not shown).

7.3 Examination of PACs by ESI^+/ESI^-

7.3.1 ESI^+/ESI^- of PACs by Capillary-mediated Electrochemical Generation

7.3.1.1 ESI^+/ESI^- of PACs with 99% MeCN/1% acetic acid

Individual solutions of benzene, naphthalene, fluorene, phenanthrene, anthracene, 3-ethylphenanthrene, 1-methylpyrene, 1-ethylpyrene, pyrene and chrysene were prepared in 99% MeCN/1% acetic acid (defined as ES-1 standard). With the solvent as the mobile phase, the following MS conditions were set: capillary V= 4.00 kV, cone voltage = 30 V, source T = 80°C, scan range : *m/z* 70-250 in 2.90 seconds. Thirty scans of background were acquired, 10 μL of the sample was injected via a Rheodyne valve and data acquisition continued for 50 scans. All analytes were tested in both ESI^+ and ESI^- mode. Table 7.1 presents the results obtained. The results indicate that the signal intensity for the radical cations of all PACs is quite low, indicating that the electrochemical oxidation of PACs is quite inefficient. Surprisingly, despite being classified as Group 1 ions, phenanthrene and pyrene were observed. The acetic acid may be stabilising these species in a manner similar

Table 7.1. ESI^+/ESI^- of PACs in 99% MeCN-1% acetic acid

Compound	ESI^+ Signal	ESI^- Signal
Naphthalene	not detected	not detected
Fluorene	not detected	not detected
Anthracene	3.2e5	not detected
Phenanthrene	1.1e5	1.7e4
3-ethylphenanthrene	2.9e5	not detected
Pyrene	3.9e3	2.5e4
1-methylpyrene	8.1e4	not detected
1-ethylpyrene	5.6e3	1.1e3
chrysene	8.4e4	not detected

to TFA. In fact, the best yields were obtained with anthracene and 3-ethylphenanthrene. In this case, the alkyl substituents on phenanthrene and pyrene seem to enhance the electrochemical reaction, rather than blocking it as the literature holds [210]. Perhaps, they are stabilising the radical cation, permitting detection of these compounds. Clearly, the positive mode is more useful than the negative ion mode, as would be expected since it should be easier to oxidise than to reduce PACs.

7.3.1.2 ESI^+/ESI^- of PACs with MeCN/acetic acid and MeCN/ethylamine

Using ES-1 standard, the electrospray response of biphenyl, biphenylene, 9,10-dihydroanthracene, and 9,10-dihydrophenanthrene was studied in both positive and negative mode. Acetic acid should enhance the formation of ions in the positive mode while the base should enhance negative ion formation. The results, presented in Table 7.2, indicate that 1) PAHs are more readily oxidised than they are reduced, 2) the addition of acetic acid greatly

enhances signal strength and 3) the addition of ethylamine was not helpful. The lack of response for 9,10-dihydroanthracene relative to 9,10-dihydrophenanthrene in the presence of acetic acid provides a means of isomer discrimination.

Table 7.2. ESI^+/ESI^- Response with MeCN, MeCN/1% acid and MeCN/1% base

	$ESI^+ (M^{+\bullet})$		$ESI^- (M^{-\bullet})$
Compound	**MeCN**	**MeCN + acid**	**MeCN + base**
Biphenyl	3.7e4	5.9e5	not detected
Biphenylene	1.5e5	1.7e6	not detected
9,10-dihydroanthracene	7.0e4	not detected	not detected
9,10-dihydrophenanthrene	5.2e4	4.8e5	not detected

7.3.1.3 ESI^+/ESI^- of PACs with dichloromethane – hexanes (1:4)

The same standards and electrospray conditions as above were used to observe the response of PACs in dichloromethane– hexanes (1:4). The results presented in Table 7.3 indicate that this solvent choice is inappropriate for negative ion mode electrospray analysis of PACs. It is applicable to a narrower range of compounds than the acetonitrile-acetic acid combination. As noted previously, it is difficult to observe pyrene by this means but there appears to be sufficient energy to permit detection of naphthalene and benzene, which was not possible with the acetonitrile-acetic acid mix. Therefore, as mentioned in the introduction, the choice of solvent is critical to experimental success and needs to be made for the particular samples of interest.

Table 7.3 ESI+/ESI- Response of PACs in 20%dichloromethane-80%hexanes

Compound	ESI+ Response	ESI- Response
benzene	1.6e5	not detected
naphthalene	1.4e5	not detected
biphenyl	not detected	not detected
fluorene	8.3e5	7.1e3
phenanthrene	6.2e5	not detected
2-ethylphenanthrene	4.8e4	not detected
1-methylpyrene	not detected	not detected
pyrene	not detected	not detected

7.4 Comparison of ESI^+ and $APCI^+$

A solution of 1 mM biphenylene (representative of the mono- and diaromatic compounds which are difficult to introduce via liquid introduction) was prepared in acetonitrile and in acetonitrile + 1% acetic acid. These solutions were then analysed in both ESI^+ and $APCI^+$ modes. Table 7.4 presents the total signal intensity (sum of the signals due to protonated molecular ion and molecular ion) as a function of ion mode and solvent.

Table 7.4. Comparison of $APCI^+$ and ESI^+ for the Signal for Biphenylene

Solvent	Mode	Total Signal
MeCN	ESI^+	4.8e6
MeCN + acetic acid	ESI^+	2.9e7
MeCN	$APCI^+$	1.6e6
MeCN + acetic acid	$APCI^+$	4.0e6

Galceran and Moyano [192] had shown that both ESI and APCI could be successfully employed for the analysis of hydroxy-PACs with comparable sensitivity. This work indicates

that both of these methods can also be used for PAH analysis. Electrospray was shown to be more efficient with the addition of acetic acid, which is consistent with the work of Van Berkel [208], was more sensitive than APCI, more variable, and more difficult to use as the probe plugged easily when not subjected to thorough rinsing with pure solvent. The signal enhancement, when coupled to HPLC, is unlikely to be beneficial as the whole column effluent can be introduced into an APCI source but a 99:1 split is required with electrospray. The addition of acetic acid was also beneficial. Acetic acid is likely to be a better gas phase acid than acetonitrile so it should enhance proton transfer, as was observed.

7.5. Chemical Electron Transfer Reagents for ESI Analysis of PACs

2,3-Dichloro-5,6-dicyano-1,4-benzoquinone (DDQ) was first used to gauge the potential of using a chemical electron transfer reagent in conjunction with a triple quadrupole rather than an ion trap mass spectrometer, as had been used in the literature method [206 - 210] to enhance the signal strength of PACs and to determine whether it could be successfully applied to other PAHs (e.g. naphthalene, phenanthrene, pyrene and perylene).

7.5.1 Effect of Solvent

The first step consisted of using a 50 fold dilution of ES-2 to probe the applicability of DDQ to PAC oxidation and subsequent analysis by electrospray. Among the solvents tested were 70:30 (v/v) hexanes-dichloromethane, dichloromethane, dichloromethane+0.1% (by volume) trifluoroacetic acid (TFA) and 50:50 (v/v) dichloromethane/methanol. Table 7.5 presents the observed signal enhancement (in counts) for 2,3-benzanthracene ($M^{+\bullet}$) with each of these solvents as a ratio of the signal in the presence of the electron transfer reagent to the signal in the absence of electron transfer reagent.

Table 7.5. Observed Signal Enhancement of 2,3-benzanthracene with DDQ as a function of solvent

Solvent	Ratio of signal (PAC + DDQ/PAC)
70:30 (v/v) hexanes-dichloromethane	117
dichloromethane	139
dichloromethane + 0.1% TFA	240
50:50 (v/v) dichloromethane/methanol	47

It is clear from these results that the addition of methanol and less so, hexanes, to dichloromethane results in decreased electron transfer efficiency or reduced stability of the radical cation. The latter is likely with a nucleophilic solvent like methanol. The addition of trifluoroacetic acid almost doubled the signal intensity, showing that this compound is indeed associated with greater electrochemical efficiency and stabilisation of the radical cation, as observed in the literature [207 - 208]. It should be noted that this signal enhancement is almost two orders of magnitude better than that obtained with similar concentrations in the literature [206].

7.5.2 Effect of Source Gas

This is an area which has not been addressed by anyone to the knowledge of the author, likely because prior experiments were performed in ion trap instruments where helium is typically used. In a triple quadrupole instrument, it is more common to use nitrogen or air . Infusion experiments where the PAH solution was continuously introduced into the mass spectrometer source were observed to be more successful when air was used as the bath and nebuliser gas than when nitrogen was used (data not shown). In fact, the use of nitrogen results in the inability to observe ions and automatic shutdown of the machine in the middle

of data acquisition; an explanation for this phenomenon is not apparent. When air was used, a steady stream of ions was observed, likely the result of oxygen acting as an electron scavenger and thereby assisting in the abstraction of electrons from the PACs.

7.5.3 Preliminary Evaluation of Chemical Electron Transfer Reagents

Preliminary comparison of the chemical electron transfer reagents was carried out with a 1/50 dilution of ES-2 standard, and the following available electrochemically active species: DDQ, Chloranil, (2,4,7-trinitro-9-fluorenylidene)malonitrile (TNFM), tetracyano-ethylene (TCE), 7,7,8,8-tetracyanoquinodimethane (TCQ), 2,4,7-trinitro-9-fluorenone (TNF) and 6,7-dichloro-1,4-dihydroxyanthraquinone (DDAQ). As presented in section 7.1.1., these species form complexes with PACs which may be identified by characteristic isotope clusters due to chlorine substitution and/or by the mass of the observed ions will be the sum of the masses of the electron acceptor and the PAH. Table 7.6 indicates which electron acceptors and donors were observed to form complexes.

Table 7.6. Tendency of PAHs to form Complexes with Chemical Electron Transfer Reagents (CETRs)

CETR	Naph-thalene	Phenan-threne	Pyrene	2,3-benz-anthracene	Perylene
DDQ	yes	yes	yes	yes	no
Chloranil	yes	yes	no	yes	no
TNFM	yes	yes	yes	yes	yes
TCE	yes	yes	yes	yes	yes
TCQ	yes	yes	no	yes	yes
TNF	yes	yes	yes	yes	yes
DDAQ	yes	yes	yes	yes	yes

An examination of the data indicates that almost all of the CETRs form complexes with the PACs. It is therefore to be expected that all will show a signal enhancement of the PAC. The experimental results, as presented in Table 7.7, indicate that complex formation may be a prerequisite for ionisation but the observation of these complexes does not appear to be positively or negatively correlated with enhanced signal strength. Chloranil, DDQ and DDAQ were the best choices for enhancing signal through electron transfer. Chloranil and DDAQ were observed to be the most versatile of the electron transfer reagents, giving strong enhancement for all species. The lower results obtained this time as opposed to earlier

Table 7.7. Signal Enhancement (ratio of signal intensity in the presence and absence of electron transfer reagent) of PAHs with Chemical Electron Transfer Reagents

CETR	Naph-thalene	Phenan-threne	Pyrene	2,3-benz-anthracene	Perylene
DDQ	2.0	6.0	6.4	0.60	3.5
Chloranil	4.8	5.4	4.8	3.8	7.8
TNFM	4.2	5.6	2.3	2.6	5.4
TCE	3.4	2.6	1.9	3.7	3.0
TCQ	1.3	1.3	5.0	1.0	1.4
TNF	1.6	8.2	2.6	1.4	3.7
DDAQ	10.0	5.8	11	7.2	9.4

experiments can be explained on the basis of dichloromethane degradation, leading to the background and possibly, sample degradation. To counter this problem, all samples and standards were prepared in freshly distilled dichloromethane and used within the day. Among the PACs studied, phenanthrene and pyrene, as Group 1 [210] compounds, were not expected

to give any signal, yet clearly that was not the case, indicating that detection was made before the ions were able to react or that the radical cation was being stabilised. Perylene, a stable radical cation of Group 2 [210], is expected to dominate the other species, as was observed. The grouping of the other standard mixture components was not done.

7.5.4 Comparison of Chemical Electron Transfer Reagents and Phenyl-Stabilised Cations

The preliminary studies indicated that DDQ, Chloranil and DDAQ (especially with pyrene) were the best chemical electron transfer reagents. Triphenylcarbenium tetrafluoroborate (TPC), 2,3,5-triphenyl-*2H*-tetrazolium chloride (TTZ) and 2,4,6-triphenylpyrylium tetrafluoroborate (TPP) are phenyl-stabilised cations (PSCs). These were then evaluated and compared for the signal enhancement of naphthalene, phenanthrene, pyrene, 2,3-benzanthracene and perylene by forming a stable cationic adduct with PACs. These PAHs were examined individually rather than as a mixture to remove the possibility of interfering peaks or competition among species for available electrons.

The results of these studies are presented in Figure 7.7 (where the data were normalised to a constant concentration of PAH and CETR or PC) and Table 7.8, complex or adduct formation being detected by an examination of isotope clusters and a *m/z* corresponding to the sum of the mass of the chemical electron transfer reagent and the PAH. Despite the success of complexing 2,4,6-triphenylpyrylium tetrafluoroborate with PACs in capillary electrophoretic separation, it did not seem to form an adduct with the PACs and was in fact associated with a dramatic suppression of radical cation formation, especially in the case of naphthalene. The most likely explanation for this behaviour is that the TPP is acting

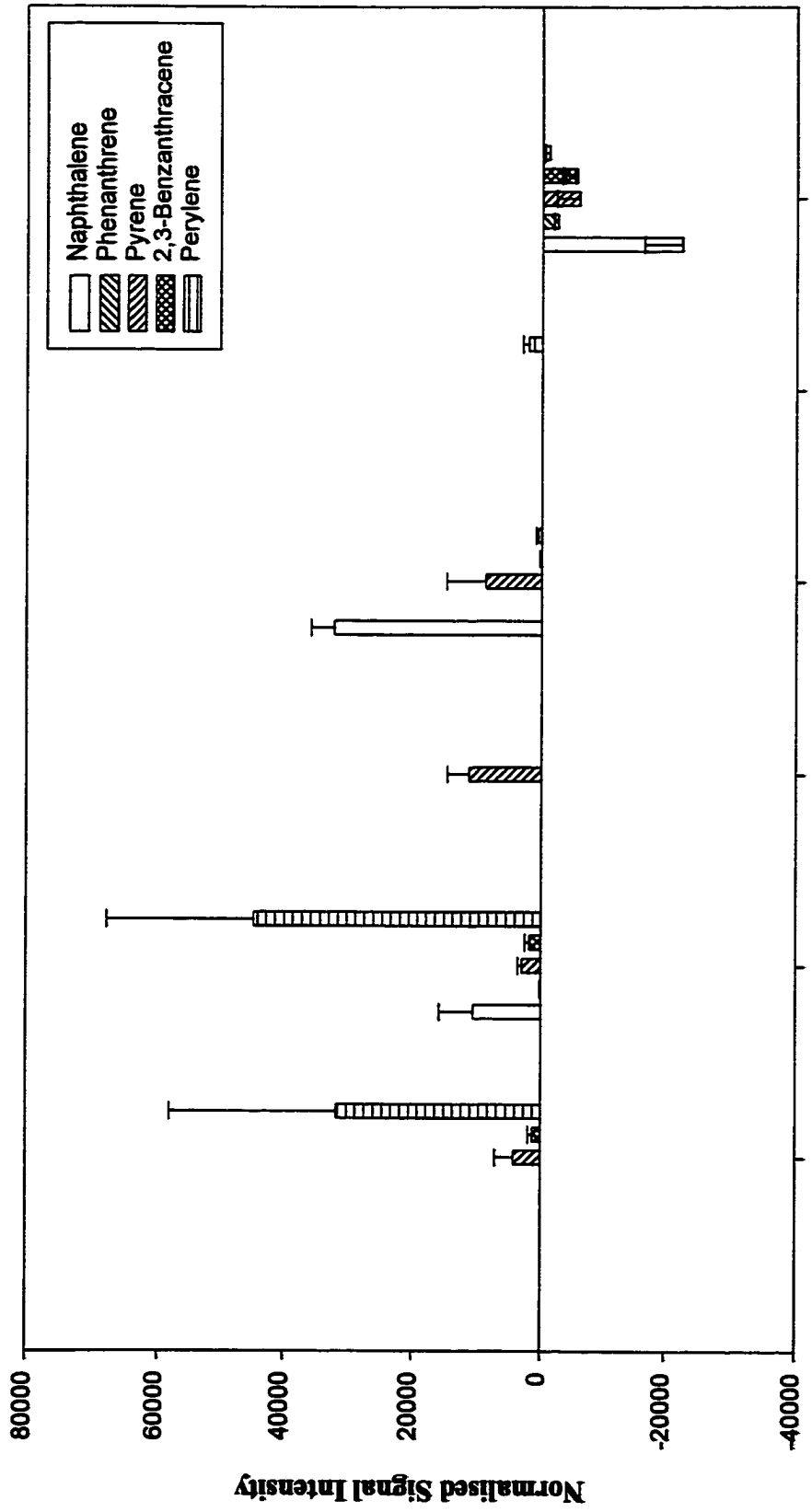

Figure 7.7. Normalised Signal Intensity for 0.020 mM solutions of PAHs (flow=1.8 mL/h) and 0.0155 mM chemical electron transfer reagent or phenyl-stabilised cation solution (flow = 4.1 mL/h).

to destabilise radical cations or is reacting with oxygen in the source, thus preventing the ionisation of PACs. TPC exhibits a tendency to complex only with naphthalene, the smallest ring system studied. TTZ demonstrated complex formation with all PACs, except 2,3-benzanthracene.

However, like in other cases, complex formation was not correlated with signal enhancement. This was the only species associated with a significant enhancement of the naphthalene signal. DDAQ is a three ring compound and should therefore exhibit steric and electrostatic barriers to complex formation, but phenanthrene did not form a complex and only the pyrene signal was enhanced. Chloranil and DDQ with no aromatic rings tended not to form complexes, yet were observed to enhance signal strength. Hence, complex formation is not positively or negatively correlated to signal enhancement.

Table 7.8. Complex Formation of PAHs with Chemical Electron Transfer Reagents

CETR	Naph-thalene	Phenan-threne	Pyrene	2,3-benz-anthracene	Perylene
DDQ	N	Y	Y	N	N
Chloranil	N	N	N	N	N
DDAQ	Y	N	Y	Y	Y
TTZ	Y	Y	Y	N	Y
TPC	Y	N	N	N	N
TPP	N	N	N	N	N

Miller *et al.* [211] suggest that pericondensed structures should complex better than catacondensed structures. This accounts for the low signal enhancement observed with phenanthrene but does not fully account for differences amongst catacondensed PACs or

differing reactivities to CETRs. A possible explanation may be related to the electron affinities of the acceptors and the electron donating capacities of species involved. The ionisation energies and electron affinities of the species studied are presented in Table 7.9. Thus, in order of increasing IE are perylene, pyrene, 2,3-benzanthracene, phenanthrene and naphthalene. Thus, it would be expected that signal enhancement would decrease in the same order. This explains some but not all of the experimental results. In terms of the CETRs, chloranil with its four chlorine substituents should have the highest electron affinity and thus, the greatest enhancements, which agrees with the experimental results. DDQ with only two chlorine substituents is likely to be a poorer electron acceptor than chloranil but better than the other species which lack chlorines or they are removed from the quinone portion of the molecule, as borne out by the experimental results. The strong enhancement of pyrene with

Table 7.9. Ionisation Energies and Electron Affinities of the Species Involved [201, 214 - 219]

Compound	Ionisation Energy (eV)	Electron Affinity (eV)
Naphthalene	8.575	-0.1908
Phenanthrene	8.479	< 0.269
Pyrene	8.029	0.500
2,3-benzanthracene	8.111	1.067
perylene	7.846	0.350
DDQ	10.58	not available
Chloranil	9.74	2.775
DDAQ	not available	not available
TTZ	not available	not available
TPC	not available	not available

DDAQ cannot be explained by reference to electron affinities or ionisation potentials. This is most likely the result of a very efficient complex formation and electron transfer.

All of these results with chloranil in particular offer a ten to one hundred fold improvement over the work of Van Berkel and Moriwaki [206, 213].

7.6 Discrimination Amongst Alkylated PACs

7.6.1 LC/APCI-MS Analysis of Alkylated PACs

An examination of naphthalene and some of its methyl, ethyl, dimethyl, propyl and butyl derivatives was undertaken in APCI$^+$. The methyl, ethyl or dimethyl, propyl and butyl derivates could be distinguished from the parent PAH by their *m/z* values, because all species gave a strong $[M-H]^+$ ion. However, isomer discrimination for compounds with the same mass was not possible. Therefore, prior isomer-selective chromatographic separation is required.

Benzene and representative mono-, di-, tri-, tetra-, penta- and hexamethyl derivatives were then evaluated to determine whether they could be distinguished and what effect substitution pattern had on mass spectral response. The results, presented in Table 7.10, indicate that APCI -MS may, in some cases, be useful in distinguishing among these species of different mass.

The softness of APCI ionisation makes it possible to observe molecular ions of even highly substituted species. Thus, species with different numbers of alkyl substituents can be readily distinguished. However, it has not been possible to distinguish among isobaric species. A solution to this problem is to resolve these isomers chromatographically before introduction into the mass spectrometer. Figures 7.8 through 7.11 depict representative LC/APCI-MS

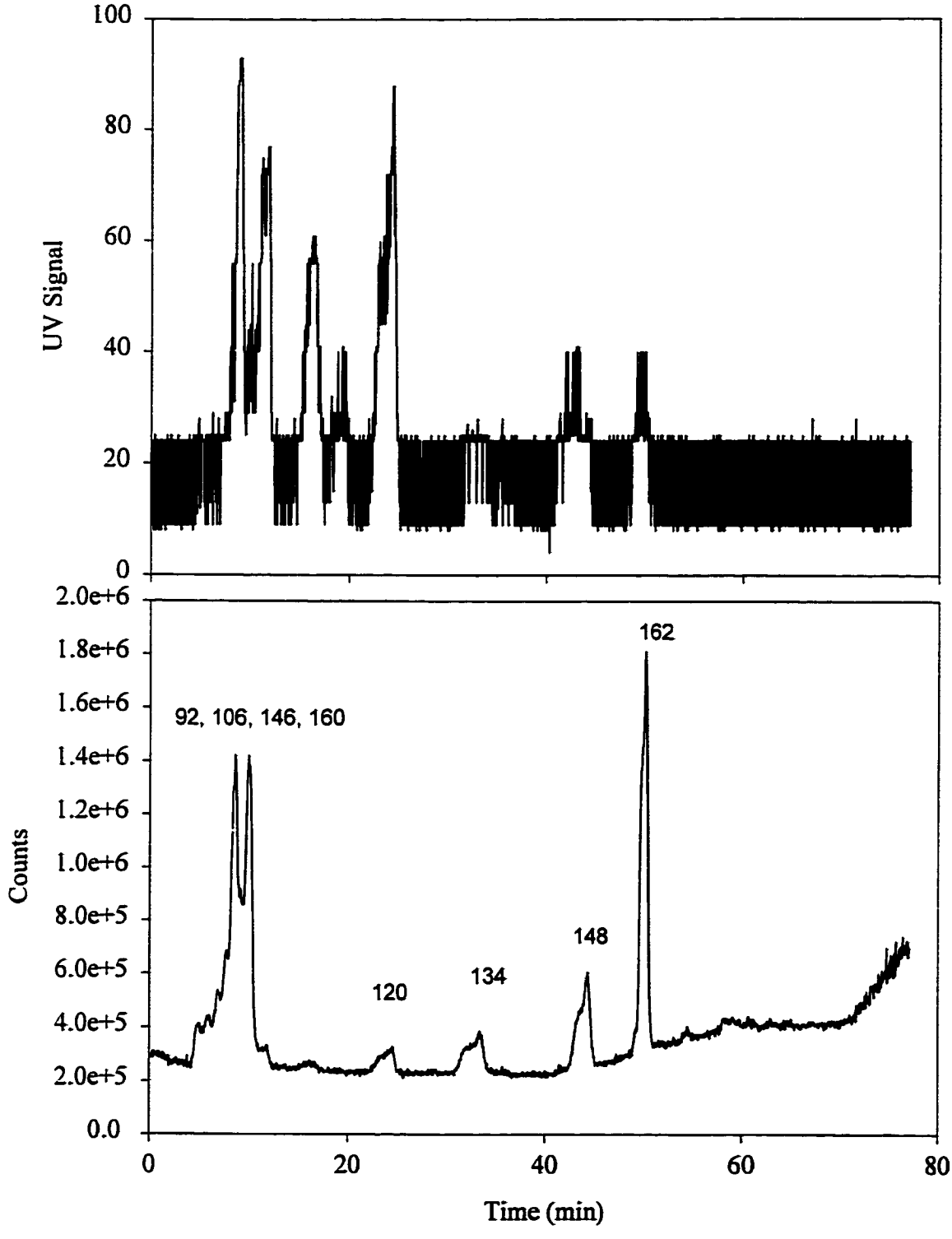

Figure 7.8. UV trace (upper) and APCI-MS trace (lower) of AB-1 eleven component standard mix in acetonitrile separated by gradient, reversed phase chromatoraphy via gradient 503010030 (50:50 (v/v) acetonitrile/water for 30 minutes, linear increase to 100% acetonitrile over following 30 minutes).

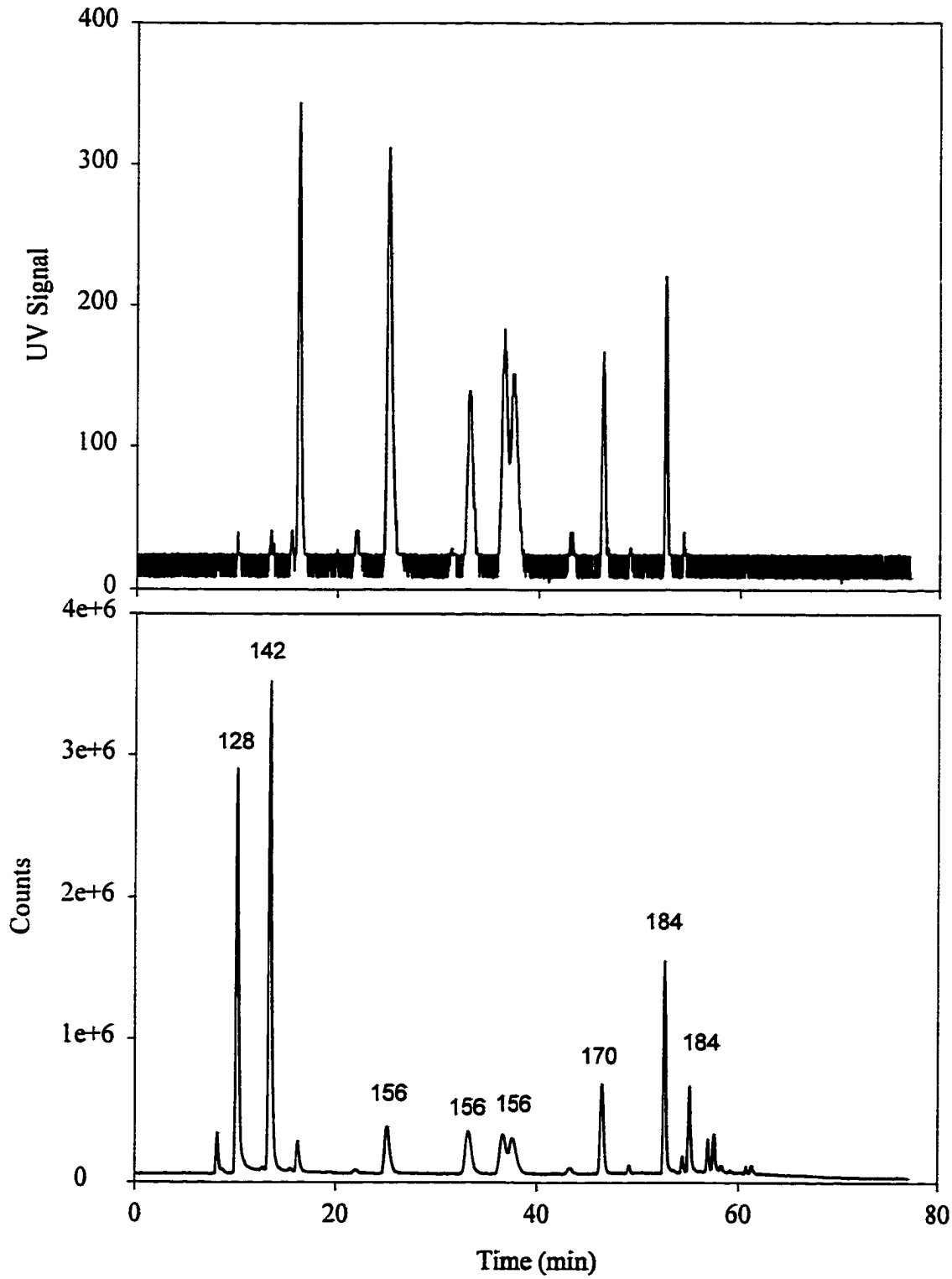

Figure 7.9. UV trace (upper) and APCI-MS trace (lower) of N-1 standard mix in acetonitrile separated by gradient, reversed phase chromatoraphy via gradient 503010030 (50:50 (v/v) acetonitrile-water for 30 minutes, linear increase to 100% acetonitrile over following 30 minutes).

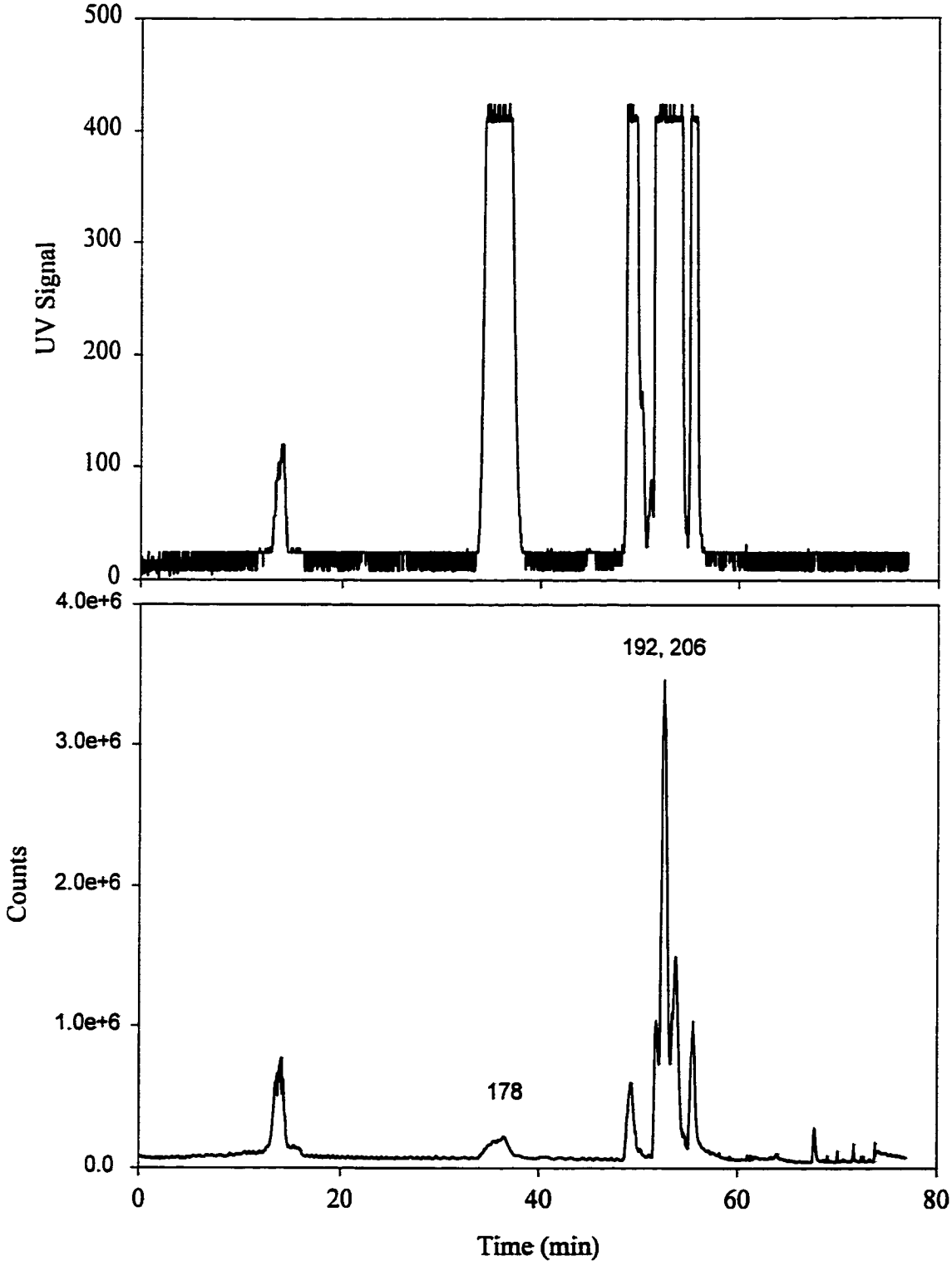

Figure 7.10. UV trace (upper) and APCI-MS trace (lower) of P-1 standard mix in acetonitrile separated by gradient, reversed phase chromatoraphy via gradient 503010030 (50:50 (v/v) acetonitrile-water for 30 minutes, linear increase to 100% acetonitrile over following 30 minutes).

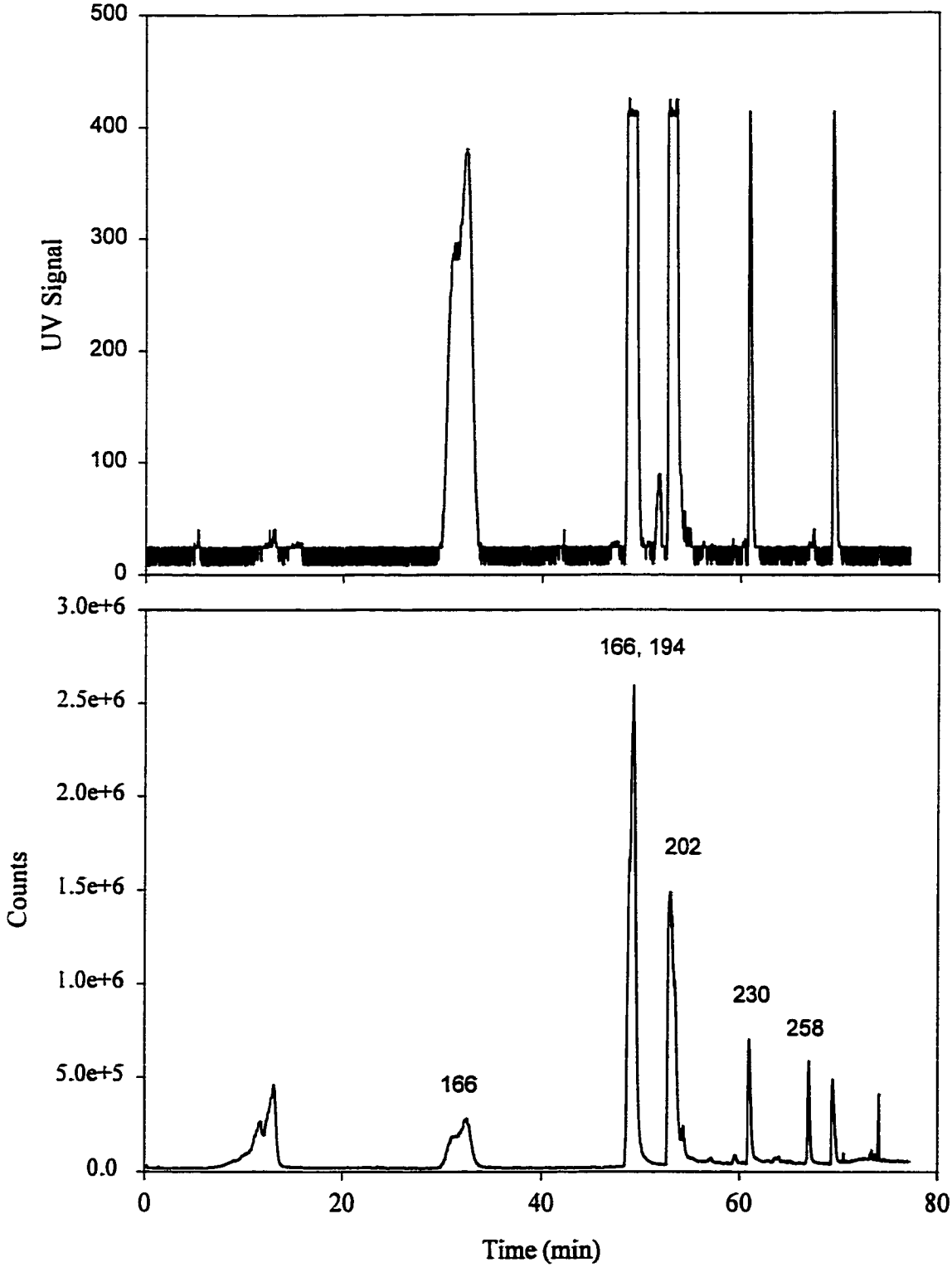

Figure 7.11. UV trace (upper) and APCI-MS trace (lower) of PF-1 six component standard mix in acetonitrile separated by gradient, reversed phase chromatoraphy via gradient 503010030 (50:50 (v/v) acetonitrile/water for 30 minutes, linear increase to 100% acetonitrile over following 30 minutes).

Table 7.10. Effect of Substitution on Observed APCI Response

# of Methyl Substituents	Response
0	3.8e4
1	2.4e4
2	3.9e4
3	5.5e4
4	2.3e5
5	1.6e5
6	8.8e4

chromatograms of standards, AB-1, N-1, P-1, and PF-1, respectively. The AB-1 fraction contains 11 compounds, mainly alkylated benzenes, but only 6 major peaks are observed. There is co-elution of compounds and much lower amounts of the tetra-, penta- and hexamethyl benzene, eluting as the last three peaks elute in the acetonitrile-rich portion of the gradient where the background is lower, explaining their relatively high signal strength. The compounds elute in the order: benzene, toluene, xylenes, mesitylene and 4-ethyltoluene co-eluting, the methyl tetralins co-eluting, 5,7-dimethyltetralin, 1,2,3,5-teramethylbenzene, pentamethylbenzene and hexamethylbenzene.

The N-1 sample contains 9 compounds, mostly alkylated naphthalenes, yet more than that number of peaks is observed. The order of elution, as expected, was naphthalene, tetralin, 2-methylnaphthalene, ethyl and dimethyl naphthalene, propyl and butylnaphthalene This indicates the presence of impurities or breakdown products.

The P-1 standard contains 6 compounds, mainly derivatives of phenanthrene, which elute as the parent, methyl, dimethyl and ethyl derivatives, yielding 6 reasonably well-resolved peaks. The peak in the earlier portion of the chromatogram is likely an impurity.

The PF mix contains 6 components, mainly pyrene and fluorene derivatives, which are clearly resolved in the chromatogram with the sequential elution of fluorene, ethylfluorenes, pyrene, 1-ethylpyrene and 9,10-dihydrobenzo[*a*]pyrene.

From these chromatograms, it is clear that the detection of chemical species in the high organic portion of the gradient is much easier than that in the high water portion, consistent with the results presented in Chapter 5. Alkylbenzenes and naphthalenes prefer a high water content in the mobile phase, putting them in a region of poor signal-to-noise. These volatile compounds are likely to be more amenable to GC/MS analysis. The phenanthrenes, pyrenes and fluorenes prefer a more organic-rich mobile phase and are thus more amenable to detection. Structural isomers cannot be distinguished by mass and can only be analysed after prior chromatographic separation, if possible.

7.6.2 Discrimination among Alkylated PACS by ESI$^+$

The effect of the number and position of substituents on PAHs on their ability to undergo electron transfer was evaluated for naphthalene and pyrene derivatives.

In the case of the naphthalenes, the parent and selected alkyl derivatives were evaluated with DDQ and chloranil. A plot of the normalised signal intensity as a function of naphthalene derivative for the two chemical electron transfer reagents is presented in Figure 7.12. A number of observations can be made. Species of different masses could be clearly distinguished by their mass even in the presence of chemical electron transfer reagents.

Isomers could not be distinguished by mass but there were observable differences in their behaviour with the two chemical electron transfer reagents. The less stable of the two isomers of methylnaphthalene, 1-methylnaphthalene, was unreactive to both DDQ and chloranil while the 2-methyl derivative was reactive to DDQ but not Chloranil. Therefore to distinguish 1- and 2-methyl naphthalene in a chromatographic separation, for example, it would be necessary to run two analyses, one with no CETR and one with a stream of DDQ. Only the 2-methyl derivative would show signal enhancement with DDQ, permitting discrimination from 1 -methyl. It is also possible that the position of the methyl group mediates the ability to form complexes. In the case of the dimethyls, 2,6, 2,7-, 1,7- and 1,8-dimethylnaphthalene were particularly reactive but this cannot be clearly explained based on type of substitution pattern. In general, DDQ was more reactive with alkylnaphthalenes than was chloranil. To identify the peaks in a chromatographic separation consisting of unsubstituted, mono-, di- and trimethylnaphthalene, the first step is to break them down by mass, thus identifying the number of methyl substituents. The separation should then be repeated with the introduction of a stream of DDQ post-column but pre-mass spectrometer and the effect on signal intensity noted, including the magnitude of any enhancement. This should then be repeated with chloranil. The magnitude of the signal enhancements with each of these electron transfer reagents and reference to Figure 7.12 should help resolve the isomers.

A similar technique should be successful with pyrene derivatives except that a fourth run with DDAQ and Figure 7.13 will be required. This was examined experimentally with parent, two methyl, a mixture of ethylmethyls, an ethyl, three diethyl, a tetrahydro, a hexahydro and a naphtha pyrene derivative analysed with DDQ, Chloranil and DDAQ. The

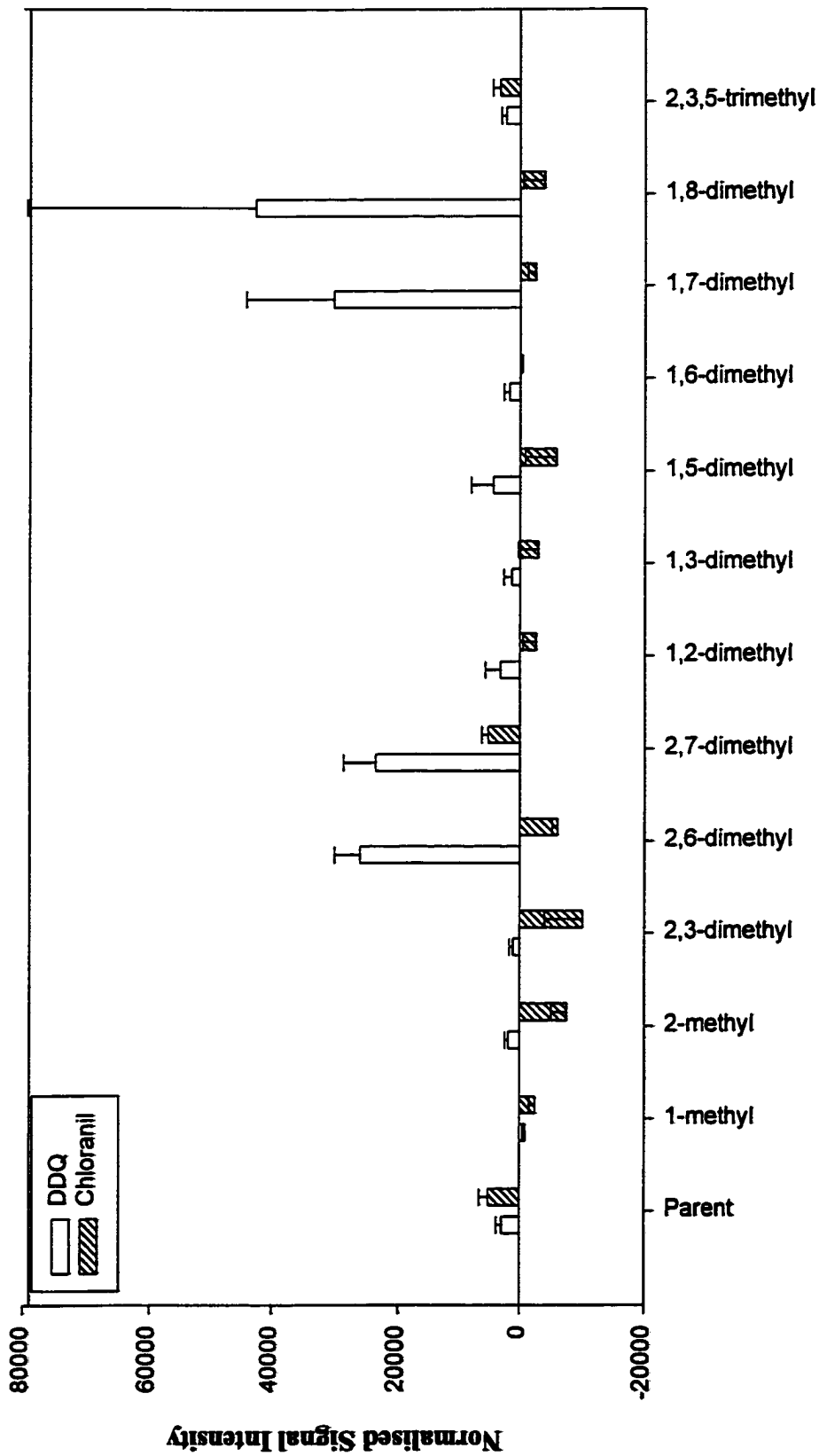

Figure 7.12. Signal Intensity for 0.010 mM alkylnaphthalene solutions (flow= 1.8 mL/h) and 0.155 mM solutions of chemical electron transfer reagents and phenyl-stabilised cations (flow= 4.1 mL/h).

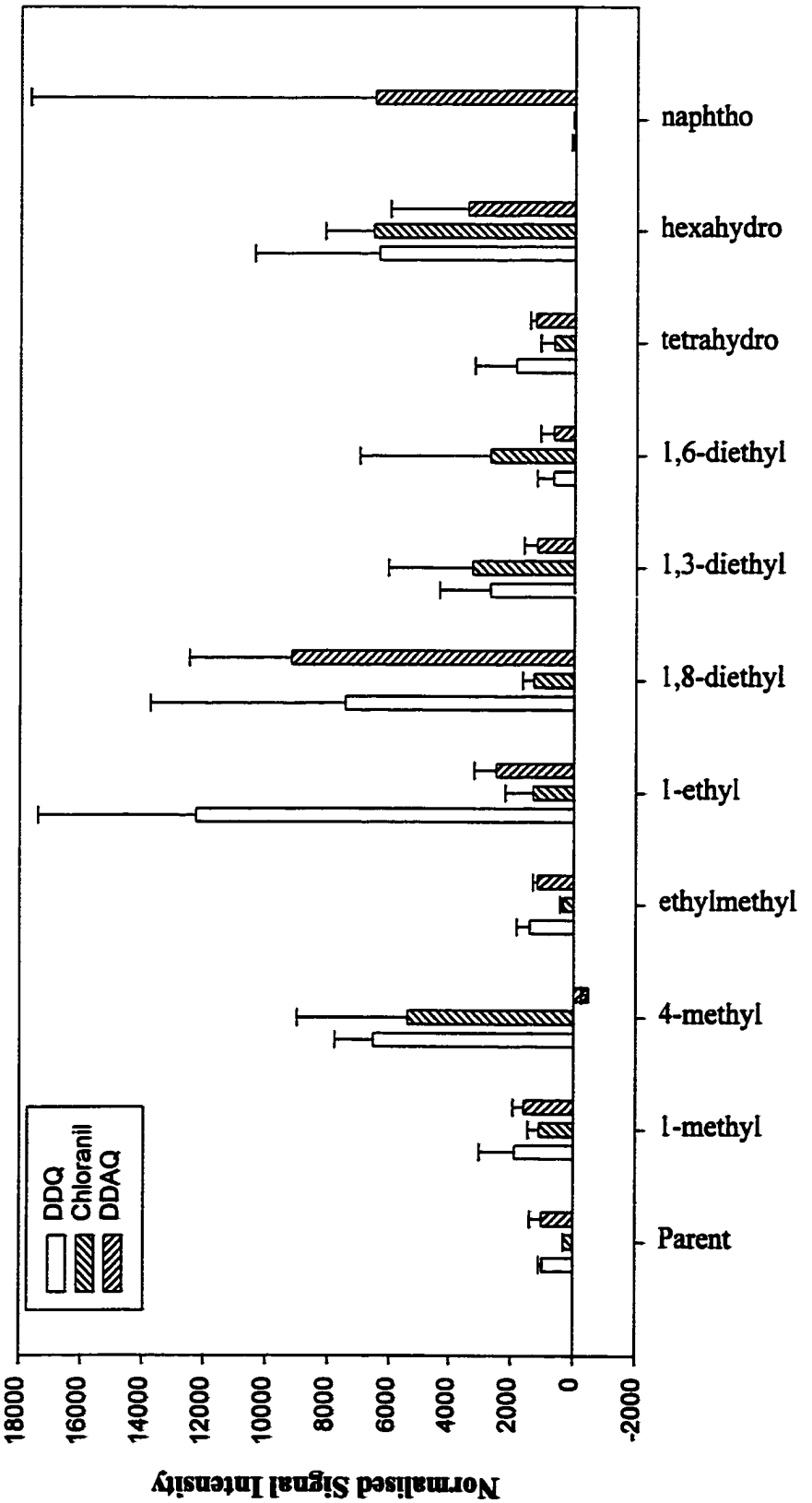

Figure 7.13. Signal Intensity for 0.010 mM solutions of pyrene derivatives (flow = 1.8 mL/h) and 0.155 mM solutions of chemical electron transfer reagent or phenyl-stabilised cations (flow= 4.1 mL/h).

results are presented in Figure 7.13. All compound classes of different masses could be readily distinguished by mass. DDAQ was the most useful and selective reagent for pyrene analysis as it 1) was the only species to enhance the signal of naphtho[2,3-*a*]pyrene, 2) permitted discrimination among non-equivalent structures such as 1- and 4-methyl derivatives and 1,8 versus 1,3 and 1,6-diethylpyrenes (the latter two being distinguishable by their reactivity with DDQ) and 3) its generally high level of signal enhancement. It is interesting that reducing the conjugation in a pyrene system by 2 (tetrahydropyrene) and 3 (hexahydropyrene) double bonds actually improved the ability of pyrene to be oxidised. This does not eliminate the aromaticity of the compounds but increasing the aliphatic portion of the molecule should increase its ionisation energy, making it more difficult to abstract an electron. It is unclear why this should confer better electron transfer properties to these molecules.

Chapter 8

Conclusions and Future Work

8.1 Conclusions

This thesis has been an examination of the liquid introduction-atmospheric pressure ionisation (API) mass spectrometric response to polycyclic aromatic compounds (PACs) typically encountered in petroleum samples. Both electrospray ionisation (ESI) and atmospheric pressure chemical ionisation (APCI) are API-MS techniques which were studied as possible means by which to examine PACs. The latter technique is more tolerant of flow rate and mobile phase composition than the former, mainly because the two techniques greatly differ in the mechanisms of ionisation and operating parameters. The results of these studies illustrated the impact of instrumental parameters, solvent identity and purity, nature of the source gas(es) used and the analyte structure on ion yield and ionisation mechanism,. The knowledge gained from these studies was also applied to the characterisation of the PAC content of a light gas oil distillation fractions and the gap between pyrene peaks by APCI-MS. A new potential means of discriminating amongst isomers and alkylated derivatives by ESI was demonstrated.

Optimisation of the APCI-MS response indicated that the corona voltage, cone voltage, solvent composition, source gas identity and sheath gas flow rate were major factors in both the ion yield and ionisation mechanism. This is consistent with a system where analytes are ionised in the gas phase in a sequence of reactions initiated by the application of a high voltage to the corona needle, which mainly ionises the sheath gas, initiating a cascade of reactions leading to the formation of solvent or gas derived ions which then ionise

the analyte by ion/molecule reactions. At lower corona voltages, lower amounts of analyte are detected and relative protonation is high. This could be related to 1) the nature of the ionising species changing with changes in corona voltage, 2) shorter residence times giving less opportunity for protonation and 3) some loss of $H^{\bullet}$ due to fragmentation with a high corona voltage. The cone voltage results indicated that solvent ionisation or fragmentation must proceed far enough to yield a substantial stock of reagent ions. When the production of these reagent ions is optimal, signal intensity of the analytes is maximised. Whether species are ionised by charge exchange or by proton transfer is principally affected by the nature of the solvent and analyte. The source gas is important from two considerations - their purity and the ions generated with them in an APCI plasma. Hence, gases of low purity are associated with significant chemical noise, a plethora of possible reagent ions, potential *m/z* interferences, and a poor signal-to-noise ratio for sample analysis. The presence of oxygen, regardless of the solvent present, will promote charge exchange in $APCI^{-}$ mode due to oxygen's high electron affinity. The sheath gas was demonstrated to be the gas most implicated in the sequence of reactions leading to ionised analyte species since the nature and flow rate of this gas impacted the ionisation of the solvent, which affects analyte ionisation. Other instrumental parameters are important for maximising response to any analyte and are involved in ion formation, transmission and detection efficiency but not in ionisation mechanism.

The optimisation of the electrospray response by the manipulation of instrumental parameters clearly demonstrated that ion formation is mainly occurring in the solution phase via redox chemistry and that instrumental parameters need only be manipulated to enhance

ion transmission and detection. To improve the ionisation efficiency, the solvent composition must be altered, wither by the addition of ionisable additives or by altering the mobile phase. This is consistent with the current understanding of electrospray as a solution phase phenomenon. However, the ability to observe PACs by electrospray in acetonitrile demonstrates that the capillary is capable of electrochemically ionising PACs, as proposed by van Berkel [206].

Due to the greater flow rate tolerance of APCI, it was originally applied to the uni- and multi-dimensional liquid chromatographic-mass spectrometric study of the distillation cuts of Syncrude Lot #2HPP 1106 synthetic crude oil. The results indicated the presence of alkylated derivatives of naphthalene, phenanthrene and pyrene. Normal phase separations with UV, fluorescence and mass spectrometric detection were able to detect the major components of the silica-fractionated naphthalene peak and pyrene peaks 1 through 4, though the sensitivity to minor components was much lower than that of the laser fluorescence detector and was inadequate for characterisation. The sensitivity in the reversed phase work was worse, allowing determination of components present only in high concentration or eluting in the organic-rich portion of the gradient due to solvent effects.

These limitations of high water concentration, solvent incompatibility between the HPLC and mass spectrometer systems and the low sensitivity to PACs by APCI_MSwere addressed by striving to understand and counter the solvent effects, by evaluating electrospray and APCI as LC/MS interface techniques, and by attempting to understand the nature of the chemical reactions occurring in the APCI plasma in an effort to maximise response to PACs.

Among the solvent effects studied were the impact of solvent identity, solvent purity and solvent additives. The comparison of various solvents indicated that aprotic organic solvents rather than aqueous solvents are preferred for APCI. This may be related to improved solvation, the types of reagent ions generated and the physical properties of the solvent (boiling point, viscosity, surface tension). Hence, the highest signal intensities for select PACs were observed in dichloromethane (highest solvation efficiency, lowest boiling point) while acetonitrile/water produced the lowest. In the former case, dichloromethane generates only select ions and exhibits little tendency to cluster, resulting in a simple, low background. At the other extreme is aqueous acetonitrile which readily generates a range of ions and clusters, resulting in complex, high backgrounds. The ions derived from the solvent determine to a great extent the ionisation mechanism of the analytes. Hence, dichloromethane in $APCI^-$ mode is a very poor gas phase acid but a good electron acceptor, thereby promoting charge exchange. Alkane solvents from *m/z* 43 ($C_3H_7^+$) and *m/z* 57 ($C_4H_9^+$) which readily transfer protons to analytes which are better gas phase bases. Water tends to form protonated water clusters capable of transferring protons to PACs, though proton affinity will decrease with increasing cluster size (due to solvation of the hydronium ion). There was no obvious correlation between ionisation mechanism and response.

It was observed that although the solvent is present in large excess relative to the analyte, a reduction of water content from 100 to 90% (with acetonitrile or methanol) resulted in a dramatic drop in protonation efficiency, likely the result of formation of other clusters from which proton transfer is less energetically favourable. These conditions would

never be used with reversed phase separations but were used to probe any possible correlation between solvent ions and clusters and degree of protonation.

The comparison of C_5 to C_9 alkane solvents indicated that these solvents will fragment predictably, giving predominantly *m/z* 43 and *m/z* 57. Heptane, octane and isooctane were associated with the highest signal intensity for select PACs but no correlation between signal intensity and ionisation mechanism was observed. There was a correlation between the nature of the fragment ion from the solvent and the degree of protonation, protonation being influenced by the abundance of *m/z* 43 which is consistent with *m/z* 43 being a better gas phase acid than *m/z* 57.

Solvent purity, as expected, was observed to have a large impact on signal intensity and ionisation mechanism in APCI. The cleaner Milli-Q water was associated with better signal-to-noise for PACs and reduced chemical noise relative to distilled water. Alumina purification of hexanes and dichloromethane appeared to remove oxygen-containing species in the solvent background which resulted in some alteration in signal intensity and ionisation mechanism of PACS. An strong ion in the background of hexanes and dichloromethane, *m/z* 59, might be arising in the source or from other probe materials.

The use of additives to break up water clusters or to improve the protonation of PACs in APCI failed to a large extent to have the desired effect. In the case of the additives used to break up water clusters, the solvent background was observed to increase and only trifluorinated toluene improved the response of PAC standards, perhaps by better solubilising the PACs. The addition of species designed to improve the protonation of PACs had the opposite effect but signal intensity was somewhat improved with formic acid.

Electrospray and APCI were evaluated as techniques for the analysis of PACs. Capillary-mediated and solvent-initiated ionisation of PACs for electrospray analysis was observed to be most efficient with the use of acetontirile-acetic acid, implicating the acetic acid in stabilisation of cations or charge-transfer complexes. A comparison of this form of electrospray with APCI indicated that although ESI gave a more intense response, it was successful for a narrower range of compounds, was less reproducible and more difficult to interface with an HPLC column because of its low flow rate tolerance. To make ESI truly competitive with APCI, the signal enhancement must be far greater, as much of the improvement will be lost in the 99:1 split from the HPLC to the ESI source. One means of doing so was the use of chemical electron transfer reagents. These species can form donor-acceptor complexes with PACs which then dissociate to yield a radical cation of the PAC and a radical anion of the chemical electron transfer reagent. Of the transfer agents evaluated, chloranil was observed to be the most versatile reagent, DDAQ was particularly useful for the ionisation of pyrene and DDQ was of intermediate reactivity. The enhancement of the molecular ion of a given PAC was solvent, gas and analyte-dependent. Dichloromethane + 0.1 % trifluoroacetic acid resulted in the best signal enhancement of 2,3-benzanthracene with DDQ, presumably by good dissolution of the PAC and stabilisation of the resulting radical cation. Oxygen, as an electron scavenger, greatly enhanced ionisation of PACs relative to nitrogen and so air was preferred to nitrogen as a source gas for electrospray. This may indicate either gas phase ionisation or could be a surface interaction between the PAC and the surrounding oxygen. In general, perylene was the most readily ionised, consistent with its low ionisation energy, while naphthalene with its high ionisation energy was poorly

enhanced. At its optimal performance, chloranil increased the signal of perylene by 45000 counts relative to the signal without chloranil. This increase in signal is two orders of magnitude better than the literature enhancement of 400 of 2,3-benzanthracene with DDQ. It is unknown whether this enhancement would be observed if the chemical electron transfer was added post-column to chromatographically-separated perylene.

However, both APCI and ESI offer some potential for discrimination amongst parent and alkylated PAHs and amongst isomers. Parent PAHs and the their alkylated analogues are clearly distinguishable by mass. With APCI, isomers cannot be distinguished but where they can be separated chromatographically, APCI can assist in isomer detection. In ESI, isomers of alkylated naphthalene were distinguishable by their differing reactivity to DDQ and chloranil. In the case of pyrene derivatives, reactivity to DDQ, chloranil and DDAQ could be used to distinguish isomers and degree of double bond reduction was correlated with signal enhancement in the presence of DDQ, DDAQ and chloranil. These offer the possibility not only of distinguishing isomers but also providing insights into the structure of the molecule at a given *m/z* value.

At this point, APCI appears to be the most versatile mass spectrometric technique but electrospray does have some advantages, particularly in isomer discrimination, which might prove useful in more detailed characterisation of PAC content of fuels, especially where liquid chromatography is unable to separate isomers.

It is believed that the application of a high voltage to the tip of the corona discharge needle ionises the surrounding gas ions [92-93], initiating a series of reactions leading to the formation of protonated water clusters if water is present which will exchange protons with

analytes of a greater gas phase basicity, the reaction being controlled kinetically or thermodynamically depending on the difference in basicity between the analyte and the protonated water cluster. The effect of the input of solvent, if any, has not been addressed.

The results presented in this thesis indicate that the observed response, both in magnitude and in ionisation mechanism with APCI, to PACs are highly dependent on the analyte, solvent and gases present in the source. The ketone, fluorenone, is more readily detected and protonated than β-phenanthrol, the phenol. 6-methyl-1,2,3,4-tetrahydrocarbazole (MTC), a much poorer gas phase base than carbazole, is also less readily detected and protonated. Attempts to correlate ionisation energy, gas phase basicity or proton affinity with observed response were only moderately successful- indicating that there is a competition among ionisation mechanisms.

Pyrene, with its relatively low ionisation energy and high gas phase basicity, is probably the best probe of the conditions in the APCI plasma. Where conditions, such as hydrogen in the plasma, favour proton transfer, the $[M+H]^+$ predominates whereas charge exchange conditions, O_2 or N_2 in the source, favour the formation of the molecular ion of pyrene. With skimmer cone A, the sheath gas was the most crucial gas as demonstrated in the one, two and three gas experiments. These gas experiments demonstrated that CI reactions were not a good basis for understanding the nature of the reactions in the APCI plasma, as typical CI reagent ions (CH_5^+, H_3^+) were not being formed. Carbon monoxide, methane and hydrogen provided no strong enhancement in PAC analysis and their explosive and/or toxic properties led to the abandonment of the study of the effects of these gases. Hydrogen in particular was associated with probe cooling and source heating (due to its high

heat capacity) and deposition and corrosion of the corona discharge needle made it unattractive for use. The combination of Extradry™ air with carbon dioxide for aqueous acetonitrile, acetonitrile and dichloromethane and nitrogen-carbon monoxide with hexanes were most beneficial with skimmer cone A. No relationship could be determined between protonation efficiency and signal intensity - therefore efforts should be directed to improving signal intensity and not manipulating ionisation mechanism.

The comparison of the three skimmer cones indicates the importance of orifice size. Ion transmission is most efficient with skimmer cone C (the largest skimmer cone orifice, at the normal) which indicates that skimmer cone A was partially obstructed, leading to decreased instrument performance.

The analysis of the gas background with skimmer cone C indicates a low level of water clusters, indicating that they are not forming or are being consumed before they reach the detector. The backgrounds are dominated by gas-derived ions (e.g. CO_2H^+ for CO_2), a ubiquitous contaminant at *m/z* 214 and its breakdown products, and probably phthalates. The gas + solvent background are dominated by solvent-derived species (e.g. *m/z* 42 for acetonitrile and *m/z* 43 for hexanes). The dichloromethane background was dominated by species unrelated to the solvent though *m/z* 83/85 ($CHCl_2^+$) and 49/51 (CH_2Cl^+) could be observed for some gas combinations. In terms of PAC response, nitrogen in the bath and sheath gas streams with carbon dioxide in the nebuliser gas stream or Extradry™ air in all streams were ideal for aqueous acetonitrile, acetonitrile and dichloromethane and carbon dioxide in all streams for hexanes. No obvious correlation could be made between signal intensity and ionisation mechanism. However, the solvent background was strongly

implicated in the degree of protonation. Hence gases like building air and carbon dioxide which permitted significant acetonitrile clustering were associated with poor protonation of samples while gases like tank nitrogen which did not seem to promote clustering resulted in enhanced protonation. Thus, it appears that the sequence of reactions leading to protonation is: the gas ionise the solvent which then ionises the analyte. With charge exchange, the reaction sequence is less clear and other processes like direct ionisation of the analyte by the corona discharge needle, gas ions or solvent impurities cannot be dismissed. Physical properties of the gases, solvent and analytes involved are inadequate to explain the observed ionisation mechanisms.

The three to fourfold improvement in the signal intensity by single ion monitoring of PACs in a real world sample, particularly of components which were difficult to determine previously, offers the distinct promise of allowing characterisation of minor constituents of the PAC fractions. These minor constituents were not previously amenable to LC/APCI-MS analysis even in SIR mode.

8.2 Future Work

Future research should focus both on basic research and on applications of LC-APCI-MS to real-world sample analysis. In terms of basic research, work should continue to explore the electrospray analysis of PACs by means of CETRs, on studying the effect of highly reactive gases and on broadening the PAC range studied.

It is of interest to determine whether the trends in PAC ionisation in the presence of DDQ, chloranil and DDAQ are preserved if the CETR is added post-column and if so, whether isomer discrimination of chromatographically separated PAC derivatives is possible

and practical. It is also of interest to continue to pursue a quantum mechanical understanding of the interactions between the CETRs/PSCs and the PACs to explain the experimental results. At the moment, geometry optimisations are still ongoing. Initial attempts to explain the behaviour as being due to the energies of lowest unoccupied molecular orbital and highest occupied molecular orbitals have not been fruitful.

Most of the gases studied as part of the APCI plasma characterisation experiments did not differ greatly in their reactivity. It is of interest to determine whether highly reactive gases (like NO, SF_6), introduced in tightly controlled amounts into the nebuliser or sheath gas streams have a significant impact on PAC signal or ionisation, or offer the possibility of isomer discrimination due to differing reactivity toward gas-derived ions.

It is also of interest to extend the range of PACs that can be detected. Specifically, heterocyclic and high mass compounds in environmental samples should be studied. Both ESI and APCI offer promise for these studies.

The CETR-mediated electrospray detection of PACs and the results of the gas studies should be applied to real-world sample characterisation. Assuming that CETRs can be coupled to chromatographic separation, they can be used to improve PAC ionisation (thus signal) and discriminate amongst isomers, providing a mechanism for isomer discrimination.

In $APCI^+$ mode, the combination of N_2-CO_2 has been successfully coupled with chromatography to permit detection of pyrene and phenanthrene derivatives. These studies should be extended to other fractions of the synthetic oil chromatograms and to the detection of PACs in air samples. The applicability of the N_2-CO_2 combination to normal phase separations (isocratic and gradient) of PACs should be studied.

Chapter 9
References

1. Neidle, S. *Nature*, **1976**, *263*, 92.

2. Kennaway, E.L. and Hieger, I. *Br. Med. J.*, **1930**, *ii*, 1044.

3. Cook, J.W., Hewett, C.L. and Hieger, I. *J. Chem. Soc.*, **1933**, 395.

4. Vo-Dinh, Tuan. *Chemical Analysis of Polycyclic Aromatic Compounds*. New York: John Wiley and Sons, Inc. 1989.

5. Yu, M.-L. and Hites, R.A. *Anal. Chem.* **1981**, *53*, 951.

6. Dunn, B.P. and Stich, H.F. *Proc. Soc. Exp. Biol. Med.*, **1975**, *150*, 49.

7. Badger, G.M. and Kimber, R.W.L. *J. Chem. Soc.*, **1960**, 266.

8. Badger, G.M. and Kimber, R.W.L. *J. Chem. Soc.*, **1960**, 2746.

9. Badger, G.M., Lewis, G.E.and Napier, I.M. *J. Chem. Soc.*, **1960**, 2825.

10. Badger, G.M., and Spotswood, T.M. *J. Chem. Soc.*, **1960**, 4431.

11. Badger, G.M., Donnelly, J.K. and Spotswood, T.M. *Austr. J. Chem.*, **1962**, *15*, 605.

12. Badger, G.M., Donnelly, J.K. and Spotswood, T.M. *Austr. J. Chem.*, **1964**, *17*, 1147.

13. Badger, G.M. and Novotny, J. *Nature*, **1963**, *198*, 1086.

14. Khan, A.U., Pitts, J.N. Jr., and Smith, E.B. *Environ. Sci. Technol.*, **1967**, *1*, 656.

15. Foote, C.S *Acc. Chem. Soc.*, **1968**, *1*, 104.

16. Pitts, J.N. Jr., Khan, A.U., Smith, E.B. and Wayne, R.P. *Environ. Sci. Technol.*, **1969**, *3*, 241.

17. Bailey, P.S. *Chem. Rev.*, **1958**, *58*, 925.

18. Bailey, P.S., Batterbee, J.E. and Lane, A.G. *J. Am. Chem. Soc.*, **1968**, *90*, 1027.

19. Erickson, P.G., Bailey, P.S. and Davis, J.C. Jr. *Tetrahedron*, **1962**, *18*, 388.

20. Moriconi, E.J., Rakoczy, B. and O'Connor, W.F. *J. Am. Chem. Soc.*, **1961**, *83*, 4618.

21. Moriconi, E.J. and Taranko, L.B. *J. Org. Chem.*, **1963**, *28*, 1831.

22. Moriconi, E.J. and Taranko, L.B. *J. Org. Chem.*, **1963**, *28*, 2526.

23. Moriconi, E.J. and Salce, L. *Adv. Chem. Ser.*, **1968**, *77*, 65.

24. Greenberg, A.J. and Darack, F.B. Atmospheric Reactions and Reactivity Indices of Polycyclic Aromatic Hydrocarbons in *Molecular Structure and Energetics*, Vol. 4, Deerfield Beach: VCH Publishers, 1987. p.1

25. Biermann, H.W., Mac Leod, H., Atkinson, R., Winer, A.M. and Pitts, J.N. Jr. *Environ. Sci. Technol.*, **1985**, *19*, 244.

26. Atkinson, R., Aschmann, S.M. and Pitts, J.N. Jr. *Environ. Sci. Technol.*, **1984**, *18*, 110.

27. Pitts, J.N. Jr., Zielinska,B., Sweetman, J.A., Atkinson, R., and Winer, A.M. *Atmos. Environ.*, **1985**, *19*, 911.

28. National Academy of Sciences, *Particulate Polycyclic Organic Matter*, Washington, D.C.: National Academy Sciences, 1972.

29. Junge, C.E. *Adv. Environ. Sci. Technol.*, **1977**, *8*, 7.

30. Thrane, K.E. and Mikalsen, A. *Atmos. Environ.*, **1981**, *15*, 909.

31. Yamasaki, H., Kuwata, K. and Hiyamoto, H. *Environ. Sci. Tech.*, **1982**, *16*, 189.

32. Lee, M.L. and Hites, R.A. *Anal. Chem.*, **1976**, *48*, 1890.

33. Gelboin, H.V. and T'so, P.O.P (eds). *Polycyclic Hydrocarbons and Cancer*. New York: Academic Press, 1978.

34. Grimmer, G. (Ed.) *Environmental Carcinogens: Polycyclic Aromatic Hydrocarbons*. Boca Raton: CRC Press, 1983.

35. Glover, P.L. (Ed.) *Chemical Carcinogens and DNA*. Vol. 1 and 2. Boca Raton: CRC Press, 1979.

36. Harvey, R.G. (Ed.) *Polycyclic Hydrocarbons and Carcinogenesis*. ACS Symposium Series 283, Washington, D.C.: American Chemical Society, 1985.

37. Wogan, G.N. and Corelick, N.J. *Environ. Health Perspect.*, **1985**, *62*, 5.

38. Later, D.W., Lee, M.L., Bartle, K.D., Kong, R.C. and Vassilaros, D.L. *Anal. Chem.*, **1981**, *53*, 1616.

39. Selucky. M.L., Chu, Y., Ruo, T., and Strausz, O.P. *Fuel*, **1977**, *56*, 369.

40. Chrones, J. and Germain, R.R. *Fuel Sci. Tech. Int'l*, **1989**, *7*, 783.

41. Izquierdo, A., Carbognani, L., Leon, V. and Parisi, A. *Fuel Sci. Tech. Int'l*, **1989**, *7*, 561.

42. Waller, P.R., Williams, A., and Battle, K.D. *Fuel*, **1989**, *68*, 520.

43. Casalini, A., Mascharpa, A. and Vecchi, C. *Fuel Sci. Tech. Int'l*, **1990**, *8*, 427.

44. Sullivan, R.F., Boduszynski, M.M. and Fetzer, J.C. *Energy and Fuels*, **1989**, *3*, 603.

45. Shue, F.F. and Yen, T.F. *Anal. Chem.*, **1981**, *53*, 2081.

46. Wise, S.A., Schatz, M.M., Benner, B.A., Hays, M.J. and Schiller, S.B. *Anal. Chem.*, **1995**, *67*, 1171.

47. White, F.A. and Wood, G.A. *Mass Spectrometry: Applications in Science and Engineering.* Toronto: John Wiley and Sons, 1986.

48. Duckworth, H.E., Barber, R.C. and Venkatasubramanian, V.S. *Mass Spectrometry.* New York: Cambridge University Press, 2nd ed., 1986.

49. Personal communication with DRs. R.K. Boyd and L. Ramaley. (Dalhousie Chemistry 6502 Class Notes)

50. Karasek, F.W. and Clement, R.E. *Basic Gas Chromatography-Mass Spectrometry: Principles and Techniques.* New York: Elsevier, 1988.

51. Davis, R. and Frearson, M. *Mass Spectrometry: Analytical Chemistry by Open Learning.* Toronto: John Wiley and Sons, 1987.

52. McLafferty, F.W. *Interpretation of Mass Spectra.* Mill Valley: University Science Books, 3rd ed., 1980.

53. Steel, C. and Henchman, M. *J.Chem.Ed.*, **1998**, *75*, 1049.

54. *VG-Fisons-Micromass™ Users Guide*. Altrincham: VG-Fisons-Micromass, 1995.

55. Bruins, A.P. *Adv. Mass Spectrom.*, **1986**, *10*, 119.

56. Drabner, G., Poppe, A. and Budzikiewicz, H. *Int. J. Mass Spectrom. Ion Processes*, **1990**, *97*, 1.

57. Burrows, E.P. *Mass Spectrom. Reviews*, **1995**, *14*, 107.

58. Vairamani, M. *Org. Mass Spectrom.*, **1993**, *28*, 1498.

59. Roussis, S.G. and Fedora, J.W. *Anal. Chem.*, **1997**, *69*, 1550-1556.

60. Moneti, G., Pieraccini, G., Dani, F.R., Catinella, S. and Traldi, P. *Rapid Commun. Mass Spectrom.*, **1996**, *10*, 167.

61. Srinivas, R., Devi, A.R. and Rao, G.K.V. *Rapid Commun. Mass Spectrom.*, **1996**, *10*, 12.

62. Clemens, D. and Munson, B. *Anal. Chem.*, **1985**, *57*, 2022.

63. Partanen, T. and Vainiotalo, P. *Rapid Commun. Mass Spectrom.*, **1997**, *11*, 881.

64. Sellier, N.M. and Bordier, C.G. *J. Am. Oil Chem. Soc.*, **1997**, *74*, 923.

65. Dearth, M.A., Asano, K.G., Hart, K.J., Buchanan, M.V., Goeringer, D.E. and McLuckey, S.A. *Anal. Chem.*, **1997**, *69*, 5121.

66. Hazell, S.J., Bowen, R.D. and Jennings, K.R. *Org. Mass Spectrom.*, **1988**, *23*, 597.

67. Elson, C.M. and Sim, P.G. *Rapid Commun. Mass Spectrom.*, **1990**, *4*, 37.

68. Sim, P.G. and Elson, C.M. *Rapid Commun. Mass Spectrom*, **1988**, *2*, 137.

69. Hilpert, L.R. *Biomed. Environ. Mass Spectrom.*, **1987**, *14*, 383.

70. Daishima, S., Iida, Y., Shibata, A. and Kanda, F. *Org. Mass Spectrom.*, **1992**, *27*, 571.

71. Isemura, T., Kakita, R., Tamaoki, A. and Yonemori, S. *J. Fluorine Chem.*, **1996**, *80*, 81.

72. Bourcier, S. Hoppilliard, Y. and Kargar, T. *Rapid Commun. Mass Spectrom.*, **1997**, *11*, 1046.

73. Sim, P.G., Jamieson, W.D. and Boyd, R.K. *Rapid Commun. Mass Spectrom.*, **1987**, *2*, 28.

74. Robinson, M.R., Botswick, D.E., Abbey, L.E. and Moran, T.F. *Rapid Commun. Mass Spectrom.*, **1988**, *2*, 210.

75. Natalis, P. and Franklin, J.L. *J. Phys. Chem.*, **1965**, *69*, 293.

76. Carroll, D.I., Dzidic, I., Horning, E.C., and Stillwell, R.N. *Appl.Spectrosc. Rev.*, **1981**, *17*, 337.

77. Horning, E.C., Horning, M.G., Carroll, D.I., Dzidic, I., and Stillwell, R.N. *Anal. Chem.*, **1973**, *45*, 936.

78. Dzidic, I., Carroll, D.I., Stillwell, R.N. and Horning, E.C. *Anal. Chem.*, **1976**, *48*, 1763.

79. Good, A., Durden, D.A. and Kebarle, P. *J. Chem. Phys.*, **1970**, *52*, 212.

80. Horning, E.C., Carroll, D.I., Dzidic, I., Haegele, K.D., Horning, M.G., and Stillwell, R.N.. *J. Chromatogr. Sci.*, **1974**, *12*, 725.

81. Carroll, D.I., Dzidic, I., Stillwell, R.N.. and Horning, E.C. in *Trace Organic Analysis: A New Frontier in Analytical Chemistry*. (Special Publication 519), Washington, D.C.: National Bureau of Standards, 1949. p.655.

82. Maquestiau, A., Flammang, R., and Nielsen, L. *Org. Mass Spectrom.*, **1980**, *15*, 376.

83. Carroll, D.I., Nowlin, J.G., Stillwell, R.N.. and Horning, E.C. *Anal. Chem.*, **1981**, *53*, 2007.

84. Cooks, R.G. and Kruger, T.L. *J. Am. Chem. Soc.*, **1977**, *99*, 1279.

85. van der Hart, W.J., Luijten, W.C.M.M., and van Thuijl, J. *Org. Mass Spectrom.*, **1980**, *15*, 463.

86. Szulejko, J.E., Howe, I., Beynon, J.H. and Schlunegger, U.P. *Org. Mass Spectrom.*, **1980**, *15*, 263.

87. Lovelock, J.E. and Gregory, N.L. *Gas Chromatography*. New York: Academic Press, 1962. p. 219

88. Crow, F..W., Bjorseth, A., Knapp, K.T. and Bennett, R. *Anal. Chem.*, **1981**, *53*, 619.

89. Dzidic, I., Carroll, D.I., Stillwell, R.N. and Horning, E.C. *J. Am. Chem. Soc.*, **1974**, *96*, 5258.

90. Dougherty, R.C. *Anal. Chem.*, **1981**, *53*, 625A.

91. Shahin, M.M. *J. Chem. Phys.*, **1967**, *45*, 2600.

92. Sunner, J., Nicol, G., and Kebarle, P. *Anal. Chem.*, **1988**, *60*, 1300.

93. Sunner, J., Ikonomou, M.G. , and Kebarle, P. *Anal. Chem.*, **1988**, *60*, 1308.

94. Ketkar, S.N., Penn, S.M. and Fite, W.L.. *Anal. Chem.*, **1991**, *63*, 924.

95. Bruins, A.P. *Mass Spectrom. Rev.*, **1991**, *10*, 53.

96. Gall, L.N. and Muradymov, M.Z *J. Anal. Chem.*, **1998**, *53*, 419.

97. Kambara, H. and Kanomata, I. *Anal. Chem.*, **1977**, *49*, 270.

98. Lane, D.A., Thomson, B.A., Lovett, A.M. and Reid, N.M. *Adv. Mass Spectrom.*, **1980**, *8B*, 1480.

99. Dzidic, I., Carroll, D.I., Stillwell, R.N. Horning, M.G. and Horning, E.C. *Adv. Mass Spectrom.*, **1978**, *7*, 359.

100. Horning, E.C., Horning, M.C., Carroll, D.I., Stillwell, R.N. and Dzidic, I. *Life Sci.*, **1973**, *13*, 1331.

101. Bell, S.E., Ewing, R.G., Eiceman, G.A. and Karpas, Z. *J. Am. Soc. Mass Spectrom.*, **1994**, *5*, 177.

102. Shiea, J., Wang, W.-S., Wang, C.H., Chen, P.-S. and Chou, C.-H. *Anal. Chem.*, **1996**, *68*, 1062.

103. Galceran, M.T., and Moyano, E. *J. Chromatogr. A*, **1994**, *683*, 9.

104. Shushan, B. and Boyd, R.K. *Org. Mass Spectrom.*, **1980**, *15*, 445.

105. Shushan, B., Safe, S.H. and Boyd, R.K. *Anal. Chem.*, **1979**, *51*, 156.

106. Růžička, J. and Hansen, E.H. *Flow Injection Analysis*. Toronto: John Wiley and Sons, Inc., 1981.

107. Jaramillo, L.F. and Driscoll, J.N. *J. High Resol. Chromatogr. Chromatogr. Commun.*, **1979**, *2*, 536.

108. Driscoll, J.N. *J. Chromatogr. Sci.*, **1982**, *20*, 91.

109. Driscoll, J.N. *J. Chromatogr. Sci.*, **1985**, *23*, 488.

110. Lubkowitz, J.A., Glajch, J.L., Semonian, B.P. and Rogers, L.B. *J. Chromatogr.*, **1977**, *133*, 37.

111. Semonian, B.P., Lubkowitz, J.A., and Rogers, L.B. *J. Chromatogr.*, **1978**, *151*, 1.

112. Antek Instruments, Houston, Texas.

113. Uden, P.C. and Henderson, D.E. *Analyst*, **1977**, *102*, 889.

114. Eckhoff, M.A., Ridgway, T.H. and Caruso, J.A. *Anal. Chem.*, **1983**, *55*, 1004.

115. Bruce, M.L. and Caruso, J.A. *Appl. Spectrosc.*, **1985**, *39*, 942.

116. Klassson-Wehler, E., Bergman, A., Kowalski, B. and Brandt, I. *Xenobiotica*, **1987**, *17*, 477.

117. Sinkkoken, E., Kolehmainen, E. and Koistinen, J. *Int. J. Environ. Anal. Chem.*, **1992**, *47*, 7.

118. Heath, D., Moffat, B., Lowry, R. and Rowland, S. *Anal. Proc. Anal. Commun.*, **1995**, *32*, 485.

119. Bemgard, A., Colmsjõ, A., and Lundmark, B.O. *J. Chromatogr.*, **1992**, *595*, 7.

120. Lee, H.K. *J. Chromatogr. A*, **1995**, *710*, 79.

121. Houdiere, F., Fowler, P.W.J., and Djordjevic, N.M. *Anal. Chem.*, **1997**, *69*, 2589.

122. Heinsch, S. and Rocca, J.L. *Chromatographia*, **1995**, *41*, 544.

123. Green, J.B., Reynolds, J.W. and Yu, S. K.-T. *Fuel Sci. Tech. Int'l*, **1989**, *7*, 1327.

124. Nishioka, M., Campbell, R.M., Lee, M.L. and Castle, R.N. *Fuel*, **1986**, *65*, 270.

125. Engelhart, H. and Elgass, R.J. in *High Performance Liquid Chromatography-Advances and Perspectives*. Vol. 2. Horvath, C. (ed). New York: Academic Press, 1980. p 57.

126. Wise, S.A., Bonnett, W.J., and May, W.E. in *Polynuclear Aromatic Hydrocarbons:Chemical and Biological Effects, 4th International Symposium*. Bjorseth, A. and Deniis, A.J. (eds.). Columbus:Batelle Press, 1980. p. 791

127. Karlesky, D., Shelley, D.C., and Warner, I.M. *J. Liq. Chromatogr.*, **1983**, *6*, 471.

128. Jinno, K. and Kawasaki, K. *Chromatographia*, **1984**, *18*, 44.

129. Grizzle, P.L. and Thomson, J.S. *Anal. Chem.*, **1982**, *54*, 1071.

130. Wallace, D., Henry, D., Pongar, K. and Zimmerman, D. *Fuel*, **1987**, *66*, 44.

131. Dong, M.W. and DiCesare, J.L. *J. Chromatogr. Sci.*, **1982**, *20*, 517.

132. Sander, L.C. and Wise, S.A. *Adv. Chromatogr.*, **1986**, *25*, 139.

133. McNalley, M.E. and Rogers, L.B. *J. Chromatogr.*, **1985**, *331*, 23.

134. Shah, P., Rogers, L.B. and Fetzer, J.C. *J. Chromatogr.*, **1987**, *388*, 411.

135. Wise, S.A, Sander, L.C. and May, W.E. *J. Chromatogr.*, **1993**, *642*, 329.

136. Giles, C.H. and Easton, L.A. *Adv. Chromatogr.*, **1966**, *3*, 67.

137. Wan, Q.H., Ramaley, L. and Guy, R.D. *Anal. Chem.*, **1996**, *69*, 4581.

138. Wise, S.A., Bonnett, W.J., Guenther, F.R and May, W.E. *J. Chromatogr. Sci.*, **1981**, *19*, 457.

139. Ohmacht, R., Kele, M. and Matus, Z. *Chromatographia*, **1994**, *39*, 668.

140. Schmit, J.A., Hnery, R.A., Williams, R.C., and Dieckman, J.F. *J. Chromatogr. Sci.*, **1971**, *9*, 645.

141. Crini, G., Torri, G., Lekchiri, Y., Martel, B., Janus, L. and Morcellet, M. *Chromatographia*, **1995**, *41*, 424.

142. Chmielowiec, J. and Sawatzky, H. *J. Chromatogr. Sci.*, **1979**, *17*, 245-252.

143. Hesselink, W., Schiffer, R.H.N.A., and Koostra, P.R. *J. Chromatogr A*, **1995**, *697*, 165.

144. Höner, A., Arnold, M., Hüsers, N. and Kleiböhmer, W. *J. Chromatogr. A*, **1995**, *710*, 129.

145. Levy, J.M. and Ritchey, W.M. *J. Chromatogr. Sci.*, **1986**, *24*, 242.

146. Fuhr, B.J., Holloway, L.R. and Reichert, C. *Fuel Sci. Tech. Int'l*, **1989**, *7*, 643.

147. Blilie, A.L. and Greibrokk, T. *Anal. Chem.*, **1985**, *57*, 2239.

148. Coulombe, S. and Sawatzky, H. *Fuel*, **1986**, *65*, 552.

149. Peaden, P.A., Lee, M.L., Hirata, Y. and Novotny, M. *Anal. Chem.*, **1980**, *52*, 2268.

150. Williams, P.T. and Bottrill, R.P. *Fuel*, **1995**, *74*, 736.

151. Brown, R.S., Luong, J.H.T., Szolar, O.H.J., Halasz, A. and Hawari, J. *Anal. Chem.*, **1996**, *68*, 287.

152. Nguyen, A.-L. and Luong, J.H.T. *Anal. Chem.*, **1997**, *69*, 1726.

153. Boyd, R.K. *Rapid Commun. Mass Spectrom.*, **1993**, *7*, 257.

154. Poirier, M.-A. and Das, B.S. *Fuel*, **1984**, *63*, 361-367.

155. Dzidic, I., Balicki, M.D., Rhodes, I.A.L. and Hart, H.V. *J. Chromatogr. Sci.*, **1988**, *26*, 236.

156. Low, G. K.-C., Batley, G.E., Lidgard, R.O., and Duffield, A.M. *Biomed. Environ. Mass Spectrom.*, **1986**, *13*, 95.

157. Bayona, J.M., Barcelo, D. and Albaiges, J. *Biomed. Environ. Mass Spectrom.*, **1988**, *16*, 461.

158. Canton, L. and Grimalt, J.O. *J. Chromatogr. A*, **1992**, *607*, 279.

159. Brotherton, S.A. and Gulick, W.M. Jr. *Anal. Chim. Acta*, **1986**, *186*, 101.

160. Pyle, S.M., Betowski, L.D., Marcus, A.B., Winnik, W. and Brittain, R.D. *J. Am. Soc. Mass Spectrom.*, **1997**, *8*, 183.

161. Mosi, A.A., Reimer, K.J. and Eigendorf, G.K. *Talanta*, **1997**, *44*, 985.

162. Ramaley, L., personal communication.

163. Millington, D.S, Yorke, D.A. and Burns, P. *Adv. Chromatogr.*, **1980**, *8B*, 1819.

164. Dark, W.A. and McFadden, W.H. *J. Chromatogr. Sci.*, **1978**, *16*, 289.

165. Linscheid, M. and Westmoreland, D.G. *Pure & Appl. Chem.*, **1994**, *66*, 1913.

166. Lee, E.D. and Henion, J.D. *J. Chromatogr. Sci.*, **1985**, *23*, 253.

132. Gremm, T.J. and Frimmel, F.H. *Chromatographia*, **1994**, *38*, 781.

168. Dark, W.A., McFadden, W.H., and Bradford, D.L. *J. Chromatogr. Sci.*, **1977**, *15*, 454.

169. Pace, C.M. and Betowski, L.D. *J. Am. Soc. Mass Spectrom.*, **1995**, *6*, 597.

170. Robins, R.H. and Guido, J.E. *Rapid Commun. Mass Spectrom.*, **1997**, *11*, 1661.

171. Wachs, T., Conboy, J.C., Garcia, F. and Henion, J.D. *J. Chromatogr. Sci.*, **1991**, *29*, 357.

172. Nabeshima, T., Takada, Y. and Sakairi, M. *Rapid Commun. Mass Spectrom.*, **1997**, *11*, 715.

173. Siegel, M.M., Tabei, K., Lambert, F., Candela, L. and Zoltan, B. *J. Am. Soc. Mass Spectrom.*, **1998**, *9*, 1196.

174. Covey, T.R., Lee, E.D., Bruins, A.P. and Henion, J.D. *Anal. Chem.*, **1986**, *58*, 1451A.

175. Windig, W., Phalp, J.M. and Payne, A.W. *Anal. Chem..*, **1996**, *68*, 3602.

176. Thomas, D., Crain, S.M., Sim, P.G. and Benoit, F.M. *J. Mass Spectrom.*, **1995**, *30*, 1034.

177. Gehring, T.A., Rushing, L.G., Churchwell, M.I., Doerge, D.R., McErlane, K.M. and Thompson, H.C. Jr. *J. Agric. Food Chem.*, **1996**, *44*, 3164.

178. Gilbert, J.D., Olah, T.V., Barrish, A. And Greber, T.F. *Biol. Mass Spectrom.*, **1992**, *21*, 341.

179. Avery, M.J., Mitchell, D.Y., Falkner, F.C. and Fouda, H.G. *Biol. Mass Spectrom.*, **1992**, *21*, 353.

180. Mück, W.M. and Henion, J.D. *Biomed. Environ. Mass Spectrom.*, **1990**, *19*, 37.

181. Holder, C.L., Preece, S.W., Conway, S.C., Pu, Y.-M. And Doerge, D.R. *Rapid Commun. Mass Spectrom.*, **1997**, *11*, 1667.

182. Mansoori, B.A. *Rapid Comm. Mass Spectrom.*, **1998**, *12*, 712.

183. Thomson, B.A., Iribarne, J.V. and Dziedzic, P.J. *Anal. Chem.*, **1982**, *54*, 2219.

184. Arpino, P.J. and Cousin, J. *Rapid Commun. Mass Spectrom.*, **1987**, *2*, 29.

185. Musser, S.M. and Callery, P.S. *Biomed. Environ. Mass Spectrom.*, **1990**, *19*, 348.

186. Anacleto, J.F., Ramaley, L., Boyd, R.K., Pleasance, S., Quilliam, M.A., Sim, P.G., and Benoit, F.M. *Rapid Commun. Mass Spectrom.*, **1991**, *5*, 149.

187. Jewett, B. M.Sc. Thesis, Dalhousie University, 1997.

188. Pleasance, S., Anacleto, J.F., Bailey, M.R. and North, D.H. *J. Am. Soc. Mass Spectrom.*, **1992**, *3*, 378.

189. Fouda, H., Nocerini, M., Schneider, R. and Gedutis, C. *J. Am. Soc. Mass Spectrom.*, **1991**, *2*, 164.

190. Gilbert, J.D., Hand, E.L., Yuan, A.S., Olah, T.V. and Covey, T.R *Biol. Mass Spectrom.*, **1992**, *21*, 63.

191. Anacleto, J.F., Perreault, H., Boyd, R.K., Pleasance, S., Quilliam, M.A., Sim, P.G., Howard, J.B., Makarovsky, Y. and Lafleur, A.L. *Rapid Commun. Mass Spectrom.*, **1992**, *6*, 214.

192. Galceran, M.T. and Moyano, E. *J. Chromatogr. A*, **1996**, *731*, 75.

193. Lafleur, A.L., Taghizadeh, K., Howard, J.B. Anacleto, J.F. and Quilliam, M.A. *J. Am. Soc. Mass Spectrom.*, **1996**, *7*, 276.

194. Schaefer, W.H. and Dixon, F., Jr. *J. Am. Soc. Mass Spectrom.*, **1996**, *7*, 1059.

195. Carroll, D.I., Dzidic, I., Stillwell, R.N., Haegele, K.D. and Horning, E.C. *Anal. Chem.*, **1975**, *47*, 2369.

196. Simonsick, W.J., Jr., and Hites, R.A. *Anal. Chem.*, **1984**, *56*, 2749.

197. Schönemann, A.T., Lago, V. and Dudeck, M. *J. Thermophys. Heat Transfer*, **1996**, *10*, 419.

198. Schönemann, A. and Auweter-Kurtz, M. *J. Thermophys. Heat Transfer*, **1995**, *9*, 620.

199. Fasoulas, S., Sleziona, P.C., Auweter-Kurtz, M., Habiger, H.A., Laure, S.H. and Schönemann, A.T. *J. Thermophys. Heat Transfer*, **1995**, *9*, 422.

200. Asselin, P., Cayet, S., Lasgorceix, P., Lago, V. and Dudeck, M. *J. Thermophys. Heat Transfer*, **1995**, *9*, 416.

201. Hunter, E.P. and Lias, S.G. *J. Phys. Chem. Reference Data*, **1998**, *27*, 413.

202. Centineo, G., Fragala, I., Bruno, G., and Spampinato, S. *J. Mol. Struct.*, **1978**, *44*, 203.

203. Terlouw, J.K., Herima, W., Frintrop, P.C.M., Dijkstra, G. and Meinemo, H.A. *J. Organomet. Chem.*, **1974**, *64*, 205.

204. Potapov, V.K., Kardash, I.E., Sorokin, V.V., Sokolov, S.A. and Evlasheva, T.I. *Khim. Vys. Energ.*, **1972**, *6*, 392.

205. Anacleto, J.F. Ph.D. Thesis, Dalhousie University, 1993.

206. Van Berkel, G.J. and Zhou, F. *Anal. Chem.*, **1995**, *67*, 2916.

207. Van Berkel, G.J., McLuckey, S.A. and Glish, G.L. *Anal. Chem.*, **1991**, *63*, 2064.

208. Van Berkel, G.J., McLuckey, S.A. and Glish, G.L. *Anal. Chem.*, **1992**, *64*, 1586.

209. Van Berkel, G.J., Asano, K.G. and McLuckey, S.A. *J. Am. Soc. Mass Spectrom.*, **1994**, *5*, 689.

210. Xu, X., Lu, W. and Cole, R.B. *Anal. Chem.*, **1996**, *68*, 4244.

211. Miller, J.L., Khaledi, M.G. and Shea, D. *Anal. Chem.*, **1997**, *69*, 1223.

212. Anacleto, J.F., Quilliam, M.A., Boyd, R.K., Howard, J.B., Lafleur, J.B., and Yadav, T. *Rapid Commun. Mass Spectrom.*, **1993**, *7*, 229.

213. Moriwaki, H., Imaeda, A., and Arakawa, R. *Anal. Commun.*, **1999**, *36*, 53.

214. Burrow, P.D., Michejda, J.A. and Jordan, K.D. *J. Chem. Phys.*, **1987**, *86*, 9.

215. Wojńavorits, L., and Földiák, G. *J. Chromatogr.* , **1981**, *206*, 511.

216. Lyons, L.E., Morris, G.C., and Warren, L.J. *J. Phys. Chem.*, **1968**, *72*, 3677.

217. Crocker, L., Wang, T.B. and Kebarle, P. *J. Am. Chem. Soc.*, **1993**, *115*, 7818.

218. Chen, G. and Cooks, R.G. *J. Mass Spectrom.*, **1995**, *30*, 1167.

219. Heinis, T., Chowdhury, S., Scott, S.L. and Kebarle, P. *J. Am. Chem. Soc.*, **1988**, *110*, 400.